



Delft University of Technology

## The Duchenne ARm ORthosis Project

### Advancing motorized arm support technology for severe muscle weakness

Filius, S.J.

#### DOI

[10.4233/uuid:b195a0eb-7fe0-4d3c-aefd-d066d362ad8b](https://doi.org/10.4233/uuid:b195a0eb-7fe0-4d3c-aefd-d066d362ad8b)

#### Publication date

2025

#### Document Version

Final published version

#### Citation (APA)

Filius, S. J. (2025). *The Duchenne ARm ORthosis Project: Advancing motorized arm support technology for severe muscle weakness*. [Dissertation (TU Delft), Delft University of Technology].  
<https://doi.org/10.4233/uuid:b195a0eb-7fe0-4d3c-aefd-d066d362ad8b>

#### Important note

To cite this publication, please use the final published version (if applicable).  
Please check the document version above.

#### Copyright

Other than for strictly personal use, it is not permitted to download, forward or distribute the text or part of it, without the consent of the author(s) and/or copyright holder(s), unless the work is under an open content license such as Creative Commons.

#### Takedown policy

Please contact us and provide details if you believe this document breaches copyrights.  
We will remove access to the work immediately and investigate your claim.

# DUCHENNE ARM ORTHOSIS

# The DAROR Project

# ADVANCING MOTORIZED ARM SUPPORT TECHNOLOGY FOR SEVERE MUSCLE WEAKNESS



**SUZANNE J. FILIUS**



# **The Duchenne ARm ORthosis Project**

Advancing motorized arm support technology for severe  
muscle weakness



# **The Duchenne ARm ORthosis Project**

Advancing motorized arm support technology for severe  
muscle weakness

## **Dissertation**

for the purpose of obtaining the degree of doctor  
at Delft University of Technology,  
by the authority of the Rector Magnificus Prof.dr.ir. T.H.J.J. van der Hagen,  
chair of the Board for Doctorates,  
to be defended publicly on,  
Friday 2 May 2025 at 12:30 o'clock.

by

**Suzanne J. FILIUS**

Master of Science in Biomedical Engineering  
Delft University of Technology, Delft,  
Master of Science in Human Movement Science:  
Sport, Exercise and Health,  
Vrije Universiteit Amsterdam, Amsterdam  
born in Uithoorn, Netherlands.

This dissertation has been approved by the promotor.

Composition of the doctoral committee:

Rector Magnificus,	Chairperson
Prof. dr. ir. J. Harlaar,	Delft University of Technology, promotor
Prof. dr. ir. H. van der Kooij,	University of Twente, promotor
Dr. M.M.H.P. Janssen,	Radboud University Medical Center, copromotor

*Independent members:*

Prof. dr. H.E.J. Veeger,	Delft University of Technology, The Netherlands
Prof. dr. ir. J. Herder,	Delft University of Technology, The Netherlands
Prof. dr. J.S. Rietman,	University of Twente, The Netherlands
Dr. C.S.M. Straathof,	University of Leiden, The Netherlands

*Reserve member:*

Prof. dr. ir. P. Breedveld	Delft University of Technology
----------------------------	--------------------------------

Keywords:      Advanced Orthosis, Exoskeleton, Upper extremity,  
Duchenne Muscular Dystrophy, Passive joint impedance,  
Weight Compensation

Printed by:      Gildeprint  
Cover design:    S. J. Filius

Copyright © 2024 by S.J. Filius

ISBN 978-94-6384-689-9

An electronic version of this dissertation is available at: <http://repository.tudelft.nl>



This work is part of the research programme Wearable Robotics with project number P16-05, which is financed by the Dutch Research Council (NWO), Duchenne Parent Project, Yumen Bionics, Spieren voor Spieren, Baat Medical, the FSHD society and Festo.

*The ideal engineer is a composite ... [S]He is not a scientist, [s]he is not a mathematician, [s]he is not a sociologist or a writer; but [s]he may use the knowledge and techniques of any or all of these disciplines in solving engineering problems.*

Nathan W. Dougherty



# Contents

<b>Preface</b>	<b>xiii</b>
<b>Summary</b>	<b>xv</b>
<b>Samenvatting</b>	<b>xvii</b>
<b>Wearable Robotics Program</b>	<b>xxi</b>
<b>1 Introduction</b>	<b>1</b>
1.1 Background . . . . .	2
1.2 Problem statement and possible solution . . . . .	4
1.3 State-of-the-art. . . . .	5
1.4 Knowledge gap. . . . .	6
1.5 Research objective . . . . .	7
1.6 Approach and outline . . . . .	7
<b>I User Analysis and Design Requirements</b>	<b>15</b>
<b>2 Design Requirements of Arm Supports for Daily Use in DMD with Severe Muscle Weakness</b>	<b>17</b>
2.1 Introduction . . . . .	18
2.1.1 Muscular Dystrophy affecting upper limb . . . . .	18
2.1.2 Intended target population . . . . .	19
2.1.3 Availability of arm supports . . . . .	19
2.1.4 Aim . . . . .	20
2.2 Method. . . . .	20
2.2.1 Data collection . . . . .	20
2.2.2 Literature search . . . . .	21
2.2.3 Functional requirements and arm model definitions . . . . .	21
2.3 Results . . . . .	22
2.3.1 Characteristics of the intended target population. . . . .	22
2.3.1.1 Muscle strength . . . . .	22
2.3.1.2 Range of motion . . . . .	24
2.3.1.3 Functional ability . . . . .	25
2.3.1.4 Joint impedance . . . . .	25
2.3.1.5 Anthropometry . . . . .	26
2.3.1.6 Comorbidities and medication . . . . .	26
2.3.2 Functional requirements . . . . .	26
2.3.2.1 Prioritizing activities of daily living . . . . .	26
2.3.2.2 Range of motion . . . . .	27

2.3.2.3	Velocity . . . . .	27
2.3.2.4	Support level . . . . .	28
2.3.3	Technical requirements . . . . .	29
2.3.3.1	Mechanical structure . . . . .	33
2.3.3.2	Human interface . . . . .	34
2.3.3.3	Actuator technology . . . . .	34
2.3.3.4	Control approach . . . . .	34
2.3.3.5	Safety . . . . .	35
2.4	Discussion . . . . .	36
2.5	Conclusion . . . . .	38
<b>3</b>	<b>Passive Joint Impedance Identification in the Upper Extremity</b>	<b>47</b>
3.1	Introduction . . . . .	48
3.2	Methods . . . . .	49
3.2.1	Literature search . . . . .	49
3.2.2	Screening . . . . .	50
3.3	Results . . . . .	51
3.3.1	Definition of passive joint impedance . . . . .	51
3.3.2	Experimental methods to quantify the joint impedance. . . . .	52
3.3.2.1	Static . . . . .	53
3.3.2.2	Frequency perturbations . . . . .	53
3.3.2.3	Ramp and variations . . . . .	53
3.3.3	Properties of joint impedance and parameters affecting it . . . . .	54
3.3.3.1	Fixed or biologically dependent parameters . . . . .	54
3.3.3.2	Time or environmentally dependent parameters . . . . .	63
3.3.3.3	Training related . . . . .	64
3.3.3.4	Reflexes or volition dependent parameters . . . . .	64
3.4	Discussion . . . . .	65
3.5	Conclusion . . . . .	67
<b>II</b>	<b>Subsystem Design, Module Design, and Unit Testing</b>	<b>77</b>
<b>4</b>	<b>Comparison of Weight and Passive Elbow Joint Impedance Compensation</b>	<b>79</b>
4.1	Introduction . . . . .	80
4.2	Methods . . . . .	81
4.2.1	Participants . . . . .	81
4.2.2	Equipment . . . . .	81
4.2.3	Outcome measures . . . . .	82
4.2.4	Study design . . . . .	83
4.2.5	Data processing . . . . .	84
4.2.6	Statistics . . . . .	84
4.3	Results . . . . .	85
4.3.1	Outcome measures . . . . .	85
4.4	Discussion . . . . .	87
4.4.1	Comparison of the compensation strategies . . . . .	87
4.4.2	Limitations of the study . . . . .	88



4.5	Conclusion . . . . .	89
<b>5</b>	<b>The Efficacy of Different Torque Profiles for Weight Compensation of the Hand</b>	<b>93</b>
5.1	Introduction . . . . .	94
5.2	Methods . . . . .	95
5.2.1	Participants . . . . .	95
5.2.2	Experiment design . . . . .	95
5.2.2.1	Parameter calibrations . . . . .	95
5.2.2.2	Experiments . . . . .	96
5.2.3	Equipment . . . . .	96
5.2.3.1	Imposing wrist torque profiles . . . . .	96
5.2.3.2	sEMG . . . . .	98
5.2.4	Data processing . . . . .	98
5.2.5	Statistics . . . . .	98
5.3	Results . . . . .	99
5.3.1	Participants . . . . .	99
5.3.2	sEMG activity . . . . .	99
5.3.2.1	ECR . . . . .	99
5.3.2.2	FCR . . . . .	100
5.4	Discussion . . . . .	101
5.4.1	Limitations of the study . . . . .	102
5.4.2	Recommendations . . . . .	103
5.5	Conclusion . . . . .	103

### III System Design and System Testing 107

<b>6</b>	<b>The Design of the Dummy Arm: a Verification Tool for Arm Exoskeleton Development</b>	<b>109</b>
6.1	Introduction . . . . .	110
6.2	Materials and methods . . . . .	112
6.2.1	Dummy Arm design requirements . . . . .	112
6.2.2	Dummy Arm design . . . . .	112
6.2.2.1	Shoulder joint . . . . .	113
6.2.2.2	Elbow joint . . . . .	113
6.2.2.3	Passive elbow joint impedance . . . . .	113
6.2.2.4	Connection frame . . . . .	113
6.2.2.5	Mass and Center of Mass of the Upper and Lower Arm . . . . .	114
6.2.2.6	Verification of design . . . . .	114
6.3	Results . . . . .	115
6.3.1	Joint impedance realization . . . . .	115
6.3.2	Activities of daily living . . . . .	117
6.3.3	Cost-analysis . . . . .	117
6.4	Discussion . . . . .	118
6.4.1	Limitations . . . . .	118
6.4.2	Recommendations . . . . .	119

6.5	Conclusions . . . . .	120
<b>7</b>	<b>A 4DOF Motorized Upper Limb Assistive Exoskeleton with Weight and Elbow Stiffness Compensation</b>	<b>125</b>
7.1	Introduction . . . . .	126
7.2	Design . . . . .	129
7.2.1	Mechanical skeleton design . . . . .	129
7.2.2	Actuator design . . . . .	129
7.2.3	Software and system architecture . . . . .	129
7.2.4	Mobile power station design . . . . .	129
7.2.5	Sensor performance . . . . .	130
7.2.5.1	Joint angle resolution . . . . .	130
7.2.5.2	SEA torque sensor performance . . . . .	130
7.2.5.3	F/T force sensor performance . . . . .	130
7.2.6	Safety measures . . . . .	131
7.3	Modeling and Control . . . . .	131
7.3.1	Kinematics . . . . .	131
7.3.2	Weight compensation model . . . . .	132
7.3.3	Elbow stiffness compensation . . . . .	132
7.3.4	Parameters of the compensation model. . . . .	133
7.3.4.1	ID(+) . . . . .	133
7.3.4.2	AP(+) . . . . .	134
7.3.5	Control for compensation and transparency . . . . .	134
7.4	Verification tests . . . . .	134
7.4.1	Range of motion . . . . .	135
7.4.2	DAROR support torque. . . . .	137
7.4.3	High-level compensation and transparency performance. . . . .	137
7.5	Discussion . . . . .	140
7.5.1	Verification of the design requirements. . . . .	140
7.5.1.1	Comparison AP(+) and ID(+) . . . . .	142
7.5.1.2	Intuitiveness of the control interface . . . . .	142
7.5.2	Study Limitations . . . . .	142
7.5.3	Conclusions . . . . .	143
<b>IV</b>	<b>General Discussion</b>	<b>149</b>
<b>8</b>	<b>Discussion</b>	<b>151</b>
8.1	Overview of main results. . . . .	152
8.1.1	Part I – User Analysis and Design Requirements . . . . .	152
8.1.2	Part II – Subsystem Design, Module Design, and Unit Testing . . . . .	152
8.1.3	Part III – System Design and System Testing . . . . .	154
8.2	General Discussion. . . . .	154
8.2.1	System verification and refinement of design requirements. . . . .	155
8.2.1.1	High-level compensation and transparency performance . . . . .	155
8.2.1.2	Semi-personalized or personalized parameter estimation? . . . . .	156
8.2.2	The importance of joint stiffness compensation . . . . .	156

8.2.3	Kinematic design alterations . . . . .	157
8.2.4	Preliminary validation results from co-creation . . . . .	157
8.3	Lessons learned . . . . .	159
8.3.1	Applying the V-model: Test, Test, and... Test!. . . . .	159
8.3.2	Collaboration is key . . . . .	160
8.4	Study limitations and recommendations . . . . .	161
8.5	Future outlook . . . . .	162
8.5.1	Alternative control approaches. . . . .	162
8.5.2	Generalization of the results . . . . .	163
8.5.3	Alternative hardware configurations . . . . .	163
8.5.4	Compensate for additional lifted objects . . . . .	163
8.5.5	Towards a product phase. . . . .	164
<b>9</b>	<b>Conclusion</b>	<b>169</b>
	<b>Appendices</b>	<b>171</b>
<b>A</b>	<b>Appendix A</b>	<b>173</b>
A.1	Search terms used in literature review of Chapter 3 . . . . .	173
<b>B</b>	<b>Appendix B</b>	<b>177</b>
B.1	Direction dependency of passive joint moments . . . . .	177
<b>C</b>	<b>Appendix C</b>	<b>179</b>
C.1	Torque models . . . . .	179
C.2	Effect of movement direction. . . . .	180
C.3	Effect of different levels of compensation. . . . .	181
<b>D</b>	<b>Appendix D</b>	<b>185</b>
D.1	Sensor Analysis . . . . .	185
D.1.1	Theoretical sensor resolution. . . . .	185
D.1.2	SEA . . . . .	185
D.1.3	F/T sensor . . . . .	186
D.1.4	Sensor performance . . . . .	186
D.1.4.1	Accuracy and sensitivity analysis . . . . .	186
D.1.5	Precision analysis . . . . .	187
D.1.6	SEA linearity and hysteresis . . . . .	188
D.2	Kinematic model of the HEC . . . . .	192
D.2.1	Kinematic Model . . . . .	192
D.2.1.1	Exoskeleton forward kinematics . . . . .	192
D.2.1.2	Human arm, shoulder frame and kinematics . . . . .	192
D.2.2	Solving the inverse kinematics problem for trajectory generation . . . . .	193
D.2.2.1	Kinematic Error Correction . . . . .	194
D.2.2.2	Constrained Differential Inverse Kinematics . . . . .	194

D.3	Derivation of the HEC gravity model. . . . .	195
D.4	Enforcing workspace limits during minimal impedance mode . . . . .	196
D.5	Parameter identification procedure. . . . .	197
D.5.1	Configurations and Motions for Identification . . . . .	197
D.5.1.1	Configurations . . . . .	197
D.5.1.2	Trajectory generation . . . . .	198
D.5.2	Parameter identification as a fitting problem . . . . .	198
D.5.2.1	Uniqueness of solution . . . . .	198
D.6	Zeroing of F/T sensor offset and post-sensor brace contribution . . . . .	199
D.6.1	F/T Sensor Workings. . . . .	199
D.6.2	Determining bias forces and torques . . . . .	199
D.6.3	Compensating bias forces and torques . . . . .	200

<b>End Matter</b>	<b>203</b>
<b>Acknowledgments</b>	<b>205</b>
<b>List of Publications</b>	<b>211</b>
<b>Curriculum Vitæ</b>	<b>213</b>

# Preface

For me personally, moving my body and being able to exercise is one of the key elements of happiness and overall well-being. Doing the sports I like is a way to express myself and interact with the people around me. The thought of losing this ability overwhelms me, and I cannot imagine how I would cope without it. For people with muscle dystrophies, such as Duchenne Muscular Dystrophy, the reality is that with each sunset, their muscles are tired and moving their body becomes harder as they get older. At an early age, they lose the ability to run, walk, and later independently eat, drink, or 'simply' itch their nose.

How great would it be if we could restore their arm function to give back some independence and improve their quality of life?



# Summary

Duchenne Muscular Dystrophy (DMD) is a neuromuscular condition from a genetic origin. It causes progressive muscle weakness, mainly affecting males. To date, there is no cure, and treatment focuses on managing symptoms and delaying disease progression. In the early teenage years, walking becomes increasingly difficult, and the use of an (electric) wheelchair becomes necessary. This makes the upper limb function increasingly important for daily activities. Simultaneously, the arm strength declines, implying the need for supportive arm devices. Yet, no arm support adequately meets the needs of individuals in the advanced stages of DMD (Brooke Scale 4). People with a functional ability of Brooke Scale 4 can still reach their mouth but cannot lift a glass of water.

Developing suitable arm supports, or *exoskeletons*, is complex for this population due to variations in muscle strength, body measurements, range of motion, and joint stiffness. Additionally, secondary conditions such as reduced bone mineral density and scoliosis present safety risks that must be carefully considered. At the start of this project, we identified a need for precise design requirements tailored to individuals with DMD Brooke Scale 4. In addition, considering the state of the art, control and actuator technology advancements were needed. Ideally, arm support assists the arm movement intuitively, allowing the user to engage their residual muscle strength without a joystick or predefined trajectories. Moreover, the device should not be bulky or stigmatizing while being strong enough to lift at least the arm's weight. This requires small but strong actuators to fit within the limited design space.

The aim of this project was fourfold: 1) define design requirements for assistive arm support tailored to individuals with DMD at Brooke Scale 4, 2) compare strategies to estimate and compensate the arm's weight and elbow stiffness using an intuitive human-exoskeleton control interface, 3) develop an exoskeleton prototype, the Duchenne ARM ORthosis (DAROR), and 4) verify that the design meets the formulated requirements.

The first part of this thesis, **Part I**, translates the clinical characteristics of individuals with DMD Brooke Scale 4 into functional and technical requirements (Chapter 2). These findings indicated that motorized arm exoskeletons that compensate for weight and *passive joint impedance* (pJimp) - the resistance of a joint to motion - seem necessary for the advanced stages of DMD. The pJimp is often elevated in individuals with DMD, making it an important characteristic to consider in developing compensation strategies. However, quantitative data on pJimp was lacking, making it difficult to model its behavior. Therefore, Chapter 3 reviewed methods used to examine pJimp in the upper limb.

In **Part II**, one of these identified methods was used to measure the pJimp in the elbow joint using a motorized elbow support (Chapter 4). Four compensation strategies were compared. These strategies compensated either the weight of the forearm, using known body measures, or the combined weight and identified elbow pJimp. For this experiment, the first version of the custom-made actuator was used. The results showed that even in individuals without DMD the pJimp plays a substantial role for compensation. It was also found that its behavior could be captured in a mathematical model together with the weight of the forearm. When applied to the entire arm, the gravitational model becomes more complex, as gravity's direction depends on the orientation of the other joints. The latter holds also for the wrist joint. Therefore, in Chapter 5, we explored simplified weight compensation strategies that depend only on the forearm orientation (instead of both forearm and wrist). The simplified torque profile showed no statistical difference in muscle

effort of the forearm muscles compared to the ‘theoretical ideal’ profile that was dependent on both forearm and wrist orientation. This makes future (semi-)passive solutions for the wrist more feasible.

In **Part III**, first, the design of the *Dummy Arm* is presented. The Dummy Arm mimics the human arm, including variable elbow joint stiffness profiles (Chapter 6). This Dummy Arm was an effective tool for developing and evaluating control strategies. Next, Chapter 7 covers the realized integration of the hardware and software components into the Duchenne ARm ORthosis, the *DAROR*. This final chapter presents the design, control, and verification results of the exoskeleton. The DAROR compensates the user’s arm weight and, optionally, the stiffness component of the pJimp in the elbow joint using an impedance controller. This controller calculates the required support torque based on the joints’ orientations. The user can use its residual muscle strength to reposition the arm to the next configuration. In this way, the user only needs to overcome the friction in the system, which requires much less muscle force than to hold the weight of the arm. This control strategy is considered more intuitive than a position controller that is controlled by a joystick or buttons. Alternatively, using electromyography (EMG) by surface electrodes to measure muscle activity as movement intention could also be intuitive but is considered less practical. Additionally, in Chapter 7 we verified the DAROR using the Dummy Arm, a healthy reference user and our co-creator with DMD. The results showed that the design requirements were sufficiently met for people with DMD Brooke Scale 4. Moreover, Chapter 7 compares two strategies to estimate and compensate for the arm weight and the elbow stiffness, both inspired on the methods explored in Chapter 4. One method is *semi-personalized* and makes use of a few body measurements (e.g., segment length, body weight) to determine the level of support. The other method is *personalized* and determines the required support torques based on an identification procedure. Although the semi-personalized approach is quicker and more robust against measurement inaccuracies, this method is considerably less accurate for individuals whose body measurements deviate from standardized tables. Since this is often the case in DMD, the personalized approach seems more promising.

Finally, in the general discussion the preliminary results of the user acceptance tests with our co-creator with DMD are presented. Although most design requirements were met, these preliminary validation tests also revealed some limitations on the system transparency (i.e., low mechanical impedance) and torque sensing (i.e., accuracy and precision). Therefore, refinements of the formulated design requirements are proposed to enhance the performance of future arm supports.

In future work, alternative control interfaces or improvements on the DAROR could extend the DAROR’s suitability to a broader population, including individuals with lower muscle strength (e.g., higher Brooke Scales). The DAROR hardware is designed to allow for the comparison of various control strategies (e.g., EMG- or force-based admittance control), facilitating a comparison in feasibility and intuitiveness of the control approaches within the same hardware.

Through this research, and by delivering the investigational DAROR exoskeleton, we facilitate well-informed development of effective motorized arm supports to address the gap in commercially available solutions. This work aligns with my personal ambition to create technology to enhance movement independence of people with limited mobility.



# Samenvatting

Duchenne Spierdystrofie (DMD) is een progressieve spierziekte die leidt tot toenemende spierzwakte en treft vooral jongens. Tot op heden bestaat er nog geen genezing en is de behandeling gericht op symptoombestrijding en het vertragen van de ziekte. Rond de eerste tienerjaren wordt lopen vaak onmogelijk, waardoor het gebruik van een (elektrische) rolstoel noodzakelijk wordt. Hierdoor wordt de armfunctie steeds belangrijker voor dagelijkse activiteiten. Ondertussen neemt ook de armkracht verder af en stijgt de behoefte aan ondersteunende hulpmiddelen voor de arm functie. Echter, op dit moment is er nog geen beschikbare armondersteuning die voldoet aan de behoeften van de gevorderde stadia van DMD (Brooke Schaal 4). Met Brooke Schaal 4 kun je de mond nog bereiken, maar zelfstandig een glas water optillen is te zwaar.

Het ontwikkelen van geschikte armondersteuning, ofwel *exoskeletten*, voor deze groep, is complex vanwege de variaties in spierkracht, lichaamsafmetingen, bewegingsbereik en gewrichtsstijfheid. Daarnaast zorgen secundaire aandoeningen, zoals verminderde botdichtheid en scoliose (kromming van de ruggenwervel), voor belangrijke veiligheidsrisico's waar rekening mee gehouden moet worden. Bij aanvang van dit project was er een behoefte aan duidelijke ontwerpeisen toegespitst op individuen met DMD Brooke Schaal 4. Bovendien, gezien de bestaande oplossingen, was er behoefte aan technologische verbeteringen op het gebied van aansturing en actuatoren (actuator: motor, sensoren, versnellingsmechanismen en controle-elektronica). Idealiter ondersteunt de armondersteuning de beweging van de arm op een intuïtieve manier, waarbij de gebruiker zijn resterende spierkracht kan inzetten zonder dat hij een joystick of vooraf ingestelde bewegingen hoeft te gebruiken. Verder moet het apparaat compact en niet stigmatiserend zijn, maar ook sterk genoeg om ten minste het gewicht van de arm te dragen. Hiervoor zijn kleine, maar krachtige, actuatoren nodig die in de beperkte ontwerpruimte passen.

Het doel van dit project was viervoudig: 1) vaststellen van ontwerpeisen voor een armondersteuning toegespitst op individuen met DMD op Brooke Schaal 4, 2) strategieën vergelijken om het arm gewicht en de elleboogstijfheid in te schatten en te compenseren met een intuïtieve aansturingsmethode, 3) ontwikkelen van de Duchenne ARM ORthesis (DAROR), en 4) verifiëren in hoeverre het ontwerp voldoet aan de gestelde eisen.

Het eerste deel van dit proefschrift, **Deel I**, vertaalt de klinische kenmerken van individuen met DMD Brooke Schaal 4 naar functionele en technische eisen (Hoofdstuk 2). Hieruit kwam naar voren dat gemotoriseerde arm exoskeletten die zowel het gewicht als de weerstand van een gewricht tegen beweging (ofwel de *passieve gewrichtsimpedantie*) kunnen compenseren, geschikt zijn voor gevorderde stadia van DMD. Deze zogenaamde gewrichtsimpedantie is vaak verhoogd bij individuen met DMD, waardoor het extra belangrijk is om deze mee te nemen in de ontwikkeling van compensatiestrategieën. Er is echter onvoldoende kwantitatieve data beschikbaar over gewrichtsimpedantie. Dit bemoeilijkt het modelleren van de gewrichtsimpedantie. Daarom is in Hoofdstuk 3 eerst een systematisch literatuuronderzoek gedaan naar methoden om de gewrichtsimpedantie in de arm te meten.

In **Deel II** werd een van deze methoden gebruikt om de gewrichtsimpedantie in het ellebooggewricht te meten met behulp van een gemotoriseerde elleboog ondersteuning (Hoofdstuk 4). Vier compensatiestrategieën werden vergeleken. Deze strategieën compenseerden ofwel het gewicht van de onderarm op basis van bekende lichaamsmetingen, of het gecombineerde gewicht en de geïdentificeerde elleboog impedantie (buigweerstand). Voor dit experiment werd de eerste testversie van de op maat gemaakte actuatoren ge-

bruikt. De resultaten toonden aan dat de gewrichtsimpedantie zelfs bij individuen zonder DMD een substantiële rol speelt bij de compensatie. We konden het gedrag van deze gewrichtsimpedantie, samen met het gewicht van de onderarm, nauwkeurig beschrijven met een wiskundig model. Echter, wanneer dit werd toegepast op de gehele arm, wordt het zwaartekrachtmodel complexer. Dit komt doordat de richting van de zwaartekracht afhankelijk is van de oriëntatie van andere gewrichten. Dit laatste geldt ook voor het polsgewricht. Daarom is in Hoofdstuk 5 gekeken naar versimpelde gewichtscompensatiestrategieën die alleen afhankelijk zijn van de oriëntatie van de onderarm (in plaats van zowel de onderarm als de pols). Deze versimpelde strategie liet geen statistisch verschil zien in de spieractiviteit van de onderarmspiers vergeleken met het ‘theoretisch ideale’ profiel, die afhankelijk was van de oriëntatie van de onderarm en de pols. Hiermee worden toekomstige (semi-)passieve oplossingen voor de pols beter haalbaar.

In **Deel III** wordt eerst het ontwerp van de *Dummy Arm* gepresenteerd. De *Dummy Arm* is een kunstarm met menselijke eigenschappen, waaronder variabele stijfheidsprofielen van de elleboog om de gewrichtsimpedantie na te bootsen (Hoofdstuk 6). De *Dummy Arm* was een effectief hulpmiddel voor het ontwikkelen en evalueren van de compensatiestrategieën. Vervolgens beschrijft Hoofdstuk 7 de integratie van de hardware- en softwarecomponenten zoals gerealiseerd in de Duchenne ARM ORthesis, de *DAROR*. Dit laatste hoofdstuk presenteert het ontwerp, de regelaar en verificatieresultaten van het *DAROR*-exoskelet. De *DAROR* compenseert het gewicht van de arm van de gebruiker en, optioneel, de stijfheidscomponent van de gewrichtsimpedantie van het ellebooggewricht. De mate van compensatie die nodig is voor de ondersteuning wordt berekend op basis van de gewrichtsoriëntaties van de arm. Op iedere positie weet de *DAROR* hoeveel ondersteuning nodig is. Hierdoor kan de gebruiker zijn resterende spierkracht gebruiken om de arm naar een volgende positie te brengen. Op deze manier hoeft de gebruiker alleen de weerstand in het systeem te overwinnen, wat veel minder spierkracht vereist dan het optillen van de arm zelf. Deze aansturingsstrategie (impedantie-regeling) wordt als intuïtiever beschouwd dan een positie-regeling die wordt aangestuurd met een joystick of knoppen. Bovendien is deze benadering praktischer dan het gebruik van elektromyografie (EMG) elektroden waarbij de bewegingsintentie wordt gemeten met spieractiviteit.

In Hoofdstuk 7 hebben we ook de *DAROR* getest met de *Dummy Arm*, een gebruiker zonder spierzwakte en onze co-creator met DMD. De resultaten toonden aan dat het gerealiseerde ontwerp van de *DAROR* voldoet aan de ontwerpeisen die specifiek zijn opgesteld voor individuen met DMD Brooke Schaal 4. In dit hoofdstuk worden ook twee strategieën vergeleken voor het schatten en compenseren van het armgewicht en de elleboogstijfheid, beide geïnspireerd op de methoden uit Hoofdstuk 4. Eén methode is *semi-gepersonaliseerd* en maakt gebruik van enkele lichaamsmaten (zoals segmentlengte en lichaamsgewicht) om de benodigde ondersteuning te bepalen. De andere methode is meer *gepersonaliseerd* en bepaalt de vereiste ondersteuning op basis van een identificatieprocedure (ofwel kalibratiemeting). Hoewel de semi-gepersonaliseerde aanpak sneller is en minder gevoelig voor onnauwkeurigheden tijdens de kalibratiemeting, is deze methode aanzienlijk minder nauwkeurig voor individuen met lichaamsmaten die afwijken van de standaardtabellen. Omdat dit vaak het geval is bij DMD, lijkt de gepersonaliseerde aanpak het meest geschikt voor onze toepassing.

Tot slot wordt er in de algemene discussie, de voorlopige resultaten met onze co-creator

met DMD gepresenteerd. Hoewel de DAROR aan de ontwerpisen voldeed, onthulden deze exploratieve validatietesten ook enkele beperkingen op het gebied van mechanische wrijving in het systeem en beperkingen van de sensoren in de actuatoren. Daarom worden enkele verfijningen van de geformuleerde ontwerpisen voorgesteld om de prestaties van toekomstige armondersteuningn verder te verbeteren.

In toekomstig onderzoek zouden verbeteringen aan de DAROR-hardware of alternatieve aansturingsmethodes (zoals EMG- of krachtgestuurde admittance-regelingen) de inzetbaarheid kunnen uitbreiden naar een bredere doelgroep, inclusief mensen met nog minder spierkracht (bijv. hogere Brooke schalen). De DAROR-hardware is zo ontworpen dat het de vergelijking van verschillende aansturingstrategieën (zoals EMG- of kracht besturing) mogelijk maakt binnen dezelfde hardware. Hierdoor is de haalbaarheid en intuïtiviteit van de diverse aansturingstrategieën in het vervolg goed te onderzoeken.

Met dit onderzoek, en het ontwikkelen van het DAROR-exoskelet als onderzoeksprototype, dragen we bij aan de goed geïnformeerde ontwikkeling van effectieve gemotoriseerde armondersteuningn voor individuen met DMD die momenteel wachten op geschikte oplossingen. Hiermee hopen we de ontwikkeling van commercieel beschikbare armondersteuningn te versnellen. Dit project sluit perfect aan bij mijn persoonlijke ambitie om technologie te creëren die de bewegingsonafhankelijkheid van mensen met beperkte mobiliteit vergroot.



# Wearable Robotics Program

From 2018 to 2024, the Wearable Robotics Project consortium was conducted in the Netherlands. This consortium has the ambition to develop wearable robots that you can wear and work in favor of the human body to protect, assist, or amplify movements. The program consists of seven projects, of which four are technical projects with the ambition to develop innovative, commercially viable, and enabling technologies in the areas:

1. Lightweight and energy efficient actuation
2. Sensing combined with biomechanical modeling for user intention detection
3. Soft and shell-like structures for lightweight and comfortable wearables
4. Balance and shared control of leg exoskeletons for stability

Together with three application projects in various fields:

5. To restore locomotion mobility in people with a spinal cord injury
6. To improve the functional ability of the arms in people with Muscular Dystrophy
7. To prevent work-related musculoskeletal back injuries

The consortium was funded by NWO-TTW and sponsors, and a fruitful collaboration was established between various expertise centers and users from industry within the Netherlands: Delft University of Technology, University of Twente, Radboud UMC, VU University Medical Center, Eindhoven University of Technology, TNO, Roessingh, St. Maartenskliniek, Motek Forcelink, XSense, FSHD Stichting, Duchenne Parent Project, Spieren voor Spieren, Yumen Bionics, Festo, Baat Medical, Laevo, Oceanz, Opteq BV, By-Wire.net, IM Systems, Hankamp Gears, Ottobock, Hocoma, TMSi, Ultimaker, Bond3D, Demcon, Dwarslaesie Organisatie nederland, i-Botics, and Landelijke Vereniging Operatieassistenten. More information can be found on <https://www.wearablerobotics.nl/>.

This thesis contains the work of Project 7, and special thanks go to our funders and user committee members: Dutch Research Council (NWO-TTW 16-05), Duchenne Parent Project, Yumen Bionics, Spieren voor Spieren, FSHD Stichting, Festo, and Baat Medical.

Within Project 7, we build further on the research projects of the FlexTension A-Gear project, an initiative of the Dutch Duchenne Parent Project, which was conducted between 2011 and 2019. Within the FlexTension A-Gear project, the work of Janssen [2] explored the progressive arm function loss of people with DMD, the work of Dunning [1] investigated how the design could be slender and close-to-body, and the work of Lobo Pratt [3] researched what sensor interfaces can be used for intuitive control of active arm supports.



Wearable Robotics

## References

- [1] A. G. Dunning. *Slender spring systems*. PhD thesis, Delft University of Technology, 2016.
- [2] M. Janssen. *Upper extremity function in Duchenne Muscular Dystrophy, Mechanisms of declined task performance*. PhD thesis, Radboud University Nijmegen, 2017.
- [3] J. Lobo Pratt. *Control interfaces to actively support the arm function of men with Duchenne Muscular Dystrophy*. PhD thesis, University of Twente, 2016.

# 1

## Introduction

## 1.1 Background

DMD is a neuromuscular disease that results in progressive breakdown of muscle tissue. At an early age, they lose the ability to run, walk (5-12 years old), and later independently eat, drink, or 'simply' itch their nose (10-20 years old) [13, 15, 25, 46]. It is caused by a mutation of the dystrophin gene on the X-chromosome and, therefore, mainly affects boys and men. It is the most common subtype of muscular dystrophies, with a live male birth incidence of 1:5000 [10]. The lack of this dystrophin protein, which is a cytoskeletal protein that provides strength and stability to myofibers [1], makes the muscle cells highly vulnerable to breakdown. After repetitive damage, the muscle fibers lose their ability to repair, leading to permanent degradation and replacement by fat (adipose tissue) and connective tissue (fibrosis) [6, 23, 34, 45]. Contractures, which result from muscle shortening and fibrosis, limit the passive range of motion (pROM) of the joints and induce disuse. These morphological adaptations in the muscles and surrounding tissue also increase the so-called *passive joint impedance* (pJimp) [32], which is the mechanical resistance in response to an exerted motion [3]. Basically, the joints feel stiffer when being moved, which progresses over the disease [6, 22].

In their early twenties, often cardiac and respiratory complications arise [2]. Life expectancy is increased from around 14 years (in the 1960's) to over 39 years [29] by advancements in medical interventions, such as corticosteroid treatment and mechanical ventilation [29]. This also implies that the years people with DMD make use of an (electric) wheelchair become longer, leading to an increased dependency on the upper extremity function [24, 30, 31]. Consequently, supporting their arm function becomes increasingly important to improve their independence in activities of daily living (ADL), social participation and their quality of life.

Assistive arm supports reduce the need for muscle strength to perform arm movements by compensating the weight of the arm and manipulated objects. Figure 1.1 categorizes the different types and levels of support in assistive devices that support arm function.

A distinction can be made between *external manipulators* that overtake the arm function, and *arm supports* that physically assist the arm. External manipulators are devices such as robotic manipulators or feeding aids, which can be controlled with a joystick or button. One issue with the control of such robotic manipulators by joystick is that the user has to control multiple joints (e.g., grip fingers, arm) over movement directions with only limited user inputs (e.g., two axis joystick) [36]. Moreover, a drawback is that they do not involve the arm in motion. Since disuse further leads to muscle atrophy and consequent functional loss, sub-maximal exercises, along with the use of splints and stretching exercises, are prescribed as therapy to help maintain muscle length and joint mobility [1, 5, 8, 19–21, 46]. By keeping the arms engaged, blood flow, muscle activity, and joint mobility are stimulated. This potentially slows down disuse atrophy and reduces the formation of contractures. So, arm supports are preferred over external manipulators, but the latter is a good alternative for people with extremely limited pROM by joint contractures.

Within the arm supports, a distinction can be made between an *end-effector* system and *exoskeletons* design. End-effector designs are interfaced with the forearm with a brace and do not follow the human arm's anatomy, while *exoskeletons* do follow the anatomy of the arm [17]. Both can be *wearable*, i.e., body-worn, or be *environmentally supported*, either by wheelchair, table or device frame. The level of support can vary. Examples of



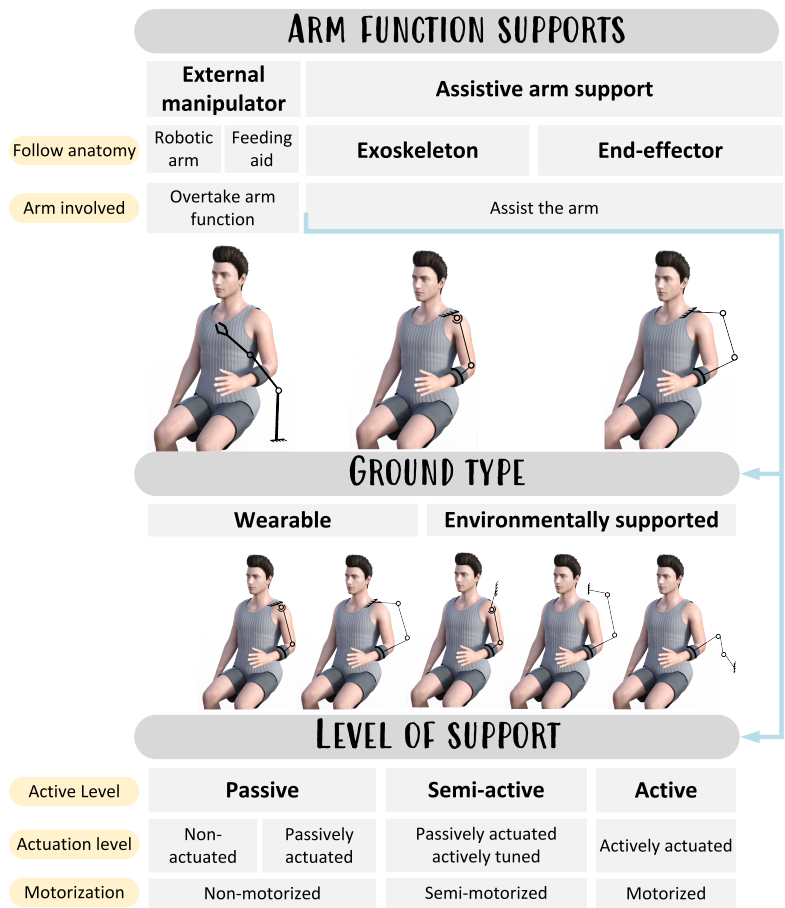


**Figure 1.1:** Categories of arm function support systems and the activation level types.

non-motorized (i.e., passive) arm supports are, for instance, devices that support the arm in a horizontal plane for tabletop activities by low resistance joints or passively actuated supports that use springs (i.e., elastic bands) or counterweights to balance the arm [43]. Additionally, semi-active arm supports exist, where the support itself comes from a passive element, e.g., a mechanical spring, while the level of pre-tension of this spring can be tuned with a motor [43]. This helps to adjust the level of support to the required level but to the drawback of button-use with the contra-lateral arm to re-adjust the support level [31], hindering bimanual tasks. Finally, there are fully active actuated systems where energy is added by a form of actuation [17, 31]. The amount of actuated degrees of freedom (DOF) and plane of assistance (e.g., vertical [33], or horizontal [39]) can vary.

## 1.2 Problem statement and possible solution

As the disease progresses, the need to support the arms increases. Most currently available arm supports are passive or semi-active orthosis [11, 43], that perform well, but provide insufficient support in the more advanced disease stages [31, 38]. A frequently used method to express the functional decline of the upper extremity in DMD is the Brooke Scale [4], which gives an indication of the disease stage, see Table 1.1. For people within Brooke Scale of 4 and above, it becomes too difficult to raise the arms above the head, lift objects with additional weight [37] and perform downward movements [27] with the passive arm supports [7]. Their residual muscle strength becomes insufficient to overcome the friction and inertia of the passive supports and their pJimp, which is not compensated [8, 9, 28]. These more severely impaired patients could benefit from active (i.e., motorized) arm support [8, 31]. Motorized arm supports allow for tuning of the support over the progression of the disease, can adapt the support to the different lifting heights automatically, and compensate for the elevated pJimp. Moreover, it could potentially detect and adapt to the additional weight of a lifted object.

However, to the author's knowledge, there are no successful active arm supports for daily use that are commercially available for this population yet. This leaves a gap in the available arm supports for the disease stage where the arms pROM is too good for external robotic manipulators and muscle strength too weak for the commercially available passive and semi-active arm supports, as depicted in Figure 1.2 [41].

**Table 1.1:** Description of the Brooke scores. Reproduced from [4]

Grade	Functional description
1	Starting with arms at the sides, the patient can abduct the arms in a full circle until they touch above the head
2	Can raise arms above head only by flexing the elbow (i.e., shortening the circumference of the movement) or using accessory muscles
3	Cannot raise hands above head but can raise an 8-oz glass of water to the mouth
4	Can raise hands to the mouth, but cannot raise an 8-oz glass of water to the mouth
5	Cannot raise hands to the mouth but can use hands to hold a pen or pick up pennies from the table
6	Cannot raise hands to the mouth and has no useful function of hands

## GAP IN COMMERCIALY AVAILABLE ARM SUPPORTS

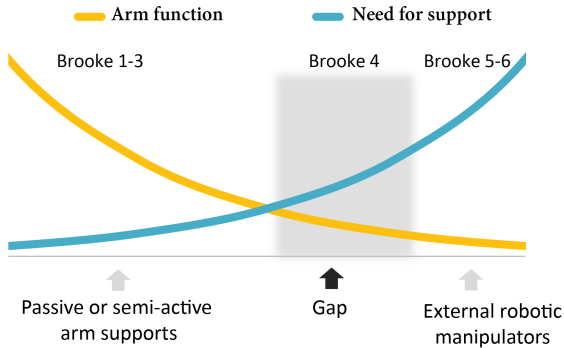


**Figure 1.2:** Gap in commercially available arm support. Note: Adapted with permission from van der Heide (2017)

### 1.3 State-of-the-art

A few research projects have attempted to address this gap but have not yet been valorized. The most promising is the Power-Assist (Talem Technologies, US) described in [9, 33]. That is, in fact, a ‘hybrid’ system, since it is a semi-motorized system, but unlike others, it automatically adjusts the level of support to the desired work plane height using force-based admittance control. This seems promising, however, similar to the commercially available semi-motorized systems, this device has an end-effector design and does not consider pJump compensation.

An exoskeleton design that follows the human arm’s anatomy is expected to allow for better alignment and natural movement [14, 16], resulting in a sleek design that remains closer to the body compared to an end-effector design. This approach is assumed to offer better aesthetics and be less stigmatizing [27].

As far as the researcher’s awareness, only three motorized *exoskeletons* intended for daily use in people with DMD have been explored in the past. One of them is the Bridge [12, 18], which is position-controlled using a joystick. Position-controlled systems that make use of a joystick or predefined trajectories (e.g., using voice or GUI control) are considered less intuitive than force-based control methods that stimulate and utilize the patient’s residual muscle strength in a natural way. Such position-controlled approaches are more suitable for the higher disease stages where the muscle strength is further reduced (Brooke Scale  $\geq 5$ ) because they do not require residual muscle strength to move the arm.

Two projects, the Active A-Gear [28] and the Powered WREX [37], have explored force-based control; however, to the best of the authors’ knowledge, neither has advanced to the stage of testing with individuals with DMD. The Active A-Gear [28] is our predecessor from the FlexTension project. It motorizes the shoulder and elbow (4DOF) using admittance control and calculates the voluntary movement intention by subtracting the identified weight and pJump of the arm. From unpublished results, we know that the motors were not strong enough to support a relaxed human arm, making it unsuitable for testing

in individuals with DMD. The Powered WREX [37], combines the 4DOF passive WREX (JAECO Orthopedic, US) with two series elastic actuators (SEA), one at the shoulder and one at the elbow. This prototype uses an external force/torque (F/T) sensor to send a feed-forward torque amplification. To the authors' knowledge, this project has not been tested with human participants, nor has it been continued.

Moreover, two commercial products that have been announced are the Assist (AbiliTech, USA) and ExoArm (Focal Meditech Inc., The Netherlands), but are, from what is known, out of business or still under development.

## 1.4 Knowledge gap

The development of appropriate arm supports is challenging and complex because, within this target population, you deal with variations in residual muscle strength, pROM, pJimp, anthropometry, comorbidities, and user needs. A mismatch between the user needs and design realization can result in device abandonment. There are several reasons for device abandonment [40, 44, 47, 48], for instance, imprecise weight compensation, conspicuous aesthetic designs, the device size or weight (e.g., being stigmatizing [27] and unpractical), and practicalities such as too much hassle to don and doff, or interference with other activities [30]. The exact design requirements that match the user needs are still vaguely defined, some even unknown. This poses challenges and risks for commercial companies developing successful motorized arm supports, particularly because the Duchenne population is small, making financial profitability difficult.

Besides this, we face several technological challenges. Ideally, the arm support assists the arm in such a way that the user can still use its own residual muscle strength in an intuitive way, requiring an intuitive human-exoskeleton interaction (e.g., no use of a joystick or predefined trajectories). Concerning the intuitiveness of force-based control approaches, *impedance*-based control is assumed to be more intuitive than *admittance*-based since this is how people usually interact with objects in the environment. With an impedance control approach, the required support torques are determined on a joint level, where the orientation of the arm determines the level of support. Whereas, with an admittance-based controller, as used in the Active A-gear [28] and Power-Assist [33], a force-sensor is used to measure the movement intention and translate this to a movement of the arm. This has the disadvantage that the device is effectively blind to forces acting on the device, such as collisions with a table or the user's body. Moreover, poorly tuned admittance controllers can become unstable in interactions with users or objects in the environment [26], making it inherently more unsafe. This will not be the case with impedance control. None of the mentioned exoskeletons in the state-of-the-art utilized impedance control or tested this with individuals with DMD.

Additionally, the device is preferably not bulky or stigmatizing [27], but strong enough to lift the weight of the arm. Unlike with advanced prosthetics, where the limb is replaced by technology, orthotics or exoskeletons encompass the limb. This results in a high torque demand within a limited design space, requiring small but strong actuators. This makes it technologically challenging. A more accurate definition of the design requirements that match the user's needs, along with advancements in actuator technology, are the first steps toward the development of suitable motorized arm supports that will be accepted.

## 1.5 Research objective

This project aims to 1) define the design requirements for an assistive motorized arm support to assist individuals with severe muscle weakness (i.e., Brooke Scale 4) due to DMD in their daily activities. It further aims to 2) develop a method to estimate and compensate for weight and the stiffness component of pJimp by impedance control. Moreover, 3) design an investigational platform to evaluate those methods. Finally, this project aims to 4) verify the formulated design requirements.

## 1.6 Approach and outline

A pitfall in the biomedical engineering field may be to embrace a new technology before a suitable application for it arises. This approach might lead to developing solutions for non-existent problems or innovations that are not adopted by the intended user [42]. To avoid this, we followed the V-model concept for system development [35]. Figure 1.3 represents the stepped breakdown of the V-model, combined with the outline of this thesis. At each breakdown, the requirements need to be *verified* against the intended design requirements to ensure that what is built matches the design requirements. Eventually, the system as a whole, needs to be *validated* to ensure that what was intended truly matches the user needs on a higher system acceptance level. Here a clear distinction is made between *verification* (i.e., are we building the product right?), and *validation* (i.e., are we building the right product?). The outline of this thesis follows this development cycle.

The left side of the ‘V’ illustrates the project definition phase, which includes the decomposition of requirements and system specifications. The bottom and right sides of the ‘V’ represent the realization and test phase, integrating the parts and verifying the subsystems or module designs against the requirements.

This thesis is divided into three parts. Part I addresses the *user analysis*, considering the clinical characteristics of the target population, and translates these into functional and technical *design requirements* (Chapter 2). It also reviews methodologies for measuring the pJimp in individuals with DMD, an important yet relatively unknown characteristic of the target population (Chapter 3).

Part II compares different compensation strategies in an active elbow support as a *subsystem* of the overall arm support (Chapter 4) and in a potential add-on wrist support *module* (Chapter 5), both including *unit testing*.

Part III covers the *system testing* of the realized integration of the hardware and software components into a motorized arm support system that assists the elbow and shoulder joints. First, it presents the design of the verification tool, the Dummy Arm, used to verify the device’s performance. The Dummy Arm mimics the characteristics of a human arm (Chapter 6). Then, it presents the design of the Duchenne ARm Orthosis (DAROR) and compares two control strategies that are tested with our co-creator with DMD (Chapter 7), who was closely involved through multiple phases of the development cycle. With that, a first preliminary validation of the system’s *acceptance testing* was explored.

The discussion reflects on the lessons learned and proposes future directions.

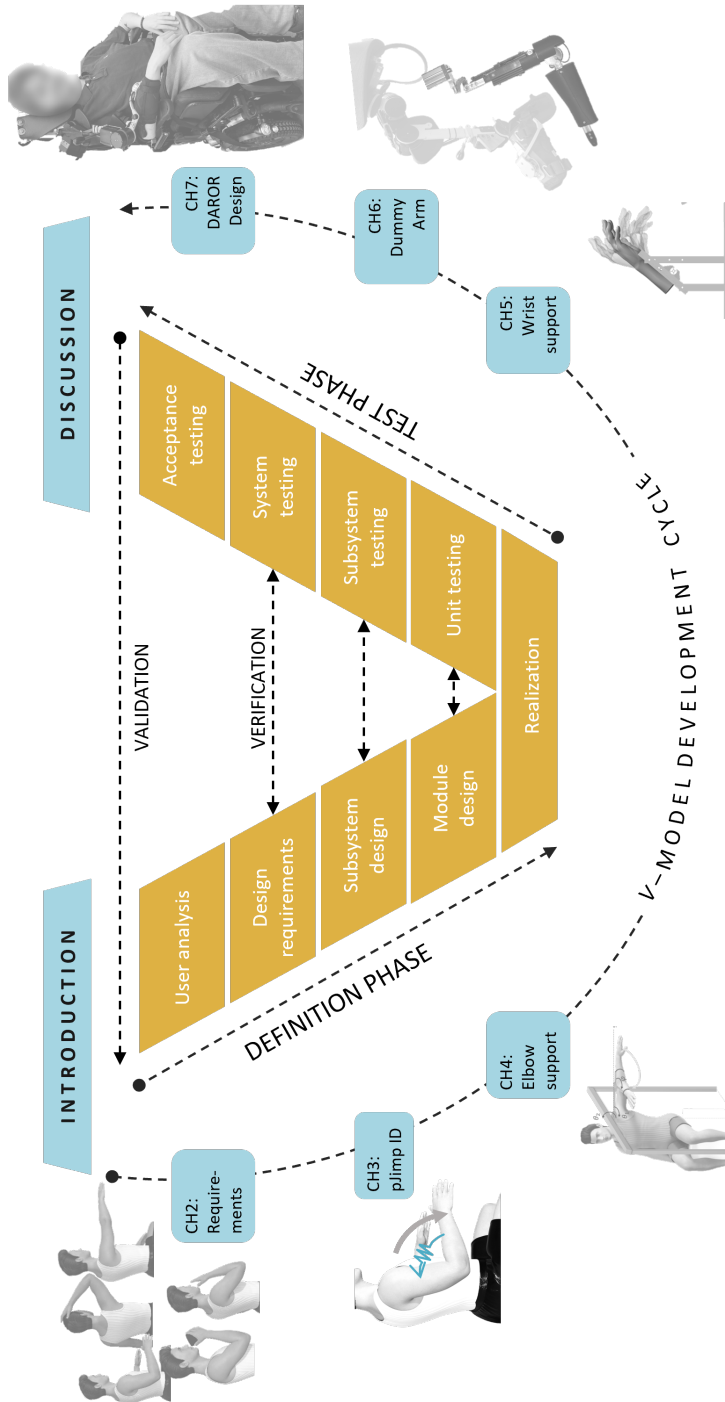


**Figure 1.3:** The outline of this thesis is represented using the V-model. Note: this V-model is adapted from [35].

## References

- [1] D. J. Birnkrant, K. Bushby, C. M. Bann, S. D. Apkon, A. Blackwell, D. Brumbaugh, L. E. Case, P. R. Clemens, S. Hadjiyannakis, S. Pandya, N. Street, J. Tomezsko, K. R. Wagner, L. M. Ward, and D. R. Weber. Diagnosis and management of Duchenne muscular dystrophy, part 1: diagnosis, and neuromuscular, rehabilitation, endocrine, and gastrointestinal and nutritional management, mar 2018.
- [2] D. J. Blake, A. Weir, S. E. Newey, and K. E. Davies. Function and genetics of dystrophin and dystrophin-related proteins in muscle. *Physiological Reviews*, 82(2):291–329, 2002. doi: 10.1152/physrev.00028.2001.
- [3] K. L. Boon, A. L. Hof, and W. Wallinga-de Jonge. The Mechanical Behaviour of the Passive Arm. *Medicine and Sport*, 8(Biomechanics III):243–248, 1973.
- [4] M. H. Brooke, R. C. Griggs, J. R. Mendell, G. M. Fenichel, J. B. Shumate, and R. J. Pellegrino. Clinical trial in Duchenne dystrophy. I. The design of the protocol. *Muscle & nerve*, 4(3):186–197, 1981. doi: 10.1002/mus.880040304.
- [5] K. Bushby, R. Finkel, D. J. Birnkrant, L. E. Case, P. R. Clemens, L. Cripe, A. Kaul, K. Kinnett, C. McDonald, S. Pandya, J. Poysky, F. Shapiro, J. Tomezsko, and C. Constantin. Diagnosis and management of Duchenne muscular dystrophy, part 1: diagnosis, and pharmacological and psychosocial management. *The Lancet Neurology*, 9(1):77–93, 2010. doi: 10.1016/S1474-4422(09)70271-6.
- [6] C. Cornu, F. Goubel, and M. Fardeau. Muscle and joint elastic properties during elbow flexion in Duchenne muscular dystrophy. *The Journal of Physiology*, 533(2):605–616, 2001. doi: 10.1111/j.1469-7793.2001.0605a.x.
- [7] M. C. Corrigan and R. A. Foulds. A Novel Approach to Increase Upper Extremity Active Range of Motion for Individuals with Duchenne Muscular Dystrophy Using Admittance Control: A Preliminary Study. In José González-Vargas, Jaime Ibáñez, Jose L Contreras-Vidal, Herman van der Kooij, and José Luis Pons, editors, *Wearable Robotics: Challenges and Trends*, pages 349–353, Cham, 2017. Springer International Publishing. doi: 10.1007/978-3-319-46532-6\_57.
- [8] M. C. Corrigan and R. A. Foulds. Evaluation of admittance control as an alternative to passive arm supports to increase upper extremity function for individuals with Duchenne muscular dystrophy. *Muscle and Nerve*, 61(6):692–701, 2020. doi: 10.1002/mus.26848.
- [9] M. C. Corrigan, B. Mathie, and R. A. Foulds. Translation of an upper extremity exoskeleton to home and community use for individuals with duchenne muscular dystrophy. *2017 International Symposium on Wearable Robotics and Rehabilitation, WeRob 2017*, pages 1–2, 2018. doi: 10.1109/WEROB.2017.8383820.
- [10] S. Crisafulli, J. Sultana, A. Fontana, F. Salvo, S. Messina, and G. Trifirò. Global epidemiology of Duchenne muscular dystrophy: An updated systematic review and meta-analysis. *Orphanet Journal of Rare Diseases*, 15(1), 2020. doi: 10.1186/s13023-020-01430-8.

- [11] A. Cruz, L. Callaway, M. Randall, and M. Ryan. Mobile arm supports in Duchenne muscular dystrophy: a pilot study of user experience and outcomes. *Disability and Rehabilitation: Assistive Technology*, 16(8):880–889, 2021. doi: 10.1080/17483107.2020.1749892.
- [12] S. Dalla Gasperina, M. Gandolla, A. Manti, L. Aquilante, V. Longatelli, M. G. D’Angelo, F. Molteni, E. Biffi, M. Rossini, M. Gfoehler, M. Puchinger, F. Braghin, and A. Pedrocchi. Upper-limb actuated exoskeleton for muscular dystrophy patients: Preliminary results. *Proceedings of the Annual International Conference of the IEEE Engineering in Medicine and Biology Society, EMBS*, pages 4431–4435, 2019. doi: 10.1109/EMBC.2019.8857725.
- [13] W. B. Drake and S. K. Charles. Passive stiffness of coupled wrist and forearm rotations. *Annals of Biomedical Engineering*, 42(9):1853–1866, 2014. doi: 10.1007/s10439-014-1054-0.
- [14] A. G. Dunning, M. M. H. P. Janssen, P. N. Kooren, and J. L. Herder. Evaluation of an arm support with trunk motion capability. *Journal of Medical Devices, Transactions of the ASME*, 10(4):1–4, 2016. doi: 10.1115/1.4034298.
- [15] A. E. Emery. The muscular dystrophies. *The Lancet*, 359(9307):687–695, feb 2002. doi: 10.1016/S0140-6736(02)07815-7.
- [16] J. M. Essers, A. Murgia, A. A. Peters, M. M. H. P. Janssen, and K. Meijer. Recommendations for studies on dynamic arm support devices in people with neuromuscular disorders: a scoping review with expert-based discussion. *Disability and Rehabilitation: Assistive Technology*, 0(0):1–14, 2020. doi: 10.1080/17483107.2020.1806937.
- [17] M. Gandolla, A. Antonietti, V. Longatelli, and A. Pedrocchi. The Effectiveness of Wearable Upper Limb Assistive Devices in Degenerative Neuromuscular Diseases: A Systematic Review and Meta-Analysis. *Frontiers in Bioengineering and Biotechnology*, 7(January):1–16, 2020. doi: 10.3389/fbioe.2019.00450.
- [18] M. Gandolla, S. Dalla Gasperina, V. Longatelli, A. Manti, L. Aquilante, M. G. D’Angelo, E. Biffi, E. Diella, F. Molteni, M. Rossini, M. Gföhler, M. Puchinger, M. Bocciolone, F. Braghin, and A. Pedrocchi. An assistive upper-limb exoskeleton controlled by multi-modal interfaces for severely impaired patients: development and experimental assessment. *Robotics and Autonomous Systems*, 143, 2021. doi: 10.1016/j.robot.2021.103822.
- [19] S. L. Houwen-Van Opstal, Y. M. Van Den Elzen, M. Jansen, M. A. Willemsen, E. H. Cup, and I. J. De Groot. Facilitators and Barriers to Wearing Hand Orthoses by Adults with Duchenne Muscular Dystrophy: A Mixed Methods Study Design. *Journal of Neuromuscular Diseases*, 7(4):467–475, 2020. doi: 10.3233/JND-200506.
- [20] M. Jansen, I. J. de Groot, N. van Alfen, and A. C. Geurts. Physical training in boys with Duchenne Muscular. *Biomed Central Pediatrics*, 10(55), aug 2010. doi: 10.1186/1471-2431-10-55.



- [21] M. Jansen, N. Van Alfen, A. C. Geurts, and I. J. De Groot. Assisted bicycle training delays functional deterioration in boys with Duchenne muscular dystrophy: The randomized controlled trial "no use is disuse". *Neurorehabilitation and Neural Repair*, 27(9):816–827, 2013. doi: 10.1177/1545968313496326.
- [22] M. M. H. P. Janssen, A. Bergsma, A. C. Geurts, and I. J. De Groot. Patterns of decline in upper limb function of boys and men with DMD: An international survey. *Journal of Neurology*, 261(7):1269–1288, 2014. doi: 10.1007/s00415-014-7316-9.
- [23] M. M. H. P. Janssen, J. Harlaar, B. Koopman, and I. J. M. de Groot. Dynamic arm study: Quantitative description of upper extremity function and activity of boys and men with duchenne muscular dystrophy. *Journal of NeuroEngineering and Rehabilitation*, 14(1):45, 2017. doi: 10.1186/s12984-017-0259-5.
- [24] M. M. H. P. Janssen, J. Horstik, P. Klap, and I. J. de Groot. Feasibility and effectiveness of a novel dynamic arm support in persons with spinal muscular atrophy and duchenne muscular dystrophy. *Journal of NeuroEngineering and Rehabilitation*, 18(1):1–13, 2021. doi: 10.1186/s12984-021-00868-6.
- [25] I. Y. Jung, J. H. Chae, S. K. Park, J. H. Kim, J. Y. Kim, S. J. Kim, and M. S. Bang. The correlation analysis of functional factors and age with Duchenne muscular dystrophy. *Annals of Rehabilitation Medicine*, 36(1):22–32, 2012. doi: 10.5535/arm.2012.36.1.22.
- [26] A. Q. Keemink, H. van der Kooij, and A. H. Stienen. Admittance control for physical human–robot interaction. *International Journal of Robotics Research*, 37(11):1421–1444, 2018. doi: 10.1177/0278364918768950.
- [27] P. N. Kooren, A. G. Dunning, M. M. H. P. Janssen, J. Lobo-Prat, B. F. Koopman, M. I. Paalman, I. J. De Groot, and J. L. Herder. Design and pilot validation of A-gear: A novel wearable dynamic arm support. *Journal of NeuroEngineering and Rehabilitation*, 12(1):1–12, 2015. doi: 10.1186/s12984-015-0072-y.
- [28] P. N. Kooren, J. Lobo-Prat, A. Q. Keemink, M. M. H. P. Janssen, A. H. Stienen, I. J. de Groot, M. I. Paalman, R. Verdaasdonk, and B. F. Koopman. Design and Control of the Active A-Gear: a Wearable 5 DOF Arm Exoskeleton for Adults with Duchenne Muscular Dystrophy. *6th IEEE RAS/EMBS International Conference on Biomedical Robotics and Biomechatronics (BioRob) June 26-29, 2016. UTown, Singapore, 2016-June (26-29):637–642, 2016. doi: 10.1109/BIOROB.2016.7523801.*
- [29] E. Landfeldt, R. Thompson, T. Sejersen, H. J. McMillan, J. Kirschner, and H. Lochmüller. Life expectancy at birth in Duchenne muscular dystrophy: a systematic review and meta-analysis. *European Journal of Epidemiology*, 35(7):643–653, 2020. doi: 10.1007/s10654-020-00613-8.
- [30] J. Lobo Pratt. *Control interfaces to actively support the arm function of men with Duchenne Muscular Dystrophy*. PhD thesis, University of Twente, 2016.
- [31] V. Longatelli, A. Antonietti, E. Biffi, E. Diella, M. G. D’Angelo, M. Rossini, F. Molteni, M. Bocciolone, A. Pedrocchi, and M. Gandolla. User-centred assistive SystEm

- for arm Functions in neUromuscuLar subjects (USEFUL): a randomized controlled study. *Journal of NeuroEngineering and Rehabilitation*, 18(1):1–17, 2021. doi: 10.1186/s12984-020-00794-z.
- [32] S. Maggioni, A. Melendez-Calderon, E. Van Asseldonk, V. Klamroth-Marganska, L. Lünenburger, R. Riener, and H. Van Der Kooij. Robot-aided assessment of lower extremity functions: A review. *Journal of NeuroEngineering and Rehabilitation*, 13(1):1–25, 2016. doi: 10.1186/s12984-016-0180-3.
- [33] B. Mathie, M. Grimm, J. Cavanaugh, R. Foulds, Z. Smith, and R. Smith. Restoration of Arm Mobility with Power-Assist Exoskeletons for Young Men with Duchenne Muscular Dystrophy. 2020.
- [34] C. M. McDonald, R. T. Abresch, G. T. Carter, W. M. J. Fowler, E. R. Johnson, D. D. Kilmer, and B. J. Sigford. Profiles of neuromuscular diseases. *American Journal of Physical Medicine and Rehabilitation*, 74(5 Suppl.):S70–92, 1995. doi: 10.1097/00002060-199509001-00003.
- [35] A. Oppermann. What Is the V-Model in Software Development? website, 2023. URL <https://builtin.com/software-engineering-perspectives/v-model>.
- [36] S. Poirier, F. Routhier, and A. Campeau-Lecours. Voice control interface prototype for assistive robots for people living with upper limb disabilities. *IEEE International Conference on Rehabilitation Robotics*, 2019-June:46–52, 2019. doi: 10.1109/ICORR.2019.8779524.
- [37] D. Ragonesi, S. Agrawal, W. Sample, and T. Rahman. Series elastic actuator control of a powered exoskeleton. *Proceedings of the Annual International Conference of the IEEE Engineering in Medicine and Biology Society, EMBS*, pages 3515–3518, 2011. doi: 10.1109/IEMBS.2011.6090583.
- [38] T. Rahman, R. Ramanathan, S. Stroud, W. Sample, R. Seliktar, W. Harwin, M. Alexander, and M. Scavina. Towards the control of a powered orthosis for people with muscular dystrophy. *Proceedings of the Institution of Mechanical Engineers, Part H: Journal of Engineering in Medicine*, 215(3):267–274, 2001. doi: 10.1243/0954411011535858.
- [39] P. T. Straathof, J. Lobo-Prat, F. Schilder, P. N. Kooren, M. I. Paalman, A. H. Stienen, and B. F. Koopman. Design and control of the A-Arm: An active planar arm support for adults with Duchenne muscular dystrophy. *Proceedings of the IEEE RAS and EMBS International Conference on Biomedical Robotics and Biomechatronics*, 2016-July: 1242–1247, 2016. doi: 10.1109/BIOROB.2016.7523801.
- [40] L. Tedesco Triccas, B. McLening, W. Hendrie, and G. Peryer. Is there a standard procedure for assessing and providing assistive devices for people with neuro-disabling conditions in United Kingdom? A nation-wide survey. *Disability and Health Journal*, 12(1):93–97, 2019. doi: 10.1016/j.dhjo.2018.08.003.
- [41] L. van der Heide. *Dynamic arm supports; matching user needs and preferences with technology*. PhD thesis, Maastricht Univeristy, 2017.

- [42] L. A. van der Heide, G. J. Gelderblom, and L. P. De Witte. Dynamic arm supports: Overview and categorization of dynamic arm supports for people with decreased arm function. *IEEE International Conference on Rehabilitation Robotics*, pages 1–6, 2013. doi: 10.1109/ICORR.2013.6650491.
- [43] L. A. Van Der Heide, B. Van Nijhuijs, A. Bergsma, G. J. Gelderblom, D. J. Van Der Pijl, and L. P. De Witte. An overview and categorization of dynamic arm supports for people with decreased arm function. *Prosthetics and Orthotics International*, 38(4): 287–302, 2014. doi: 10.1177/0309364613498538.
- [44] L. A. van der Heide, G. J. Gelderblom, and L. P. De Witte. Effects and effectiveness of dynamic arm supports: A technical review. *American Journal of Physical Medicine and Rehabilitation*, 94(1):44–62, 2015. doi: 10.1097/PHM.0000000000000107.
- [45] J. F. Wang, J. Forst, S. Schröder, and J. M. Schröder. Correlation of muscle fiber type measurements with clinical and molecular genetic data in Duchenne muscular dystrophy. *Neuromuscular Disorders*, 9(3):150–158, 1999. doi: 10.1016/S0960-8966(98)00114-X.
- [46] J. Weichbrodt, B. M. Eriksson, and A. K. Kroksmark. Evaluation of hand orthoses in Duchenne muscular dystrophy. *Disability and Rehabilitation*, 40(23):2824–2832, 2018. doi: 10.1080/09638288.2017.1347721.
- [47] R. Wessels, B. Dijcks, M. Soede, G. J. Gelderblom, and L. D. Witte. Non-use of provided assistive technology devices, a literature overview. 15:231–238, 2003.
- [48] R. D. Wessels, B. P. Dijcks, M. Soede, G. J. Gelderblom, and L. P. De Witte. Non-use of assistive technology in the Netherlands: A non-issue? *Disability and Rehabilitation: Assistive Technology*, 1(1-2):97–102, 2006. doi: 10.1080/09638280500167548.



# I

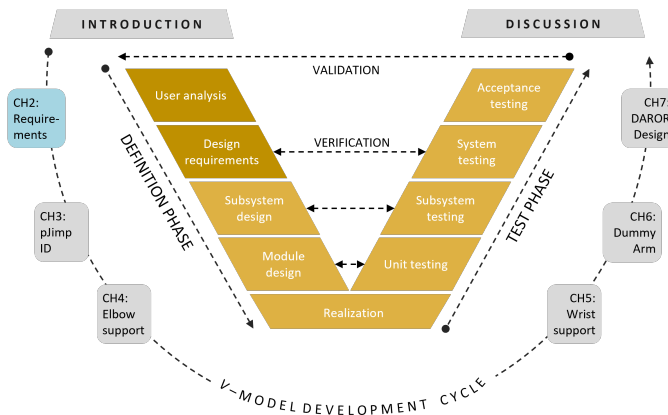
## User Analysis and Design Requirements



# 2

## Design Requirements of Arm Supports for Daily Use in DMD with Severe Muscle Weakness

Part I, will describe the left side of the V-model, the *user analysis* and *design requirements*.



This chapter further analyzes the clinical characteristics of the target population and formulates the functional and technical design requirements for an appropriate arm support that matches their needs. It reveals that some of the design requirements require further investigation. A more in-depth *user analysis* of a clinical characteristic of the population is further discussed in the next Chapter 3.

This chapter was published as:

Suzanne J Filius, Jaap Harlaar, Lonneke Alberts, Saskia Houwen-van Opstal, Herman van der Kooij, and Mariska MHP Janssen, 2024. Design requirements of upper extremity supports for daily use in Duchenne muscular dystrophy with severe muscle weakness. *Journal of Rehabilitation and Assistive Technologies Engineering* , 11:1-18, doi:10.1177/20556683241228478. Note: small adaptations are made in section titles.

## Design requirements of upper extremity supports for daily use in DMD with severe muscle weakness

**Abstract** People with Duchenne muscular dystrophy (DMD) cope with progressive muscular weakness and consequential upper extremity function loss. They benefit from arm supports, or arm exoskeletons, to assist arm function. Especially for severe muscle weakness (DMD  $\geq$  Brooke Scale 4), the design of such arm support is challenging. This study aims to structurally develop functional and technical design requirements of arm supports for people with DMD Brooke Scale 4. An overview of clinical characteristics and a classification of clinically meaningful activities were derived from data from the Dutch Dystrophinopathy Database and available literature. Based on these, functional and technical design requirements of arm supports were developed and matched to the achievable needs of the user. First, the clinical characteristics of the target population, such as strength, range of motion, and functional ability, are given. Next, clinically relevant activities of daily living are translated to functional requirements categorized in a ‘must’, ‘should’, and ‘could’ category. Last, the technical requirements to realize these functional goals are presented. The recommendations following from the functional user needs, technical requirements, and safety considerations can be used to make the development of assistive arm supports for people with DMD Brooke Scale 4 more user centered.

## 2.1 Introduction

### 2.1.1 Muscular Dystrophy affecting upper limb

Duchenne muscular dystrophy (DMD) is a progressive neuromuscular disease (NMD) caused by a dystrophin gene mutation that results in a lack of the dystrophin protein. An absence of dystrophin makes the muscle cells highly vulnerable to stress during muscle contraction [57]. As a result, the muscles of DMD patients weaken over time. DMD is often diagnosed around the age of 5 [6], and around the age of 10, DMD patients start using a wheelchair and cope with loss of upper extremity function [32]. At present, no cure has been found, but since 1960, life expectancy has increased from around 14 years to over 39 years due to medical interventions such as corticosteroid use and (eventually) mechanical ventilation [40]. Especially for wheelchair users, loss of upper extremity function has a great impact on their independence, social participation and quality of life [33, 46, 47]. Since the timespan that DMD patients make use of a wheelchair becomes longer, it becomes more important to focus on possibilities to support functions of the upper extremity.



### 2.1.2 Intended target population

Figure 2.1 summarizes the general characteristics of DMD patients per Brooke Scale [4] to highlight how the selected population fits within the spectrum of DMD. In this paper, we will specifically focus on patients within Brooke Scale 4 (i.e., “can raise hands to the mouth, but cannot raise an 8 oz [ $\sim 230$ g] glass of water to the mouth” [4, p.193]). This population is often in the late non-ambulatory stage [6]. About 4-10% of the DMD patients have an upper extremity classification of Brooke Scale 4 [9, 24, 28, 31, 34, 48, 68], over 25,000 patients worldwide. We focused on this population since these patients are often too weak to use a non-motorized arm support [47]. However, external robotic manipulators are not intuitive and potentially worsen disease progression by taking over the execution of tasks completely, contributing to disuse. These specific functional needs contribute to the lack of arm support availability for this population. This will be further discussed in the next section.

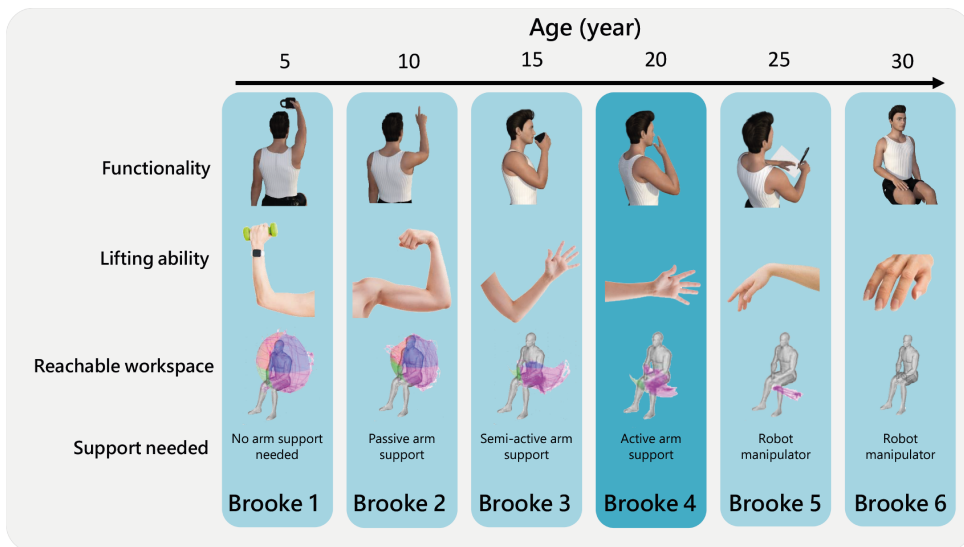


**Figure 2.1:** Summary of the functional user characteristics classes per Brooke Scale. Range of motion images are retrieved and adapted from [24, 25]. Functionality models were retrieved from DAZ Productions[76]. Lifting ability figures were retrieved from Internet [vecteezy.com; pexels.com; splash.com].

### 2.1.3 Availability of arm supports

Compensation for the weight of the arms can reduce the net joint moments to perform activities of daily living (ADL) to benefit people with arm disabilities [18]. Over the past century, many attempts have been made to design supportive devices for people with arm disabilities [33, 73]. Currently, passive (i.e., non-motorized weight support through springs or counterweights) and semi-active (i.e., passive weight support with motorized adjustment) systems are commercially available.

A major functional limitation of passive systems is that they do not support the weight of the arms over the entire workspace equally. The level of support determined by device provision is often set to function well in the frontal and horizontal workspace. As the disease progresses, it becomes too difficult to raise the arms above the head, lift objects [59], and perform downward movements with passive arm supports [37, 47]. Semi-active systems allow the users to adapt the support level for the required workspace by using a button with the contralateral arm [47], making the interaction cumbersome.

Besides passive and semi-passive arm support systems, external robotic manipulators are commercially available. These are active systems controlled by a joystick for endpoint control of the manipulator that overtakes the function of the human arm. These devices interact directly with the objects in the environment without the human arm. Robotic manipulators might be a solution when no or very limited passive range of motion (pROM) is left (e.g., due to shortened muscle and joint contractures), often seen in higher disease stages (Brooke  $\geq 5$ ). However, it has been shown that physical arm training slows down the progression and prevents contractures that may develop from disuse [30]. So, as long as the pROM is sufficient, it is essential to keep the arm muscles involved and provide assistance as needed.

Unfortunately, the authors are unaware of commercially available systems appropriate for the severe disease stages, i.e., Brooke Scale 4 in DMD, encompassing and involving the human arm in motion. Therefore, there remains a need for dedicated assistive arm support to be developed, with specific functional and technical design requirements. These requirements should be based on the clinical characteristics of people with DMD classified in Brooke Scale 4, focusing on the most meaningful and feasible upper extremity tasks.

### 2.1.4 Aim

This paper aims to develop functional and technical arm support design requirements for people with DMD classified in Brooke Scale 4.

## 2.2 Method

The data presented in this study are based on PubMed prior to October 2022, reference snowballing and data from the Dutch Dystrophinopathy Database (DDD).

### 2.2.1 Data collection

The DDD is a national register for Duchenne and Becker muscular dystrophy patients in the Netherlands. The database contains natural history data collected from annual clinical care assessments. In the database, 39 DMD patients with Brooke Scale 4 are included. Access to this database was granted by the Duchenne Center Netherlands (DCN), a collaboration between the Leiden University Medical Center (LUMC), the Radboud University Medical Center (Radboudumc), Kempenhaeghe-MUMC+, the Duchenne Parent Project (DPP) patient organization and 'Spierziekte Nederland' (SN) patient association. We requested data for muscle strength, range of motion (ROM), and performance of upper limb (PUL) scores.

### 2.2.2 Literature search

For the characteristics of the intended target population and the functional requirements, literature was mainly searched using a combination of the terms (or their synonyms) DMD, upper extremity, muscle force/torque, active range of motion (aROM) and pROM, joint impedance, reachable workspace, and PUL. Only papers in which patients with Brooke Scale 4 participated or where it could be determined what data corresponded with patients in Brooke Scale 4 were included. More literature has been published on these characteristics in DMD. Yet, in several papers, the clinical characteristics of the patients are not categorized per Brooke Scale but based on age or other functional scales. For the literature search of the technical requirements, additional search terms were added: ADL, angular velocities, arm support and its accompanying synonyms (e.g., exo- skeleton, assistive device, dynamic arm supports, orthosis). Also motorized upper extremity arm supports for ADL used in different pathologies (e.g., stroke, incomplete spinal cord injury) were included. Not all data we found in the literature could directly be used for our results. Therefore, we used additional literature and made several assumptions to interpret the data. For example, literature-based assumptions on anthropometrics and body weight were used for recalculating forces to joint torques or to estimate arm segment weights.

### 2.2.3 Functional requirements and arm model definitions

To state the functional requirements, the ADLs that are identified as clinically meaningful for DMD (i.e., high-level functional requirements) were first categorized into a ‘must’, ‘should’, and ‘could’ category based on an estimated required strength and workspace score. Next, we dissected these activities into ‘low-level functional requirements’ (i.e., ROM, velocity, and support level) by brief analyses of the required ROM and support level. For the support level analysis, a custom kinematic rigid body model of the arm was created to estimate the internal shoulder and elbow joint moments for a set of ADL poses. The segment parameters used for this kinematic model were taken from [74].

**Arm model** The custom kinematic rigid body arm model followed the ISB recommendations [15, 77] with adaptations of Stienen and Keemink [72] to define the joint rotations of the arm. Within these definitions the wrist joint is approximated by three axes of rotation (sequence flexion/extension, ulnar/ radial deviation, pronation/supination), the elbow joint is approximated by a hinge joint (flexion/extension) and the shoulder joint as ball-and-socket joint relative to the thorax [15] with three axes of rotation (sequence horizontal rotation, elevation rotation, axial rotation). Where *horizontal* rotation, also referred to as ‘(angle of) plane of elevation’, is the rotation around the y-axis fixed to the thorax coordinate system, *elevation* is the rotation around the x-axis fixed to the humerus coordinate system. *Axial* rotation is the rotation around the y-axis fixed to the humerus coordinate system, see Figure 2.2.

In literature, the classical medical definition (i.e., shoulder ab-/adduction, flexion/extension, internal-external rotation) is often used. For the ROM analysis, we translated, when possible, the medical definition into the ISB recommendations.

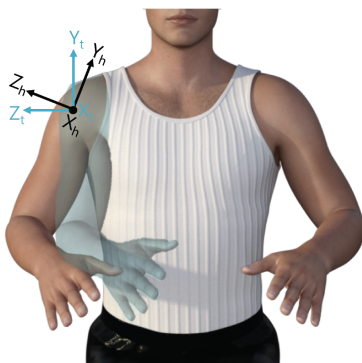


**Figure 2.2:** Representation of the thorax (t) and humerus (h) coordinate systems according to the ISB recommendations [77]. The x-axis points outwards of the paper. The human model shows elevation rotation in the frontal plane around  $x_h$  with respect to the thorax coordinate system [72]

## 2.3 Results

### 2.3.1 Characteristics of the intended target population

This part of the paper overviews the patient characteristics commonly described in DMD patients with Brooke Scale 4. Table 2.1 describes data on upper extremity muscle strength, ROM and the functional ability of this population. The average age of the DMD patients with Brooke Scale 4 within this overview is approximately 15 years (5 – 29 years).

#### 2.3.1.1 Muscle strength

When designing an arm support, it is essential to know how much joint torque patients can provide to a varying degree. We found three sources that described the muscle strength of in total eight patients in Brooke Scale 4 (see Table 2.1). Different methods were used to measure muscle strength. Unfortunately, in most sources, only force and no joint torques were reported. [5] and [32] used a fixed-frame dynamometer to measure strength, while a hand-held dynamometer was used in the DDD.

To relate the reported joint forces to joint torques and healthy reference values, we translated the forces measured with a dynamometer to torques using an average forearm length of 26.5 cm and a combined upper arm and forearm length of 60.6 cm [17, 74]. On average, elbow flexion strength varied between 3 N and 18 N, which relates to estimated torque values between .8 and 4.8 Nm, about 2% – 10% of the torques measured in a healthy reference population [27]. Elbow extension strength varied between 3 N and 25 N (i.e., .8 – 6.6 Nm), about 3% – 22% of the torques measured in a reference population. Shoulder abduction strength varied between 3 N and 15 N (i.e., 1.8 – 9.1 Nm), about 4% – 184% of the torques measured in the healthy reference population.

The elbow flexion strength is barely sufficient for lifting the weight of the forearm and hand, which is about 2.5% body weight [26], approximately 15.9 N, and shoulder abduction strength is not sufficient to lift the entire arm, which is about 5.5% body weight, [26] approximately 35.1 N with an estimated body weight of 65 kg [1].

**Table 2.1:** Characteristics of DMD patients in Brooke Scale 4 (B4).

Author	Nr. DMD B4	Outcome as Average (reported measure on data variability)
<i>Muscle strength<sup>a</sup></i>		
Brussock et al. [5]	1	Shoulder abduction <sup>b</sup> : R = 2.9 N, L = 3.4 N Elbow flexion: R = 2.9 N, L = 2.9 N Elbow extension: R = 2.9 N, L = 2.9 N
Janssen et al. [32]	3	Shoulder abduction: R = 15 N (95% CI 3; 26 N), 5.6 Nm (95% CI 4.9; 6.2 Nm) Elbow flexion: R = 7 N (95% CI -3; 17), 1.7 Nm (95% CI -1.2; 4.5 Nm) Elbow extension: R = 8 N (95% CI 2; 14), 1.8 Nm (95% CI -0.4; 4.0 Nm)
Dutch Duchenne Database	4	Shoulder abduction: R = 5.1 N (range 0-10.5 N) Elbow flexion: R = 18.1 N (range 9.3; 35.3 N) Elbow extension: R = 25.4 N (range 17.3-41.2 N)
<i>pROM</i>		
Dutch Duchenne Database	36	Shoulder flexion <sup>b</sup> : R = 150°(range 70; 180), L = 146°(range 70; 180) Shoulder abduction: R = 145°(range 70; 180), L = 145°(range 70; 180) Elbow flexion: R = 141°(range 120; 150), L = 142°(range 110; 155) Elbow extension <sup>c</sup> : R = 23°(range -20; 85), L = 27°(range -20; 90)
Janssen et al. [32]	3	Shoulder abduction: R = 128°(95% CI 97°; 160°) Elbow flexion: R = 135°(95% CI 124°; 155°) Elbow extension <sup>c</sup> : R = 50°(95% CI -45°; 146°)
<i>aROM</i>		
Janssen et al. [32]	3	Shoulder abduction: R = 0°(95% CI 0°; 0°) Elbow flexion (against gravity): R = 110°(95% CI 16°; 204°) Elbow extension <sup>c</sup> : R = 40°(95% CI -24°; 104°)
<i>Reachable workspace (RSA<sup>c</sup>)</i>		
Han et al. [24]	4	RSA right and left = 0.90 (SD 0.06 I)
Corrigan and Foulds [13]	5	RSA right = 0.0858 (range 0.025; 0.165) RSA left = 0.0226 (range 0.011; 0.037)
Janssen et al. [33]	1	RSA right = 0.2 RSA left = 0.17
<i>PUL (1.2)<sup>e</sup>[% of max]</i>		
Gandolla et al. [20]	4	PUL total = 56% (range 46; 64%) PUL shoulder dimension = 0% (range 0; 0%) PUL elbow dimension = 59% (range 38; 71%) PUL wrist and finger dimension = 91% (range 88; 96%)

Author	Nr. DMD B4	Outcome as Average (reported measure on data variability)
Janssen et al. [32]	3	PUL total = 43% (95% CI 28; 58%) PUL shoulder dimension = 0% (95% CI 0; 0%) PUL elbow dimension = 29% (95% CI 12; 44%) PUL wrist and finger dimension = 83% (95% CI 63; 108%)
<i>PUL (2.0)<sup>e</sup> % of max</i>		
Pane et al. [55]	28 <sup>f</sup>	PUL total = 36% PUL shoulder dimension = 0% PUL elbow dimension = 29% PUL wrist and finger dimension = 77%
Janssen et al. [33]	1	PUL shoulder dimension = 6% PUL elbow dimension = 65%
Cruz et al. [14]	4 <sup>g</sup>	PUL total = 36% (range 29; 45%) PUL shoulder dimension = 0% (range 0; 0%) PUL elbow dimension = 29% (range 12; 41%) PUL wrist and finger dimension = 77% (range 69; 92%)
Dutch Database	21	PUL total = 38% (range 29; 50%) PUL shoulder dimension = 0% (range 0; 0%) PUL elbow dimension = 35% (range 18; 53%) PUL wrist and finger dimension = 77% (range 69; 92%)

<sup>a</sup>Muscle strength values consist of both force and torque, depending on the data collection or reporting method. If handheld dynamometry is used, force (N) is often reported while torque is measured. Moment arms, however, are usually not reported.

<sup>b</sup>Where shoulder abduction in the classical medical definition is defined as elevation rotation with 0° horizontal rotation, and shoulder flexion is defined as elevation rotation with 90° horizontal rotation.

<sup>c</sup>Note that a positive value for elbow extension means that there is no full elbow extension, see Figure 4.

<sup>d</sup>The Relative Surface Area (RSA) ranges between 0.0 and 1.0, where 1.0 corresponds to the reachable workspace envelope of the entire frontal hemisphere the subject reached.

<sup>e</sup>PUL refers to the Performance of Upper Limb scale, a functional scale to measure upper extremity function [20]. There are two versions of this scale. The PUL 1.2 has a maximum score of 74 (16 for shoulder dimension, 34 for elbow dimension and 24 for wrist and finger dimension), The PUL 2.0 has a maximum score of 42 (12 for shoulder dimension, 17 for elbow dimension and 13 for wrist and finger dimension).

<sup>f</sup>Number of participants is based on both Brooke Scale 3 and 4, so number of participants with solely Brooke Scale 4 is not available. The data presented, however, is only from patients with Brooke Scale 4. No data on variability between subjects is available.

<sup>g</sup>Not clear if Brooke Scale 4 and 5 were included or Brooke Scale 4 alone.

### 2.3.1.2 Range of motion

The pROM in shoulder abduction (elevation rotation in the frontal plane) is around 130°, which is about 30° less than in the reference population [21]. Elbow flexion of DMD patients with Brooke Scale 4 is about 130°, compared to 150° in the reference population [70]. Elbow extension is most limited in DMD patients. On average, DMD patients show a passive elbow extension of 30° of flexion, compared to the reference population who can, on average (hyper)extend the elbow about -5° of extension [70]. Note that different methods for measuring ROM were used. Janssen et al. [32] used 3D motion analysis to determine the aROM and pROM, while DDD used goniometry to determine pROM.

Regarding aROM, no movement is possible at the shoulder level, and for the elbow, the aROM was similar to the pROM. The limited aROM can also be observed when looking at the reachable workspace. With a relative surface area (RSA) of .02 to .2, almost no shoulder movement is observed (a value of 1.0 corresponds to the envelope of the entire frontal hemisphere that the subject can reach).

### 2.3.1.3 Functional ability

Functional ability of the arms in DMD patients is usually measured with the PUL scale [52], see footnote<sup>e</sup> Table 2.1. Table 2.1 shows that DMD patients in Brooke Scale 4 have no function left in the shoulder dimension. The scores in the elbow dimension are about 30% of the maximal possible score and only minor functional limitations are seen in the wrist and finger dimension.

### 2.3.1.4 Joint impedance

In DMD patients, the joint impedance, often referred to in the clinical field as muscle or joint stiffness, is elevated compared to the healthy reference population [11, 43, 60]. At some point in time during the progression of the disease, the muscle strength becomes too low to overcome the elevated joint impedance in an extensive range of the functional workspace [11, 43, 45].

The term joint impedance describes all the mechanisms in the joint that contribute to the resistance of motion [39, 42, 50], including all motion-dependent effects such as stiffness or non-elastic forces (i.e., pose dependent), viscosity or damping (i.e., velocity dependent), and inertia (i.e., acceleration dependent) [50]. Joint impedance results from passive components (i.e., biomechanical properties such as tendons, tissue, and inertia) and active components (i.e., muscle reflexes or neural-driven contractions) [50]. The elevated joint impedance experienced in DMD presumably results from the passive components, such as shortened muscles, high levels of connective tissue, and joint contractures majorly developed by disuse and fibrosis.

Lobo-Prat et al. [43], Ragonesi et al. [60] identified the combined passive joint moments (e.g., weight and passive joint impedance components) in NMD patients for arm support applications. Lobo-Prat et al. [43] showed a great improvement in the vertical and horizontal workspace with passive joint impedance compensation with respect to solo weight compensation in a DMD patient (Brooke Scale not mentioned). Especially in combination with the low muscle strength in DMD, this passive joint impedance becomes an important factor to consider when developing the control of an arm support.

Three other studies [11, 31, 39] report an increased (experienced) joint stiffness in DMD determined with varying methods. According to the results of [11] the mean total joint stiffness is ~ 20 times higher in DMD (Brooke Scale not specified, age range 9 – 21 years) than that of healthy children. Measured during fast (4 – 12 Hz) sinusoidal perturbations (3°) to the right elbow during an active task (35% – 75% maximally voluntary contraction). They state that the total joint stiffness increases exponentially with disease progression [11]. Moreover, [39] concluded that the index of muscle stiffness, measured by shear wave elastography using ultrasound, was significantly higher (up to 136%) in DMD patients (Brooke Scale not specified, age range 8 – 23 years) compared to healthy controls. Moreover, [31] found that the experienced stiffness increases throughout the stages of DMD with a



substantial increase in the late non-ambulatory stage, which includes DMD patients with Brooke Scale 4.

The results indicate that joint impedance increases over disease progression in DMD and that the passive joint impedance is a relevant component to consider in arm support compensation strategies.

### 2.3.1.5 Anthropometry

The intended target population's body dimensions might deviate from the healthy reference population and should be considered when developing an arm support. DMD patients are prone to have a higher body mass index (BMI) and be overweight or obese [29, 61]. In addition, it is known that children with DMD exhibit a different growth pattern and are typically smaller than the healthy reference population [53, 65]. Deviating sizes are expected for the arm length, arm circumference and shoulder width. Besides the fitting, this might influence the position of the center of mass (COM), affecting kinematic arm models.

### 2.3.1.6 Comorbidities and medication

Regarding the design of an arm support, important comorbidities should be considered. Scoliosis (an aberrant curvature of the spine) is common in DMD patients. Scoliosis leads to a skewed posture and a worse sitting balance; this might influence both the fitting and the effectiveness of an arm support. In addition, DMD patients have decreased bone mineral density, which commonly leads to fractures [75], so high loads exerted on the bones should be avoided. Finally, based on clinical observation, it is important to take the occurrence of shoulder subluxations into account, by limiting extreme shoulder ROM.

Another factor that should be considered is medication use (i.e., corticosteroids). Many DMD patients use an intermittent corticosteroid regime (10 days on and then 10 days off). Although this has not been studied, patients anecdotally report more functional difficulties and muscle weakness during the 10-day off period. These variations should be taken into account when developing the control and level of support of an arm support.

## 2.3.2 Functional requirements

### 2.3.2.1 Prioritizing activities of daily living

The DMD Upper Limb Patient-Reported Outcome Measure (DMD UL PROM), not to be confused with pROM ('passive range of motion'), is an outcome measure used in DMD to track upper limb function decline in ADL. It includes activities that are identified as meaningful in the daily lives of people with DMD and impact their quality of life [36].

We used the DMD UL PROM to define the high-level functional requirements. Authors SF and MJ ranked the DMD UL PROM activities on the required workspace and required strength needed to perform the activity, according to the scores presented in Table 2.2.

Next, we classified these activities into a 'must', 'could' and 'should' category, see Figure 2.3. Where 'must' defines the requirements necessary for arm supports to assist the most feasible ADL. 'Should' describes the recommendable requirements that would increase the usability to gain function in the less feasible but important ADL, potentially to



**Table 2.2:** Workspace and strength scores

	Score	Workspace (cm)	Strength (g)	Category
1		Small movements in horizontal plane (< 10)	Hand movement with finger pressure < 50	Must
2		Large movements in horizontal plane (> 10)	Forearm movement no/weight < 50	Must
3		Movement in sagittal plane close to body	Forearm movement with weight < 100	Must
4		Movement in sagittal plane far from body	Entire arm no/weight < 50 or forearm with weight < 200	Should
5		Movements that require trunk movement	Entire arm with weight < 100 or forearm with weight > 200	Could
6	-		Entire arm with trunk no/weight < 200	Could
7	-		Entire arm with trunk with weight > 200	Could

the drawback of increased complexity and bulkiness of the device. Where ‘could’ describe the nice-to-haves but hard to realize functional ADL gains.

According to our categorization based on the workspace and strength scores, activities with movements in the horizontal plane, such as tabletop activities and movements close to the body in the sagittal plane while lifting small objects (<100 g), fall under the ‘must’ category. Reaching movements, such as pressing an elevator button or putting on a light switch, which require lifting the entire arm in the sagittal plane far from the body or lifting the lower arm with medium weight (<200 g), fall under the ‘should’ category. Finally, arm movements that require high forces to lift heavy weight (>200 g), manipulate objects (i.e., open a can, open a door, or drawer), or require trunk movements (i.e., picking up pen from floor) fall under the ‘could’ category.

### 2.3.2.2 Range of motion

For the ROM analysis, we looked into studies that analyzed the required ROM for daily activities. We searched for the activities of the DMD UL PROM items and presented the largest ROM required for the ‘must’ and ‘should’ categories, see Figure 2.4. Since the activities in the ‘could’ category were hardly reported in the literature, the found values gave an underrepresentation of the actual ROM needed in the ‘could’ category. Moreover, the required trunk movements were not reported, and therefore, the ‘could’ category was excluded from this analysis.

### 2.3.2.3 Velocity

Limited literature was found on movement velocities for the DMD UL PROM activities. Two studies were identified that reported the angular joint velocity during ADL in the healthy reference population. According to Rosen et al. [64] the upper extremity movement velocities measured in four activities (i.e., arm reach to head level, move object at waist level, pick up phone on wall/hang up, and eat with spoon) ranged between -141 and 172°/s

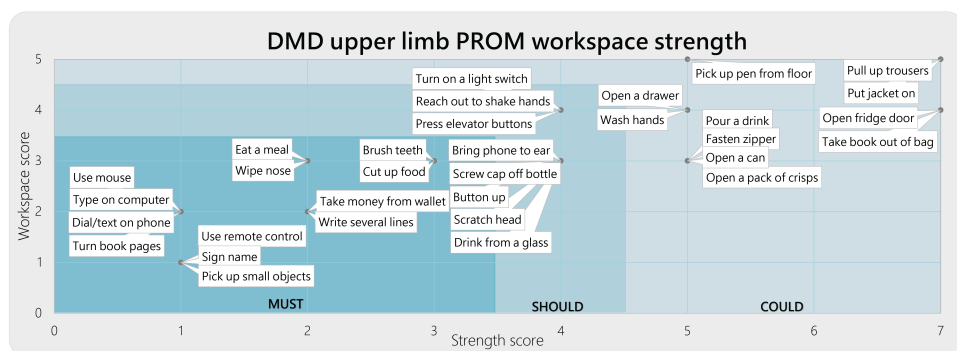


**Figure 2.3:** Classification of DMD UL PROM activities in the functional must, should, could requirement categories.

for the shoulder joint, and  $-172$  and  $145^\circ/\text{s}$  for the elbow joint. The mean velocity over the four activities was  $\pm 85^\circ/\text{s}$  for the shoulder, and  $\pm 93^\circ/\text{s}$  for the elbow joint. Karner et al. [35] report the average and peak angular velocity over four ADL (e.g., combing hair, drinking from bottle with straw, interacting with own body, and move other hand). They found  $101^\circ/\text{s}$  (peak  $228^\circ/\text{s}$ ) for the elevation rotation,  $34^\circ/\text{s}$  (peak  $82^\circ/\text{s}$ ) for horizontal rotation,  $83^\circ/\text{s}$  (peak  $134^\circ/\text{s}$ ) for axial rotation and  $98^\circ/\text{s}$  (peak  $181^\circ/\text{s}$ ) for elbow flexion.

More research is required on the movement velocity to determine the functional requirements in a ‘must,’ ‘should’ and ‘could’ categorization. We think it is more important to give back independent task execution at an albeit lower but stable and predictable movement velocity than moving fast on a natural arm velocity equal to the healthy reference population. Moreover, too quickly might feel unsafe, but too slowly may lead to frustration.

### 2.3.2.4 Support level

The required support levels need to be known to be able to choose the appropriate actuation (e.g., type, size and power). The results of the simplified analysis to estimate the static kinematic joint moments of the human shoulder and elbow joint required in movements of the ‘must,’ ‘should’ and ‘could’ categories are displayed in Table 2.3. We looked at a tabletop and feeding activity for the ‘must’ category. When taking the maximum values, an internal joint torque of approximately 2 Nm is generated in the elbow and 5 Nm in the shoulder joint (elevation rotation). For the ‘should’ category, we looked into a ‘reaching at top of head level,’ ‘bring an object (<200 g) to head level’ and ‘reaching at shoulder level’ pose. Approximately -2 Nm (extension moment) is generated with the elbow and 11 Nm with the shoulder joint (elevation rotation). For the ‘could’ category, approximately 3 Nm with the elbow and 13 Nm with the shoulder joint is required to ‘reach at shoulder level while holding an object (200 g)’. This activity is meant to correspond to ‘wash hands,’ ‘open drawer’ or ‘open fridge door’. The other DMD UL PROM activities in the could category, such as ‘pick pen from floor,’ ‘take book out of bag,’ and ‘put jacket on,’ require a substantial trunk inclination angle, which was not considered for this analysis.

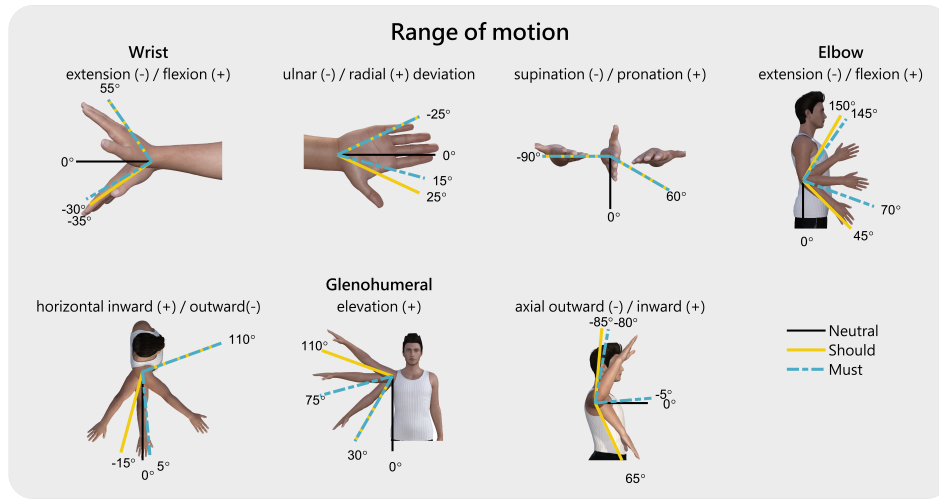








**Figure 2.4:** Indication of the range of motion of the wrist, elbow and glenohumeral joints required for the must and should categories. Note: The data in this figure is based on the ADL activities included in the DMD UL PROM items [2, 63], including: (*must*) turn book pages, eat a meal, wipe nose, brush teeth; (*should*), drink from a glass, bring phone to ear, scratch head, button up, press elevator buttons, turn on a light switch, reach out to shake hands. The values are rounded to 5°.

These joint moments are in accordance with the findings of Karner et al. [35]. However, it should be noted that the numbers presented here are only rough estimations to indicate the required support level. These calculations are based on static poses of a dynamic movement, so the moments of inertia are not taken into account. However, considering the relatively low speeds and angular accelerations, the expected relative contribution is fairly limited. Additionally, the weight of the device is not considered since this depends on the technology but should be considered when choosing the appropriate (actuation) technology. Furthermore, the additional joint moments required to overcome the (elevated) passive joint impedance must be considered. Lobo-Prat et al. [43], Ragonesi et al. [60] concluded that passive joint impedance is a relevant component and that the arm dynamics cannot be modelled by a simplified gravitational kinematic model alone. For proper compensation of the passive joint impedance, it is essential to know its behavior over the pROM among DMD Brooke Scale 4, either generalized or personalized. Unfortunately, these studies Lobo-Prat et al. [43], Ragonesi et al. [60] do not provide enough quantitative data on the level and behavior of the passive joint impedance and are therefore not included to define the required support level.

### 2.3.3 Technical requirements

The technical requirements are divided into four categories: *mechanical structure*, *actuator technology*, *control approach*, and *human interface*. The requirements are expressed in Table 2.4. Each category is subdivided into ‘performance’ and ‘safety’. Supplementary details to the table are given below.

**Table 2.3:** SEA joint moments in ADL poses (Nm)

Activity	Must		Could		Should	
	Tabletop activities	Feeding activities (50g)	Reach top head	Bring object (200g) to head	Reach shoulder level	Reach at shoulder height with object (200g)
						
Elbow	2.3	1.1	-1.8	-0.3	-	3.1
Shoulder						
Horizontal	-	-	-	-	-	-
Elevation	3.2	5.4	6.2	7.4	11.2	12.5
Axial	0.8	1.3	1.2	2.2	-	-

Model representing activities retrieved from DAZ Productions [76].

**Table 2.4:** Technical requirements.

Requirement	Should/Could	Must	Source
<b>Mechanical structure</b>			
<i>Performance</i>			
Anatomy	Follow the human anatomical structure <sup>1</sup>	Allow 3D motion in shoulder and elbow joint	<sup>1</sup> [16, 19]
DOF	<ul style="list-style-type: none"> <li>· Could: Allow trunk movements<sup>1</sup></li> <li>· 5 DOF (e.g., glenohumeral horizontal, elevation, axial rotation, elbow extension/flexion and forearm supi-/pronation)</li> <li>· Include (passive) dynamic wrist support</li> </ul>	<ul style="list-style-type: none"> <li>· 4 DOF (no glenohumeral axial rotation or forearm supi-/pronation)</li> <li>· Include static passive wrist at rest position</li> </ul>	<sup>1</sup> [14, 16, 19, 23]
Singularity	Prevent singularity by design e.g.: 1) configure singularity outside the movement range, 2) use redundant linkages, or 3) optimize the length of the linkages	Solve for singularity (e.g., by end-stops, control limits)	[7, 56]
Joint alignment	<ul style="list-style-type: none"> <li>· Misalignment &lt; 3.5<sup>1</sup></li> <li>· Implementation of a form of passive or active misalignment adaptation (i.e., self-aligning joints)<sup>1,2</sup></li> </ul>	<ul style="list-style-type: none"> <li>· Misalignment &lt; 10 cm</li> <li><i>Note:</i> 10 cm joint misalignment can result in high interaction torques (&lt; ±1.46 Nm) or forces (&lt; ±230 N)<sup>3</sup></li> </ul>	<sup>1</sup> [54] <sup>2</sup> [78] <sup>3</sup> [66]
Fitting	Adjustable fitting for 95% of intended target population, e.g., fully adjustable to (upper) arm length, circumference, shoulder width, hunchback angle	Use of multiple sized components, e.g., small, medium, large	

**Table 2.4** (Continued)

Requirement	Should/Could	Must	Source
Obtrusiveness	<ul style="list-style-type: none"> <li>·Not wider than an electric wheelchair (<math>\pm 700 \times 1500</math> mm)</li> <li>·No voluminous components at radial or ulnar side of forearm and frontal side of the upper arm</li> </ul>	<ul style="list-style-type: none"> <li>·Passes through doorway</li> <li>·No hinder in arm relaxation, e.g., clash with tabletop</li> </ul>	[19]
Outdoor use	Device protected from rain and dust (IP66) and robust to oscillations and collisions to environment	Usable inside and robust to oscillations and collisions to environment	[41]
<i>Safety</i>			
Angle limits	Personalized hardware end-stops to limit device ROM to user pROM	Device should not exceed pROM of user	
Sharp edges, skin pinching, hair entanglement	No scissor mechanisms or pinch points by design, and protection of rotating parts	No sharp edges, mitigation measures to prevent risk of pinched skin or hair entanglement	
<b>Actuator technology</b>			
<i>Performance</i>			
Maximum motor torque	20 Nm	$> 10 \text{ Nm}^1$ Note: Up to 12.5 Nm required for human arm in ADL <sup>2</sup> , additional torques are required to move the device itself.	<sup>1</sup> [54] <sup>2</sup> Table 2.3
Motor torque bandwidth	100 Hz	40 Hz	[54]
Delivered torque resolution	$< .5 \text{ Nm}$	$< 1 \text{ Nm}$	[71]
Movement intention detection directions			
Force-based	Joint torques accurately measured for movement intention in all assisted joints (impedance compensation-based)	A 6DOF force sensor at each interface point to determine $x, y, z$ intention direction (admittance control)	
sEMG-based	Joint angles/torques estimated from muscles that contribute to the supported motion using pattern-recognition or regression-based algorithms	3 agonist/antagonist pairs muscles for $x, y, z$ direction	[44]
Movement intention detection accuracy			
Force-based (interface-level)	Force sensors used for admittance control with DMD are: <ul style="list-style-type: none"> <li>·ATI Industrial Automation Mini45 Force/ Torque sensor, measurement resolution of <math>1/4 \text{ N}^{1,2}</math></li> <li>·Nano 25, ATI Industrial Automation, Apex, USA 3</li> </ul>	No clear measured resolution requirements were found for interface force-based methods (e.g., admittance control), therefore the used force sensors used in literature are reported in the could/ should column.	<sup>1</sup> [12] <sup>2</sup> [43] <sup>3</sup> [38]
Force-based (joint-level)	0.1 Nm (measured torque resolution on joint level)	$< 1 \text{ Nm}$	[71]
sEMG-based	SNR $< 25\%$	SNR $< 50\%$	[44]

**Table 2.4** (Continued)

Requirement	Should/Could	Must	Source
<i>Safety</i>			
Movement velocity [ $^{\circ}/s$ ]	Glenohumeral: ~66 to 59 $^{\circ}$ Elevation with 0 $^{\circ}$ horizontal rotation ~68 to 76 $^{\circ}$ Elevation with 90 $^{\circ}$ horizontal rotation ~95 to 90 $^{\circ}$ Axial rotation Elbow: ~89 to 83 $^{\circ}$ extension/flexion	Give independent task execution back while moving at a safe and predictable speed.	Data present mean ADL angular velocities based on the recorded kinematic data reported in [64].
Temperature	< skin temperature	< 48 $^{\circ}$ <sup>1</sup>	<sup>1</sup> IEC 60601-1:2005 standard
Audible acoustic energy	< 30 dBA <sup>1</sup>	< 80 dBA <sup>2</sup>	<sup>1</sup> [38] <sup>2</sup> IEC 60601-1:2005 standard
<b>Control approach</b>			
<i>Performance</i>			
Support gain	Gain optimized over ROM, tuneable support gain depending on variable needs on daily basis (e.g., fatigue, morning stiffness, temperature)	Gain similar over ROM, no static floating in space when relaxed (i.e., 80% > gain < 100%)	[19, 38]
Compensation strategy	Detect and compensate for additional load of grasped object in hand. Distinguish between interaction with environment (e.g., table, caregiver push against arm) and users' movement intention	Distinguish between voluntary movement and intrinsic passive joint impedance	<sup>1</sup> [43]
Transparency	Residual actuator impedance < .3 Nm	Residual actuator impedance < .4 Nm (50% of elbow flexion strength, $\approx .8 - 4.8$ Nm) <sup>1</sup>	<sup>1</sup> Muscle strength section
<i>Safety</i>			
ROM limits	System ROM = pROM	System ROM < pROM user Prevent hardware-to-hardware collisions Prevent singular configurations	
Torque limits	More research is required to find safe general torque limit within the pROM	Subject-specific limit determined at device provision; physiotherapist checks stretch values for pROM	
Velocity limits	Predictable and stable at ADL movement velocities.	Predictable stable velocity < ADL velocities	More research required
<b>Human interface</b>			
<i>Performance</i>			
Donning/Doffing	< 10 min a day	< 15 min	[38]

**Table 2.4** (Continued)

Requirement	Should/Could	Must	Source
Comfortability			
Usage duration	> 8 h/day	> 4 h/day	
Skin pressure	Pressure on skin <sup>1</sup> : ·Upper arm: 21.6 ± 8.7 mmHg ·Forearm: 20.1 ± 7.7 mmHg	·Pressure on skin: <sup>2</sup> < 30 mmHg ·No stiff material on top of a bony structure to prevent pressure points	<sup>1</sup> [66] <sup>2</sup> [58]
Shear forces	No shear forces	No sliding in interface on skin	
<i>Safety</i>			
Risk of fall-out	No sliding in the interface	The arm of the user should not be able to fall out the interface in all possible configurations	
Fire-proof	Fabrics and material used are fire resistant	Fabrics and materials used do not melt or catch fire when in contact with fire	16CFR1610: standard for the flammability of clothing textiles
Biocompatible and hygiene	Easily detachable and robust to was-/dry-machine	Skin-friendly, breathable, and detachable to wash	ISO 10993-1:2009
Quick release	Intuitive interface quick release design that any bystander could use in case of emergencies	User interface attachments should be quickly releasable < 30 s by a trained caregiver who knows how to handle the arm support that stays near the user to assist in case of emergencies	

3D: three dimensional; DOF: degrees of freedom; IP: international protection; (P)ROM: (passive) range of motion; sEMG: surface electromyography; DMD: Duchenne muscular dystrophy; SNR: signal to noise ratio; ADL: activities of daily living.

### 2.3.3.1 Mechanical structure

The mechanical structure should not add additional load to the spine to prevent deterioration of potential scoliosis, a frequent comorbidity in DMD, since trunk muscles are also weakened. Therefore, it is recommended to connect the arm support to the (electrical) wheelchair to carry the weight of the device.

Moreover, the mechanical design of the device must not restrict the user's already limited pROM [54] and allow the ROM required for the in the 'must' and preferably 'should' defined categories. However, it is also crucial to be aware of the aforementioned joint contractures, which people with DMD suffer from. To assist the ADL in the 'could' category, the mechanical structure should also allow for trunk movements. This is important for the large workspace reaching tasks [14].

Moreover, the arm support should not be obstructive, e.g., it must fit through a standard-sized doorway [14]. Preferably it looks slender and slim instead of bulky and stigmatizing [46].

Finally, the mechanical axes must be optimally aligned to the human joints because joint misalignment can result in high interaction forces and injury [3, 66, 67]. There will always be some degree of joint misalignment since human joints are not pure revolute joints, have complex geometries, and the axes of rotation translate during rotation [67].

To prevent adverse events, misalignment can be limited by design, e.g., self-alignment mechanisms or compliant actuators [3, 54].

### 2.3.3.2 Human interface

The human interface that transmits the forces from the exoskeleton to the body must be comfortable and fit the dimensions of the individual user. A well-balanced consideration should be made between comfortability (e.g., skin pressure, shear forces, displacements) and safety (e.g., sliding or falling out, skin irritation, bruises, or discomfort). Preferably, the interface is easily personalized, detachable and easy to clean (e.g., washing machine-resistant and cleanable surfaces).

For the user's independence and compliance, the device should be easy to don and doff with the help of a caregiver, but preferably independently by the user itself. Note that the aforementioned joint misalignments between the human and system joints could also result in displacement and shear forces at the human interface [22, 66] This should be minimized and checked during donning.

### 2.3.3.3 Actuator technology

Based on required joint torques and the limitations mentioned above of the (semi-)passive systems, a form of motorized support for the intended target population will be needed. For a motorized arm support, a choice should be made considering the type and placement of the actuator technology. The actuator type can vary from electrical motors (e.g., servo, step motor, series elastic actuator) to hydraulics or pneumatic (artificial muscles) [49, 51].

For the placement of the actuator technology, a choice between directly on the joint or teleported (i.e., externally positioned), such as cable-driven systems, can be made. The advantage of directly placing the actuator on the joint is that the design can be simple since no transmission mechanisms are required. The disadvantage is that a heavy and more distally placed motor negatively influences the mass distribution, i.e., effective weight and inertia [51]. Moreover, multiple actuators around a single joint negatively affect the device ROM (e.g., colliding motors at the shoulder joint for example). The advantage of teleported actuators, such as cable-driven systems, is lower limb inertia and enlarged ROM. However, the disadvantage of cable-driven systems is that for a bi-directional motion, two cables and two motors are required (e.g., cables can only pull) and that the cables introduce (non-linear) friction [51, 71].

### 2.3.3.4 Control approach

Preferably, the device supports the arm naturally and intuitively without the use of the contralateral arm or pre-defined trajectories but must detect the movement intention from a (physiological) signal that is intuitively related to the supported motion.

Control interfaces such as surface electromyography (sEMG) and force-based interfaces are promising strategies for achieving fine control movements [45]. With sEMG control, the muscle activity of selected muscles indicates the user's movement intention. Often, the agonist and antagonist muscles are used for opposite movements, for example, the m. biceps brachii and m. triceps brachii for elbow flexion and extension. The options with the force-based approaches are broad, from admittance control [13, 43] to impedance compensation-based (e.g., of weight and passive joint impedance) approaches. With admittance control,



a force sensor is used to measure the interaction forces between the user and device at interface level to measure the movement direction and intention of the user. The forces are then translated into a movement of the arm. With impedance compensation-based methods, the required support torques are determined on a joint level, where the orientation of the arm determines the level of support.

Lobo-Prat et al. [44, 45] compared sEMG and force-based admittance control interfaces in adults with DMD. They concluded that sEMG-based control was perceived as less fatiguing but force-based control as more intuitive since force-based control is closer to the natural way of interacting with the environment. They recommended the use of force-based control interfaces for people with more voluntary forces and sEMG-based for people where voluntary forces are below the intrinsic forces (e.g., weight and passive joint impedance) of the arm. This aligns with their findings that the participant with Brooke Scale 4 preferred the force-based methods, while participants with Brooke Scale 5 and 6 preferred the sEMG interface. With sEMG-based interfaces, it is easier to distinguish between voluntary movement intention and the intrinsic forces of the arm [44]. However, sEMG-based interfaces have the practical drawback that it is a difficult and time-consuming installation, due to the sensitivity of proper electrode placement. Moreover, it can become uncomfortable to have multiple electrodes in contact with the skin for a longer period, and long-term sEMG measurement stability is poor [13, 44]. Although both methods have pros and cons, based on Lobo-Prat et al. [44, 45] we recommend force-based methods for people with DMD Brooke Scale 4 since this is reported as more intuitive and has practical advantages.

### 2.3.3.5 Safety

Obviously, the device must be safe for the user and bystanders. The mechanical design should be strong and stiff enough to prevent bending (which can result in control issues) and breakage, also considering unintended usage. Considering the actuator placement, the configuration should not allow for singularity (i.e., configurations where the actuators mechanically get ‘stuck’).

Audible acoustic energy should be considered when choosing the actuator technology. Most types of actuators make noise, while the shoulder actuators might be placed close to the ear. The system should not hinder communication with others, let alone the risk of hearing damage [IEC 60601-1:2005 standard]. Similarly, the electric magnetic radiation of the actuator technology should be considered. This might affect active implants (e.g., pacemakers) of the user or bystander [IEC 60601-1-2:2014 standard].

The device should move as the user intended, which is an important safety aspect for selecting the control approach. If the robot moves differently, it can cause an unsafe situation, e.g., spilling hot water over its own or bystander’s skin. It is expected to have higher precision with impedance compensation-based approaches over sEMG approaches [44]. Other vital safety aspects for the control software are to warrant the torque, velocity and angle limits. Overstretching due to high torque, unexpected fast movement, or movement outside of the pROM of the patient could lead to trauma of soft tissue, such as (shortened) muscles and ligaments, or even damage to the cartilage and bones. Stretching the joints with elevated joint impedance can be beneficial [69], but care should be taken with stretching beyond the rigid contractures. From consultation with clinicians, stretching

exercises performed by therapists can break a bone in patients with severely reduced bone mineral density. Unfortunately, the patient is not always aware of the reduced bone mineral density. Therefore, it is crucial that the ROM of the device does not exceed the pROM of the user. Since the level of contractures, and thus the pROM, varies among the target population, user-specific end-stops are recommended to limit the device ROM. Physical hardware end-stops should be provided to prevent overstretching of the human joint in case of a software error or unexpected behavior. Moreover, it is recommended to identify the maximal allowable joint torque at the joint limits that are comfortable to the user before using the device.

Furthermore, end-application restrictions should apply, e.g., the device should not be used in people with involuntary movement intentions such as spasticity or epilepsy. Additional safety requirements are expressed in Table 2.4.

## 2.4 Discussion

This paper provides the functional and technical design requirements of wearable assistive arm support technology for people with DMD Brooke Scale 4.

The clinical characteristics show that the intended target population of DMD presents severe muscle weakness, with muscle strength of approximately 2% – 22% of the healthy reference population. On average, their functional ability without arm support is limited to tabletop activities because of their severely impaired shoulder function. However, some variation in functional abilities is present, along with a great variety in the level of joint contractures, arm circumferences, and BMI among patients. This implies that a certain level of individual customization is necessary.

The functional requirements show that activities with light weights (< 100 g) close to the body, such as computer(gaming), personal hygiene, feeding activities (incl. drinking with a straw), and writing, are a ‘must.’ Activities further away from the body or with heavier weights (< 200 g), such as turning on a light switch, scratching your head, or drinking from a glass, fall under the ‘should’ category. Activities requiring trunk movement for reaching and lifting heavy weights (> 200 g) fall under the ‘could’ category and are less feasible to realize. Considering the support level requirements, a form of motorized support is preferable for the intended target population. The advantage of a motorized system is that it can automatically adjust to the required compensation levels at different heights in the workspace (which is not yet the case in the semi-active systems), it allows for passive joint impedance compensation, and theoretically is able to detect and compensate for additional lifted objects. Moreover, it will enable the user to tune the level of support to a level that is required and feel comfortable, this level might vary between or even during the day(s) depending on the fatigue levels. It may need some experience for the user to find the right balance between sufficient training of the arms and preventing the risk of overuse.

Unfortunately, there are not enough quantitative data available on the level and behavior of the passive joint impedance over the pROM in DMD Brooke Scale 4 yet. Therefore, further investigation of the behavior (e.g., position, velocity, acceleration dependence) of the (elevated) passive joint impedance in DMD and whether it can be captured in a generalized model or should be personalized is needed. Furthermore, no clear literature was found on acceptable torque and velocity limits that are safe and comfortable for the user. Follow-up

studies should examine safe levels for the torque and velocity limits. It is expected that the performance of the control of the device (e.g., robustness, predictability, and safety) affects the acceptable movement velocity that feels safe to the user. Finally, no standards are yet available to quantify the comfortability of existing arm supports [22], making it difficult to compare and construct design requirements. However, within this paper, we have provided an educated guess for these requirements to highlight their importance because safety and comfort remain critical aspects of user acceptance. Future studies could aim to compare existing arm supports on comfortability.

The limitations are a lack of available data and literature concerning the target population and the requirements. In the case of limited literature, we verbally and by email consulted with three clinicians specialized in DMD (physiotherapist, occupational therapist and paediatric rehabilitation physician) to get more clarification on some of the clinical topics. Moreover, several assumptions had to be made to interpret reported values to be relevant for this paper.

Although the narrative focus is on DMD Brooke Scale 4, the concluding design requirements might also apply to other pathologies with a similar functional profile (e.g., other muscular dystrophies, spinal muscular atrophy, or amyotrophic lateral sclerosis) or more severely affected DMD (e.g., Brooke Scale 5). However, the importance of starting with specific patient needs should be stressed to ensure a good match between needs and design. The target population can be expanded after the functional gain and compliance is proven. In this way, the device is fit to the user instead of fitting the user to the technology, a commonly seen pitfall in assistive technology companies [10, 73].

One of the biggest challenges in the design of a (motorized) arm support is to improve the arm function without limiting the residual function of the user. Since the technology needs to encompass the arm, the design space is limited, while high support torques are required, making it hard to render the design into a slender construction. Moreover, arm supports (e.g., orthotics) deal with the residual arm function of the user that can vary among users. It is essential not to restrict the residual function to prevent further function loss or abandonment of the device. Moreover, the extreme muscle weakness of the DMD population increases the complexity of the control approach and the required safety measures. Another challenge is finding the right balance between adding complexity to the assistive technology and the user's gain in functionality. To prevent technology-driven overdesign and reduce the technology's complexity and costs, we categorized the requirements into 'must', 'should', and 'could' categories and recommend starting with a minimal viable product that supports the 'must' requirements. When sufficient functionality and acceptance are proven, the system is ready to implement more complexity for the next iteration. Although it is challenging to fulfil the needs of the target population, they are expected to benefit significantly from motorized arm supports to assist arm function. As the disease progresses, arm supports are expected to slow down the functional loss by the involvement of the arms as daily practice, which is beneficial for muscle maintenance, bone mineral density [8], and prevention of contractures caused by disuse [30]. Nevertheless, arm supports can provide more independence, social participation and, thereby, improve their quality of life.

In addition and beyond our scheme, other personal and environmental barriers (e.g., awareness, acceptance, financial situation, the device provision process, a lack of follow-up

procedures, and coordination between service and funding) should be tackled. These factors will differ between counties. Unfortunately, motorized arm supports' expected (development) costs are high. On the other hand, using arm supports can also reduce healthcare costs due to the aforementioned clinical benefits. A large study on the effectiveness and cost-effectiveness of assistive technology for impaired arm function is currently ongoing in the Netherlands, and results are expected in the upcoming years [62].

This work will be followed up by developing a dedicated assistive arm support based on the identified requirements. Although multiple solutions are possible from the specified requirements, we expect a motorized arm support with intuitive force-based weight and passive joint impedance compensation best match the needs of the DMD Brooke Scale 4.

## 2.5 Conclusion

In the development process of assistive technology, it is essential to start with the specific needs of the intended user. People with DMD Brooke Scale 4 have severe muscle weakness ( $< 22\%$  arm strength compared to the healthy reference population), which leads to severe functional impairments, with almost no active movement in the shoulders and limited movement in the elbow. This paper categorizes the functional requirements for assistance arm supports in people with DMD Brooke Scale 4 into a 'must', 'should', and 'could' category and links this to the technical requirements. A form of motorized actuator technology with intuitive movement intention detection is recommended because it allows the implementation of control algorithms to adjust for the correct workspace height, allows for passive joint impedance compensation, can adapt to muscle fatigue and can compensate for the additional weight of lifted objects. Due to the severe muscle weakness, this population is vulnerable, and extra care should be taken with the safety considerations raised in the technical requirements. The design must not limit or restrict the residual function of the user nor increase the risk of injury. This paper can be used for the development of arm supports for people with DMD Brooke Scale 4 and make them more user centered.

## References

- [1] Disabled World, 2017. URL <https://www.disabled-world.com/calculators-charts/height-weight-teens.php#mteen>.
- [2] J. Aizawa, T. Masuda, T. Koyama, K. Nakamaru, K. Isozaki, A. Okawa, and S. Morita. Three-dimensional motion of the upper extremity joints during various activities of daily living. *Journal of Biomechanics*, 43(15):2915–2922, 2010. doi: <https://doi.org/10.1016/j.jbiomech.2010.07.006>.
- [3] M. O. Ajayi, K. Djouani, and Y. Hamam. Interaction Control for Human-Exoskeletons. *Journal of Control Science and Engineering*, 2020, 2020. doi: 10.1155/2020/8472510.
- [4] M. H. Brooke, R. C. Griggs, J. R. Mendell, G. M. Fenichel, J. B. Shumate, and R. J. Pellegrino. Clinical trial in Duchenne dystrophy. I. The design of the protocol. *Muscle & nerve*, 4(3):186–197, 1981. doi: 10.1002/mus.880040304.
- [5] C. M. Brussock, S. M. Haley, T. L. Munsat, and D. B. Bernhardt. Measurement of isometric force in children with and without Duchenne’s muscular dystrophy. *Physical therapy*, 72(2):105–114, feb 1992. doi: 10.1093/ptj/72.2.105.
- [6] K. Bushby, R. Finkel, D. J. Birnkrant, L. E. Case, P. R. Clemens, L. Cripe, A. Kaul, K. Kinnett, C. McDonald, S. Pandya, J. Poysky, F. Shapiro, J. Tomezsko, and C. Constantin. Diagnosis and management of Duchenne muscular dystrophy, part 1: diagnosis, and pharmacological and psychosocial management. *The Lancet Neurology*, 9(1):77–93, 2010. doi: 10.1016/S1474-4422(09)70271-6.
- [7] M. N. Castro. *Development of a passive orthosis for upper extremity assistance*. PhD thesis, Aalborg: Aalborg University, 2019.
- [8] P. D. Chilibeck, D. G. Sale, and C. E. Webber. Exercise and Bone Mineral Density. *Sports Medicine*, 19(2):103–122, 1995. doi: 10.2165/00007256-199519020-00003.
- [9] A. M. Connolly, E. C. Malkus, J. R. Mendell, K. M. Flanigan, J. P. Miller, J. R. Schierbecker, C. A. Siener, P. T. Golumbek, C. M. Zaidman, C. M. McDonald, L. Johnson, A. Nicorici, P. I. Karachunski, J. W. Day, J. M. Kelecic, L. P. Lowes, L. N. Alfano, B. T. Darras, P. B. Kang, J. Quigley, A. E. Pasternak, J. M. Florence, P. Anand, C. O. Wulf, E. Goude, J. C. Dalton, L. Viollet-Callendret, K. K. Buser, E. Shriber, and R. Parad. Outcome reliability in non-Ambulatory Boys/Men with duchenne muscular dystrophy. *Muscle and Nerve*, 51(4):522–532, 2015. doi: 10.1002/mus.24346.
- [10] A. M. Cook, J. M. Polgar, and P. Encarnação. Principles of Assistive Technology. In *Assistive Technologies*, pages 1–15. 2020. doi: 10.1016/b978-0-323-52338-7.00001-9.
- [11] C. Cornu, F. Goubel, and M. Fardeau. Muscle and joint elastic properties during elbow flexion in Duchenne muscular dystrophy. *The Journal of Physiology*, 533(2):605–616, 2001. doi: 10.1111/j.1469-7793.2001.0605a.x.

- [12] M. Corrigan and R. Foulds. Admittance Control of the Intelligent Assistive Robotic Manipulator for Individuals with Duchenne Muscular Dystrophy: A Proof-of- Concept Design. *Journal of Rehabilitation Robotics*, 3(May):1–5, 2015. doi: 10.12970/2308-8354.2015.03.01.
- [13] M. C. Corrigan and R. A. Foulds. Evaluation of admittance control as an alternative to passive arm supports to increase upper extremity function for individuals with Duchenne muscular dystrophy. *Muscle and Nerve*, 61(6):692–701, 2020. doi: 10.1002/mus.26848.
- [14] A. Cruz, L. Callaway, M. Randall, and M. Ryan. Mobile arm supports in Duchenne muscular dystrophy: a pilot study of user experience and outcomes. *Disability and Rehabilitation: Assistive Technology*, 16(8):880–889, 2021. doi: 10.1080/17483107.2020.1749892.
- [15] C. A. M. Doorenbosch, J. Harlaar, and D. H. E. J. Veeger. The globe system: An unambiguous description of shoulder positions in daily life movements. *Journal of Rehabilitation Research and Development*, 40(2):147–155, 2003. doi: 10.1682/jrrd.2003.03.0149.
- [16] A. G. Dunning, M. M. H. P. Janssen, P. N. Kooren, and J. L. Herder. Evaluation of an arm support with trunk motion capability. *Journal of Medical Devices, Transactions of the ASME*, 10(4):1–4, 2016. doi: 10.1115/1.4034298.
- [17] T. Edmond, A. Laps, A. L. Case, N. O’Hara, and J. M. Abzug. Normal Ranges of Upper Extremity Length, Circumference, and Rate of Growth in the Pediatric Population. *Hand*, 15(5):713–721, 2020. doi: 10.1177/1558944718824706.
- [18] J. M. Essers, K. Meijer, A. Murgia, A. Bergsma, and P. Verstegen. An inverse dynamic analysis on the influence of upper limb gravity compensation during reaching. *IEEE International Conference on Rehabilitation Robotics*, pages 1–5, 2013. doi: 10.1109/ICORR.2013.6650368.
- [19] J. M. Essers, A. Murgia, A. A. Peters, M. M. H. P. Janssen, and K. Meijer. Recommendations for studies on dynamic arm support devices in people with neuromuscular disorders: a scoping review with expert-based discussion. *Disability and Rehabilitation: Assistive Technology*, 0(0):1–14, 2020. doi: 10.1080/17483107.2020.1806937.
- [20] M. Gandolla, A. Antonietti, V. Longatelli, and A. Pedrocchi. The Effectiveness of Wearable Upper Limb Assistive Devices in Degenerative Neuromuscular Diseases: A Systematic Review and Meta-Analysis. *Frontiers in Bioengineering and Biotechnology*, 7(January):1–16, 2020. doi: 10.3389/fbioe.2019.00450.
- [21] T. K. Gill, E. M. Shanahan, G. R. Tucker, R. Buchbinder, and C. L. Hill. Shoulder range of movement in the general population: age and gender stratified normative data using a community-based cohort. *BMC Musculoskeletal Disorders*, 21(1):676, 2020. doi: 10.1186/s12891-020-03665-9.

- [22] M. A. Gull, S. Bai, and T. Bak. A review on design of upper limb exoskeletons. *Robotics*, 9(1):1–35, mar 2020. doi: 10.3390/robotics9010016.
- [23] M. A. Gull, M. Thøgersen, S. H. Bengtson, M. Mohammadi, L. N. Andreasen Struijk, T. B. Moeslund, T. Bak, and S. Bai. A 4-dof upper limb exoskeleton for physical assistance: design, modeling, control and performance evaluation. *Applied Sciences (Switzerland)*, 11(13), 2021. doi: 10.3390/app11135865.
- [24] J. J. Han, G. Kurillo, R. T. Abresch, E. De Bie, A. Nicorici, and R. Bajcsy. Upper extremity 3-dimensional reachable workspace analysis in dystrophinopathy using Kinect. *Muscle and Nerve*, 52(3):344–355, 2015. doi: 10.1002/mus.24567.
- [25] J. J. Han, E. de Bie, A. Nicorici, R. T. Abresch, C. Anthonisen, R. Bajcsy, G. Kurillo, and C. M. McDonald. Reachable workspace and performance of upper limb (PUL) in duchenne muscular dystrophy. *Muscle and Nerve*, 53(4):545–554, 2016. doi: 10.1002/mus.24894.
- [26] R. Hari Krishnan, V. Devanandh, A. K. Brahma, and S. Pugazhenth. Estimation of mass moment of inertia of human body, when bending forward, for the design of a self-transfer robotic facility. *Journal of Engineering Science and Technology*, 11(2): 166–176, 2016.
- [27] L. J. Hébert, D. B. Maltais, C. Lepage, J. Saulnier, and M. Crête. Hand-Held Dynamometry Isometric Torque Reference Values for Children and Adolescents. *Pediatric Physical Therapy*, 27(4):414–423, 2015. doi: 10.1097/PEP.0000000000000179.
- [28] L. B. Hiller and C. K. Wade. Upper extremity functional assessment scales in children with Duchenne muscular dystrophy: a comparison. *Archives of physical medicine and rehabilitation*, 73(6):527–534, jun 1992.
- [29] S. L. Houwen-van Opstal, L. Rodwell, D. Bot, A. Daalmeyer, M. A. Willemsen, E. H. Niks, and I. J. de Groot. BMI-z scores of boys with Duchenne muscular dystrophy already begin to increase before losing ambulation: a longitudinal exploration of BMI, corticosteroids and caloric intake. *Neuromuscular Disorders*, 32(3):236–244, 2022. doi: 10.1016/j.nmd.2022.01.011.
- [30] M. Jansen, N. Van Alfen, A. C. Geurts, and I. J. De Groot. Assisted bicycle training delays functional deterioration in boys with Duchenne muscular dystrophy: The randomized controlled trial "no use is disuse". *Neurorehabilitation and Neural Repair*, 27(9):816–827, 2013. doi: 10.1177/1545968313496326.
- [31] M. M. H. P. Janssen, A. Bergsma, A. C. Geurts, and I. J. De Groot. Patterns of decline in upper limb function of boys and men with DMD: An international survey. *Journal of Neurology*, 261(7):1269–1288, 2014. doi: 10.1007/s00415-014-7316-9.
- [32] M. M. H. P. Janssen, J. Harlaar, B. Koopman, and I. J. M. de Groot. Dynamic arm study: Quantitative description of upper extremity function and activity of boys and men with duchenne muscular dystrophy. *Journal of NeuroEngineering and Rehabilitation*, 14(1):45, 2017. doi: 10.1186/s12984-017-0259-5.



- [33] M. M. H. P. Janssen, J. Horstik, P. Klap, and I. J. de Groot. Feasibility and effectiveness of a novel dynamic arm support in persons with spinal muscular atrophy and duchenne muscular dystrophy. *Journal of NeuroEngineering and Rehabilitation*, 18(1):1–13, 2021. doi: 10.1186/s12984-021-00868-6.
- [34] I. Y. Jung, J. H. Chae, S. K. Park, J. H. Kim, J. Y. Kim, S. J. Kim, and M. S. Bang. The correlation analysis of functional factors and age with Duchenne muscular dystrophy. *Annals of Rehabilitation Medicine*, 36(1):22–32, 2012. doi: 10.5535/arm.2012.36.1.22.
- [35] J. Karner, W. Reichenfelser, and M. Gfoehler. Kinematic and kinetic analysis of human motion as design input for an upper extremity bracing system. *Proceedings of the 9th IASTED International Conference on Biomedical Engineering, BioMed 2012*, (February): 376–383, 2012. doi: 10.2316/P.2012.764-105.
- [36] K. Klingels, A. G. Mayhew, E. S. Mazzone, T. Duong, V. Decostre, U. Werlauff, E. Vroom, E. Mercuri, N. M. Goemans, and A. Others. Development of a patient-reported outcome measure for upper limb function in Duchenne muscular dystrophy: DMD Upper Limb PROM. *Developmental Medicine and Child Neurology*, 59(2):224–231, 2017. doi: 10.1111/dmcn.13277.
- [37] P. N. Kooren, A. G. Dunning, M. M. H. P. Janssen, J. Lobo-Prat, B. F. Koopman, M. I. Paalman, I. J. De Groot, and J. L. Herder. Design and pilot validation of A-gear: A novel wearable dynamic arm support. *Journal of NeuroEngineering and Rehabilitation*, 12(1):1–12, 2015. doi: 10.1186/s12984-015-0072-y.
- [38] P. N. Kooren, J. Lobo-Prat, A. Q. Keemink, M. M. H. P. Janssen, A. H. Stienen, I. J. de Groot, M. I. Paalman, R. Verdaasdonk, and B. F. Koopman. Design and Control of the Active A-Gear: a Wearable 5 DOF Arm Exoskeleton for Adults with Duchenne Muscular Dystrophy. *6th IEEE RAS/EMBS International Conference on Biomedical Robotics and Biomechanics (BioRob) June 26-29, 2016. UTown, Singapore*, 2016-June (26-29):637–642, 2016. doi: 10.1109/BIOROB.2016.7523801.
- [39] L. Lacourpaille, R. Gross, F. Hug, A. Guével, Y. Péréon, A. Magot, J. Y. Hogrel, and A. Nordez. Effects of Duchenne muscular dystrophy on muscle stiffness and response to electrically-induced muscle contraction: A 12-month follow-up. *Neuromuscular Disorders*, 27(3):214–220, 2017. doi: 10.1016/j.nmd.2017.01.001.
- [40] E. Landfeldt, R. Thompson, T. Sejersen, H. J. McMillan, J. Kirschner, and H. Lochmüller. Life expectancy at birth in Duchenne muscular dystrophy: a systematic review and meta-analysis. *European Journal of Epidemiology*, 35(7):643–653, 2020. doi: 10.1007/s10654-020-00613-8.
- [41] S. Landsberger, P. Leung, V. Vargas, J. Shaperman, J. Baumgarten, Y. L. Yasuda, E. Sumi, D. McNeal, and R. Waters. Mobile arm supports: History, application, and work in progress. *Topics in Spinal Cord Injury Rehabilitation*, 11(2):74–94, 2005. doi: 10.1310/FCDG-QHTV-M9KL-5478.
- [42] M. L. Latash and V. M. Zatsiorsky. Joint stiffness: Myth or reality? *Human Movement Science*, 12(6):653–692, 1993. doi: 10.1016/0167-9457(93)90010-M.



- [43] J. Lobo-Prat, A. Q. L. Keemink, B. F. J. M. Koopman, A. H. A. Stienen, and P. H. Veltink. Adaptive gravity and joint stiffness compensation methods for force-controlled arm supports. In *IEEE International Conference on Rehabilitation Robotics*, volume 2015-Sept, pages 478–483. IEEE, 2015. doi: 10.1109/ICORR.2015.7281245.
- [44] J. Lobo-Prat, P. N. Kooren, M. M. H. P. Janssen, A. Q. Keemink, P. H. Veltink, A. H. Stienen, and B. F. Koopman. Implementation of EMG-and force-based control interfaces in active elbow supports for men with duchenne muscular dystrophy: a feasibility study. *IEEE Transactions on Neural Systems and Rehabilitation Engineering*, 24(11):1179–1190, 2016. doi: 10.1109/TNSRE.2016.2530762.
- [45] J. Lobo-Prat, K. Nizamis, M. M. H. P. Janssen, A. Q. Keemink, P. H. Veltink, B. F. Koopman, and A. H. Stienen. Comparison between sEMG and force as control interfaces to support planar arm movements in adults with Duchenne: A feasibility study. *Journal of NeuroEngineering and Rehabilitation*, 14(1):1–17, 2017. doi: 10.1186/s12984-017-0282-6.
- [46] J. Lobo Pratt. *Control interfaces to actively support the arm function of men with Duchenne Muscular Dystrophy*. PhD thesis, University of Twente, 2016.
- [47] V. Longatelli, A. Antonietti, E. Biffi, E. Diella, M. G. D’Angelo, M. Rossini, F. Molteni, M. Bocciolone, A. Pedrocchi, and M. Gandolla. User-centred assistive SystEm for arm Functions in neUromuscuLar subjects (USEFUL): a randomized controlled study. *Journal of NeuroEngineering and Rehabilitation*, 18(1):1–17, 2021. doi: 10.1186/s12984-020-00794-z.
- [48] Y. J. Lue, R. F. Lin, S. S. Chen, and Y. M. Lu. Measurement of the Functional Status of Patients with Different Types of Muscular Dystrophy. *Kaohsiung Journal of Medical Sciences*, 25(6):325–333, 2009. doi: 10.1016/S1607-551X(09)70523-6.
- [49] P. Maciejasz, J. Eschweiler, K. Gerlach-Hahn, A. Jansen-Troy, and S. Leonhardt. A survey on robotic devices for upper limb rehabilitation. 2014.
- [50] S. Maggioni, A. Melendez-Calderon, E. Van Asseldonk, V. Klamroth-Marganska, L. Lünenburger, R. Riener, and H. Van Der Kooij. Robot-aided assessment of lower extremity functions: A review. *Journal of NeuroEngineering and Rehabilitation*, 13(1):1–25, 2016. doi: 10.1186/s12984-016-0180-3.
- [51] S. K. Manna and V. N. Dubey. Comparative study of actuation systems for portable upper limb exoskeletons. *Medical Engineering and Physics*, 60:1–13, 2018. doi: 10.1016/j.medengphy.2018.07.017.
- [52] A. Mayhew, E. S. Mazzone, M. Eagle, T. Duong, M. Ash, V. Decostre, M. Vandenhauwe, K. Klingels, J. Florence, M. Main, F. Bianco, E. Henrikson, L. Servais, G. Campion, E. Vroom, V. Ricotti, N. Goemans, C. McDonald, and E. Mercuri. Development of the Performance of the Upper Limb module for Duchenne muscular dystrophy. *Developmental Medicine and Child Neurology*, 55(11):1038–1045, nov 2013. doi: 10.1111/dmcn.12213.

- [53] C. M. McDonald, R. T. Abresch, G. T. Carter, W. M. J. Fowler, E. R. Johnson, D. D. Kilmer, and B. J. Sigford. Profiles of neuromuscular diseases. *American Journal of Physical Medicine and Rehabilitation*, 74(5 Suppl.):S70–92, 1995. doi: 10.1097/00002060-199509001-00003.
- [54] A. Otten, C. Voort, A. Stienen, R. Aarts, E. Van Asseldonk, and H. Van Der Kooij. LIMPACT: A Hydraulically Powered Self-Aligning Upper Limb Exoskeleton. *IEEE/ASME Transactions on Mechatronics*, 20(5):2285–2298, 2015. doi: 10.1109/TMECH.2014.2375272.
- [55] M. Pane, G. Coratti, C. Brogna, E. S. Mazzone, A. Mayhew, L. Fanelli, S. Messina, A. D. Amico, M. Catteruccia, M. Scutifero, S. Frosini, V. Lanzillotta, G. Colia, F. Cavallaro, E. Rolle, R. De Sanctis, N. Forcina, R. Petillo, A. Barp, A. Gardani, A. Pini, G. Monaco, M. G. D. Angelo, R. Zanin, G. L. Vita, C. Bruno, T. Mongini, F. Ricci, E. Pegoraro, L. Bello, A. Berardinelli, R. Battini, V. Sansone, E. Albamonte, G. Baranello, E. Bertini, L. Politano, M. P. Sormani, and E. Mercuri. Upper limb function in Duchenne muscular dystrophy: 24 month longitudinal data. *PLoS ONE*, 13(6):4–11, 2018. doi: 10.1371/journal.pone.0199223.
- [56] J. C. Perry, J. M. Powell, and J. Rosen. Isotropy of an upper limb exoskeleton and the kinematics and dynamics of the human arm. *Applied Bionics and Biomechanics*, 6(2): 175–191, 2009. doi: 10.1080/11762320902920575.
- [57] B. J. Petrof. The molecular basis of activity-induced muscle injury in Duchenne muscular dystrophy. *Molecular and Cellular Biochemistry*, 179(1-2):111–124, 1998. doi: 10.1023/A:1006812004945.
- [58] J. L. Pons. *Rehabilitation Exoskeletal Robotics*, volume 29. 2010. doi: 10.1109/MEMB.2010.936548.
- [59] D. Ragonesi, S. Agrawal, W. Sample, and T. Rahman. Series elastic actuator control of a powered exoskeleton. *Proceedings of the Annual International Conference of the IEEE Engineering in Medicine and Biology Society, EMBS*, pages 3515–3518, 2011. doi: 10.1109/IEMBS.2011.6090583.
- [60] D. Ragonesi, S. K. Agrawal, W. Sample, and T. Rahman. Quantifying anti-gravity torques for the design of a powered exoskeleton. *IEEE Transactions on Neural Systems and Rehabilitation Engineering*, 21(2):283–288, 2013. doi: 10.1109/TNSRE.2012.2222047.
- [61] V. Ricotti, M. R. Evans, C. D. Sinclair, J. W. Butler, D. A. Ridout, J. Y. Hogrel, A. Emira, J. M. Morrow, M. M. Reilly, M. G. Hanna, R. L. Janiczek, P. M. Matthews, T. A. Yousry, F. Muntoni, and J. S. Thornton. Upper limb evaluation in duchenne muscular dystrophy: Fat-water quantification by MRI, muscle force and function define endpoints for clinical trials. *PLoS ONE*, 11(9):1–15, 2016. doi: 10.1371/journal.pone.0162542.
- [62] U. R. Roentgen, L. A. D. Heide, I. E. Kremer, H. Creemers, M. A. Brehm, J. T. Groothuis, E. A. Hagedoren, R. Daniëls, and S. M. Evers. Effectiveness and cost-effectiveness of an optimized process of providing assistive technology for impaired upper extremity function: Protocol of a prospective, quasi-experimental non-randomized study (OMARM). *Technology and Disability*, 33(3):207–220, 2021. doi: 10.3233/TAD-210335.

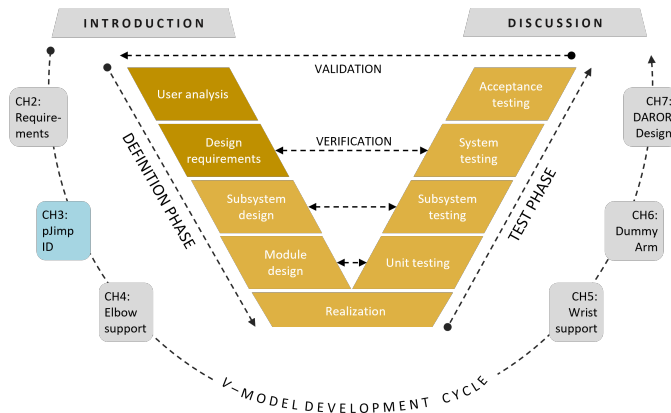
- [63] D. P. Romilly, C. Anglin, R. G. Gosine, C. Hershler, and S. U. Raschke. A Functional Task Analysis and Motion Simulation for the Development of a Powered Upper-Limb Orthosis. *IEEE Transactions on Rehabilitation Engineering*, 2(3):119–129, 1994. doi: 10.1109/86.331561.
- [64] J. Rosen, J. C. Perry, N. Manning, S. Burns, and B. Hannaford. The Human Arm Kinematics and Dynamics During Daily Activities – Toward a 7 DOF Upper Limb Powered Exoskeleton. *Brain Research*, 2005.
- [65] E. Sarrazin, M. V. D. Hagen, U. Schara, K. Von Au, and A. M. Kaindl. Growth and psychomotor development of patients with Duchenne muscular dystrophy. *European Journal of Paediatric Neurology*, 18(1):38–44, 2014. doi: 10.1016/j.ejpn.2013.08.008.
- [66] A. Schiele and F. C. van der Helm. Influence of attachment pressure and kinematic configuration on pHRI with wearable robots. *Applied Bionics and Biomechanics*, 6(2): 157–173, 2009. doi: 10.1080/11762320902879961.
- [67] A. Schiele and F. C. T. van der Helm. Kinematic design to improve ergonomics in human machine interaction. *IEEE Transactions on Neural Systems and Rehabilitation Engineering*, 14(4):456–469, 2006. doi: 10.1109/TNSRE.2006.881565.
- [68] L. Servais, N. Deconinck, A. Moraux, M. Benali, A. Canal, F. Van Parys, W. Vereecke, S. Wittevrongel, M. Mayer, I. Desguerre, K. Maincent, C. Themar-Noel, S. Quijano-Roy, N. Serari, T. Voit, and J. Y. Hogrel. Innovative methods to assess upper limb strength and function in non-ambulant Duchenne patients. *Neuromuscular Disorders*, 23(2): 139–148, 2013. doi: 10.1016/j.nmd.2012.10.022.
- [69] A. J. Skalsky and C. M. McDonald. Prevention and management of limb contractures in neuromuscular diseases. *Physical Medicine and Rehabilitation Clinics of North America*, 23(3):675–687, 2012. doi: 10.1016/j.pmr.2012.06.009.
- [70] J. M. Soucie, C. Wang, A. Forsyth, S. Funk, M. Denny, K. E. Roach, and D. Boone. Range of motion measurements: Reference values and a database for comparison studies. *Haemophilia*, 17(3):500–507, 2011. doi: 10.1111/j.1365-2516.2010.02399.x.
- [71] A. H. Stienen, E. E. Hekman, H. T. Braak, A. M. Aalsma, F. C. Van Der Helm, and H. Van Der Kooij. Design of a rotational hydroelastic actuator for a powered exoskeleton for upper limb rehabilitation. *IEEE Transactions on Biomedical Engineering*, 57(3):728–735, 2010. doi: 10.1109/TBME.2009.2018628.
- [72] A. H. A. Stienen and A. Q. L. Keemink. Visualization of shoulder range of motion for clinical diagnostics and device development. *IEEE International Conference on Rehabilitation Robotics*, 2015-Sept:816–821, 2015. doi: 10.1109/ICORR.2015.7281303.
- [73] L. A. van der Heide, G. J. Gelderblom, and L. P. De Witte. Dynamic arm supports: Overview and categorization of dynamic arm supports for people with decreased arm function. *IEEE International Conference on Rehabilitation Robotics*, pages 1–6, 2013. doi: 10.1109/ICORR.2013.6650491.

- [74] H. E. J. Veeger, B. Yu, K. An, and R. H. Rozendal. Parameters for modeling the upper extremity. *Journal of Biomechanics*, 30(6):647–652, 1997. doi: [https://doi.org/10.1016/S0021-9290\(97\)00011-0](https://doi.org/10.1016/S0021-9290(97)00011-0).
- [75] L. M. Ward, S. Hadjiyannakis, H. J. McMillan, G. Noritz, and D. R. Weber. Bone health and osteoporosis management of the patient with Duchenne muscular dystrophy. *Pediatrics*, 142(Suppl 2):S34–S42, 2018. doi: 10.1542/peds.2018-0333E.
- [76] R. Whisenant, C. Jones, A. Diether, and B. Lamming. DAZ 3D Studio, 2023. URL <https://www.daz3d.com/>. Version 4.10.0.123 Pro Edition (64-bit) For Windows.
- [77] G. Wu, F. C. T. Van Der Helm, H. E. J. Veeger, M. Makhsous, P. Van Roy, C. Anglin, J. Nagels, A. R. Karduna, K. McQuade, X. Wang, F. W. Werner, and B. Buchholz. ISB recommendation on definitions of joint coordinate systems of various joints for the reporting of human joint motion - Part II: Shoulder, elbow, wrist and hand. *Journal of Biomechanics*, 38(5):981–992, 2005. doi: 10.1016/j.jbiomech.2004.05.042.
- [78] K. Wu, Y. Su, Y. Yu, K. Lin, and C. Lan. Series Elastic Actuation of an Elbow Rehabilitation Exoskeleton with Axis Misalignment Adaptation. pages 1–6, 2017.

# 3

## Passive Joint Impedance Identification in the Upper Extremity

Chapter 2 recommended to consider passive joint impedance (i.e., resistance from passive structures) in compensation strategies, though data on its levels and behavior in individuals with DMD remain sparse. Moreover, there exist confusion about the terminology and the methodologies to identify passive joint impedance vary greatly.



This chapter reviews methodologies for identifying passive joint impedance, while Chapter 4 will focus on measuring it the elbow joint and compare different compensation strategies.

This chapter was submitted for publication to *Journal of NeuroEngineering and Rehabilitation* on September 23, 2024 as: Filius, S.J., Papa, K., Harlaar, Jaap., (*under revision*). Review of Upper Extremity Passive Joint Impedance Identification in People with Duchenne Muscular Dystrophy.

# Review of Upper Extremity Passive Joint Impedance Identification in People with Duchenne Muscular Dystrophy

**Abstract** *Duchenne Muscular Dystrophy (DMD) progressively leads to loss of limb function due to muscle weakness. The incurable nature of the disease shifts the focus to improving quality of life, including assistive supports to improve arm function. Over time, the passive joint impedance (Jimp) of people with DMD increases. Force-based controlled motorized arm supports require a clear distinction between the user's movement intention and passive forces, such as passive Jimp. Therefore, Jimp identification is essential. This review aims to define Jimp, identify factors influencing it, and outline experimental methods used for quantification, with a focus on the upper extremities in DMD. A literature review was performed in May 2021 and updated in March 2024 using SCOPUS, PubMed, IEEEExplore, and WebOfScience. The results reveal confusion in definitions and show various Jimp measuring practices for both DMD and individuals without muscle weakness. This study presents an overview and lists important parameters affecting passive Jimp, such as the joint's position, velocity and the multi-articular nature of the upper arm muscles. For personalized passive Jimp compensation in arm supports, ramp-type perturbations with constant velocity across the full joint range appear most optimal for identifying the elevated and non-linear nature of the passive Jimp in DMD.*

## 3.1 Introduction

Duchenne Muscular Dystrophy (DMD) is an inherited disease resulting from the mutation of the X-chromosome dystrophin gene, leading to the absence of the structural protein dystrophin [47, 52, 77]. It is the most prevalent muscular dystrophy, mainly affecting boys, with an incidence rate of about 1:5000 live male births [14, 53]. Patients cope with loss of ambulation, loss of upper extremity (UE) function, scoliosis, and respiratory and cardiovascular complications, with the latter two eventually leading to death [10, 47, 52, 74, 77]. The lack of dystrophin causes various muscle morphological changes, with muscle fibers losing their ability to repair after several deterioration-regeneration cycles, leading to permanent degradation and replacing them with adipose (i.e., fat) and connective tissue (i.e., fibrosis) [13, 31, 52, 77]. This process causes muscle loss [52] and the formation of joint contractures [47]. Further weakening of the muscles, combined with joint contractures limiting the joint's range of motion (ROM) [13, 52, 61]. This results in arm-function deterioration, hindering the activities of daily living and social participation [30, 51, 61], making them more dependent on family and caretakers [47].

Arm-assistive devices can improve the quality of life of people with DMD by compensating for the arm's weight and assisting the arm functionality [47, 66]. An example of such a device is the passive Wilmington Robotic Exoskeleton (JAECO Orthopedic, Hot Springs, AR). Unfortunately, as the disease progresses, even with passive assistance, the muscle strength becomes insufficient, making boys with DMD unable to overcome the friction and inertia of the passive supports, and the passive forces exerted on their arms [45, 47, 66]. This makes it difficult to raise their arms above their head, lift objects with additional weight [66], and perform downward movements [35].

Due to muscle weakness and morphological changes in the muscles, the so-called passive joint impedance (Jimp) increases, making movement even more difficult. Jimp refers to the resistance against a movement, often referred to as joint stiffness in the clinical field. As a consequence, the functional ability decreases even further. Even with arm supports that compensate for the arm's weight, the functional ability can be limited by this passive Jimp [45] and compensating for the passive Jimp in assistive arm supports seems promising.

Straathof et al. [74] showed in their study with people with DMD that providing Jimp compensation with the planar active A-Arm support system (Flexextension Project, The Netherlands) increased the functional ROM of the users' arm. Moreover, [45, 47] showed with the UR5 Robotic arm (Universal Robots, Denmark) that compensating for both arm weight and passive Jimp leads to an increased horizontal and vertical workspace of the arm in an individual with DMD, compared to weight compensation alone.

Unlike passive, active-assistance devices can compensate not only for the weight of the arm but also for its passive Jimp, including stiffness, damping, and inertia forces [45, 47, 74]. While different control methods of these devices exist, force-based control requires a clear distinction between the user's voluntary and passive forces (weight and passive Jimp) [47]. Thus, the passive Jimp and the gravity component must be correctly estimated to properly identify the user's intention and improve the device's control [46, 47, 66, 74].

Unfortunately, the literature lacks sufficient quantitative data on the levels and behavior of passive Jimp in individuals with DMD, limiting the development of force-based compensation models in assistive technologies [21]. Moreover, specialists in various fields [5, 6, 45, 66, 75] use different terms and methods to describe and quantify passive Jimp. Therefore, there is a need to clarify the definitions used for passive Jimp, and the parameters that affect it. For this reason, the study provides (1) an insight into what passive Jimp is, (2) parameters affecting Jimp, and (3) an overview of the experimental methods in the literature measuring the Jimp of the upper extremities in individuals with DMD and without muscle weakness.

## 3.2 Methods

The Prisma flowchart in Figure 3.1 displays an overview of the process.

### 3.2.1 Literature search

In May 2021, a single reviewer (KP) conducted a literature study in four electronic databases: SCOPUS, PubMed, IEEEExplore, and WebOfScience. This search was updated in March 2024. The following keywords and Medical Subject Headings (MeSH) Terms were used in the

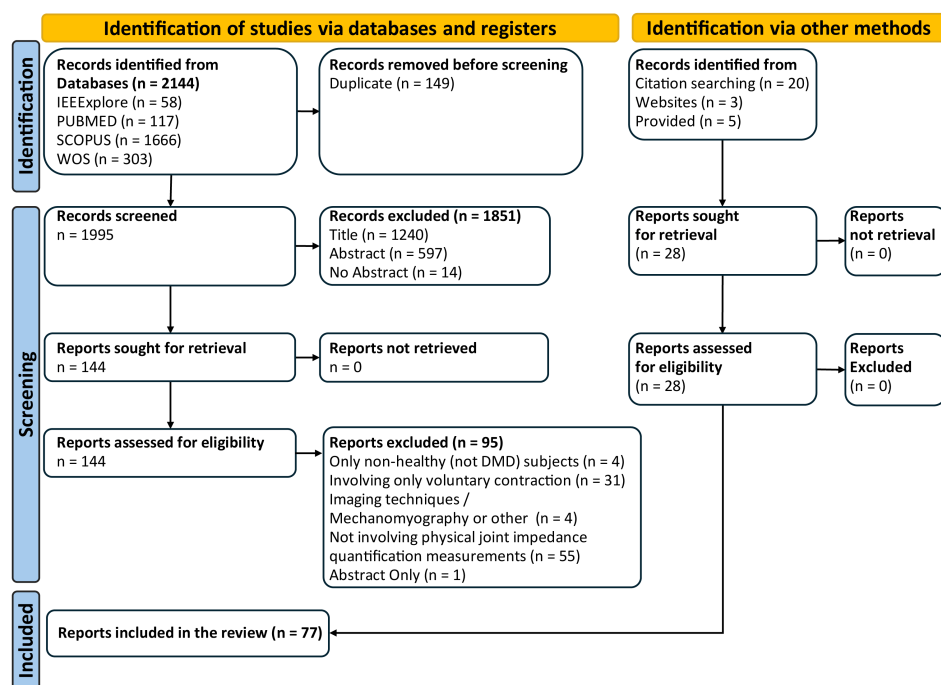


**Figure 3.1:** Prisma Flowchart process for the selection of the results of the review [59].

search: *stiffness, co-activation, contractures, ROM, elasticity, excursion, and fibrosis*, focused only on the muscles and joints (*shoulder, elbow, wrist*) of the *upper extremities and limbs*. Finally, the terms *Duchenne, Becker, muscular dystrophy/ies and neuromuscular diseases* were used. The terms were refined by reviewing multiple results to ensure relevance and were explicitly adjusted for each database. Where applicable, they were combined with additional filters. In all databases, only studies involving adolescents and adults were included. Where possible, non-human results were excluded. Detailed database-specific search strings are available in Appendix A.1. Next, all the results were imported into EndNote X9.3.3 software (Clarivate) and cleared from duplicates.

### 3.2.2 Screening

Based on the title and abstract, results written in a non-English language, contained no abstract, and papers that concern DMD but describe treatments with toxin or surgery, gene, or protein mutations were excluded. Moreover, papers that only used imaging techniques to measure the stiffness or rigidity of the muscles were excluded. Additionally, papers describing assistive arm supports for people with DMD, that do not consider passive Jimp identification, modeling or compensation were excluded.

Since the number of results related to passive Jimp identification and DMD was very small (5), also papers describing experiments to identify passive Jimp in non-disabled



participants were included. However, papers focused solely on sports and athletes or those only involving experiments requiring a form of voluntary muscle contraction during identification were excluded. So, studies quantifying Jimp in people with DMD (with or without voluntary contraction) and non-disabled participants (including only those describing experiments without voluntary contraction) were included. Moreover, studies providing general information about relevant definitions, and parameters affecting the Jimp were included.

Finally, a full review of the selected papers was carried out. Any cross-references to studies about experiments and Jimp attributes were added to the pool for further examination.

### 3.3 Results

#### 3.3.1 Definition of passive joint impedance

Various terms like stiffness, impedance, elastic coefficient, tonus, hypertonia, spasticity, and rigidity were identified in the (clinical) literature, with professionals having difficulty distinguishing some of them [5, 6]. We quoted the definitions in Table 3.1 for clarity. To illustrate, Roberson and Giurintano [68] define ‘*joint stiffness*’ as “a limitation in the ROM of a joint or a resistance encountered while the joint is moved through its ROM”. While Boon et al. [8] defined ‘*mechanical impedance*’ as “the mechanical resistance that is exerted in response to passive motion”, which is also referred to as ‘*rigidity*’ in the medical terminology [8]. Moreover, ‘*muscle tone*’ characterizes the resistance to an externally forced movement [63]. Wiegner and Watts [80] refer to ‘*tone*’ and ‘*stiffness*’ as the same thing, similar to Malhotra et al. [50] who describe tone as stiffness [24]. Chuang et al. [11] mention poor discrimination between increased muscle tone and soft-tissue stiffness. Similar to ‘*spasticity*’ [24] and ‘*rigidity*’ [20], muscle tone is influenced by the innervation of the muscles [11, 63]. A clear definition for tonus and spasticity is provided in Table 3.1.

Maggioni et al. [49] give a clear definition of joint impedance and distinguish it from the clinically often used term joint stiffness. They describe ‘*joint impedance*’ as the “force generated by changes in position (e.g., stiffness, non-elastic forces), in velocity (e.g., viscosity, damping) and in acceleration (e.g., inertia)” [41, 49]. Therefore, the term joint impedance is, in this case, better than joint stiffness since it consists of more components than pure stiffness. Joint stiffness alone can only describe the static property of a joint, while joint viscosity and limb inertia are needed to characterize its dynamic resistance against an external perturbation [86], where perturbation refers to an externally applied force or motion that alters the state of the limb.

Moreover, they clearly distinguish the active and passive forms of Jimp. *Passive* Jimp results from the passive biomechanical properties of the muscles, tendons, and tissues around the joint and limb inertia [49]. In contrast, the *active* form is a result of the response to reflexes or resistance produced by (non-reflexive) muscle contractions, such as tone and spasticity, which both are absent in DMD [52]. Therefore, *passive* Jimp is the primary focus of this paper.

**Table 3.1:** Comparison of descriptions.

Term	Descriptions
Joint stiffness	“A limitation in the ROM of a joint or a resistance encountered while the joint is moved through its ROM” [68].
Mechanical Impedance	“The mechanical resistance that is exerted in response to passive motion” [8]. “Mechanical impedance is the force resistance to perturbations of state” [22].
Mechanical admittance	Denotes the deformation change in response to a load disturbance. The inverse of mechanical impedance [69].
Tonus	“The state of activity or tension of a muscle beyond that related to its physical properties, that is, its active resistance to stretch. In skeletal muscle, tonus is dependent upon efferent innervation” [58].
Myotonia	“Prolonged failure of muscle relaxation after contraction. This may occur after voluntary contractions, muscle percussion, or electrical stimulation of the muscle. Myotonia is a characteristic feature of myotonic disorders” [57].
Rigidity	“Continuous involuntary sustained muscle contraction which is often a manifestation of basal ganglia diseases. When an affected muscle is passively stretched, the degree of resistance remains constant regardless of the rate at which the muscle is stretched. This feature helps to distinguish rigidity from muscle spasticity” [56].
Spasticity	“A motor disorder characterized by a velocity dependent increase in tonic stretch reflexes (muscle tone) with exaggerated tendon jerks, resulting from hyper excitability of the stretch reflex, as one component of the upper motor neurone syndrome” [39].

### 3.3.2 Experimental methods to quantify the joint impedance

This literature review yielded 47 studies looking into the mechanical properties of the UE, dating from 1973 to 2022. Table 3.3 summarizes the identified experimental studies. The studies varied in the imposed movements, the joints of the upper extremity in focus, and the study population.

We first categorized them based on the type of study population, resulting in five studies including people with DMD, 29 with no pathology, and 13 with and without pathology.

A secondary categorization based on the investigated joint, dividing them between the entire arm, shoulder, elbow, wrist, wrist and fingers combined, and only fingers (1, 8, 20, 15, 2 and 1, respectively).

The third categorization is based on the imposed movement or perturbation. The number of studies implementing each perturbation type is shown in Table 3.2, where each study may include more than one perturbation type. Most studies perturbed the joints by a static hold position, applying a constant velocity (ramp type), or through frequency perturbations.

Out of the five studies examining solely DMD subjects, four applied ramp movements [45–47, 74] and one included both quick release and frequency perturbations experiments [13], with three investigating the full-arm and two the elbow joint. A description of the most frequently imposed movements follows.

### 3.3.2.1 Static

In five studies they measured the steady-state passive Jimp at static positions of the joint [17, 26, 40, 65, 66, 72]. With sufficient static torque measurements of a combination of positions over the ROM of two joints, a surface area can be created to describe the static passive Jimp, just as Ragonesi et al. [65, 66] did for different elbow and shoulder positions.

**Table 3.2:** Number of studies implementing each perturbation.

Perturbation Type	#
Static	5
Ramp	11
Repeating Ramp	9
Ramp-and-hold	8
Frequency Perturbations	5
Quick-Release	1
Step	2
Pendulum Swing Motion	1
Torque Pulses	3
Pseudo-Random Binary Sequence	5
Random Torque Perturbations	1
Static Torque Displacement	1

### 3.3.2.2 Frequency perturbations

Frequency perturbations are sinusoidal perturbations that are usually applied for system identification techniques and creating a model of the investigated system [13, 84, 86, 87]. However, these techniques are more appropriate for linear systems [33]. Consequently, to avoid any non-linearities, the frequency perturbations are applied in a typically narrow ROM of less than  $5^\circ$  [13, 84, 86, 87]. The studies identified in this review utilized frequencies of 0.4 to 12 Hz [13, 48, 84], and the majority of joint displacements are in the range of 0.005 to 0.1 rad ( $0.3^\circ$  to  $5.7^\circ$ ), except for MacKay et al. [48], who also investigated 0.5 rad ( $\approx 29^\circ$ ). The only study that implemented frequency perturbation techniques for studying the joint impedance of people with DMD was that of Cornu et al. [13], which applied perturbations of  $3^\circ$  at frequencies of 4 to 12 Hz.

### 3.3.2.3 Ramp and variations

Ramp experiments introduce a linear increment of force or position (i.e., constant velocity) to move the joint over a particular ROM. Where constant velocity perturbations allow for the examination of Jimp, linear increment of force perturbations reveal the joint's compliance (i.e., 'admittance'). Repeating the same experiment continuously over multiple cycles gives a repeating ramp experiment. As in Lobo-Prat et al. [45, 47], Straathof et al. [74], ramp perturbations can be applied on a single joint or on multiple joints simultaneously to obtain the arm's combined passive Jimp over the workspace.

Another variation, ramp-and-hold, introduces a pause at the end of the movement before switching direction. This pause can be a constant [16, 20, 27, 36] or a random value [33,

34]. Different velocities are used in ramp experiments ranging from slow velocities of 0.05 rad/s (2.86 °/s) [46] up to 500 °/s [63]. The investigated ROM can vary. For example, the perturbation ROMs for the elbow joint identified are as narrow as 2° [33], wide as  $\approx 143^\circ$  [71] or even cover the arm's (horizontal) workspace [46, 47, 74, 76].

Unlike frequency perturbations, the non-linearities over the workspace do not necessarily limit the perturbation's ROM in ramp studies. However, Drake and Charles [18], Klomp et al. [33, 34] still investigated only a small range of the wrist joint where the stiffness is linear.

Slower velocities (e.g., around 3 °/s, [46]) can be used to examine the passive Jimp, while higher velocities (e.g.,  $\geq 60^\circ$ /s, [76]) can be used to elicit a reflex response affecting the active Jimp [75, 76]. Reflex responses will be further discussed in the Reflex paragraph 3.3.3.4.

As a variation to the rotational ramp-type experiments, Azarsa et al. [4] evaluated the inferior translational admittance of the glenohumeral joint. They evaluated the inferior direction displacement of the shoulder when applying an incremental load of 10 to 80 N in a supine position with 90° abduction and external rotation. Also, Gibo et al. [27], reports a linear displacement perturbation (7 mm) of the hand while investigating the contribution of co-contraction of the arm muscles to the Jimp.

### 3.3.3 Properties of joint impedance and parameters affecting it

This review has identified several parameters affecting Jimp that should be considered when designing experiments. We divided them into four categories: (1) fixed or biologically dependent, (2) time- or environmentally dependent, (3) training-related, and lastly, (4) reflexes or volition-dependent.

#### 3.3.3.1 Fixed or biologically dependent parameters

Some attributes are always present and define the Jimp regardless of the time of day, environmental conditions or the person's physical condition. During a joint's movement, velocity and acceleration produce dynamic torque components, which add to the total Jimp [17].

**Positional dependence** With movement, the length changes in musculotendon structures, joint capsules, ligaments, and connective tissues can create passive moments around a joint [17, 40]. Within the muscles, the cross-bridges have spring-like properties [73], which contribute to the positional dependence (i.e., stiffness) component of the passive Jimp [19, 48].

Like a spring's equilibrium point, the static passive Jimp is at its minimum near the joint's neutral position of the joint [36]. Around the neutral position, the passive Jimp is linear [18, 80]. Around the neutral position of the wrist (around 15°, Drake and Charles [18]) and the elbow (around 30°, Wiegner and Watts [80]), the passive Jimp is linear. However, this is not true for the extreme positions [36].

For a 90° abducted arm, Wiegner and Watts [80] identified this neutral elbow position (equilibrium point) to be in the range of  $73^\circ \pm 10^\circ$  (107° relative to the humerus). When the arm is resting besides the subject's body and pulled by gravity, Jones et al. [32] identified the equilibrium point in the range of 10° to 20°. Whereas, according to Wiegner and Watts [80], the National Aeronautics and Space Administration [12] report a neutral elbow position in

a weightless condition to be  $58^\circ \pm 24^\circ$ . Endo et al. [20] made a distinction in the equilibrium for the flexion ( $0^\circ$  to  $110^\circ$ ) and extension ( $110^\circ$  to  $10^\circ$ ) movement direction. They report an equilibrium of  $58.1^\circ$  (95% CI:  $55.3^\circ$  to  $60.9^\circ$ ) for the flexion perturbation and  $61.1^\circ$  (95% CI:  $59.2^\circ$  to  $62.9^\circ$ ) for the extension perturbation. For the glenohumeral joint, the intrinsic mechanical properties are coupled over the different rotational axes of the shoulder (e.g., internal/external rotation and horizontal abduction/adduction) [84]. Therefore, different arm positions can lead to variations in the mechanical stiffness and viscous damping [84].

**Multiarticular effects** In the human body, the force-producing musculotendon structures can span multiple joints, wherein movement at one joint alters the moments applied to an adjacent joint. Consequently, cross-coupling moments between adjacent joints connected by multiarticular muscles can be investigated when moving one of the joints [17, 81, 88].

One such muscle is the m. Triceps Brachii (TB), spanning over the shoulder and elbow joints and acting as an extensor for both of them [40]. The length and moment arm of m. TB changes with varying shoulder and elbow joint angles [40] affecting the passive shoulder extension moment. Landin and Thompson [40] measured the static extension shoulder moments under different elbow and shoulder position combinations. Their reported results of the interaction between the two joints seem contradicting. However, they do identify that the overall passive tissue around the shoulder joint constituted a large proportion of the maximum shoulder extension moment (60-80 %) [40].

Moreover, the passive Jimp of the wrist joint is affected by the muscles and joint position of the forearm and metacarpophalangeal joints [17]. Park et al. [62] measured a 13 % coupled stiffness between wrist flexion/extension (FE) and radio-ulnar deviation and Drake and Charles [18] identified in the literature that the forearm rotation counters the pulling direction of the wrist muscles by 12 %. Furthermore, the resting position of the fingers can be altered with changes in the wrist position, which change the length of the muscles in the forearm, actuating the fingers [26]. Due to the small weight of the fingers and the hand, the passive musculotendon stiffness properties dominate over the multi-joint arm dynamics, causing the fingers to move towards the resting position [26].

**Contractures** Joint contractures are typical in DMD, and their development increases with mobility reduction, which increases with wheelchair reliance [52]. Contractures affect the muscle's operation ROM [80] and can be painful [64]. Combined with connective tissues, adhesions, and abnormal muscle shortening, the passive Jimp rises and the ROM declines [40, 54]. These alter the resting position and the joint's passive torque-angle relationship [80]. Consequently, passive Jimp directly indicates the contractures [88]. Shortening of the long finger flexor muscles [29, 79] and surgical treatment or conservative management such as splinting, and stretching to elongate the muscle-tendon complex of the joint are common in DMD [29, 64, 79].

**Table 3.3:** Studies investigating the joint impedance of the upper extremities.

Perturbation <sup>a</sup>	ROM	Joint(s)	Subjects	D/E	Experiment Description	Source
<b>Duchenne Muscular Dystrophy Subjects</b>						
Ramp	Full horizontal arm's workspace (2D planar)	Full Arm	3 DMD (Brooke 4-6) (18-23 yr)	D	Measured the passive forces of the relaxed arm by passively moving it in the horizontal plane.	[47]
Ramp	Full joint workspace (1D)	Elbow	3 DMD (Brooke 5) (21-22 yr)	D	Measured elbow compensation (gravity and joint stiffness) forces with a constant velocity while the arm is relaxed.	[46]
Ramp	Full horizontal arm's workspace (2D planar) $\approx 32 \text{ cm} \times 17 \text{ cm} = 544 \text{ cm}^2$	Full Arm	1 DMD (Brooke 5) (24 yr)	D	Low-velocity passive arm movement creates a 2D force field in the transverse plane.	[74]
Ramp	Full horizontal arm's workspace (2D planar)	Full Arm	1 DMD (23 yr)	D	Passive arm forces by sweeping the arm in the horizontal plane in front of the subject's workspace.	[45]
(1) QR, (2) FP	(1) Not Specified, (2) $3^\circ$ peak-to-peak harmonic angular displacement	Elbow	22 DMD boys ( $13.55 \pm 3.03$ yr, 9-21 yr), 15 healthy boys ( $11.02 \pm 1.66$ yr, 9-15 yr)	D	Performed isometric Maximum Voluntary Contraction (MVC) tests, Quick-Release (QR) and sinusoidal perturbations (SP) tests with sub-maximal MVCs.	[13]
<b>Healthy Subjects</b>						
Static	Nine hand positions, 10 cm apart forming a $3 \times 3$ grid (shoulder $12^\circ - 70^\circ$ , elbow $48^\circ - 110^\circ$ )	Full Arm	9 (22-41yr) (8 Right-Handed (RH) males)	D	While the subject was relaxed, they estimated arm stiffness ellipses by obtaining measurements immediately before applying perturbations to the hand.	[72]
Ramp-and-Hold	7 mm	Shoulder, Elbow	11 "young" (4 males) ( $27 \pm 5$ yr) and 11 "old" (7 males) ( $58 \pm 12$ yr)	D	(1) Baseline session measuring the passive arm impedance and (2) Perturbation sessions (clockwise and isotropic) with subjects resisting force perturbations in eight different directions ( $0^\circ$ , $\pm 45^\circ$ , $\pm 90^\circ$ , $\pm 135^\circ$ and $180^\circ$ ).	[27]

**Table 3.3** (Continued)

Perturbation	ROM	Joint(s)	Subjects	D/E	Experiment Description	Source
PRBS	$\pm 2.5^\circ$ ( $\pm 0.045$ rad) in IER and $\pm 1.5^\circ$ ( $\pm 0.025$ rad) in horizontal ABD/ADD	Shoulder	15 males and females ( $29 \pm 5$ yr)	D	Rapid perturbations in different directions (IER, ABD and ADD) while subjects maintained different MVC torque levels of 0 % (passive) to 40 %, at 10 % increments.	[84]
Ramp	Not Specified	Shoulder	20 males ( $37 \pm 7.47$ yr)	D	Involved inferior-directed translation of the glenohumeral joint where they gradually applied to the humeral head a preload of 10 N followed by a target load of 80 N.	[4]
Step	Max $\approx 150^\circ$ to $195^\circ$	Shoulder	10 males (24–29 yr) ( $25.9 \pm 1.79$ yr)	E	Examiner applied a tensile load of 30 N to the humerus until achieving a 4 Nm IER. Tested for humerus elevation ( $30^\circ$ , $45^\circ$ , $60^\circ$ , $90^\circ$ , $120^\circ$ and $135^\circ$ ), and planes anterior and posterior to the scapula ( $30^\circ$ and $60^\circ$ ).	[44]
Static	Not Specified	Shoulder, Elbow	18 females ( $19.8 \pm 1.3$ yr)	D	Measured the mean passive shoulder joint extension moment before stimulation at different shoulder and elbow positions.	[40]
FP	Small Amplitude	Shoulder	7 males ( $33 \pm 7.9$ yr)	D	Small-amplitude abduction perturbations to the shoulder while the user is relaxed or minimizing the background torque error with sub-maximal MVCs.	[86]
Ramp-and-Hold	$10^\circ$	Elbow	10 RH (5 males) ( $24.4 \pm 2.7$ yr)	D	Examining elbow joint movement at different muscle contraction levels and velocities.	[36]
Repeating Ramp	$60^\circ$ and $120^\circ$	Elbow	9 ( $24.4 \pm 4.2$ yr)	E	Measured neural and non-neural torques, position, and velocity while the examiner moved the subject's elbow joint passively.	[15]
PRBS	0.03 rad	Elbow	15 ( $53.5 \pm 9.6$ yr)	D	Applied pseudo-random perturbations to the elbow joint to measure the intrinsic and reflex dynamic stiffness.	[55]

**Table 3.3** (Continued)

Perturbation	ROM	Joint(s)	Subjects	D/E	Experiment Description	Source
FP	Amplitude standard deviation $\sigma = 1.5^\circ$	Elbow	5 (25–40 yr)	D	Applying standard perturbations to the elbow joint to evaluate intrinsic and reflex properties before and after fatigue with 0–50% MVCs.	[87]
(1) Torque Pulses, (2) Ramp	(1) 1 to 7 Nm (2) $\approx 60^\circ$ (4 $\times$ EXT and then 4 $\times$ FLX sequences)	Elbow	19 (11 males) (20–78 yr, median 32 yr)	D	Conducted preliminary and formal experiments to examine limb velocity and muscle reflex contraction of the relaxed joint. Used torque pulses of varying levels and different levels of torque for elbow FE movements.	[80]
(1) FP, (2) STD, (3) Torque Pulse	(1) 0.005 to 0.5 rad (2) Varying amount $0 \pm 0.5$ rad (3) Superimposed for pulse amplitudes up to 0.05 rad	Elbow	5 (3 males) (21–37 yr)	D	Investigated (1) the Frequency Response of the elbow joint over different amplitudes and frequencies, applied (2) Static torque displacements and (3) Test Pulse simulations over different joint positions.	[48]
(1) Step, (2) Ramp	(1) Not Specified, (2) $2^\circ$	Elbow	1 male adult	D	Examine the passive and reflex-mediated muscle stiffness of the relaxed elbow through (1) step (different amplitudes) and (2) ramp (different velocities) tests, with different isometric contraction levels preceding the perturbation onset.	[7]
Repeating Ramp	(1) 0.06 rad and (2) $\leq 0.4$ rad at elbow $90^\circ$	Elbow	5 (4 males) (20–26yr)	D	Measured the passive joint impedance of the elbow for different velocities over the same amplitude and vice versa.	[8]
Ramp	$18^\circ$ in 2D FE-RUD space	Wrist	13 (7 RH males) (19–55 yr), 3 LH males (23–60 yr)	D	Different target positions of passive wrist FE and Radio-Ulnar Deviation (RUD) movements.	[19]
Ramp-and-Hold	0.15 rad peak-to-peak	Wrist	8 (5 males), (33 $\pm$ 9 yr)	D	Wrist dynamic model behavior parameters are estimated through ramp-and-hold perturbations of different torque levels and velocities. Subjects were both relaxed and applying torque against the manipulator.	[34]



**Table 3.3** (Continued)

Perturbation	ROM	Joint(s)	Subjects	D/E	Experiment Description	Source
Random Torque Perturbations	Mean displacement amplitude across subjects: (FE, RUD and PS) = (5.4°, 5.1° and 4.1°)	Forearm and Wrist	8 RH (6 males) (27.1 ± 3.4 yr)	D	Applied random force perturbations in three directions to investigate wrist FE, RUD, and forearm pronation/supination (PS).	[62]
PRBS	0 ± 10°	Wrist	14 RH (3 males) (27 ± 2.9 yr)	D	Used small amplitude, high velocity (100°/s) wrist displacements to evaluate wrist biomechanical properties ( $S_{MECH}$ ) and wrist position sense before and after a fatigue task.	[1]
Torque Pulse	Peak wrist FLX (33.2 ± 9.1°) and EXT (32.8 ± 5.8°) angles	Wrist	10 RH males (22.7 ± 2.7 yr)	D	Wrist-joint rotational stiffness estimation through perturbations with three sub-maximal hand-grip MVCs. Examined the effect of co-contraction and perturbation anticipation.	[28]
Ramp	Sphere radius 15° in PS-FE-RUD space	Wrist	10 RH (5 males) (24 ± 5.42 yr)	D	Passive Wrist FE at different forearm PS and RUD positions.	[18]
Repeating Ramp	37° FLX to 36° EXT and from 16° RD to 28° UD	Wrist	15 RH (7 males) (20-27 yr)	D	Examined wrist stiffness from its neutral position to 24 peripheral targets around the FE/RUD workspace of the wrist joint.	[60]
Ramp-and-Hold	2°, 4° and 8°	Wrist	7 (3 males), (38 ± 12 yr)	D	Assessed wrist joint properties with ramp-and-hold perturbations at different amplitudes and FLX torque combinations.	[34]
Ramp-and-Hold	(1) FE: -0.8–0.6rad, RUD: -0.3–0.3rad, PS: -0.8–0.8rad, (2) 0.3 rad	Wrist	10 RH (7 males), mean age 34 yr, 34-42 yr	D	Conducted (1) 1D (FE, RUD, PS) and (2) 2D (FE-RUD space) passive wrist movements with a constant velocity (< 0.2rad).	[23]
Ramp-and-Hold	Not Specified	Wrist	8 (4 males) (25 ± 4 yr)	D	Applied random Ramp-and-Hold wrist extension perturbations of different combinations of angular velocities and target torques to examine the dependency of the SRS elastic limit on joint velocity.	[16]

**Table 3.3** (Continued)

Perturbation	ROM	Joint(s)	Subjects	D/E	Experiment Description	Source
Static	10° increments of MCP joint at 60°, 0° and -60° wrist FE angles	Wrist, Fingers (MCP)	6 (3 males) (25-28yr)	D	Examined metacarpophalangeal (MCP) joint stiffness for three different wrist positions with incremental fingertip force measurement.	[17]
Static	Maximum FE limits of the MCP joint in 10° increments for wrist FE angles: 60°, 0° and -60°	Wrist, Fingers	4 (2 males) (25-28yr)	D	Measuring total passive torque at different wrist and fingertip positions.	[26]
Repeating Ramp	50°	Wrist	48 (24 males) (21-70 yr, mean age 45.3 ± 13.7)	D	Measured the Intrinsic Stiffness Index, Total Stiffness Index and Stretch Reflex Threshold Speed through different velocity wrist extension ramp tests.	[63]
Ramp	≈ 45°	Fingers	5 RH males (29.3 ± 0.2 yr)	D	Passive extension of the two fingers in five different equally spaced velocities ranging from 0.75 to 45 rad/s.	[22]
<b>Healthy and Non-Healthy<sup>b</sup></b>						
Repeating Ramp	Not Specified	Shoulder, Elbow, Wrist	3 healthy, (7 Stroke patients)	D	Investigating the effect of strenuous stretching exercise on (individual & cross-coupling) joint stiffness through different velocities passive range of motion (pROM) movements.	[88]
Static	10° to 150°, 0° to 140°, for shoulder and elbow respectively, with increments of 20°	Shoulder, Elbow	5 healthy adults (25-50 yr), 5 healthy children (13-19 yr), 5 children with disabilities (SMA, MD, Arthrogryposis) (13-18 yr)	D	Measuring the (1) static and (2) maximal isometric push-pull end-point forces and torque in the sagittal plane at different shoulder and elbow joint positions.	[65, 66]
Repeating Ramp	Full	Elbow	10 healthy (6 males) (48.5 ± 15.2 yr) and 16 Stroke patients (11 males) (51.6 ± 14.1 yr)	E	A clinician moved the subject's forearm through the elbow's full ROM at three different velocities: (1) slow (60 to 99°/s), (2) moderate (100 to 139°/s) and (3) fast (140 to 180°/s).	[76]

**Table 3.3** (Continued)

Perturbation	ROM	Joint(s)	Subjects	D/E	Experiment Description	Source
Repeating Ramp	Healthy: $107.6 \pm 8.7^\circ$ , Stroke: $74.2 \pm 21.5^\circ$	Elbow	9 healthy (9 males), ( $51.4 \pm 24.9$ yr) and 12 chronic Stroke patients (10 males), ( $53.0 \pm 8.5$ yr)	E	The therapist passively moved the subject's elbow joint at different speeds over the subject's pROM until a mechanical stop or a 3 Nm torque limit was reached.	[82]
Ramp-and-Hold	0.15 rad	Elbow	7 healthy (2 males) (21-52 yr) and 5 Obstetric brachial plexus lesion patients (1 male) (24-50 yr)	D	FE ramp-and-hold rotations (0.15 rad, 4 rad/s) while subjects applied four different torque levels (including relaxed 0 Nm).	[3]
Ramp-and-Hold	Max ROM from max extension to max FLX	Elbow	20 healthy (5 males) ( $71.2 \pm 7.2$ yr), 24 PD patients (17 males) ( $69.8 \pm 7.6$ yr)	E	Examiner passively flexed and extended the subjects' forearm from maximum EXT to maximum FLX and vice versa for 60 s with short rest in-between direction change.	[20]
Repeating Ramp	Healthy ( $142.84 \pm 10.51^\circ$ ), PD ( $125.6 \pm 14.35^\circ$ )	Elbow	11 healthy (10 males) (30-68 yr), 41 Rigidity Dominant patients (35 males) (36-75 yr)	D	Constant speed FE pROM elbow joint movement.	[71]
PRBS	0.03 rad	Elbow	14 healthy, 14 Stroke patients	D	Pseudo-random perturbations (PRBS) are applied to the elbow joint at different positions ( $45^\circ$ FLX: $15^\circ$ : $75^\circ$ EXT) around its neutral position.	[54]
FP	$60^\circ - 120^\circ$	Elbow	15 healthy, 15 Hemiparetic (Stroke) patients ( $57 \pm 10.2$ years)	D	The examiner applied sinusoidal stretches of different frequencies of manual stretch to the elbow joint.	[42]
Pendulum Swing Motion	$\approx 50^\circ$	Elbow	11 healthy RH ( $59.5 \pm 11.8$ yr), 11 Stroke patients ( $57.7 \pm 16.1$ yr)	D	Modelled the swing motion of the elbow joint from $130^\circ$ ( $0^\circ$ full extension) until it reached an equilibrium with the subject lying on a bed and relaxed.	[43]
Ramp	$20^\circ$ FLX to $30^\circ$ EXT	Wrist	17 healthy (12 males) ( $48 \pm 10$ yr), (17 Stroke patients, 5 Stroke validation group)	D	Investigated the wrist's stretch reflex through passive movements (FLX to EXT) at two different constant velocities.	[78]

**Table 3.3** (Continued)

Perturbation	ROM	Joint(s)	Subjects	D/E	Experiment Description	Source
PRBS	$\approx 2^\circ$	Wrist	14 healthy (4 males) ( $62.9 \pm 8.5$ yr), (14 PD, 4 males) ( $62.6 \pm 9.1$ yr)	D	Applied perturbations to the wrist joint to investigate the intrinsic and reflex contributions.	[83]
Repeating Ramp	$\approx 30^\circ$	Wrist	18 healthy ( $67.7 \pm 10.9$ yr), (19 PD patients) ( $69.1 \pm 9.6$ yr)	D	Investigated the co-contraction of muscles during passive movements through two different constant velocities.	[37]

The  $\approx$  sign is used to denote approximate values. D/E: Device/Examiner; PRBS: Pseudo-Random Binary Sequence joint displacement; FP: Frequency Perturbations; TP: Torque Pulse; QR: Quick Release; STD: Static Torque Displacement; MVC: Maximum Voluntary Contraction; MCP: Metacarpophalangeal; FLX: Flexion; EXT: Extension; FE: Flexion/Extension; ABD: Abduction; ADD: Adduction; IER: Interna/External Rotation; RUD: Radio-Ulnar Deviation; PS: Pronation/Supination; MD: Muscular Dystrophy; SMA: Spinal Muscular Atrophy; PD: Parkinson's Disease; RH: Right-Handed; LH: Left-Handed.

<sup>a</sup>The Perturbation column, for Duchenne Muscular Dystrophy subjects lists experiments carried out with either active or passive components. The remaining groups report only the measurement of the passive joint impedance and not additional measurements with an active component.

<sup>b</sup>Experiments investigating both healthy and non-healthy (excluding BMD and DMD) subjects, are included only for their healthy-related measurements.

**Velocity** Passive Jimp values tend to increase with rotational speed (from  $11$  to  $16^\circ/\text{s}$  and  $43$  to  $67^\circ/\text{s}$ ), for a given initial elbow joint position of ( $60^\circ$  and  $90^\circ$ ), both with and without muscle contraction [36].

Drake and Charles [18] presented that average velocities lower than  $12^\circ/\text{s}$  do not affect wrist stiffness, and Wu et al. [82] concluded that for velocities of  $90$  to  $270^\circ/\text{s}$ , the maximum resistance of the elbow increases. Moreover, high velocities can elicit a reflex response at the movement onset (see Reflex paragraph 3.3.3.4).

**Hysteresis** Evaluating the Jimp with continuous movement instead of static poses allows for observing the joint's viscous behavior and direction dependence during the loading and unloading phases of the torque-angle curve. The curves between these two phases differ, and the area between them indicates the dissipated energy. This energy dissipation results from dry friction (not velocity-dependent) and viscosity (velocity-dependent) and is typical in soft tissues, such as muscles, tendons, and connective tissue [8, 71]. In literature, this phenomenon is also referred to as the hysteresis loop [23]. The shape of the hysteresis loop can change with different amplitude and velocity perturbations [8]. Perturbing a joint around its neutral position reveals the direction dependence of the FE resistance torques [8].

Unlike conventional approaches, [20] models the passive Jimp not with a hysteresis loop, but uses two distinct linear regressions for the flexion and extension phases of the elbow joint, with the cutoff point at the elbow's equilibrium. The perturbation was, however, manually performed by a single examiner with a simple measurement instrument. So skepticism towards their results is warranted.

**Inertia - Acceleration** The limb's inertia affects the passive Jimp when high accelerations occur during the onset of a joint movement or a sudden switch in direction [71]. The inertia of a limb can vary significantly depending on a person's height and weight [86]. To exclude the effects of inertia from the passive Jimp measurements, studies like Pisano et al. [63], Sepehri et al. [71] have trimmed the data around the areas of increased acceleration.

### 3.3.3.2 Time or environmentally dependent parameters

Some parameters vary throughout the day due to environmental changes, the subject's condition, or muscle state.

**Thixotropy and Temperature** A skeletal muscle-fiber biological trait, called thixotropy, changes the muscle stiffness depending on the length and contraction history of the muscle [70]. Thixotropy develops through muscle contraction with the detachment of cross-bridges [70] and once the agitated cross-bridge is released it requires time to be re-established. This process transforms the movement from a gel-like to a soluble-like form [38]. A joint's movement is more prone to the thixotropic effect when lower frequency (e.g., 1 to 3.5 Hz) perturbations are applied to it [38]. Even a 2 s pause still results in an increased stiffness when perturbed in this frequency range [38]. Anguelova et al. [3] incorporated a 15 s rest period between their fast stretch ramp-and-hold protocol to prevent thixotropic force reductions.

Thixotropy is also affected by temperature. The bonding of cross-bridges is greater in cold conditions, as it reduces the muscle's relaxation rate and diminishes cross-bridge release. In contrast, the cross-bridges release more easily in warmer temperatures [38].

**Short-range stiffness** The Short-Range Stiffness (SRS) is a biomechanical property of the musculotendon complex that describes the higher initial stiffness at the beginning of a brief low-amplitude stretch or perturbation. It can be used as a clinical outcome measure of co-contraction and muscle weakness levels [3]. The SRS is attributed to the cross-bridges not detaching quickly enough during rapid movements. It enhances the stability and control of joints during quick transient movements or unexpected forces. The stiffness response is a time-varying parameter since it occurs at an initial perturbation after a 1 % change in the length of a muscle after a resting period of about 15 s [18]. In the wrist, this translates to the first 2° to 4° of the movement [18].

The elastic limit of SRS increases with the perturbation velocity but disappears after approximately 30 ms. Once the elastic limit is reached, the stiffness returns to its 'normal' resting levels where, assuming a linear system, the muscle behaves like a viscous damper [16]. However, at slower velocities, the SRS is not consistently observed [16].

MacKay et al. [48], observed SRS in the elbow joint with two frequency perturbations (natural frequency in the range of 2 to 3 Hz) and static displacements. During static displacements, SRS stiffness reached values of 4 to 5 Nm/rad (four times the stiffness of greater displacements), while with oscillations, SRS reached 14 to 18 Nm/rad at the initial 0.1 rad (5.7°) of the perturbation. When SRS is not of interest, the initial response to the perturbation can be excluded from the analysis. For instance, Pando et al. [60] neglected the first 2° of the wrist movement in their analysis.

**Fatigue** In fatigability, a distinction is made between central (e.g., changes in motor neurons) and peripheral fatigue (e.g., changes at the muscle level). However, these two are interdependent [1]. When fatigued, more motor units are recruited to match the pre-fatigue torque levels. Additionally, an individual's homeostasis and psychological state influence perceived fatigability [1]. Early onset of fatigue is typical in muscle dystrophies [1, 2] and can affect both Jimp and muscle strength.

Zhang et al. [87] observed a reduction in producible torque after investigating the effects of fatigue on the elbow joint in five healthy individuals. They found reduced stiffness and increased viscosity in the elbow as participants actively resisted the perturbations at various torque levels [87]. Similarly, Albanese et al. [1] found that wrist stiffness, modelled using a linear second-order mass-spring-damper system, decreased after fatigue. Here, the participants were asked to naturally grasp the wrist perturbation handle and not intervene or resist the perturbations. These effects are presumably restored within 60 to 90 min [1, 38]. To avoid fatigue during experiments, rest periods can be incorporated between measurements. For instance, Pisano et al. [63] used 10 s rest intervals, whereas Zhang et al. [87] avoided acute fatigue with 10 min breaks.

In contrast to fatigue-induced decreases in Jimp levels, Jones et al. [32] found that the passive muscles were mechanically stiffer, and the resting joint position shifted to a more flexed angle of 6° to 20° following damaging exercise with repetitive eccentric MVC elbow contractions. These damaging effects were observed as early as the next day and lasted up to a week. Bottas et al. [9] also conducted a similar study on exercise-induced muscle damage and found increased passive Jimp and reduced elbow ROM lasting more than eight days.

### 3.3.3.3 Training related

Engaging in physical activities frequently alters muscle anatomy and can lead to changes in passive Jimp. For instance, Wiegner and Watts [80] found that the upper arm volume significantly correlates with elbow Jimp [80]. Moreover, compared to the non-dominant hand, the dominant hand shows greater stiffness [19]. This could result from changes in the myofibril structure, leading to a higher percentage of slow-twitch fibers in the dominant arm [19]. A higher cross-sectional muscle area is associated with power activities.

On the contrary, stretching exercises can reduce Jimp. A half-hour strenuous stretching session of the shoulder, elbow and wrist joints resulted in a reduced elbow coupling torque in stroke subjects [88]. Additionally, stretching can have a short-term positive effect on the Jimp and both active and passive ROM in chronic stroke patients [67]. This can also be, however, the result of increased tolerance to stretching [67].

### 3.3.3.4 Reflexes or volition dependent parameters

This category lists parameters which depend on an active response from reflexes or voluntary contraction.

**Co-contraction** In addition to passive Jimp, agonist-antagonist muscle activation can substantially increase the overall Jimp improving the stability of a joint [11, 18, 27, 28, 37], either voluntary or as a result of a reflex response. The increase caused by the active Jimp components can vary depending on the joint's position [37] and there is a trade-off

between the gained stability and the metabolic efficiency, as co-contraction is energetically costly [27].

Moreover, anticipation can play a role in the active Jimp. Holmes et al. [28] compared the wrist FE torque between an anticipated and unknown perturbation. They discovered that an anticipated perturbation can lead to an increased Jimp.

**Stretch reflex** Several studies have investigated the reflex response to high velocity perturbations [9, 34, 42, 48, 63, 73, 78, 82]. The reflex loop differentiates reflex contributions from active Jimp by introducing a delay [87]. MacKay et al. [48] identified the onset of this response at approximately 90 ms after the perturbation onset. This response increases the number of active cross-bridges, thereby increasing the active Jimp [73]. At slow velocities, the reflex response is minimal or absent [18, 78, 82, 88]. According to Pisano et al. [63], Wiegner and Watts [80], Wu et al. [82], no reflex response is observed for velocities lower than 10, 20 and 30 °/s, respectively.

Several studies [1, 9, 34, 42, 63, 82, 85] used high velocities (60, 100, 171, 180, 230, 270, 280 and 500 °/s, respectively) to induce a reflex response. In some participants, Pisano et al. [63] identified the stretch reflex threshold ranging between 60 and 500 °/s, whereas in others, there was no reflex response observed at all. Wiegner and Watts [80] report a reflex threshold of 100 °/s and since the reflex occurs less frequently when the subjects relax more, they discovered that the reflex response is also a function of the applied torque and relaxation state of the subject.

Additionally, the response amplitude varies between muscles and joint positions [85] and ischemia can completely block the reflex response [73].

### 3.4 Discussion

This study highlights the importance of accurately identifying passive Jimp in individuals with DMD. Unfortunately, in DMD, very little is known about the elevated and non-linear nature of the passive Jimp over the variable passive ROM. Accurate models of Jimp behavior can help differentiate between voluntary movement intentions, the effects of gravity, and passive Jimp in the UE. This differentiation is crucial for developing force-based control in active assistive arm supports. This review clarifies the terminology around the passive Jimp and provides an overview of ways to identify the passive Jimp in the UE. Additionally, it discusses the parameters that can affect passive Jimp and should be taken into consideration.

The literature reveals considerable variations in the definitions and methodologies used to measure passive Jimp across different studies. Despite differences in terminology, there is a consensus that passive Jimp refers to the resistance against an applied joint rotation caused by the passive biomechanical properties of the muscles, tendons, and tissues around the joint, as well as the limb's inertia [49]. Given an applied perturbation, the torque-angle relationship reveals the characteristics of the passive Jimp.

This study reviews the various perturbation methods used in the literature to impose a passive movement and measure the applied joint torque. Static, frequency, and ramp-type are the most frequently used movement perturbations for quantifying passive Jimp. The choice between static and dynamic methodologies is at the researcher's discretion, depending on their specific field of interest. A limitation of this study is its narrative focus

on individuals with DMD and the healthy population, which may have restricted the range of identified experimental methods.

Static experiments yield a measure of passive Jimp before movement onset, excluding the velocity effects. Velocity can affect the passive Jimp, with no, to little increase when the movement is slow [18], and higher increase at higher velocities [82]. With frequency perturbations, fast movements over small ROM are provided. Frequency perturbations allow for system identification techniques to model the biomechanical behavior of a human joint [13, 86, 87]. However, since they only consider a small ROM and assume linear biomechanical behavior within the considered ROM [33], they do not include the non-linearities over the entire ROM.

When performing the perturbations, the ‘fixed or biologically dependent parameters’ mentioned, such as joint position, velocity, and movement direction, should be considered. The movement direction affects the torque-angle relationship showing a hysteresis loop [8]. The position and velocity parameters can affect the passive Jimp over the entire ROM. Due to the anatomy of the UE muscles, the multiarticular muscles cause cross-coupling torques between the joints, causing the ‘position’ to be a multi-dimensional parameter. Velocities higher than  $60^\circ/\text{s}$  [63] and  $100^\circ/\text{s}$  [80] could trigger a reflex response [63, 80, 82]. The reflex response should be avoided when examining only the ‘passive’ Jimp components. For instance, Wiegner and Watts [80] selected a maximal velocity of  $20^\circ/\text{s}$  to ensure that reflexes would not confound. When perturbations are applied with changing velocities, accelerations and the limb’s inertia also play a role. Understanding the relation of the position and velocity perturbations to the passive Jimp, could provide a basic model of the passive Jimp behavior. Additional effects of other parameters, such as the SRS that only affects the onset of a movement [3], the environmental temperature that affects the passive Jimp in cold conditions, or the muscle’s fatigue, could be considered. Exploring the effect of one parameter while eliminating the effects of others may be impossible. However, careful consideration can minimize their impact on passive Jimp. Understanding these parameters and their effects on passive Jimp is essential when designing experiments and interpreting results.

For DMD in particular, most studies have utilized ramp-type perturbations, which involve applying a slow, constant velocity across a large ROM of the joint. These perturbation methods reveal the limited passive ROM as a result of joint contractures [40, 54] and show the non-linear behavior of the Jimp. Considering the relatively slow arm movements in this application of motorized arm supports [25], the position and velocity dependencies seem more relevant than the inertia dependency. So, ramp-type methods emerge as the most suitable technique for characterizing joint impedance over the full ROM and account for the non-linear characteristics of passive Jimp in DMD.

Standardizing the terminology around Jimp and methodologies used to identify it, including prioritizing the affecting parameters, may lead to better assistive devices. Ultimately improving the quality of life for individuals with DMD.



### 3.5 Conclusion

In conclusion, to identify the elevated and non-linear behavior of the passive Jimp in DMD, the ramp-type perturbations, where a constant velocity movement is applied to a larger ROM of the joint, seem most appropriate for the application of accurate and personalized passive Jimp compensation in active assistive arm supports. The identification of passive Jimp does, however, require careful consideration of the parameters affecting it. It is recommended to first examine the influence of the joint's position, including the influence of multiarticular muscles and the effect of different movement velocities over other parameters; to form the basis of an accurate and personalized Jimp compensation model.

## References

- [1] G. A. Albanese, V. Falzarano, M. W. Holmes, P. Morasso, and J. Zenzeri. A Dynamic Sub-maximal Fatigue Protocol Alters Wrist Biomechanical Properties and Proprioception. *Frontiers in Human Neuroscience*, 16(May):1–14, 2022. doi: 10.3389/fnhum.2022.887270.
- [2] C. Angelini and E. Tasca. Fatigue in muscular dystrophies. *Neuromuscular Disorders*, 22(Suppl. 3):S214—S220, 2012. doi: 10.1016/j.nmd.2012.10.010.
- [3] G. V. Anguelova, E. de Vlugt, A. N. Vardy, E. W. van Zwet, J. G. van Dijk, M. J. Malessy, and J. H. de Groot. Cocontraction measured with short-range stiffness was higher in obstetric brachial plexus lesions patients compared to healthy subjects. *Journal of Biomechanics*, 63:192–196, 2017. doi: 10.1016/j.jbiomech.2017.08.015.
- [4] M. H. Azarsa, A. Mirbagheri, S. R. Hosseini, A. Shadmehr, and N. Karimi. Objective measurement of Inferior-Directed stiffness in glenohumeral joint using a specially designed robotic device in healthy shoulders; Within- and Between-Session reliability. *Journal of Biomechanics*, 127(August), 2021. doi: 10.1016/j.jbiomech.2021.110663.
- [5] R. Bhimani, J. E. Gaugler, and J. Felts. Consensus Definition of Muscle Tightness From Multidisciplinary Perspectives. *Nursing research*, 69(2):109–115, 2020. doi: 10.1097/NNR.0000000000000404.
- [6] R. H. Bhimani and D. Soomar. Understanding Symptoms of Muscle Tightness, Weakness, and Rigidity From a Nursing Perspective. *Rehabilitation Nursing*, 44(5):271–281, sep 2019. doi: 10.1097/rnj.0000000000000151.
- [7] C. Billian and G. I. Zahalak. A Programmable Limb Testing System (and Some Measurements of Intrinsic Muscular and Reflex-Mediated Stiffnesses). *Journal of Biomechanical Engineering*, 105(1):6–11, 1983. doi: 10.1115/1.3138387.
- [8] K. L. Boon, A. L. Hof, and W. Wallinga-de Jonge. The Mechanical Behaviour of the Passive Arm. *Medicine and Sport*, 8(Biomechanics III):243–248, 1973.
- [9] R. Bottas, K. Miettunen, P. V. Komi, and V. Linnamo. Disturbed motor control of rhythmic movement at 2 h and delayed after maximal eccentric actions. *Journal of Electromyography and Kinesiology*, 20(4):608–618, 2010. doi: 10.1016/j.jelekin.2009.11.010.
- [10] M. H. Brooke, R. C. Griggs, J. R. Mendell, G. M. Fenichel, J. B. Shumate, and R. J. Pellegrino. Clinical trial in Duchenne dystrophy. I. The design of the protocol. *Muscle & nerve*, 4(3):186–197, 1981. doi: 10.1002/mus.880040304.
- [11] L. L. Chuang, C. Y. Wu, and K. C. Lin. Reliability, validity, and responsiveness of myotonometric measurement of muscle tone, elasticity, and stiffness in patients with stroke. *Archives of Physical Medicine and Rehabilitation*, 93(3):532–540, 2012. doi: 10.1016/j.apmr.2011.09.014.
- [12] E. Churchill, L. L. Laubach, J. T. Mcconville, and I. Tebbetts. *Anthropometry for Designers*. NASA Ref Publication 1024, 1978.

- [13] C. Cornu, F. Goubel, and M. Fardeau. Muscle and joint elastic properties during elbow flexion in Duchenne muscular dystrophy. *The Journal of Physiology*, 533(2):605–616, 2001. doi: 10.1111/j.1469-7793.2001.0605a.x.
- [14] S. Crisafulli, J. Sultana, A. Fontana, F. Salvo, S. Messina, and G. Trifirò. Global epidemiology of Duchenne muscular dystrophy: An updated systematic review and meta-analysis. *Orphanet Journal of Rare Diseases*, 15(1), 2020. doi: 10.1186/s13023-020-01430-8.
- [15] H. Dai and L. T. D’Angelo. A portable system for quantitative assessment of parkinsonian bradykinesia during deep-brain stimulation surgery. *2013 2nd International Conference on Advances in Biomedical Engineering, ICABME 2013*, pages 77–80, 2013. doi: 10.1109/ICABME.2013.6648851.
- [16] E. de Vlugt, S. van Eesbeek, P. Baines, J. Hilde, C. G. Meskers, and J. H. de Groot. Short range stiffness elastic limit depends on joint velocity. *Journal of Biomechanics*, 44(11): 2106–2112, 2011. doi: 10.1016/j.jbiomech.2011.05.022.
- [17] A. D. Deshpande, N. Gialias, and Y. Matsuoka. Contributions of intrinsic visco-elastic torques during planar index finger and wrist movements. *IEEE Transactions on Biomedical Engineering*, 59(2):586–594, 2012. doi: 10.1109/TBME.2011.2178240.
- [18] W. B. Drake and S. K. Charles. Passive stiffness of coupled wrist and forearm rotations. *Annals of Biomedical Engineering*, 42(9):1853–1866, 2014. doi: 10.1007/s10439-014-1054-0.
- [19] S. Durand, C. P. Y. Rohan, T. Hamilton, W. Skalli, and H. I. Krebs. Passive Wrist Stiffness: The Influence of Handedness. *IEEE Transactions on Biomedical Engineering*, 66(3):656–665, 2019. doi: 10.1109/TBME.2018.2853591.
- [20] T. Endo, T. Hamasaki, R. Okuno, M. Yokoe, H. Fujimura, K. Akazawa, and S. Sakoda. Parkinsonian rigidity shows variable properties depending on the elbow joint angle. *Parkinson’s Disease*, 2013:1–5, 2013. doi: 10.1155/2013/258374.
- [21] S. J. Filius, J. Harlaar, L. Alberts, S. Houwen-van Opstal, H. van der Kooij, and M. M. Janssen. Design requirements of upper extremity supports for daily use in Duchenne muscular dystrophy with severe muscle weakness. *Journal of Rehabilitation and Assistive Technologies Engineering*, 11(March):1–18, 2024. doi: 10.1177/20556683241228478.
- [22] A. E. Fiorilla, F. Nori, L. Masia, and G. Sandini. Finger impedance evaluation by means of hand exoskeleton. *Annals of Biomedical Engineering*, 39(12):2945–2954, 2011. doi: 10.1007/s10439-011-0381-7.
- [23] D. Formica, S. K. Charles, L. Zollo, E. Guglielmelli, N. Hogan, and H. I. Krebs. The passive stiffness of the wrist and forearm. *Journal of Neurophysiology*, 108(4):1158–1166, 2012. doi: 10.1152/jn.01014.2011.
- [24] K. Fujimura, M. Mukaino, S. Itoh, H. Miwa, R. Itoh, D. Narukawa, H. Tanikawa, Y. Kanada, E. Saitoh, and Y. Otaka. Requirements for Eliciting a Spastic Response

- With Passive Joint Movements and the Influence of Velocity on Response Patterns: An Experimental Study of Velocity-Response Relationships in Mild Spasticity With Repeated-Measures Analysis. *Frontiers in Neurology*, 13(March):1–9, 2022. doi: 10.3389/fneur.2022.854125.
- [25] M. Gandolla, S. Dalla Gasperina, V. Longatelli, A. Manti, L. Aquilante, M. G. D'Angelo, E. Biffi, E. Diella, F. Molteni, M. Rossini, M. Gföhler, M. Puchinger, M. Bocciolone, F. Braghin, and A. Pedrocchi. An assistive upper-limb exoskeleton controlled by multi-modal interfaces for severely impaired patients: development and experimental assessment. *Robotics and Autonomous Systems*, 143, 2021. doi: 10.1016/j.robot.2021.103822.
- [26] N. Gialias and Y. Matsuoka. A musculotendon contribution for multijoint hand control. *Annual International Conference of the IEEE Engineering in Medicine and Biology - Proceedings*, pages 4482–4485, 2006. doi: 10.1109/IEMBS.2006.259701.
- [27] T. L. Gibo, A. J. Bastian, and A. M. Okamura. Effect of age on stiffness modulation during postural maintenance of the arm. In *IEEE International Conference on Rehabilitation Robotics*, pages 1–17, 2013. doi: 10.1109/ICORR.2013.6650395.
- [28] M. W. Holmes, J. Tat, and P. J. Keir. Neuromechanical control of the forearm muscles during gripping with sudden flexion and extension wrist perturbations. *Computer Methods in Biomechanics and Biomedical Engineering*, 18(16):1826–1834, 2015. doi: 10.1080/10255842.2014.976811.
- [29] S. L. Houwen-Van Opstal, Y. M. Van Den Elzen, M. Jansen, M. A. Willemsen, E. H. Cup, and I. J. De Groot. Facilitators and Barriers to Wearing Hand Orthoses by Adults with Duchenne Muscular Dystrophy: A Mixed Methods Study Design. *Journal of Neuromuscular Diseases*, 7(4):467–475, 2020. doi: 10.3233/JND-200506.
- [30] M. M. H. P. Janssen, A. Bergsma, A. C. Geurts, and I. J. De Groot. Patterns of decline in upper limb function of boys and men with DMD: An international survey. *Journal of Neurology*, 261(7):1269–1288, 2014. doi: 10.1007/s00415-014-7316-9.
- [31] M. M. H. P. Janssen, J. Harlaar, B. Koopman, and I. J. M. de Groot. Dynamic arm study: Quantitative description of upper extremity function and activity of boys and men with duchenne muscular dystrophy. *Journal of NeuroEngineering and Rehabilitation*, 14(1):45, 2017. doi: 10.1186/s12984-017-0259-5.
- [32] D. A. Jones, D. J. Newham, and P. M. Clarkson. Skeletal muscle stiffness and pain following eccentric exercise of the elbow flexors. *Pain*, 30(2):233–242, 1987. doi: 10.1016/0304-3959(87)91079-7.
- [33] A. Klomp, J. H. D. Groot, E. D. Vlugt, C. G. M. Meskers, J. H. Arendzen, and F. C. T. V. D. Helm. Perturbation Amplitude Affects Linearly Estimated Neuromechanical Wrist Joint Properties Asbjørn. *Ieee Transactions on Biomedical Engineering*, 61(4): 1005–1014, 2014.

- [34] A. Klomp, E. de Vlught, J. H. de Groot, C. G. Meskers, J. H. Arendzen, and F. C. van der Helm. Perturbation velocity affects linearly estimated neuromechanical wrist joint properties. *Journal of Biomechanics*, 74:207–212, 2018. doi: 10.1016/j.jbiomech.2018.04.007.
- [35] P. N. Kooren, A. G. Dunning, M. M. H. P. Janssen, J. Lobo-Prat, B. F. Koopman, M. I. Paalman, I. J. De Groot, and J. L. Herder. Design and pilot validation of A-gear: A novel wearable dynamic arm support. *Journal of NeuroEngineering and Rehabilitation*, 12(1):1–12, 2015. doi: 10.1186/s12984-015-0072-y.
- [36] L. Kuxhaus, S. Zeng, and C. J. Robinson. Dependence of elbow joint stiffness measurements on speed, angle, and muscle contraction level. *Journal of Biomechanics*, 47(5):1234–1237, 2014. doi: 10.1016/j.jbiomech.2013.12.008.
- [37] Y. Kwon, J. W. Kim, Y. Ho, H. M. Jeon, M. J. Bang, G. M. Eom, and S. B. Koh. Analysis of antagonistic co-contractions with motorized passive movement device in patients with parkinson’s disease. *Bio-Medical Materials and Engineering*, 24(6):2291–2297, 2014. doi: 10.3233/BME-141042.
- [38] M. Lakie, E. G. Walsh, and G. W. Wright. Control and postural thixotropy of the forearm muscles: Changes caused by cold. *Journal of Neurology Neurosurgery and Psychiatry*, 49(1):69–76, 1986. doi: 10.1136/jnnp.49.1.69.
- [39] J. W. Lance. *Spasticity: Disordered Motor Control*, pages 485–495. Chicago: Year Book Medical Publishers, 1980.
- [40] D. Landin and M. Thompson. The shoulder extension function of the triceps brachii. *Journal of Electromyography and Kinesiology*, 21(1):161–165, 2011. doi: 10.1016/j.jelekin.2010.09.005.
- [41] M. L. Latash and V. M. Zatsiorsky. Joint stiffness: Myth or reality? *Human Movement Science*, 12(6):653–692, 1993. doi: 10.1016/0167-9457(93)90010-M.
- [42] H. Lee, J. J. Chen, M. Ju, C. K. Lin, and P. P. W. Poon. Validation of portable muscle tone measurement device for quantifying velocity-dependent properties in elbow spasticity. *Journal of Electromyography and Kinesiology*, 14(5):577–589, 2004.
- [43] C. C. Lin, M. S. Ju, and C. W. Lin. The pendulum test for evaluating spasticity of the elbow joint. *Archives of Physical Medicine and Rehabilitation*, 84(1):69–74, 2003. doi: 10.1053/apmr.2003.50066.
- [44] H. Lin, A. Hsu, C. C. Jia-Rea, and G. Chang. Quantification of shoulder joint passive rotation range of motion in vivo. *Journal of Medical and Biological Engineering*, 24: 163–169, 2004.
- [45] J. Lobo-Prat, A. Q. L. Keemink, B. F. J. M. Koopman, A. H. A. Stienen, and P. H. Veltink. Adaptive gravity and joint stiffness compensation methods for force-controlled arm supports. In *IEEE International Conference on Rehabilitation Robotics*, volume 2015-Septe, pages 478–483. IEEE, 2015. doi: 10.1109/ICORR.2015.7281245.

- [46] J. Lobo-Prat, P. N. Kooren, M. M. H. P. Janssen, A. Q. Keemink, P. H. Veltink, A. H. Stienen, and B. F. Koopman. Implementation of EMG-and force-based control interfaces in active elbow supports for men with duchenne muscular dystrophy: a feasibility study. *IEEE Transactions on Neural Systems and Rehabilitation Engineering*, 24(11):1179–1190, 2016. doi: 10.1109/TNSRE.2016.2530762.
- [47] J. Lobo-Prat, K. Nizamis, M. M. H. P. Janssen, A. Q. Keemink, P. H. Veltink, B. F. Koopman, and A. H. Stienen. Comparison between sEMG and force as control interfaces to support planar arm movements in adults with Duchenne: A feasibility study. *Journal of NeuroEngineering and Rehabilitation*, 14(1):1–17, 2017. doi: 10.1186/s12984-017-0282-6.
- [48] W. A. MacKay, D. J. Crammond, H. C. Kwan, and J. T. Murphy. Measurements of human forearm viscoelasticity. *Journal of Biomechanics*, 19(3):231–238, 1986. doi: 10.1016/0021-9290(86)90155-7.
- [49] S. Maggioni, A. Melendez-Calderon, E. Van Asseldonk, V. Klamroth-Marganska, L. Lünenburger, R. Riener, and H. Van Der Kooij. Robot-aided assessment of lower extremity functions: A review. *Journal of NeuroEngineering and Rehabilitation*, 13(1):1–25, 2016. doi: 10.1186/s12984-016-0180-3.
- [50] S. Malhotra, A. D. Pandyan, C. R. Day, P. W. Jones, and H. Hermens. Spasticity, an impairment that is poorly defined and poorly measured. *Clinical Rehabilitation*, 23(7): 651–658, 2009. doi: 10.1177/0269215508101747.
- [51] A. G. Mayhew, G. Coratti, E. S. Mazzone, K. Klingels, M. James, M. Pane, V. Straub, N. Goemans, E. Mercuri, and P. W. Group. Performance of Upper Limb module for Duchenne muscular dystrophy. *Developmental Medicine & Child Neurology*, 62(5): 633–639, 2020.
- [52] C. M. McDonald, R. T. Abresch, G. T. Carter, W. M. J. Fowler, E. R. Johnson, D. D. Kilmer, and B. J. Sigford. Profiles of neuromuscular diseases. *American Journal of Physical Medicine and Rehabilitation*, 74(5 Suppl.):S70–92, 1995. doi: 10.1097/00002060-199509001-00003.
- [53] J. R. Mendell and M. Lloyd-Puryear. Report of MDA muscle disease symposium on newborn screening for Duchenne muscular dystrophy. *Muscle & nerve*, 48(1):21–26, 2013.
- [54] M. M. Mirbagheri, L. AliBiglou, M. Thajchayapong, T. Lilaonitkul, and W. Z. Rymer. Comparison of neuromuscular abnormalities between upper and lower extremities in hemiparetic stroke. *Annual International Conference of the IEEE Engineering in Medicine and Biology - Proceedings*, pages 303–306, 2006. doi: 10.1109/IEMBS.2006.260530.
- [55] M. M. Mirbagheri, K. Settle, R. Harvey, and W. Z. Rymer. Neuromuscular abnormalities associated with spasticity of upper extremity muscles in hemiparetic stroke. *Journal of Neurophysiology*, 98(2):629–637, 2007. doi: 10.1152/jn.00049.2007.

- [56] National Library of Medicine Medical Subject Heading Descriptor Data 2022. Muscle Rigidity, 1999. URL <https://meshb.nlm.nih.gov/record/ui?ui=D009127>.
- [57] National Library of Medicine Medical Subject Heading Descriptor Data 2022. Myotonia, 1999. URL <https://meshb.nlm.nih.gov/record/ui?ui=D009222>.
- [58] National Library of Medicine Medical Subject Heading Descriptor Data 2022. Muscle Tonus, 2008. URL <https://meshb.nlm.nih.gov/record/ui?ui=D009129>.
- [59] M. J. Page, J. E. McKenzie, P. M. Bossuyt, I. Boutron, T. C. Hoffmann, C. D. Mulrow, L. Shamseer, J. M. Tetzlaff, E. A. Akl, S. E. Brennan, R. Chou, J. Glanville, J. M. Grimshaw, A. Hróbjartsson, M. M. Lalu, T. Li, E. W. Loder, E. Mayo-Wilson, S. McDonald, L. A. McGuinness, L. A. Stewart, J. Thomas, A. C. Tricco, V. A. Welch, P. Whiting, and D. Moher. The PRISMA 2020 statement: an updated guideline for reporting systematic reviews. *BMJ* 2021, 372:n71, 2021. doi: 10.1136/bmj.n71.
- [60] A. L. Pando, H. Lee, W. B. Drake, N. Hogan, and S. K. Charles. Position-dependent characterization of passive wrist stiffness. *IEEE Transactions on Biomedical Engineering*, 61(8):2235–2244, 2014. doi: 10.1109/TBME.2014.2313532.
- [61] S. Pandya, J. M. Florence, W. M. King, J. D. Robison, M. Oxman, and M. A. Province. Reliability of goniometric measurements in patients with duchenne muscular dystrophy. *Physical Therapy*, 65(9):1339–1342, 09 1985. doi: 10.1093/ptj/65.9.1339.
- [62] K. Park, P. H. Chang, and S. H. Kang. In vivo estimation of human forearm and wrist dynamic properties. *IEEE Transactions on Neural Systems and Rehabilitation Engineering*, 25(5):436–446, 2017. doi: 10.1109/TNSRE.2016.2573844.
- [63] F. Pisano, G. Miscio, R. Colombo, and P. Pinelli. Quantitative evaluation of normal muscle tone. *Journal of the Neurological Sciences*, 135(2):168–172, 1996. doi: 10.1016/0022-510X(95)00291-9.
- [64] E. Pontén, S. Gantelius, and R. L. Lieber. Intraoperative muscle measurements reveal a relationship between contracture formation and muscle remodeling. *Muscle and Nerve*, 36(1):47–54, 2007. doi: 10.1002/mus.20780.
- [65] D. Ragonesi, S. K. Agrawal, W. Sample, and T. Rahman. Quantifying anti-gravity torques in the design of a powered exoskeleton. In *Proceedings of the Annual International Conference of the IEEE Engineering in Medicine and Biology Society, EMBS*, volume 21, pages 7458–7461. IEEE, 2011. doi: 10.1109/IEMBS.2011.6091749.
- [66] D. Ragonesi, S. K. Agrawal, W. Sample, and T. Rahman. Quantifying anti-gravity torques for the design of a powered exoskeleton. *IEEE Transactions on Neural Systems and Rehabilitation Engineering*, 21(2):283–288, 2013. doi: 10.1109/TNSRE.2012.2222047.
- [67] S. Rao, M. Huang, S. G. Chung, and L. Q. Zhang. Effect of Stretching of Spastic Elbow Under Intelligent Control in Chronic Stroke Survivors—A Pilot Study. *Frontiers in Neurology*, 12(December):1–10, 2021. doi: 10.3389/fneur.2021.742260.



- [68] L. Roberson and D. J. Giurintano. Objective measures of joint stiffness. *Journal of Hand Therapy*, 8(2):163–166, 1995.
- [69] A. C. Schouten, E. de Vlugt, J. J. B. van Hilten, and F. C. T. van der Helm. Design of a torque-controlled manipulator to analyse the admittance of the wrist joint. *Journal of neuroscience methods*, 154(1-2):134–141, 2006.
- [70] C. Sekihara, M. Izumizaki, T. Yasuda, T. Nakajima, T. Atsumi, and I. Homma. Effect of cooling on thixotropic position-sense error in human biceps muscle. *Muscle and Nerve*, 35(6):781–787, 2007. doi: 10.1002/mus.20779.
- [71] B. Sepehri, A. Esteki, E. Ebrahimi-Takamjani, G. A. Shahidi, F. Khamseh, and M. Moinodin. Quantification of rigidity in Parkinson’s disease. *Annals of Biomedical Engineering*, 35(12):2196–2203, 2007. doi: 10.1007/s10439-007-9379-6.
- [72] D. Shin, J. Kim, and Y. Koike. A myokinetic arm model for estimating joint torque and stiffness from EMG signals during maintained posture. *Journal of Neurophysiology*, 101(1):387–401, 2009. doi: 10.1152/jn.00584.2007.
- [73] T. Sinkjaer and R. Hayashi. Regulation of wrist stiffness by the stretch reflex. *Journal of Biomechanics*, 22(11-12):1133–1140, 1989. doi: 10.1016/0021-9290(89)90215-7.
- [74] P. T. Straathof, J. Lobo-Prat, F. Schilder, P. N. Kooren, M. I. Paalman, A. H. Stienen, and B. F. Koopman. Design and control of the A-Arm: An active planar arm support for adults with Duchenne muscular dystrophy. *Proceedings of the IEEE RAS and EMBS International Conference on Biomedical Robotics and Biomechatronics*, 2016-July: 1242–1247, 2016. doi: 10.1109/BIOROB.2016.7523801.
- [75] J. C. van den Noort, L. Bar-On, E. Aertbeliën, M. Bonikowski, S. M. Braendvik, E. W. Broström, A. I. Buizer, J. H. Burridge, A. van Campenhout, B. Dan, J. F. Fleuren, S. Grunt, F. Heinen, H. L. Horemans, C. Jansen, A. Kranzl, B. K. Krautwurst, M. van der Krogt, S. Lerma Lara, C. M. Lidbeck, J. P. Lin, I. Martinez, C. Meskers, D. Metaxiotis, G. Molenaers, D. A. Patikas, O. Rémy-Néris, K. Roeleveld, A. P. Shortland, J. Sikkens, L. Sloot, R. J. Vermeulen, C. Wimmer, A. S. Schröder, S. Schless, J. G. Becher, K. Desloovere, and J. Harlaar. European consensus on the concepts and measurement of the pathophysiological neuromuscular responses to passive muscle stretch. *European Journal of Neurology*, 24(7):981–e38, 2017. doi: 10.1111/ene.13322.
- [76] C. Wang, L. Peng, Z. G. Hou, and P. Zhang. The Assessment of Upper-Limb Spasticity Based on a Multi-Layer Process Using a Portable Measurement System. *IEEE Transactions on Neural Systems and Rehabilitation Engineering*, 29(Mas 3):2242–2251, 2021. doi: 10.1109/TNSRE.2021.3121780.
- [77] J. F. Wang, J. Forst, S. Schröder, and J. M. Schröder. Correlation of muscle fiber type measurements with clinical and molecular genetic data in Duchenne muscular dystrophy. *Neuromuscular Disorders*, 9(3):150–158, 1999. doi: 10.1016/S0960-8966(98)00114-X.



- [78] R. Wang, P. Herman, Ekeberg, J. Gäverth, A. Fagergren, and H. Forssberg. Neural and non-neural related properties in the spastic wrist flexors: An optimization study. *Medical Engineering and Physics*, 47:198–209, 2017. doi: 10.1016/j.medengphy.2017.06.023.
- [79] J. Weichbrodt, B. M. Eriksson, and A. K. Kroksmark. Evaluation of hand orthoses in Duchenne muscular dystrophy. *Disability and Rehabilitation*, 40(23):2824–2832, 2018. doi: 10.1080/09638288.2017.1347721.
- [80] A. W. Wiegner and R. L. Watts. Elastic properties of muscles measured at the elbow in man: I. Normal controls. *Journal of Neurology, Neurosurgery & Psychiatry*, 49(10):1171–1176, 1986. doi: 10.1136/JNNP.49.10.1171.
- [81] J. M. Winters and D. G. Klewen. Effect of initial upper-limb alignment on muscle contributions to isometric strength curves. *Journal of Biomechanics*, 26(2):143–153, 1993. doi: 10.1016/0021-9290(93)90045-G.
- [82] Y. N. Wu, H. S. Park, J. Chen, Y. Ren, E. J. Roth, and L. Zhang. Position as well as velocity dependence of spasticity-four-dimensional characterizations of catch angle. *Frontiers in Neurology*, 9(OCT):1–10, 2018. doi: 10.3389/fneur.2018.00863.
- [83] R. P. Xia, A. Muthumani, Z. H. Mao, and D. W. Powell. Quantification of neural reflex and muscular intrinsic contributions to parkinsonian rigidity. *Experimental Brain Research*, 234(12):3587–3595, 2016. doi: 10.1007/s00221-016-4755-9.
- [84] Y. Yahya, I. Hunter, T. Besier, A. Taberner, and B. Ruddy. Shoulder Joint Stiffness in a Functional Posture at Various Levels of Muscle Activation. *IEEE Transactions on Biomedical Engineering*, 69(7):2192–2201, 2022. doi: 10.1109/TBME.2021.3138398.
- [85] S. I. Yamamoto, K. Nakazawa, H. Yano, and T. Ohtsuki. Differential angle-dependent modulation of the long-latency stretch reflex responses in elbow flexion synergists. *Journal of Electromyography and Kinesiology*, 10(2):135–142, 2000. doi: 10.1016/S1050-6411(99)00025-5.
- [86] L. Q. Zhang, G. H. Portland, G. Wang, C. A. Diraimondo, G. W. Nuber, M. K. Bowen, and R. W. Hendrix. Stiffness, viscosity, and upper-limb inertia about the glenohumeral abduction axis. *Journal of Orthopaedic Research*, 18(1):94–100, jan 2000. doi: 10.1002/JOR.1100180114.
- [87] L. Q. Zhang, W. Zev Rymer, and W. Z. Rymer. Reflex and intrinsic changes induced by fatigue of human elbow extensor muscles. *Journal of Neurophysiology*, 86(3):1086–1094, sep 2001. doi: 10.1152/jn.2001.86.3.1086.
- [88] L. Q. Zhang, H. Park, and Y. Ren. Shoulder, elbow and wrist stiffness in passive movement and their independent control in voluntary movement post stroke. In *2009 IEEE International Conference on Rehabilitation Robotics, ICORR 2009*, pages 805–811. 11th International Conference on Rehabilitation Robotics Kyoto International Conference Center, Japan, June 23-26, 2009. doi: 10.1109/ICORR.2009.5209489.



# II

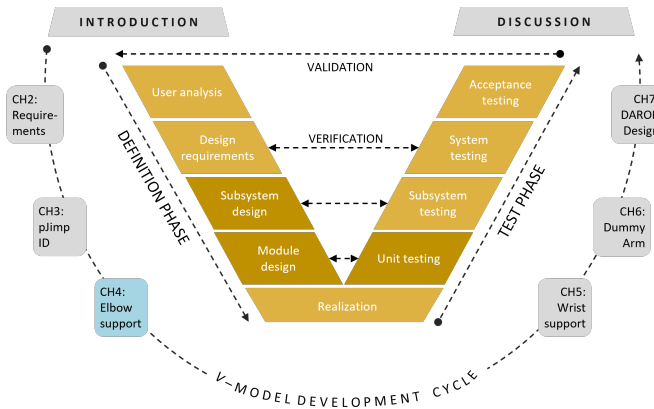
## Subsystem Design, Module Design, and Unit Testing



# 4

## Comparison of Weight and Passive Elbow Joint Impedance Compensation

Part I focused on the *user analysis* and *design requirements*. Part II focuses on *subsystem design*, *module design*, and *unit testing* of the V-model.



When the first ‘test actuator’ was ready for *unit testing*, we created a *subsystem* in the form of an elbow support. This chapter identifies the passive joint impedance and compares various compensation strategies for the elbow joint.

This chapter was published as: S. Filius, M. Janssen, H. van der Kooij and J. Harlaar, 2023. Comparison of Lower Arm Weight and Passive Elbow Joint Impedance Compensation Strategies in Non-Disabled Participants. *International Conference on Rehabilitation Robotics (ICORR)*, Singapore, Singapore, 2023, pp. 1-6. doi: 10.1109/I-CORR58425.2023.10304707. ©2024 IEEE. The data and materials allowing users to understand, verify and replicate the findings are published under restricted access on the 4TU.ResearchData repository doi: 10.4121/fc5c31ea-b4ca-45bf-830b-f0e86ece95bf and can be accessed upon request.

# Comparison of Lower Arm Weight and Passive Elbow Joint Impedance Compensation Strategies in Non-Disabled Participants

## 4

**Abstract** People with severe muscle weakness in the upper extremity are in need of an arm support to enhance arm function and improve their quality of life. In addition to weight support, compensation of passive joint impedance (*pJimp*) seems necessary. Existing devices do not compensate for *pJimp* yet, and the best way to compensate for it is still unknown. The aim of this study is to 1) identify *pJimp* of the elbow, and 2) compare four different compensation strategies of weight and combined weight and *pJimp* in an active elbow support system. The passive elbow joint moments, including gravitational and *pJimp* contributions, were measured in 12 non-disabled participants. The four compensation strategies ('scaled-model', 'measured', 'hybrid', and 'fitted-model') were compared using a position-tracking task in the near vertical plane. All four strategies showed a significant reduction (20-47%) in the anti-gravity elbow flexor activity measured by surface electromyography. The *pJimp* turned out to contribute to a large extent to the passive elbow joint moments (range took up 60%) in non-disabled participants. This underlines the relevance of compensating for *pJimp* in arm support systems. The parameters of the scaled-model and hybrid strategy seem to overestimate the gravitational component. Therefore, the measured and fitted-model strategies are expected to be most promising to test in people with severe muscle weakness combined with elevated *pJimp*.

## 4.1 Introduction

Pathologies such as Muscular Dystrophies (MD), Stroke, Spinal Muscular Atrophy (SMA) and Amyotrophic Lateral Sclerosis can result in severe arm muscle weakness and consequential functional loss. These patients are in need of arm support(s) to regain arm function and improve their independence, social participation and quality of life. It has been shown that people with arm disabilities benefit from weight compensation by arm supports to assist activities of daily living (ADL) [8, 26].

Besides the support of arm weight, compensation of passive joint impedance (*pJimp*) seems necessary in pathologies (e.g., MD, SMA) with severe muscle weakness in combination with elevated *pJimp* [22, 27]. The *pJimp* is expressed as the passive resistance in response to a joint movement [2, 25], so not the active resistance that result from (involuntary) muscle activation (e.g., spasticity). In some pathologies like Duchenne MD

(DMD) the pJimp can be 5 times the residual muscle strength [22]. Previous studies have highlighted the clinical relevance of pJimp compensation in people with DMD [6, 23, 27] and shown that with only weight compensation the functional gain was limited [22]. In weakened individuals with elevated pJimp, the ratio between the voluntary and passive forces (e.g., gravitational and pJimp) is very small and difficult to distinguish from each other [27]. Moreover, pJimp can change as the disease progresses [5, 16], but it can also vary throughout the day, through room temperature changes [21] or by doing stretching exercises [33]. This makes it difficult to model and compensate for pJimp [22].

Ragonesi et al. [27] measured the passive arm dynamics in non-disabled and adolescents with neuromuscular disabilities (i.e., MD, Arthrogryposis and SMA) for arm support purposes. They measured the passive elbow and shoulder joint moments in the vertical (e.g., sagittal) plane using static measurements over ca. 72 postures. Lobo-Prat et al. [23] measured the passive elbow joint moments in MD patients dynamically at slow velocity ( $2.9^\circ/\text{s}$ ) over the elbow range of motion (ROM) and compensated for it in an active elbow support system. Unfortunately, both methods are time consuming and become complex when translating it to multiple degrees of freedom (DOF). Moreover, since the pJimp varies over time, these calibration measurements need to be repeated regularly. Therefore, new strategies to compensate for a combination of weight and pJimp are required that are less time consuming and complex. Modeling the pJimp would reduce the need for (re)calibration processes, since it allows for parameter tuning. Another option is to add a single plane measurement of the pJimp to a scaled gravitational model. Those two approaches will be explored and compared to the existing (i.e., scaled gravitational model [18] and measured passive joint moments [23]).

This study aims to 1) identify passive elbow joint impedance, and 2) compare four different compensation strategies of weight and combined weight and pJimp in an active elbow support system in non-disabled participants.

## 4.2 Methods

### 4.2.1 Participants

For this study, 12 non-disabled male individuals between 18 and 35 years old were recruited with no history of arm injuries, joint dislocations, or movement difficulties nor active implants (e.g., pacemaker). Ethical approval was obtained from the Human Research Ethics Committee (HREC) from Technical University of Delft (ID2284). All participants gave written informed consent before participation.

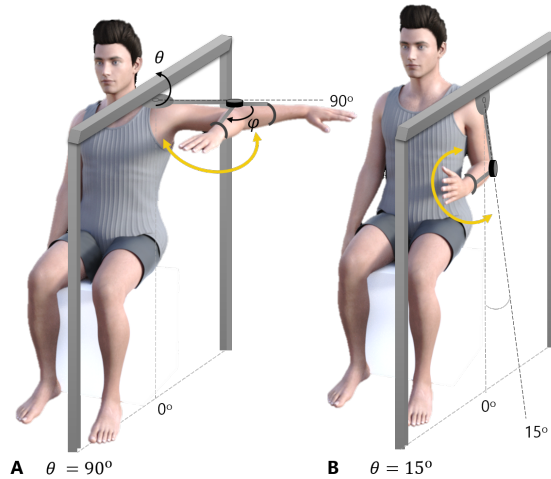
### 4.2.2 Equipment

Figure 4.2.2 shows the two configurations used in the active elbow system. The actuator is aligned with the elbow joint ( $\varphi$ ), and the frame is adjustable in shoulder abduction angle ( $\theta$ ) and height. The horizontal configuration ( $\theta = 90^\circ$ ) was used to measure pJimp and the combined passive joint moments were measured in the near vertical configuration ( $\theta = 15^\circ$ ) to avoid collision with the body. Distal of the actuator, a sleeve interface holds the forearm of the participant in a neutral orientation (thumb upward).

The elbow joint angle was measured by absolute encoders (ICHaus, Germany), with a resolution of 19 bits, attached to a custom sensor slave running at 1 kHz. A 6 DOF

force/torque (F/T) sensor (SI-40-mini F/T, Schunk, ATI Industrial Automation, USA) was placed on the forearm at the sleeve interface, to measure the interaction forces, converted to express the elbow joint torque. The analog signal of the F/T sensor was digitized to 12 bits at 1 kHz. The encoders and F/T sensor were connected over EtherCAT to a computer and interfaced using TwinCAT 3, Beckhoff Automation, Verl, Germany. For each experiment the F/T sensor was calibrated. Surface electromyography (sEMG) signals were recorded with Delsys® Trigno Avanti™ Sensors that communicate with Bluetooth BLE 4.2. The analog signal was sampled at 1.1 kHz with a 16 bits analog-to-digital converter internally. The Delsys® software EMGWorks was used for real-time visualization of the sEMG signals and storing the signals. The skin preparation and sensor placement on the short head of the m. biceps brachii and the lateral head of the m. triceps brachii were in accordance with the SENIAM guidelines [15]. The encoders, F/T sensor and sEMG signals were synchronized using a 5V trigger signal.

4



**Figure 4.1:** Experimental set-up with A) the horizontal and B) the near vertical configuration. The actuator is represented by the black disc at the elbow joint. *Note:* model was retrieved from DAZ Productions [31].

### 4.2.3 Outcome measures

The primary outcome measure was the compensation efficacy measured in the position-tracking task (day 2). This was defined by the root mean square (RMS) of the sEMG signals of biceps and triceps muscles, where a lower RMS sEMG indicates higher compensation efficacy. Secondary outcome measures were the RMS of the position-tracking error (since this affects the sEMG signals); the task workload using the NASA-Task Load index (NASA-TLX); a subjective 5-point Likert Scale (1 dislike, 5 like); and the personal preference for a specific compensation strategy. The NASA-TLX evaluates the workload of a task on 6 rating scales (e.g., mental demand, physical demand, temporal demand, performance, effort, and frustration).



#### 4.2.4 Study design

The study consisted of 3 sessions divided over 2 days. First the biometric data (i.e., body mass, body length, arm segment lengths, and hand plus forearm segment volumes) were collected to calculate weight and center of mass (COM) of the forearm and hand using anthropometric tables [32]. For the weight calculation, the segment volumes were measured using the water displacement method [19] and were multiplied with an averaged density value from cadaver studies [3, 4, 7].

Next, the actuator moved the arm of the participants held in the horizontal configuration through 80% of the range of elbow motion over 8 cycles while the participant was asked to fully relax the arm, at  $2.9^\circ/\text{s}$  [23] and at  $5.7^\circ/\text{s}$ . Next, the elbow was moved in the near vertical plane at  $5.7^\circ/\text{s}$ .

On the second day, first 2 repetitions of the maximum voluntary contraction (MVC) for 3 seconds of the biceps and triceps muscles were collected. In the position-tracking task, the participants were asked to actively follow a sinusoidal (5 cycles of 20s each) target position signal at 75% of the total elbow ROM. The target position and the real-time elbow joint position were displayed on a screen in front of the participant and the participant was asked to follow the target line as close as possible, see Figure 4.2. First a trial with the actuator turned off was performed to get familiar with the task. Then a baseline measurement was recorded, where the actuator was activated in zero-impedance mode [28]. After this, the four compensation strategies (*scaled-model*, *measured*, *hybrid*, and *fitted-model*) were compared in a randomized order and were provided with a gain of 80% since a gain of 100% is not always preferred [9, 17, 20]. Before each compensation strategy, a test trial was done to get familiar with the strategy. After each compensation strategy the (dis)like 5-point Likert scale and the NASA-TLX scores were collected. The NASA-TLX was collected using the official NASA Task Load Index (TLX) iOS app [30].

The four compensation strategies consisted of a *scaled-model* (i.e., compensates for weight only using a simplified kinetic model scaled to the individual biometric parameters), *measured* (i.e., compensates for the combined passive forces including weight and pJimp measured in the near vertical plane), *hybrid* (i.e., a combination of the scaled-model and the measured pJimp in the horizontal plane), and *fitted-model* (i.e., that combines the kinetic weight model with a linear pJimp model fitted to the measured passive forces in the near vertical plane). The formulas of the strategies are listed in Table 4.1.

**Table 4.1:** Overview of compensation strategy joint torques

Strategy	Formula	Measured at
Baseline	$\tau_{GJ} = 0$	none
Scaled	$\tau_{G_{mod}} = q \cdot m \cdot com \cdot g \cdot \sin(\varphi) \cdot \cos(\theta)$	none
Hybrid	$\tau_{G_{mod}J_{meas}} = q \cdot (\tau_{G_{mod}} + \tau_{J_{meas}})$	$\theta = 90^\circ$
Measured	$\tau_{G_{meas}J_{meas}} = q \cdot (\tau_{G_{meas}} + \tau_{J_{meas}})$	$\theta = 15^\circ$
Fitted	$\tau_{GJ_{fit}} = q \cdot (m \cdot com \cdot g \cdot \sin(\varphi) \cdot \cos(\theta) + a\varphi + b)$	$\theta = 15^\circ$

Abbreviations:  $\tau$  = torque,  $G$  = gravity,  $J$  = passive joint impedance, *mod* = modelled, *meas* = measured,  $q$  = gain,  $m$  = mass, *com* = center of mass,  $g$  = gravitational acceleration,  $\varphi$  = elbow joint angle, and  $\theta$  = shoulder abduction angle

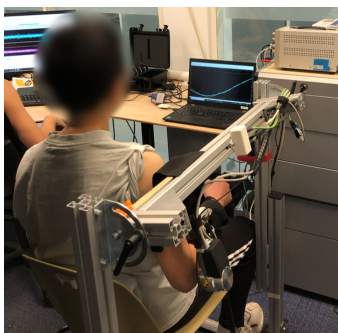


**Figure 4.2:** Picture taken on experiment Day 2, with the real-time sEMG signals on the computer screen left and the position-tracking task on the computer screen on the right.

### 4.2.5 Data processing

**Data selection** The first and last cycles and the cycles where the participant was not relaxed enough (where  $sEMG > 3 \times SD$  of the 3 cycles with lowest average sEMG, with a spike allowance of 5% within the separate cycles) were excluded from analysis.

**Passive joint moments** The measured passive joint moments depend on the movement direction [2]. For simplification, the joint moment at a specific angle was calculated by taking the average of the flexion and extension cycles. Moreover, to calculate the pJimp, the velocity conditions ( $2.9$  and  $5.7^\circ/s$ ) were combined and averaged.

**sEMG processing** The sampled raw sEMG data was filtered with a 3<sup>th</sup> order high-pass Butterworth zero-phase digital filter with a cut-off frequency of 20 Hz. Then, the envelope was taken by taking the absolute values and apply a 2<sup>nd</sup> order low-pass Butterworth zero-phase digital filter with a cutoff frequency of 1 Hz.

The MVC was determined by taking the maximal value of the 2 attempts. The sEMG recorded during the compensation strategies was normalized to the MVC. The RMS values for the sEMG signals were calculated and compared among each condition. The specific samples where participants showed an overshoot of the target position outside of the measured 80% of ROM were excluded from analysis.

**RMS tracking error** The RMS of the tracking error was calculated by taking the RMS of the error between the measured elbow joint angle and the target position signal.

All processing was done using custom programming in MATLAB®.

### 4.2.6 Statistics

Descriptive statistics were used to calculate the group mean ( $M$ ), standard error of the mean ( $SEM$ ) and standard deviation ( $SD$ ). The distributions of the outcome measures were examined for normality of distribution to select either the parametric one-way repeated measure analysis of variance (ANOVA) or the non-parametric Friedman's ANOVA. Wilcoxon Signed Rank Tests were used in addition to the non-parametric Friedman's ANOVA for the pairwise

comparison. The false discovery rate (FDR) was used to correct the level of significance for multiple pairwise comparisons [1, 12]. The effect size  $r$  was calculated by the  $z$  score divided by the number of observations squared [11]. Statistical analyses were performed using SPSS (IBM SPSS Statistics for Windows, Version 28.0.1.0, Armonk, NY, USA: IBM Corp.)

### 4.3 Results

Twelve non-disabled male individuals participated in the study, see Table 4.2 for the descriptive characteristics.

The Shapiro-Wilk test revealed that the RMS of the triceps muscle and tracking error deviated from normal. Therefore, non-parametric tests were selected for all outcome measures.

The average joint moment profiles of the four compensation strategies evolving from the measurements performed on Day 1 are displayed in Figure 4.3. The measurement of the pJimp in the horizontal plane showed a negative profile up to the equilibrium of the elbow joint (e.g., where it crosses zero) around  $65^\circ$  elbow flexion. Note that elbow flexion range presented in this graph is limited to the commonly shared ROM of the group, each individual ROM is larger. The measured pJimp was larger near the limits of the elbow joint, and varied between  $-2.2$  and  $2.1$  Nm. The individual measured joint torques in the near vertical plane crossed the zero towards the elbow extension (at ca.  $17-25^\circ$ ) in most cases and varied between  $-0.9$  and  $5.8$  Nm. On average, the range of measured pJimp took up  $60\%$  ( $\pm 14\%$ ) of the total range of the measured passive forces. The mean absolute difference between the flexion and extension cycles due to the aforementioned direction dependency in the muscles [2] was approximately  $< 0.5$  Nm on average, visualized in Appendix B.1. The mean absolute difference in slope between the two velocities measured in pJimp was  $2.7e^{-3}(\pm 2.6e^{-3})$  Nm/ $^\circ$ .

#### 4.3.1 Outcome measures

The non-parametric Friedman's ANOVA revealed that on average the sEMG RMS of the biceps muscle significantly differed among the conditions, see Table 4.3. The Wilcoxon

**Table 4.2:** Participant characteristics

$n = 12$ (Unit)	M	SD	95%CI
Age (years)	29	3.6	[26.5-31.5]
Weight (kg)	76.1	13.1	[67.1-85.1]
Body length (cm)	179.7	9.9	[172.9-186.5]
com <sub>forearm+hand</sub> (m)	16.2	1.3	[15.3-17.0]
mass <sub>forearm+hand</sub> (kg)	1.7	0.4	[1.4-1.9]
Dominant hand (r/l)	11/1	-	-
Frequency of sport (1-5)	2.6	1.1	[1.8-3.3]
Intensity of sport (1-5)	3.2	1.0	[2.5-3.8]

Abbreviations:  $n$  = number of participants;  $M$  = mean;  $SD$  = standard deviation;  $CI$  = confidence interval;  $com$  = center of mass.

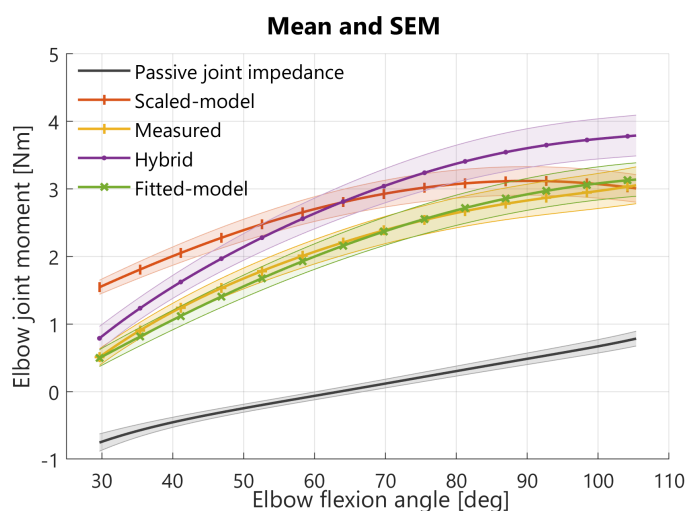


**Figure 4.3:** Group mean and standard error of the mean (SEM) results of the torque-angle profiles of the four compensation strategies and the measured pJimp. Based on the data of day 1 (relaxation task).

signed rank test revealed that on average, compared to no support (baseline), the muscle activity of the biceps muscle decreased significantly ( $p < .01$ ,  $r = -.62$ ) for the scaled-model ( $-47.7\%$ ), the measured ( $-21.3\%$ ), the hybrid ( $-39.1\%$ ) and the fitted-model ( $-31.5\%$ ) strategy. No significant differences were found between the compensation strategies for the biceps muscles.

On average, the activity in the triceps muscle decreased for the scaled-model ( $-0.7\%$ ), the measured ( $-3.2\%$ ) and the hybrid ( $-9.6\%$ ), but slightly increased for the fitted-model strategy ( $+2.2\%$ ), however these differences were not significant. See Figure 4.4.

No statistical significant differences were found for the position-tracking RMS error, the NASA-TLX and the 5-point Likert scale. The NASA-TLX score ranged on average from 31 to 37% among the conditions, meaning that the task load was rated as ‘somewhat high’ for all conditions. Out of the 12 participants, 4 preferred the scaled-model (33%), 4 preferred measured (33%), 3 preferred fitted-model (25%), and 1 the hybrid (8%) compensation strategy.

**Table 4.3:** Outcome of the non-parametric Friedman’s ANOVA and group mean and standard deviation

Outcomes	$\chi^2(4)$	$p$ -value	Units	Baseline		Scaled-model		Measured		Hybrid		Fitted-model	
				Mean	SD	Mean	SD	Mean	SD	Mean	SD	Mean	SD
sEMG Biceps RMS	25.93	<.00	%MVC	2.66	1.48	1.39	0.78	2.09	1.44	1.62	1.03	1.82	0.99
sEMG Triceps RMS	5.33	0.33	%MVC	0.95	0.53	0.95	0.47	0.92	0.61	0.86	0.40	0.97	0.65
Tracking error RMS	1.60	0.81	deg	2.60	0.62	3.04	1.17	2.85	1.01	2.95	0.78	2.77	0.86
NASA TLX	1.13	0.89	%	35	17	34	16	37	18	38	17	31	16
5-point Likert-Scale	4.34	0.36	1-5	3.58	0.67	3.50	0.80	3.42	0.90	3.08	0.79	3.58	1.00

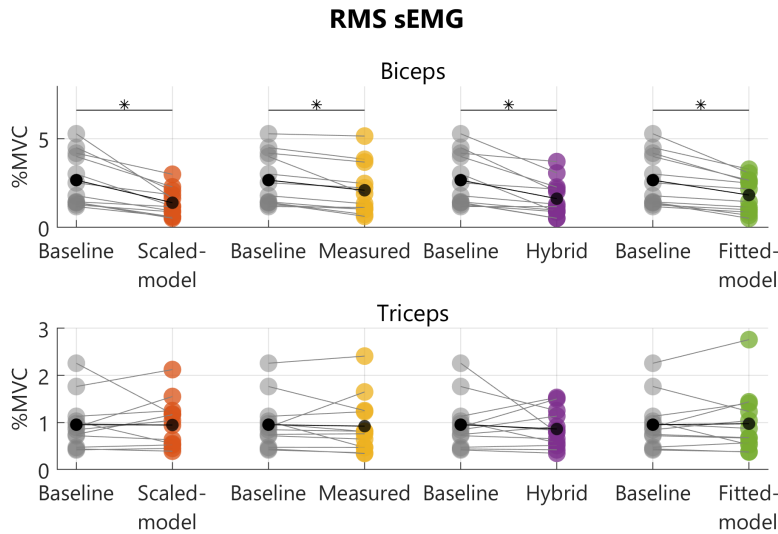


**Figure 4.4:** Scatterplot of RMS sEMG results in the near vertical configuration for biceps (top) and triceps (bottom), normalized to percentage of maximally voluntary contraction (MVC). Based on the data of day 2 (position-tracking task). The black dots represent the group mean.

## 4.4 Discussion

This study is the first exploring different arm support strategies that include weight as well as pJimp compensation. We explored two new combinations of weight and pJimp compensation strategies (hybrid and fitted-model) and compared this with the ‘conventional’ weight only (scaled-model) and measured strategy similar to Lobo-Prat et al. [23].

All four compensation strategies showed a significant reduction in the anti-gravity biceps muscle activity. No statistically significant differences were found between the compensation strategies. Therefore, it is important to look at the pros and cons of the strategies to decide which strategy is most promising.

### 4.4.1 Comparison of the compensation strategies

The *measured* strategy is expected to be most accurate since it is based on the actual passive joint moments. The disadvantage is that it needs calibration measurements in the plane of movement. This can be a time-consuming and complex process, especially in multi-DOF set-ups.

The *fitted-model* has the advantage over the measured strategy that it allows for parameter tuning of either the gravitational (e.g., for thicker clothes) or pJimp (e.g., affected by room temperature) model parameters, potentially reducing the need of re-calibration. Furthermore, the model parameters can be fitted to a set of joint configurations instead of full ROM measurements, reducing the time of the calibration process.

The advantage of the *scaled-model* strategy is that only biometric data need to be collected to set the model parameters. However, the scaled-model strategy is missing the

pJimp component. Although the pJimp component can easily be overcome by the muscle strength of non-disabled participants, it does seem to play a substantial role (range takes up 60%) in the measured passive joint moments. For the intended target population, the pJimp is much higher in relation to their muscle strength ( $\pm > 50$  times) [14, 27]. The pJimp component introduces a reduction of the passive joint moments in the extension region and an increase in the flexion region. This can be seen with the *hybrid* strategy that shows a slight tilt with respect to the scaled-model. However, this does not seem to explain all the differences between the measured joint moments and the scaled-model. It seems that there is an overestimation of the gravitational model parameters, which holds for both the scaled-model and hybrid strategy. So, a disadvantage of these two strategies is that the model parameters are easily over- or under-estimated using anthropometric tables. Moreover, it is known that the soft tissue composition in the arm of people with for example MD is different to that of non-disabled (e.g., less muscle tissue, more fat and connective tissue) [29], making it even more complex to predict the model parameters with accuracy.

The advantage of the hybrid strategy is that only the pJimp needs to be identified instead of full ROM measurements, which can save time in the calibration process. However, when the gravitational component is overestimated, adding an additional pJimp will add an extra support torque in the higher flexion region. Too high anti-gravity support will result in difficulties to move the arms down, as is seen in non-powered arm supports (e.g., by springs) due to imperfect static balancing of the arms [10, 24]. An advantage of powered systems is that the compensation gain can be adjusted in case of model inaccuracies, improving the usability. However, model inaccuracies are sub-optimal and can introduce problems when a high level of accuracy in support level is required for the target population.

Overall, our expectation is that the measured and fitted-model strategies are most promising to test in a target population with severe muscle weakness. Since the scaled-model and hybrid torque-angle profiles seem to overestimate the gravitational component. Moreover, the scaled-model does not take into account the pJimp component, and we have seen that, even in non-disabled, this affects the passive joint moments.

#### 4.4.2 Limitations of the study

It is not well known how well these results translate to pathologies with severe muscle weakness and elevated pJimp. We found a way to model and fit the passive joint moments in a combined weight and pJimp model with a linear relation for the pJimp. First of all, more research is needed to determine whether the fitted 1<sup>st</sup>-order model of the pJimp can be applied in pathologies with elevated pJimp, or that a higher order or personalized model is required. This study measured the passive joint moments within an elbow ROM of 80% due to safety reasons. Although this covers the ROM for most functional ADL, it is expected that the pJimp is higher at the joint limits, potentially resulting in a higher order fit. Furthermore, potential effects of shoulder positions by for example differences in bi-articular muscles are not taken into account. Moreover, the velocity effects are averaged out and therefore potential damping effects in the pJimp are not taken into account in the compensation strategies. This is in accordance with [13], who also found that the dynamics of the passive human arm depends mostly on the joint angle. Secondly, the non-disabled participants require only little relative muscle effort (%MVC) to perform the position-

tracking task. This makes it difficult to find and feel differences between the relatively small changes in the provided support torque. This task is expected to require much larger relative muscle effort (MVC%) in a target population with severe muscle weakness (e.g., 2% elbow flexion moment of healthy population [14, 27]), where the accuracy of the provided support levels become more critical and the compensation efficacy more distinctive. As an indication, a 1 Nm difference in support torque can take up 70% of the max elbow flexion moment in MD patients [27].

As mentioned, the parameters used for the hybrid and scaled-model strategies seem to be overestimated. More research in the anthropomorphic characteristics might improve the parameter estimation.

For the practical validity in the clinical application a powered arm support with accurate torque sensing is required, so that the system can both accurately identify the passive joint moments for calibration and provide the accurate support levels. Follow-up studies should identify whether muscle relaxation measurements during calibration is redundant.

## 4.5 Conclusion

All four compensation strategies showed a significant reduction in the anti-gravity muscle activity, but no statistically significant differences were found in the compensation efficacy between the compensation strategies.

It was found that pJimp substantially affects the passive elbow joint moments, even in non-disabled participants. This underlines the necessity of pJimp compensation, which is expected to be even more critical in people who suffer from severe muscle weakness in combination with elevated pJimp.

The profiles of the measured and fitted-model strategies were highly similar, while the scaled-model and hybrid seem to overestimate the passive joint moments.

Based on the current study, the measured and fitted-model are expected to be the most interesting and promising strategies to test in a follow-up study.

## References

- [1] Y. Benjamini and D. Yekutieli. The control of the false discovery rate in multiple testing under dependency. *The annals of Statistics*, 29(4):1165–1188, 2001.
- [2] K. L. Boon, A. L. Hof, and W. Wallinga-de Jonge. The Mechanical Behaviour of the Passive Arm. *Medicine and Sport*, 8(Biomechanics III):243–248, 1973.
- [3] R. F. Chandler, C. E. Clauser, J. T. McConville, H. M. Reynolds, and J. W. Young. Investigation of Inertial Properties of the Human Body. Technical Report March, U.S. Department of Transportation, Washington, D.C., 1975.
- [4] C. E. Clauser, J. T. McConville, and J. W. Young. Weight, volume, and center of mass of segments of the human body. Technical report, Wright-Patterson Air Force Base, Ohio, 1969. URL <http://oai.dtic.mil/oai/oai?verb=getRecord&metadataPrefix=html&identifier=AD0710622>.
- [5] C. Cornu, F. Goubel, and M. Fardeau. Muscle and joint elastic properties during elbow flexion in Duchenne muscular dystrophy. *The Journal of Physiology*, 533(2):605–616, 2001. doi: 10.1111/j.1469-7793.2001.0605a.x.
- [6] M. C. Corrigan and R. A. Foulds. Evaluation of admittance control as an alternative to passive arm supports to increase upper extremity function for individuals with Duchenne muscular dystrophy. *Muscle and Nerve*, 61(6):692–701, 2020. doi: 10.1002/mus.26848.
- [7] W. T. Dempster. Space requirements of the seated Operator. Technical report, Wright Patterson Air Force Base, 1955.
- [8] J. M. Essers, K. Meijer, A. Murgia, A. Bergsma, and P. Verstegen. An inverse dynamic analysis on the influence of upper limb gravity compensation during reaching. *IEEE International Conference on Rehabilitation Robotics*, pages 1–5, 2013. doi: 10.1109/ICORR.2013.6650368.
- [9] J. M. Essers, A. Murgia, A. A. Peters, M. M. H. P. Janssen, and K. Meijer. Recommendations for studies on dynamic arm support devices in people with neuromuscular disorders: a scoping review with expert-based discussion. *Disability and Rehabilitation: Assistive Technology*, 0(0):1–14, 2020. doi: 10.1080/17483107.2020.1806937.
- [10] T. Estilow, A. M. Glanzman, K. Powers, A. Moll, J. Flickinger, L. Medne, G. Tennekoon, and S. W. Yum. Use of the wilmington robotic exoskeleton to improve upper extremity function in patients with duchenne muscular dystrophy. *American Journal of Occupational Therapy*, 72(2):1–5, 2018. doi: 10.5014/ajot.2018.022939.
- [11] A. Field. *Discovering statistics using IBM SPSS statistics*. SAGE Publications, 4th edition, 2013.
- [12] M. E. Glickman, S. R. Rao, and M. R. Schultz. False discovery rate control is a recommended alternative to Bonferroni-type adjustments in health studies. *Journal of Clinical Epidemiology*, 67(8):850–857, 2014. doi: 10.1016/j.jclinepi.2014.03.012.



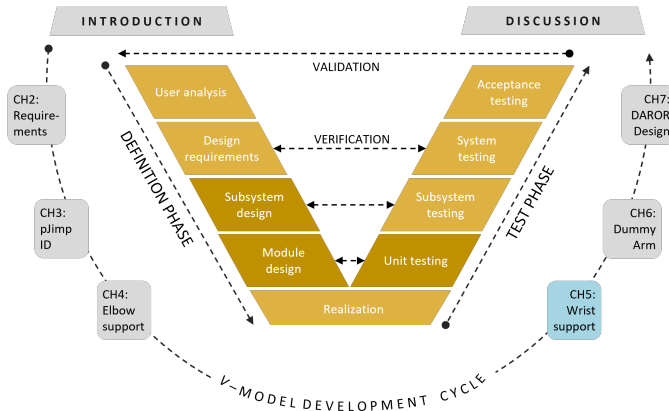
- [13] M. Guidali, U. Keller, V. Klamroth-Marganska, T. Nef, and R. Riener. Estimating the patient's contribution during robot-assisted therapy. *Journal of Rehabilitation Research and Development*, 50(3):379–394, 2013. doi: 10.1682/JRRD.2011.09.0172.
- [14] L. J. Hébert, D. B. Maltais, C. Lepage, J. Saulnier, and M. Crête. Hand-Held Dynamometry Isometric Torque Reference Values for Children and Adolescents. *Pediatric Physical Therapy*, 27(4):414–423, 2015. doi: 10.1097/PEP.0000000000000179.
- [15] H. J. Hermens, B. Freriks, C. Disselhorst-Klug, and G. Rau. Development of recommendations for SEMG sensors and sensor placement procedures. *Journal of Electromyography and Kinesiology*, 10(5):361–374, 2000. doi: [https://doi.org/10.1016/S1050-6411\(00\)00027-4](https://doi.org/10.1016/S1050-6411(00)00027-4).
- [16] M. M. H. P. Janssen, A. Bergsma, A. C. Geurts, and I. J. De Groot. Patterns of decline in upper limb function of boys and men with DMD: An international survey. *Journal of Neurology*, 261(7):1269–1288, 2014. doi: 10.1007/s00415-014-7316-9.
- [17] M. M. H. P. Janssen, J. Horstik, P. Klap, and I. J. de Groot. Feasibility and effectiveness of a novel dynamic arm support in persons with spinal muscular atrophy and duchenne muscular dystrophy. *Journal of NeuroEngineering and Rehabilitation*, 18(1):1–13, 2021. doi: 10.1186/s12984-021-00868-6.
- [18] F. Just, Ö. Özen, S. Tortora, V. Klamroth-Marganska, R. Riener, and G. Rauter. Human arm weight compensation in rehabilitation robotics: Efficacy of three distinct methods. *Journal of NeuroEngineering and Rehabilitation*, 17(1):1–17, 2020. doi: 10.1186/s12984-020-0644-3.
- [19] J. R. Karges, B. E. Mark, S. J. Stikeleather, and T. W. Worrell. Concurrent Validity of Upper-Extremity Volume Estimates: Comparison of Calculated Volume Derived From Girth Measurements and Water Displacement Volume. *Physical Therapy*, 83(2):134–145, 2003. doi: 10.1093/ptj/83.2.134.
- [20] P. N. Kooren, A. G. Dunning, M. M. H. P. Janssen, J. Lobo-Prat, B. F. Koopman, M. I. Paalman, I. J. De Groot, and J. L. Herder. Design and pilot validation of A-gear: A novel wearable dynamic arm support. *Journal of NeuroEngineering and Rehabilitation*, 12(1):1–12, 2015. doi: 10.1186/s12984-015-0072-y.
- [21] M. Lakie, E. G. Walsh, and G. W. Wright. Control and postural thixotropy of the forearm muscles: Changes caused by cold. *Journal of Neurology Neurosurgery and Psychiatry*, 49(1):69–76, 1986. doi: 10.1136/jnnp.49.1.69.
- [22] J. Lobo-Prat, A. Q. L. Keemink, B. F. J. M. Koopman, A. H. A. Stienen, and P. H. Veltink. Adaptive gravity and joint stiffness compensation methods for force-controlled arm supports. In *IEEE International Conference on Rehabilitation Robotics*, volume 2015-Sept, pages 478–483. IEEE, 2015. doi: 10.1109/ICORR.2015.7281245.
- [23] J. Lobo-Prat, P. N. Kooren, M. M. H. P. Janssen, A. Q. Keemink, P. H. Veltink, A. H. Stienen, and B. F. Koopman. Implementation of EMG-and force-based control interfaces in active elbow supports for men with duchenne muscular dystrophy: a

- feasibility study. *IEEE Transactions on Neural Systems and Rehabilitation Engineering*, 24(11):1179–1190, 2016. doi: 10.1109/TNSRE.2016.2530762.
- [24] V. Longatelli, A. Antonietti, E. Biffi, E. Diella, M. G. D’Angelo, M. Rossini, F. Molteni, M. Bocciolone, A. Pedrocchi, and M. Gandolla. User-centred assistive SystEm for arm Functions in neUromuscuLar subjects (USEFUL): a randomized controlled study. *Journal of NeuroEngineering and Rehabilitation*, 18(1):1–17, 2021. doi: 10.1186/s12984-020-00794-z.
- [25] S. Maggioni, A. Melendez-Calderon, E. Van Asseldonk, V. Klamroth-Marganska, L. Lünenburger, R. Riener, and H. Van Der Kooij. Robot-aided assessment of lower extremity functions: A review. *Journal of NeuroEngineering and Rehabilitation*, 13(1):1–25, 2016. doi: 10.1186/s12984-016-0180-3.
- [26] G. Prange. *Rehabilitation robotics: stimulating restoration of arm function after stroke*. PhD thesis, Enschede: University of Twente, 2009.
- [27] D. Ragonesi, S. K. Agrawal, W. Sample, and T. Rahman. Quantifying anti-gravity torques for the design of a powered exoskeleton. *IEEE Transactions on Neural Systems and Rehabilitation Engineering*, 21(2):283–288, 2013. doi: 10.1109/TNSRE.2012.2222047.
- [28] W. F. Rampeltshammer, A. Q. Keemink, and H. Van Der Kooij. An Improved Force Controller with Low and Passive Apparent Impedance for Series Elastic Actuators. *IEEE/ASME Transactions on Mechatronics*, 25(3):1220–1230, 2020. doi: 10.1109/TMECH.2020.2970532.
- [29] V. Ricotti, M. R. Evans, C. D. Sinclair, J. W. Butler, D. A. Ridout, J. Y. Hogrel, A. Emira, J. M. Morrow, M. M. Reilly, M. G. Hanna, R. L. Janiczek, P. M. Matthews, T. A. Yousry, F. Muntoni, and J. S. Thornton. Upper limb evaluation in duchenne muscular dystrophy: Fat-water quantification by MRI, muscle force and function define endpoints for clinical trials. *PLoS ONE*, 11(9):1–15, 2016. doi: 10.1371/journal.pone.0162542.
- [30] P. So. Nasa task load index (tlx) app, nasa human systems integration division, 2020. URL <https://humansystems.arc.nasa.gov/groups/tlx/tlxapp.php>.
- [31] R. Whisenant, C. Jones, A. Diether, and B. Lamming. DAZ 3D Studio, 2023. URL <https://www.daz3d.com/>. Version 4.10.0.123 Pro Edition (64-bit) For Windows.
- [32] D. A. Winter. *Biomechanics and Motor Control of Human Movement: Fourth Edition*. 2009. doi: 10.1002/9780470549148.
- [33] L. Q. Zhang, H. Park, and Y. Ren. Shoulder, elbow and wrist stiffness in passive movement and their independent control in voluntary movement post stroke. In *2009 IEEE International Conference on Rehabilitation Robotics, ICORR 2009*, pages 805–811. 11th International Conference on Rehabilitation Robotics Kyoto International Conference Center, Japan, June 23-26, 2009. doi: 10.1109/ICORR.2009.5209489.

# 5

## The Efficacy of Different Torque Profiles for Weight Compensation of the Hand

Chapter 4 showed that the elbow support torque also depends on the shoulder orientations. For the hand, the support torque depends on the forearm and wrist orientations. The hand could benefit from small, lightweight, preferably passive support. However, the constrained design space further complicates precise hand weight compensation.



This chapter explores simplified torque profiles to enable more feasible solutions.

This chapter was published as:

van der Burgh, B. J., Filius, S. J., Radaelli, G., and Harlaar, J. (2024). The efficacy of different torque profiles for weight compensation of the hand. *Wearable Technology* 5, e2. doi:<https://doi.org/10.1017/wtc.2023.23>. The data and materials allowing users to understand, verify and replicate the findings are published under restricted access on the 4TU.ResearchData repository and can be accessed upon request.

## The efficacy of different torque profiles for weight compensation of the hand

**Abstract** *Orthotic wrist supports will be beneficial for people with muscular weakness to keep their hand in neutral rest position and prevent potential wrist contractures. Compensating the weight of the hands is complex since the level of support depends on both wrist and forearm orientations. To explore simplified approaches, two different weight compensation strategies (constant and linear) were compared to the theoretical ideal sinusoidal profile and no compensation in 8 healthy subjects using a mechanical wrist support system. All three compensation strategies showed a significant reduction of 47%-53% sEMG activity in the anti-gravity m. extensor carpi radialis. However, for the higher palmar flexion region, a significant increase of 44%-61% in the m. flexor carpi radialis was found for all compensation strategies. No significant differences were observed between the various compensation strategies. Two conclusions can be drawn: (1) a simplified torque profile (e.g., constant or linear) for weight compensation can be considered as equally effective as the theoretically ideal sinusoidal profile; (2) Even the theoretically ideal profile provides no perfect support as other factors than weight, such as passive joint impedance, most likely influence the required compensation torque for the wrist joint.*

### 5.1 Introduction

Neuromuscular disorders are seriously impacting people's lives, for example Duchenne Muscular Dystrophy (MD), a genetic disorder that leads to progressive loss of muscle strength [23]. This results in loss of ambulation in early adolescence and progressive loss of arm function, along with the development of joint contractures. Around the age of 12 the functionality and the range of motion (ROM) of the arm decreases [20, 21].

Compensating for the weight of the arm will add to regain some functionality by reducing the muscular effort to perform a task. A variety of arm supporting devices already exists to assist the functionality of the shoulder and elbow [16]. A significant reduction ( $p < .05$ ) in muscle effort of the anti-gravity muscles was shown, such as in the m. biceps brachii ranging from 28% to 60% [10, 19, 20, 25, 26]. However, support of the wrist joint is often neglected, resulting in a flexed rest position of the hand, which may induce in wrist contractures. Especially, as the long finger flexor muscles in DMD are prone to shorten [18]. Retaining wrist and finger function is of great importance to perform daily activities and strongly add to improve quality of life [18].

To support the weight of the hand, theoretically a sinusoidal torque profile of which the magnitude and phase depend on the hand and forearm orientation is required (see

Appendix C.1). So, a straightforward solution to achieve this would be the use of a counterweight, which directly compensates the weight of the hand. This yields a considerable (-52%) decrease in extensor muscle activity [17]. However, the drawback of using a counterweight is that it either uses a large weight or long lever arm. Such a solution will obstruct movements, look conspicuous, and require additional effort to lift the arm with the added counterweight. A lighter and more slender solution is therefore preferred. So, it is worth considering alternative solutions, that include different torque profiles, that may be equally effective. For example, by using linear springs or a constant force. No studies were found that considered weight compensation methods, other than the sinusoidal torque profiles, under different orientations of the forearm.

Therefore, the aim of the current study is to explore whether a constant torque or a linear spring will show similar reductions in muscular effort compared to the theoretically ideal sinusoidal torque profile, considering both the forearm and wrist orientation.

## 5.2 Methods

### 5.2.1 Participants

For this study, non-disabled participants were recruited from a university student population, with no history of injuries to their right wrist. Ethical approval was obtained from the Human Research Ethics Committee (HREC) from Delft University of Technology (ID2288). All participants gave written informed consent.

### 5.2.2 Experiment design

The experiment design is schematically illustrated in Figure 5.1.

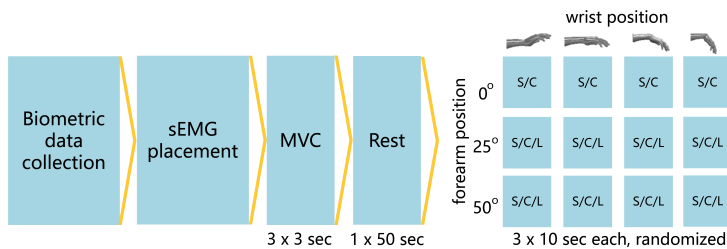


**Figure 5.1:** Schematic overview of experimental design. Abbreviations: sEMG, surface electromyography, MVC, Maximally Voluntary Contraction, S, sinusoidal, C, constant, L, linear

#### 5.2.2.1 Parameter calibrations

Biometric data collection included the weight and center of mass (CoM) of the hand. The weight of the hand was estimated using a water displacement method [5, 22] and an anthropometric table [8]. The hand CoM was estimated using anthropometric equations including adaptations to adjust for flexed fingers [5, 8].

The surface electromyography (sEMG) electrode placement was based on the recommendations from Criswell [11] and Barbero et al. [2] for the muscle bellies of the m.

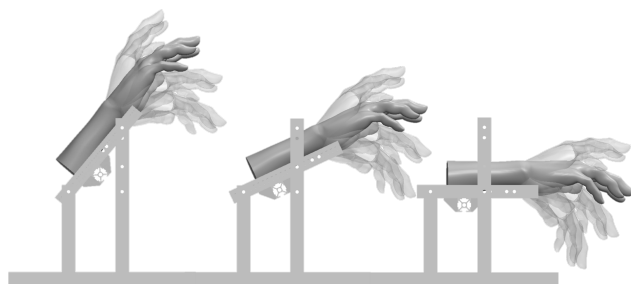


**Figure 5.2:** Schematic representation of the different positions of the forearm and hand. From left to right the forearm is positioned at 50, 25 and 0° with respect to the horizontal. The hand can be positioned at 25° dorsal flexion (-25°), neutral (0°), 25° palmar flexion (25°) and 50° palmar flexion (50°) indicated by the transparent hands. *Note:* Hand model adapted from Story [32]

## 5

extensor carpi radialis (ECR) and the m. flexor carpi radialis (FCR). The reference electrode was placed on the lateral epicondyle of the humerus. The skin preparation was according to the SENIAM recommendations [29], involving shaving and rubbing.

Three maximum voluntary contraction (MVC) tasks were performed by asking the participant to maximally flex or extend their hand against a rigid surface with a straight wrist in a pronated position for 3 seconds followed by 12 seconds of rest. During the MVC the participants were encouraged by the experimenter.

A measurement of rest activity was performed by laying the forearm and hand relaxed on a table in a pronated position for 50 seconds.

### 5.2.2.2 Experiments

For the assessment of the efficacy of the different compensation strategies the activity of the wrist muscles was evaluated using sEMG for all 12 experimental conditions.

The forearm was placed at 0, 25 and 50° with respect to the horizontal. In each successive forearm orientation the different wrist and balance methods (e.g., constant, linear, sinusoidal and no support) were evaluated. Within each sEMG recording the wrist was positioned in a pronated position for 10 seconds at 25° dorsal flexion, 0°, 25° and 50° palmar flexion (Figure 5.2), with 5 seconds rest between each position. Each condition was performed three times, but not in a consecutive order. To control the length of the finger flexors and extensors the position of the fingers was held constant throughout the experiment by gently holding a foam tube during all measurements.

The order of the wrist position and the compensation strategies were randomized to account for the influence of the prior movement direction [11] (Appendix C.2).

## 5.2.3 Equipment

### 5.2.3.1 Imposing wrist torque profiles

A wrist support system was developed to fixate the forearm in different orientations and provide different compensation torque profiles at the wrist joint (Figures 5.3 and 5.4). The human wrist joint was aligned with system by changing the position of the fixation. The constant torque profile was generated through a mass hanging from a pulley over a

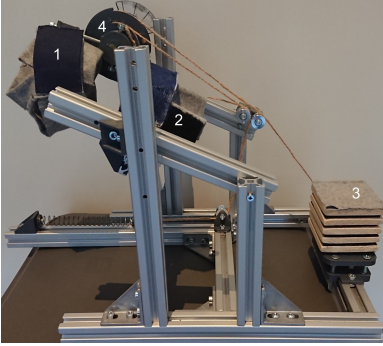


**Figure 5.3:** Side view of the setup, 1) hand interface, 2) forearm interface, 3) elbow support, 4) transmission pulley for application of the different torque profiles



**Figure 5.4:** Top view of the setup with arm and sEMG electrodes placed on the ECR and FCR

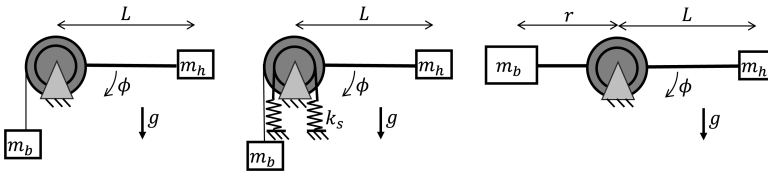


**Figure 5.5:** Schematic representation of the application methods of the constant (left), linear (middle) and sinusoidal (right) torque profiles. Here  $m_b$  and  $m_h$  are the balance mass and the mass of the hand respectively and  $k_s$  the stiffness of the springs

constant lever arm (Figure 6.2). By combining a set of six balance masses (66, 74, 97, 199, 237, 307 g) the desired compensation torque could be approximated within an error of less than 3%. The linear profile was generated by combining the balance masses in series with a spring. By using different types of springs, the slope of the torque profile could be adjusted. For this, a choice was made between four different springs (.15, .19, .25 and .47 N/mm), resulting in an effective stiffness around the wrist joint of .06, .08, .10 or .19 Nm/rad. The linear torque profile was not considered for the forearm orientation of  $0^\circ$  as it behaves as a constant torque. The sinusoidal profile was generated by attaching a counterweight to a rigid rod. By varying the distance of the weight with respect to the hinge of the rod, the magnitude of the profile was adjusted (Figure 6.2). This value could be adjusted continuously. The required weight compensation torque depends on the biometric properties of the participant's hand and forearm orientation (Figure 5.6), as explained in the mathematical wrist model presented in Appendix C.1.



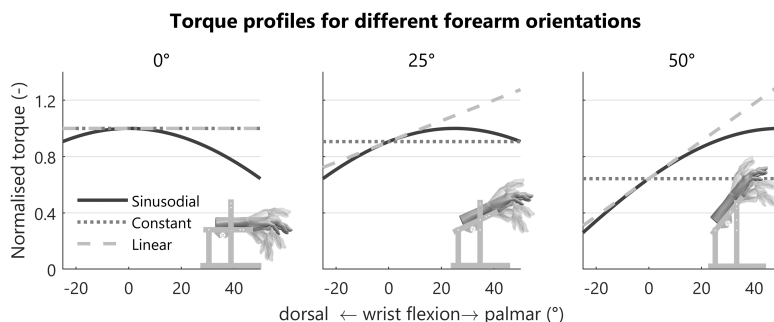


**Figure 5.6:** Torque profiles as a ratio of the maximum sinusoidal torque for the three different forearm orientations. *Note:* The constant torque is only constant with respect to the wrist flexion angle, while it is different for every forearm orientation. The constant and linear torque profiles are respectively the 0<sup>th</sup> and 1<sup>st</sup> order expansion of the Taylor series of the sinusoidal profile

## 5

### 5.2.3.2 sEMG

The sEMG recordings were made using a Bagnoli™ EMG system with DE-2.1 Single Differential Surface EMG sensors from Delsys®, consisting of an 8-channel amplifier with an output voltage range of  $\pm 5$  V (System noise (R.T.I)  $< 1.2\mu V_{rms}$ ). The sEMG sensor consist of two 10 mm long and 1 mm wide electrode contacts spaced 10 mm apart (Figure 5.4). The amplifier gain was set separately for each participant to 1k or 10k, maximizing the signal amplitude and avoiding amplifier saturation. The analogue signal was sampled with a frequency of 2000 Hz with a 16-bit ( $\pm 10$  V) ADC NI® 9215 (Input noise  $0.37mV_{rms}$ ) using NI LabVIEW™ 2018. The digitized signal was stored on a computer for offline processing with MATLAB® R2021a.

### 5.2.4 Data processing

The recorded sEMG signal was filtered by applying 2<sup>nd</sup>-order IIR Notch filter at 50 Hz to remove power line interference, followed by a 6<sup>th</sup> order band-pass Butterworth filter with lower and upper cut-off frequencies of 20 and 450 Hz respectively [24]. Then, this signal was rectified by taking its absolute value. Next, the sEMG envelope was defined by taking a 3rd order low-pass Butterworth filter of the rectified signal with a cut-off frequency of 2 Hz [7]. Finally, the sEMG envelope of both muscles were normalized with respect to its MVC. The MVC value was defined as the maximum of the sEMG envelope from the 3 repetitions of the MVC task for both ECR and FCR muscle.

For comparison of the compensation strategies the mean magnitude of the central 5.5 seconds of the sEMG envelope for the ECR and FCR muscles were averaged over the three repetitions per condition, expressed in percentage MVC [3, 4].

### 5.2.5 Statistics

For statistical analysis, a repeated measures analysis of variance (ANOVA) is performed on the outcome measures to assess the effects of the forearm orientation, wrist position and balancing method and their interactions on the sEMG activity of the ECR and FCR



muscles. The assumption of sphericity of the data is assessed using Mauchly's test. If this assumption is violated a Greenhouse-Geisser correction was applied to the degrees of freedom to account for this violation. Following the ANOVA, the results are analyzed using a multiple comparison with Bonferroni adjustment [14]. P-values < .05 are interpreted as significant. Data is reported as mean  $\pm$  standard deviation. Statistical analyses were performed using IBM SPSS® Statistics for Windows, Version 28.0.1.0 (Armonk, NY, USA: IBM Corp.).

## 5.3 Results

### 5.3.1 Participants

Nine people participated in the experiment (see Table 5.1). One participant had to be excluded due to a technical error during the experiment. All participants were right-handed.

**Table 5.1:** Participant characteristics, reported as mean and standard deviation.

Characteristic	Male (N=4)	Female (N=4)
Age (years)	24.0 $\pm$ 0.8	24.8 $\pm$ 0.5
Body weight (kg)	78.3 $\pm$ 9.6	63.8 $\pm$ 9.3
Height (m)	1.86 $\pm$ 0.06	1.70 $\pm$ 0.08
Hand weight (g)	434 $\pm$ 39	337 $\pm$ 29
Center of mass (mm)	47.3 $\pm$ 3.3	42.4 $\pm$ 1.4

### 5.3.2 sEMG activity

A representative example of the raw sEMG data is depicted in Figure 5.7 for the constant torque and no compensation. Overall, the ECR activity is lower for the constant torque support, while the FCR activity increases for larger levels of palmar flexion. Additionally, from the figure it can be observed that the signal is approximately constant throughout the central 5.5 seconds segment in each condition, showing its validity to be used in the calculation of the outcome measure. The combined results for the different participants for each condition can be found in Figure 5.8.

#### 5.3.2.1 ECR

Using Mauchly's test it was observed that the assumption of sphericity had been violated for the main effects of wrist position for the ECR,  $\chi^2(5) = 21.04, p < .001$  and balance method  $\chi^2(5) = 15.04, p = .011$ . Consequently, the degrees of freedom were corrected using Greenhouse-Geisser estimates of sphericity. The effect of wrist position and balance method were observed to be significant ( $p < .001$ ). A pairwise comparison showed that the ECR activity on average reduced ( $p < .001$ ) with 51% for constant ( $2.1 \pm 0.68$  %MVC), 53% for linear ( $2.0 \pm 0.58$  %MVC) and 46% for sinusoidal ( $2.3 \pm 0.61$  %MVC) compared to no compensation ( $4.3 \pm 1.2$  %MVC). This can also be seen from Figure 5.8 showing an overall decrease in ECR activity close to rest level. No significant effects were observed between the different types of compensation.

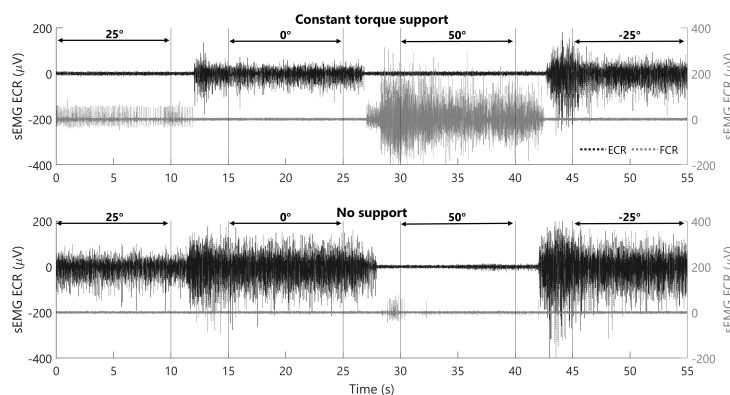


**Figure 5.7:** Raw sEMG data from one participant for a single measurement of constant torque compensation (top graph) and no compensation (bottom graph), for different levels of palmar flexion with the forearm at 0°. Note that the order of the wrist position is randomly assigned throughout the experiments. However, for clarity the results of two experiments of the same participant are depicted which follow the same order

5

### 5.3.2.2 FCR

Using Mauchly's test it was indicated that the assumption of sphericity had been violated for the main effects of wrist position for the FCR,  $\chi^2(5) = 29.78, p < .001$ . Consequently, the degrees of freedom were corrected using Greenhouse-Geisser estimates of sphericity. The effect of wrist position ( $p < .001$ ), balance method ( $p < .001$ ) and forearm orientation ( $p = .008$ ) were observed to be significant. A pairwise comparison showed that the FCR activity on average increased with 50% ( $p = .012$ ) for constant ( $2.7 \pm 1.3$  %MVC), 61% ( $p = .005$ ) for linear ( $2.9 \pm 1.4$  %MVC) and 44% ( $p = .005$ ) for sinusoidal ( $2.6 \pm 1.1$  %MVC). This is mainly caused by a large increase in FCR activity at 50° palmar flexion when a form of compensation is used, especially at the horizontal forearm position, see Figure 5.8. Considering all forearm orientations, the FCR activity increased with 134% (from 2.3 to 5.4%MVC) for the constant and sinusoidal torque profile and 187% (from 2.3 to 6.6%MVC) for the linear torque profile with respect to no compensation when flexing the wrist from 0° to 50°. No significant effects were observed between the different types of compensation.

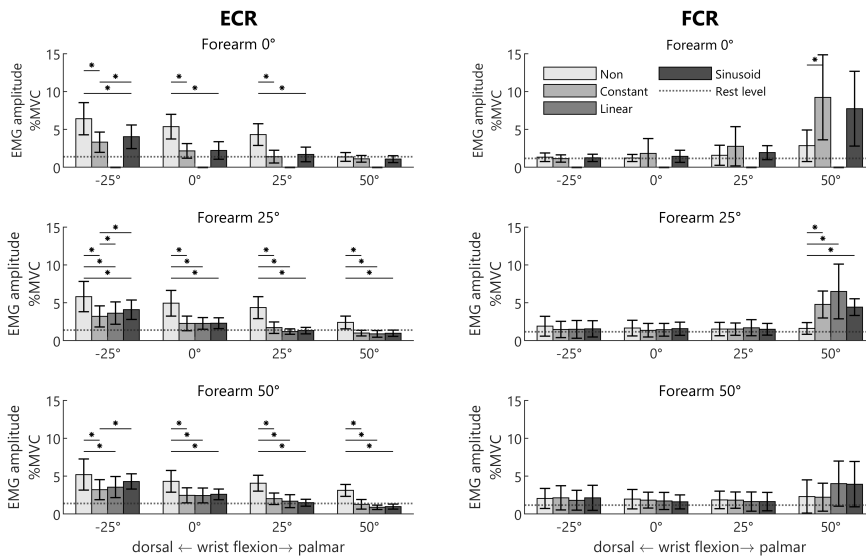


**Figure 5.8:** Mean sEMG magnitude relative to the MVC of the ECR (left) and FCR (right) for different forearm positions, wrist positions and balance methods. Reported as mean and standard deviation. \*indicates a statistically significant difference. Note, for the 0° forearm position the linear force profile is combined with the constant force profile as they are the same for this orientation (therefore no separate measurements were performed)

## 5.4 Discussion

This study was conducted to assess whether two simplified weight compensation strategies show a similar muscle activity reduction as the theoretically ideal sinusoidal strategy applied in a wrist support system to compensate the weight of the hand. Based on the pairwise comparison between the different compensation strategies combining all wrist and forearm orientations, for both the FCR and ECR, a significant difference was found between with and without compensation, while no differences were found between the different compensation strategies (constant, linear and sinusoidal). These findings indicate that the simplified constant and linear torque profiles can be regarded effective alternatives for compensation, as opposed to the sinusoidal torque profile. These findings could not be compared with literature as to the authors' knowledge there are no studies that systematically investigate the influence of different types of compensation on the activity of the wrist muscles.

Although the anti-gravity ECR muscle showed a significant reduction in muscle activity in almost all configurations, the FCR showed only an increase at 50° palmar flexion within all compensation strategies. Although this increased activity is relatively small ( $< 10\% \text{MVC}$ ), it indicates that there is an overcompensation of the required compensation at 50° palmar flexion. For the constant and linear compensation strategies this overcompensation could be explained by overestimation of the required compensation torque resulting from the simplification of the theoretical required torque, see Table 5.2. However, in case of the sinusoidal profile (and the constant profile at the 25° forearm orientation, i.e., C25) no

overestimation of the theoretical required compensation is provided and still an increase of the FCR activity was detected. This suggests that for the higher levels of palmar flexion, a lower theoretical compensation torque is required than what follows from the theoretically ideal sinusoidal strategy. This mismatch between the actual and theoretical compensation torque could be explained by the effects of passive joint impedance. Each joint in the human body demonstrates resistance against passive motion, especially near the end range of motion, resulting from muscles, ligaments, nerves, blood vessels, and skin [1, 6]. Formica et al. [15] measured the passive joint impedance of the wrist joint in healthy subjects. From their results it can be observed that for larger palmar flexion angles the magnitude of the passive joint impedance becomes equal to or even larger than the gravitational moments. Consequently, it is hypothesized that the increase in FCR activity for the higher flexion region is (partially) a result of this inherent passive joint impedance. This assumes that when no support is provided the moments generated by gravity are large enough to overcome at least partially the passive joint impedance during flexion. So, when the weight of the hand is compensated, additional forces are required to palmar flex the hand to overcome the passive joint impedance to reach a palmar flexion angle of 50°, resulting in elevated FCR activity. The influence of this joint impedance is especially of importance when translating these findings to people which suffer from an increased passive joint impedance which is often the case in chronic stroke, spinal muscular atrophy and MD patients [9, 12, 27, 31].

**Table 5.2:** Level of compensation of the simplified balancing methods compared to the theoretical required torque (e.g., sinusoidal profile) for the specific wrist and forearm positions. Larger values than 100% indicate overcompensation, whereas smaller values indicate under compensation. For the balance method C=constant and L=linear, while the adjoining number indicates the forearm orientation. A more general overview of the level of compensation is depicted in Figure 5.6

Balance method	Wrist position			
	-25	0	25	50
C 0	110%	100%	110%	156%
L 0	110%	100%	110%	156%
C 25	141%	100%	91%	100%
L 25	112%	100%	109%	141%
C 50	248%	100%	71%	64%
L 50	119%	100%	108%	131%

### 5.4.1 Limitations of the study

When inspecting the data presented in Figure 5.8, it can be observed that certain conditions exhibit a substantial standard deviation. This is especially the case for the FCR. This is likely caused by the fact that the activity was close to rest level, making it more susceptible to noise (e.g., power line interference). Additionally, some variation was potentially caused by estimation errors of the hand weight and CoM (see Appendix C.3) [10, 28]. However, the estimated masses are comparable to literature [8, 13]. Moreover, the resolution of the applied torques for the constant and linear profiles was finite. This was especially a limitation for the linear profile, due to the limited number of springs available. For some participants this

finite resolution resulted in a small deviation from the required compensation estimated. When considering the results of all participants across all experiments, on average the differences between the applied and desired compensation were  $-.011 \pm .042$  N/mm for the stiffness and  $.53 \pm 9.2$  g for the weight, resulting in a difference of less than 10%. Other possible sources for spread in the results might be due to variation in the passive joint impedance and potential misalignment of the human wrist joint with respect to the mechanical joint of the set-up.

The human wrist deviates from that of an ideal hinge joint [1]. While the impact of this deviation is minimal at smaller flexion angles, it becomes more prominent as the angles increase, due to translation of the axis of rotation of the human wrist joint [30]. Joint misalignment can introduce interaction forces between the human and the set-up, such as shear forces at the interface, requiring more effort to flex the wrist. Moreover, correctly palpating the muscle belly of the FCR was challenging in some participants, potentially resulting in a less ideal sensor placement, yielding cross talk from other muscles.

### 5.4.2 Recommendations

This study determined the constant and linear profile by making use of a Taylor expansion around the neutral position of the wrist ( $0^\circ$  flexion) of the sinusoidal profile (Appendix C.1). However, other approximations, for instance taking an average of the profile, are possible directions for further investigation for further optimization of the provided level of support. However, more importantly the influence of passive joint impedance should be taken into account, since the passive joint impedance plays a substantial role in the required level of compensation, especially in many clinical cases and near the joint limits.

## 5.5 Conclusion

This study has shown that simplified torque-angle profiles (e.g., constant or linear) can be considered as alternative to the conventional sinusoidal profile to compensate for the weight of the hand. However, the increase in FCR activity for all compensation methods, including the conventional sinusoidal, indicates a limitation of the applied compensation strategies as they do not account for passive joint impedance near the joint limits. As such, more research is needed to assess this influence of passive joint impedance on the required compensation profile. Meanwhile, the findings of this study can be used to inform the development of simplified wrist supports for people suffering from (neuro)muscular weakness.

## References

- [1] Ç. Ayhan and E. Ayhan. Chapter 13 - Kinesiology of the wrist and the hand. In Salih Angin and Ibrahim Engin Şimşek, editors, *Comparative Kinesiology of the Human Body*, pages 211–282. Academic Press, 2020. doi: <https://doi.org/10.1016/B978-0-12-812162-7.00013-8>.
- [2] M. Barbero, R. Merletti, and A. Rainoldi. Upper Limb. In *Atlas of Muscle Innervation Zones*, pages 103–120. Springer Milan, Milano, 2012. doi: 10.1007/978-88-470-2463-2.
- [3] M. Besomi, P. W. Hodges, E. A. Clancy, J. Van Dieën, F. Hug, M. Lowery, R. Merletti, K. Søgaard, T. Wrigley, T. Besier, R. G. Carson, C. Disselhorst-Klug, R. M. Enoka, D. Falla, D. Farina, S. Gandevia, A. Holobar, M. C. Kiernan, K. McGill, E. Perreault, J. C. Rothwell, and K. Tucker. Consensus for experimental design in electromyography (CEDE) project: Amplitude normalization matrix. *Journal of Electromyography and Kinesiology*, 53:102438, 2020. doi: 10.1016/j.jelekin.2020.102438.
- [4] A. Burden. How should we normalize electromyograms obtained from healthy participants? What we have learned from over 25years of research. *Journal of Electromyography and Kinesiology*, 20(6):1023–1035, 2010. doi: 10.1016/j.jelekin.2010.07.004.
- [5] R. F. Chandler, C. E. Clauser, J. T. McConville, H. M. Reynolds, and J. W. Young. Investigation of Inertial Properties of the Human Body. Technical Report March, U.S. Department of Transportation, Washington, D.C., 1975.
- [6] G. S. Chleboun, J. N. Howell, R. R. Conatser, and J. J. Giesey. The relationship between elbow flexor volume and angular stiffness at the elbow. *Clinical Biomechanics*, 12(6): 383–392, 1997. doi: 10.1016/S0268-0033(97)00027-2.
- [7] E. A. Clancy, F. Negro, and D. Farina. Single-Channel Techniques for Information Extraction from the Surface EMG Signal. In *Surface Electromyography: Physiology, Engineering, and Applications*, pages 91–125. John Wiley & Sons, Ltd, Hoboken, New Jersey, 2016. doi: 10.1002/9781119082934.ch04.
- [8] C. E. Clauser, J. T. McConville, and J. W. Young. Weight, volume, and center of mass of segments of the human body. Technical report, Wright-Patterson Air Force Base, Ohio, 1969. URL <http://oai.dtic.mil/oai/oai?verb=getRecord&metadataPrefix=html&identifier=AD0710622>.
- [9] C. Cornu, F. Goubel, and M. Fardeau. Muscle and joint elastic properties during elbow flexion in Duchenne muscular dystrophy. *The Journal of Physiology*, 533(2):605–616, 2001. doi: 10.1111/j.1469-7793.2001.0605a.x.
- [10] M. Coscia, V. C. K. Cheung, P. Tropea, A. Koenig, V. Monaco, C. Bennis, S. Micera, and P. Bonato. The effect of arm weight support on upper limb muscle synergies during reaching movements. *Journal of NeuroEngineering and Rehabilitation*, 11(1):22, 2014. doi: 10.1186/1743-0003-11-22.

- [11] E. Criswell. *Cram's introduction to surface electromyography*. Jones and Bartlett, Sudbury, MA, second edi edition, 2011.
- [12] K. L. de Gooijer-van de Groep, E. de Vlugt, H. J. van der Krogt, A. Helgadóttir, J. H. Arendzen, C. G. M. Meskers, and J. H. de Groot. Estimation of tissue stiffness, reflex activity, optimal muscle length and slack length in stroke patients using an electromyography driven antagonistic wrist model. *Clinical Biomechanics*, 35:93–101, 2016. doi: 10.1016/j.clinbiomech.2016.03.012.
- [13] J. L. Durkin and J. J. Dowling. Analysis of Body Segment Parameter Differences Between Four Human Populations and the Estimation Errors of Four Popular Mathematical Models. *Journal of Biomechanical Engineering*, 125(4):515–522, 2003. doi: 10.1115/1.1590359.
- [14] A. Field. *Discovering statistics using IBM SPSS statistics*. SAGE Publications, 4th edition, 2013.
- [15] D. Formica, S. K. Charles, L. Zollo, E. Guglielmelli, N. Hogan, and H. I. Krebs. The passive stiffness of the wrist and forearm. *Journal of Neurophysiology*, 108(4):1158–1166, 2012. doi: 10.1152/jn.01014.2011.
- [16] M. Gandolla, A. Antonietti, V. Longatelli, and A. Pedrocchi. The Effectiveness of Wearable Upper Limb Assistive Devices in Degenerative Neuromuscular Diseases: A Systematic Review and Meta-Analysis. *Frontiers in Bioengineering and Biotechnology*, 7(January):1–16, 2020. doi: 10.3389/fbioe.2019.00450.
- [17] Y. Hasegawa, S. Shimada, and K. Eguchi. Development of wrist support mechanism for muscle weakness person to work on desk work. In *2014 International Symposium on Micro-NanoMechatronics and Human Science (MHS)*, pages 1–3. IEEE, 2014. doi: 10.1109/MHS.2014.7006127.
- [18] S. L. Houwen-Van Opstal, Y. M. Van Den Elzen, M. Jansen, M. A. Willemsen, E. H. Cup, and I. J. De Groot. Facilitators and Barriers to Wearing Hand Orthoses by Adults with Duchenne Muscular Dystrophy: A Mixed Methods Study Design. *Journal of Neuromuscular Diseases*, 7(4):467–475, 2020. doi: 10.3233/JND-200506.
- [19] B. T. Iwamuro, E. G. Cruz, L. L. Connelly, H. C. Fischer, and D. G. Kamper. Effect of a Gravity-Compensating Orthosis on Reaching After Stroke: Evaluation of the Therapy Assistant WREX. *Archives of Physical Medicine and Rehabilitation*, 89(11):2121–2128, 2008. doi: 10.1016/j.apmr.2008.04.022.
- [20] M. J. A. Jannink, G. B. Prange, A. H. A. Stienen, H. van der Kooij, J. M. Kruitbosch, M. J. IJzerman, and H. J. Hermens. Reduction of muscle activity during repeated reach and retrieval with gravity compensation in stroke patients. In *2007 IEEE 10th International Conference on Rehabilitation Robotics*, pages 472–476. IEEE, 2007. doi: 10.1109/ICORR.2007.4428468.
- [21] I. Y. Jung, J. H. Chae, S. K. Park, J. H. Kim, J. Y. Kim, S. J. Kim, and M. S. Bang. The correlation analysis of functional factors and age with Duchenne muscular dystrophy. *Annals of Rehabilitation Medicine*, 36(1):22–32, 2012. doi: 10.5535/arm.2012.36.1.22.

- [22] J. R. Karges, B. E. Mark, S. J. Stikeleather, and T. W. Worrell. Concurrent Validity of Upper-Extremity Volume Estimates: Comparison of Calculated Volume Derived From Girth Measurements and Water Displacement Volume. *Physical Therapy*, 83(2): 134–145, 2003. doi: 10.1093/ptj/83.2.134.
- [23] E. Mercuri, C. G. Bönnemann, and F. Muntoni. Muscular dystrophies. *The Lancet*, 394 (10213):2025–2038, 2019. doi: 10.1016/S0140-6736(19)32910-1.
- [24] R. Merletti and G. L. Cerone. Tutorial. Surface EMG detection, conditioning and pre-processing: Best practices. *Journal of Electromyography and Kinesiology*, 54:102440, 2020. doi: 10.1016/j.jelekin.2020.102440.
- [25] G. B. Prange, L. A. C. Kallenberg, M. J. A. Jannink, A. H. A. Stienen, H. van der Kooij, M. J. IJzerman, and H. J. Hermens. Influence of gravity compensation on muscle activity during reach and retrieval in healthy elderly. *Journal of Electromyography and Kinesiology*, 19(2):e40–e49, 2009. doi: 10.1016/j.jelekin.2007.08.001.
- [26] M. Puchinger, N. B. R. Kurup, T. Keck, J. Zajc, M. F. Russold, and M. Gfoehler. The Retrainer Light-Weight Arm Exoskeleton: Effect of Adjustable Gravity Compensation on Muscle Activations and Forces. In *2018 7th IEEE International Conference on Biomedical Robotics and Biomechatronics (Biorob)*, pages 396–401. IEEE, 2018. doi: 10.1109/BIOROB.2018.8487218.
- [27] D. Ragonesi, S. K. Agrawal, W. Sample, and T. Rahman. Quantifying anti-gravity torques for the design of a powered exoskeleton. *IEEE Transactions on Neural Systems and Rehabilitation Engineering*, 21(2):283–288, 2013. doi: 10.1109/TNSRE.2012.2222047.
- [28] K. D. Runnalls, G. Anson, S. L. Wolf, and W. D. Byblow. Partial weight support differentially affects corticomotor excitability across muscles of the upper limb. *Physiological Reports*, 2(12):e12183, 2014. doi: 10.14814/phy2.12183.
- [29] E. Sarrazin, M. V. D. Hagen, U. Schara, K. Von Au, and A. M. Kaindl. Growth and psychomotor development of patients with Duchenne muscular dystrophy. *European Journal of Paediatric Neurology*, 18(1):38–44, 2014. doi: 10.1016/j.ejpn.2013.08.008.
- [30] A. Schiele and F. C. T. van der Helm. Kinematic design to improve ergonomics in human machine interaction. *IEEE Transactions on Neural Systems and Rehabilitation Engineering*, 14(4):456–469, 2006. doi: 10.1109/TNSRE.2006.881565.
- [31] B. D. Schmit, J. P. A. Dewald, and W. Z. Rymer. Stretch reflex adaptation in elbow flexors during repeated passive movements in unilateral brain-injured patients. *Archives of Physical Medicine and Rehabilitation*, 81(3):269–278, 2000. doi: 10.1053/apmr.2000.0810269.
- [32] A. Story. Right Hand Reference, 2020. URL <https://grabcad.com/library/right-hand-reference-1>.



# III

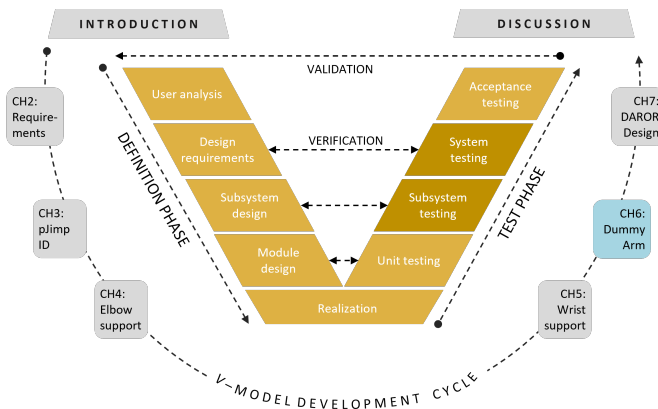
## System Design and System Testing



# 6

## The Design of the Dummy Arm: a Verification Tool for Arm Exoskeleton Development

Parts I and II covered the left side of the V-model. Parts III shifts to the right side, focusing on System Design and Testing.



This chapter introduces the Dummy Arm, a verification tool simulating the target population's load. The next Chapter 7 will detail the design of the Duchenne Arm Orthosis (DAROR) system.

---

This chapter was published as: Filius, S.J., van der Burgh, B.J., Harlaar, J. 2024. The Design of the Dummy Arm: A Verification Tool for Arm Exoskeleton Development. *Biomimetics*, 9, 579. doi:10.3390/biomimetics9100579. The CAD design of the dummy arm can be downloaded at <https://doi.org/10.4121/3c4fa57d-3fc6-4e27-933c-00a02a6e5a33>. A supporting video is available at <https://www.mdpi.com/article/10.3390/biomimetics9100579/s1>. The software to calculate the cam profile shape is available at <https://doi.org/10.4121/df7a7d4f-2e4b-428a-a3d4-16b6e153c29c>

# The Design of the Dummy Arm: A Verification Tool for Arm Exoskeleton Development

**Abstract** Motorized arm supports for individuals with severe arm muscle weakness require precise compensation for arm weight and elevated passive joint impedance (e.g., joint stiffness as a result of muscle atrophy and fibrosis). Estimating these parameters in vivo, along with the arm's center of mass, is challenging, and human evaluations of assistance can be subjective. To address this, a dummy arm was designed to replicate the human arm's anthropometrics, degrees of freedom, adjustable segment masses, and passive elbow joint impedance (eJimp). This study presents the design, anthropometrics, and verification of the dummy arm. It successfully mimics the human arm's range of motion, mass, and center of mass. The dummy arm also demonstrates the ability to replicate various eJimp torque-angle profiles. Additionally, it allows for the tuning of the segment masses, centers of mass, and eJimp to match a representative desired target population. This simple, cost-effective tool has proven valuable for the development and verification of the Duchenne ARM ORthosis (DAROR), a motorized arm support, or 'exoskeleton'. This study includes recommendations for practical applications and provides insights into optimizing design specifications based on the final design. It supplements the CAD design, enhancing the dummy arm's application for future arm-assistive devices.

## 6

### 6.1 Introduction

Assistive wearable technologies, such as motorized orthosis or exoskeletons, work in parallel to the human skeleton to support or augment human motion in terms of strength, endurance, or function [1, 7, 10, 16]. The application of such devices varies [9], from industrial [7, 17] to military [28] to medical (e.g., rehabilitative [22], or daily assistive [15]) use. Developing such devices requires extensive human testing and evaluation, which brings several challenges.

The first challenge with human testing relates to safety, especially at the beginning of the development cycle, as it is difficult to predict how new sensors or software systems behave when interacting with humans. For instance, failure in safety limits or unexpected behavior might result in fast, unexpected movements of the limb or even extend the limb beyond its natural joint limits, potentially resulting in dangerous situations. Moreover, when developing exoskeletons for a vulnerable population, such as people with severe muscle weakness or children, obtaining (medical) ethical approval and recruiting subjects

that are willing to be exposed to the potential risks are time-consuming processes and are therefore not feasible for every phase of development [1]. In addition to safety issues, developing an exoskeleton is time-consuming, labor-intensive, and, therefore, costly.

Furthermore, for exoskeletons that aim to compensate for the weight of the human limb, it is essential to accurately know the properties of the limb to verify the controller's performance. However, the properties of human limb, such as their weight and center of mass (CoM), can only be estimated indirectly (e.g., using tables from the literature [3, 4]). Especially in the case of populations with neuromuscular disorders, the anthropometrics might deviate from the available tables due to, for instance, muscle atrophy, bone density reductions, joint contractures, or deformations.

Moreover, it is difficult for humans to objectively quantify the amount of assistance provided or distinguish between small changes in controller settings, leading to subjective or even biased evaluations of the controller's performance.

During the development of the Duchenne ARm ORthosis (DAROR), as described in Chapter 7, these challenges led to the need for a mechanical phantom. Such a phantom, like a Dummy Arm, with similar human-limb characteristics, can serve as a tool for verification for various compensation strategies, and enhances the fast iteration of exoskeleton control development [1]. The DAROR is an investigational motorized arm exoskeleton that enhances arm function. It is intended to provide assistance in daily activities for people with neuromuscular diseases such as Duchenne Muscular Dystrophy (DMD) that cope with severe muscle weakness and elevated joint stiffness, or, more accurately, 'passive joint impedance' (pJimp). The impedance controller of the DAROR aims to compensate for the weight of the user's arm and the elbow pJimp (denoted as eJimp for the remainder of this work). The term pJimp describes the passive mechanical impedance against motion [19] resulting from the passive tissue around the joint and limb inertia. For instance, in people with DMD, this pJimp is elevated, presumably resulting from muscle atrophy, higher levels of connective tissue, and the development of joint contractures [14].

In the literature, few examples of dummy limbs were found, describing mannequins with a primary focus on mimicking the outer dimensions of the human limb [6, 18, 20]. Others, described rather complex and costly designs which were equipped with sensors and actuators or soft tissues [1, 2, 9, 27]. For the development of the DAROR, an upper-extremity phantom limb that is cost-effective, simple in design, and mimics the characteristics of the human arm, including eJimp, was required to serve as a verification tool for the compensation models.

This work presents the design and verification of a relatively simple, reproducible, cost-effective dummy arm that mimics human arm characteristics. The novelty of this design is that it allows us to replicate (elevated) eJimp and is easily adjustable in mass and CoM to fit various exoskeleton target populations. By sharing our design, we promote the development of future arm exoskeletons and facilitate the rapid iteration and objective evaluation of exoskeleton controllers.

# 6.2 Materials and methods

## 6.2.1 Dummy Arm design requirements

The dummy arm was required to have the following properties:

- A representative and adjustable segment mass and CoM [3–5, 8, 12];
- A representative forearm anthropometric to fit the DAROR interface sleeve(s);
- A similar DAROR range of motion; see Table 6.1;
- An attachment at the base of the frame at the shoulder joint;
- An adjustable (linear) eJimp;
- An interface to attach additional objects at the wrist location.

**Table 6.1:** DAROR shoulder range of motion.

Joint Rotation	Target
GH elevation	11° to 137°
GH horizontal	–46° to 138°
GH axial	–113° to 65°
El flexion/extension	2° to 120°

Abbreviation: GH, glenohumeral joint; El, elbow.

## 6.2.2 Dummy Arm design

The design of the dummy arm can be divided into several sub-design problems: the shoulder joint, the elbow joint, the elbow joint impedance, the connection frame, and the mass of the upper and lower arm. The design of the dummy arm, with its components together with the DAROR, is shown in Figure 6.1.

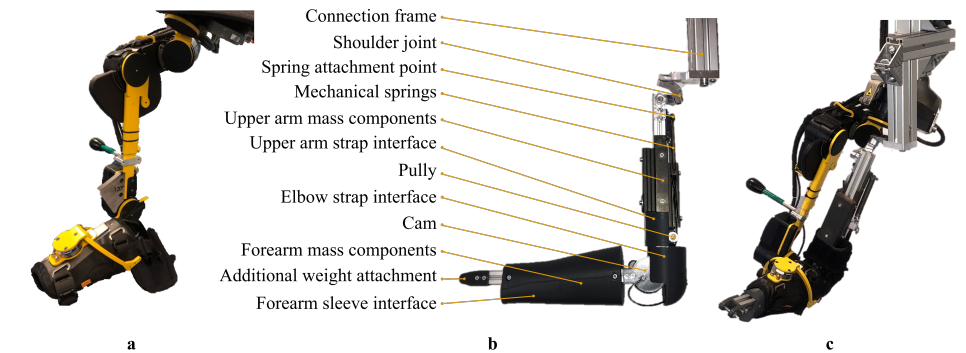


**Figure 6.1:** Picture of the a) DAROR exoskeleton, b) Dummy Arm design with its components, and c) the Dummy Arm placed inside the DAROR exoskeleton.

### 6.2.2.1 Shoulder joint

The shoulder joint is a complex joint due to its high number of degrees of freedom (e.g., glenohumeral elevation and horizontal and axial rotation, according to the ISB recommendations [11, 25, 29]), as well as its large range of motion. A serial chain of three revolute joints was used to mimic the three degrees of freedom of the shoulder. However, with three revolute joints, several configurations are possible. Each has its advantages and disadvantages with respect to its range of motion and the possible occurrence of gimbal locking. As the range of motion is primarily restricted by the exoskeleton, which consists of three actuators mounted in series at an inclination of approximately  $60^\circ$  with respect to each other (see Chapter 7), a similar configuration for the dummy arm is used. Each of the three revolute joints consists of a set of two ball bearings (MR95-2Z) to minimize friction and provide support to possible bending moments. The joints are connected through 3D-printed or milled aluminum brackets (for the final design milled aluminum brackets were used).

### 6.2.2.2 Elbow joint

The elbow joint can be considered a hinge joint. Therefore, the design of the elbow joint is relatively straightforward, consisting of two ball bearings (625ZZ) mounted to the upper arm frame on either side of an axis and attached to the forearm frame.

### 6.2.2.3 Passive elbow joint impedance

The impedance of the dummy arm elbow joint is created using a wrapping cam mechanism. This mechanism consists of a spring attached to a belt, which wraps around a cam attached to the forearm. Upon rotation of the forearm, the belt wraps/unwraps around the cam, stretching/relaxing the spring. This is shown schematically in Figure 6.2. A cam is attached on either side of the elbow with the belt either wrapping the cam in a clockwise or counterclockwise direction to simulate impedance during both the flexion and extension of the elbow. The current design aimed to mimic the linearized torque profile of the passive eJimp similar to [13], which is achieved using a circular cam. However, different torque profiles can be generated depending on the shape of the cam. The torque-angle profile can be further tuned by changing the spring stiffness ( $k_s$ ) or the spring's pretension ( $x_0$ ). An additional advantage of the wrapping cam mechanism is that the springs can be mounted parallel to the upper arm frame, resulting in a compact design.

### 6.2.2.4 Connection frame

To connect the different components (joints, springs, and weights), a skeleton for the upper and lower arm is made of aluminum extrusion beams ( $20 \times 20$  mm), which allows the various components to be attached freely along the beam's length. As a result, the system is modular, allowing for easy adjustment of different parts. Additionally, the dummy arm can mimic different human arm sizes using various lengths of beams. A rigid 3D-printed PLA shell is attached to the frame, which mimics the forearm [26] for interfacing with the exoskeleton sleeve.

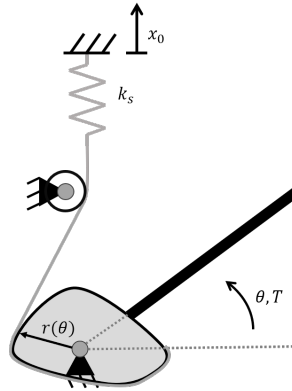


**Figure 6.2:** Schematic of the wrapping cam mechanism to generate the desired joint stiffness. Here,  $k_s$  is the spring stiffness,  $\theta$  the angle of the elbow,  $r$  is a function of  $\theta$ , defining the cam shape (for the current prototype,  $r$  is constant, resulting in a circular cam), and  $x_0$  is the pretension applied to the spring. The torque  $T$  can be expressed as  $T = T(\theta, k_s, x_0)$ . A detailed discussion on deriving the cam shape for a given torque profile can be found in [21, 24].

## 6

### 6.2.2.5 Mass and Center of Mass of the Upper and Lower Arm

Steel plates are mounted to the aluminum beams to mimic the overall mass and the CoM of the human forearm and upper arm. The location for the mounting of the steel plates is based on a CAD model, which is used to estimate the CoM. The dimensions of the dummy arm are based on the biometric data from [3], resulting in an approximate length of 250 mm for the lower arm and 300 mm for the upper arm. The segment mass parameters are based on the work of [3–5, 12], with a mass of approximately 1.6 to 2 kg for the upper arm and 0.9–1.1 kg for the forearm. The mass of the hand (ca. 400 g) is not included, but it can be attached separately alongside additional weights to mimic lifted objects in the hand if deemed necessary. The advantage of using a modular system consisting of aluminum extrusion profiles is that properties such as its mass and CoM can be easily adjusted to the desired application by removing or adding weights and shifting their position. As such, the dummy arm can be adjusted to simulate different arms.

### 6.2.2.6 Verification of design

The verification of the dummy arm consists of two parts. First, the direct measurement of the segment properties of the dummy arm is performed by weighing the segment mass and estimating the CoM in the direction of the limb with respect to the proximal joint. This latter property was measured by hanging the upper and forearm individually to a rod with two ropes connected to the endpoints of the limb segments. The location on the rod where it needed to be held fixed to keep the rod in balance (level) was taken as the CoM location. The second part verifies the realized eJimp with four different spring-type configurations. This is done using the DAROR set-up. The DAROR moves the dummy arm elbow joint (position-controlled) through a range-of-motion cycle (either ca. 10–109° or 40–116°) with approximately 8 static intervals, while the shoulder joint remained in



a neutral position (ca. GH elevation: 10°, horizontal 10°, axial 0°). A video showing this procedure is available in the Supplementary Materials. The joint torque is measured by the deflection of the series elastic element in the actuators (torque accuracy 0.5 Nm, torque precision 0.4 Nm, ref. Chapter 7) in the elbow actuator. The range-of-motion cycle is repeated with and without springs attached to the dummy arm elbow joint. First, these torque-angle profiles are fitted to a 5th-order polynomial (polyfit, polyval) using MATLAB (version 2021b). Then, these torque-angle profiles measured with and without the attached springs were subtracted to receive the measured eJimp of the dummy arm. Additionally, a first-order fit of this eJimp was created to compare the realized Jimp slope, offset, and equilibrium (zero-crossing) to the average human eJimp measured in twelve non-disabled male individuals in the study of Filius et al. [13].

## 6.3 Results

The dummy arm was developed and fabricated based on the design requirements. Table 6.2 summarizes the realized characteristics of the dummy arm in terms of its mass, CoM, and eJimp characteristics, and compares it to the intended human model and the CAD design parameters. The table shows that the mass and CoM of the realized dummy arm is comparable to the human arm model but is tunable by adjusting the position and number of steel plates, as mentioned in Section 6.2.2.5.

**Table 6.2:** Comparison of the mass and center of mass (CoM) based on CAD with real-life measurements.

	Human Model		Dummy Arm		CAD	
	Mass <sup>a</sup> kg	CoM <sup>b</sup> mm	Mass kg	CoM mm	Mass kg	CoM <sup>c</sup> mm
UA	1.6–2	137	1.8	140	1.7	$\begin{bmatrix} 2.5 \\ -140.2 \\ -2.0 \end{bmatrix}$
FA	0.9–1.1	106	1.0	110	1.0	$\begin{bmatrix} -0.2 \\ -112.7 \\ 2.6 \end{bmatrix}$

Abbreviations: UA: Upper arm; FA: Forearm; CoM, center of mass; eJimp, passive elbow joint impedance; z, zero-crossing (equilibrium point); M, mean; SD, standard deviation. All CoM values are expressed with respect to the proximal joint center. <sup>a</sup>Retrieved from [3, 4]. <sup>b</sup>Based on average locations of COM as ratio of segment length of dummy arm, retrieved from Table 4 of [3]. <sup>c</sup>The second element (y-axis) is aligned with the limb in a proximal direction, and the first element (x-axis) points laterally.

### 6.3.1 Joint impedance realization

The realized eJimp in the dummy arm is compared to the measured human eJimp from our previous work [13] and presented in Figure 6.3. This previous work used an active elbow support set-up to identify the human eJimp in twelve non-disabled male individuals. The actuator placed at the elbow joint rotated the participant's forearm over the elbow's range of motion in the horizontal plane. In this plane, the gravitational component of the passive forces exerted on the elbow joint remains constant. A six-degrees-of-freedom force/torque

sensor on the forearm interface sleeve measured the elbow joint moments, representing the human eJimp [13]. Figure 6.3 shows the human eJimp model as a group average and standard error of the mean of the identified human eJimp and compares this to the realized eJimp of the four spring types.

Depending on the selected spring type and pre-tension of the springs, different eJimp characteristics were realized; see Table 6.3. Spring type 4 has the most representative equilibrium point (i.e., where the torque-angle curve crosses the zero-line) compared to the human model. The slope of type 2 is more representative of the slope of the non-disabled eJimp, whereas the slope of spring type 4 could represent an elevated eJimp.

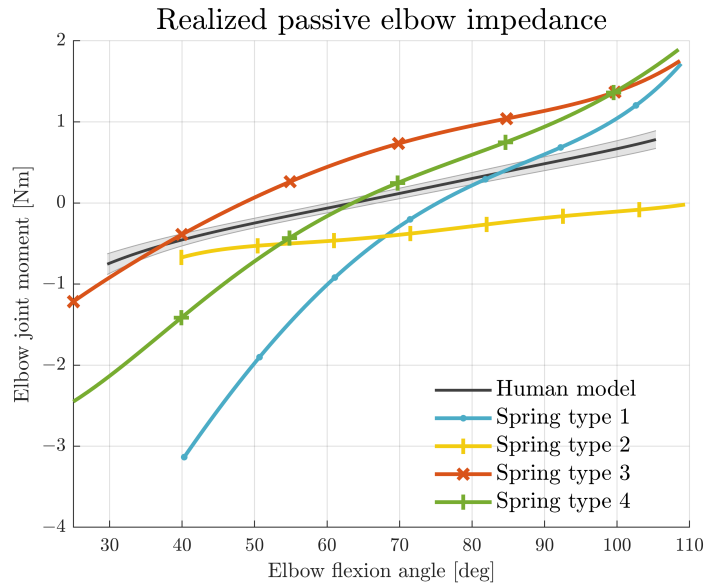


**Figure 6.3:** The realized passive eJimp using different spring types compared to the average human eJimp model of 12 non-disabled male individuals, with data retrieved from [13]. The solid grey line represents the group average, and the shaded area shows the standard error of the mean.

**Table 6.3:** Passive eJimp characteristics of different spring types compared to human model.







	1st-Order Fit Nm/rad $x$ + Nm	$z$ (M $\pm$ SD) deg
Human model	$1.14x - 1.29$	$66 \pm 11$
Spring type 1	$4.31x - 2.46$	74
Spring type 2	$1.29x + 1.45$	-
Spring type 3	$3.04x - 0.03$	48
Spring type 4	$3.67x - 1.24$	63

Abbreviations:  $z$ , zero-crossing (equilibrium point); M, mean; SD, standard deviation.

6.3.2 Activities of daily living

The achieved range of motion of the shoulder joints is larger than the shoulder range of motion of the DAROR set-up, and the elbow joint is similar to the range of motion of a human arm in the DAROR set-up, see Chapter 7. This achieved range of motion is sufficient to reach the desired activities that are considered relevant for daily living for this application. To illustrate the sufficient range of motion of the dummy arm in the DAROR set-up, some static poses of the relevant activities of daily living are displayed in Table 6.4. Moreover, the dummy arm design allows for the attachment of an additional object at the wrist location, which is illustrated in the third column (c), where a 200 g mass is attached to the attachment point to simulate a lifted object in hand.

Table 6.4: Illustration of the range of motion of the dummy arm for a set of activities of daily living.

a. Tabletop Activities	b. Feeding Activities	c. Lifted Object (200 g)
 	 	 

6.3.3 Cost-analysis

The material costs for the various components of the dummy arm are listed in Table 6.5. Here, labor costs are not included in this overview, as they are dependent on the available facilities. Moreover, the costs of a 3D-printed shoulder joint are considered. However, a milled aluminum shoulder joint will be more expensive, especially due to the involved labor and equipment costs. The approximate fabrication time is around 5 h in the case of a 3D-printed shoulder joint, and for milled aluminum joints, an additional 5–10 h should be taken into account, depending on proficiency and the available equipment.

**Table 6.5:** Material costs of the various components. If the costs depend on the material properties, the total weight or length is reported. Dimensions of the different sub-components can be retrieved from the CAD files in Supplementary Materials S1. Costs are rounded to the nearest EUR 0.50.

<b>Material</b>	<b>Costs</b>
Bearings	EUR 13.50
Frame	EUR 6.00 (550 mm)
Mounting materials	EUR 15.00
Axes	EUR 1.00 (200 mm)
Weights	EUR 12.50 (1.9 kg)
Springs	EUR 11.00
Belt and pulleys	EUR 13.00
PLA filament	EUR 6.50 (280 g)
Total	EUR 78.50

## 6.4 Discussion

This work aims to present the design of a relatively simple, reproducible, and cost-effective dummy arm that can be used as a verification and development tool for (motorized) upper-extremity exoskeletons. The dummy arm mimics the human arm mechanics with adjustable mass, CoM, and ejimp characteristics. The forearm design simulates the shape of a human forearm and allows for the attachment of additional weights at the wrist to simulate (objects lifted in) the hand.

### 6.4.1 Limitations

Some simplifications are made when comparing the dummy arm with a human arm. First of all, it is assumed that the joints are ‘ideal’ joints (e.g., having a fixed center of rotation), whereas, in reality, human joints have complex surface geometries and show shifts in their joint axis of rotation during motion [23]. This is especially apparent for the shoulder joint, as the elevation or suppression of the scapula occurs in most elevation movements. Joint misalignment might exert excessive interaction forces on the dummy arm, especially as the dummy arm joints give no slack. Therefore, there is little compensation possible against misalignment. This has practical implications, as the 3D-printed parts at the elbow joint may fatigue or fail when subjected to substantial joint misalignment. However, as opposed to human joints, the dummy arm joint centers are more easily visually aligned with the joints of the DAROR set-up.

Since the dummy arm is not instrumented with sensors like that in the work of [2, 9], no feedback on the possible effects of joint misalignment between the dummy arm and exoskeleton could be obtained. Including sensors in the design would allow us to investigate influences of joint misalignment. However, adding sensors adds complexity and costs to the design of the dummy arm. Therefore, depending on the research interest, it must be considered whether it is worth including these components, or whether a simpler version might suffice. Moreover, since human joints are not ‘ideal’ like the simplified joints of the dummy arm, the measured interaction forces in a phantom limb might deviate from real-world scenarios with a human limb.

The generalizability of the dummy arm design to other upper-extremity exoskeletons has not yet been investigated. However, by providing our CAD design in the Supplementary Materials, we enable others to make the necessary adjustments for various exoskeleton applications.

### 6.4.2 Recommendations

Although beyond the scope of the current study, it is of interest to investigate whether the realized eJimp characteristics of the dummy arm spring types are representative of people with neuromuscular disorders who cope with elevated eJimp. Different spring characteristics could approximate the human eJimp more closely. This requires more investigation. Potentially, the torque-angle profile of people with DMD is less likely to behave linearly. As mentioned above, the dummy arm eJimp profile can be further tuned by adjusting the shape of a cam (wrapping cam mechanism). Examples of this can be found in the work of [24], who used a serial wrapping cam mechanism to design an upper-limb assistive device. A more general description of the design and use of a wrapping cam mechanism can be found in the work of [21].

Although not of interest within the current application, several directions exist in which to improve the dummy arm. For instance, the force transmission between the dummy arm and the exoskeleton could be considered. In reality, due to the soft-tissue deformation of the skin and subcutaneous tissue, the transmission of the forces to the arm is different than when a rigid structure is used. A possible solution would be to use a soft outer layer for the dummy arm, similar to what is done by the authors of [1]. Moreover, since humans have no ideal joints, it might be worth investigating, depending on the research interest, making the joints more human-like to allow for small shifts in the joint axes of rotation. However, adding soft tissue, or more human-like joints, adds complexity and costs to the design of the dummy arm.

To reduce the costs of the design, the shoulder brackets could also be 3D-printed. Nevertheless, care should be taken with the load demands on the material in combination with the material selection and manufacturing techniques. Otherwise, a redesign of the brackets to strengthen these structures is recommended. After our initial PLA 3D-printed shoulder bracket failed, we decided to mill the shoulder from aluminum.

The advantage of using a modular dummy arm is that it can be adjusted to the anthropometrics for different populations, such as children or people with pathologies affecting the upper extremity (e.g., DMD, spinal muscular atrophy, amyotrophic lateral sclerosis, stroke). By making use of a more patient-like dummy arm, the burden on patients for the development of exoskeletons can be decreased, as the tests can be very exhaustive and demanding for patients. Testing time with vulnerable patients is also limited, while a dummy arm is always available. Therefore, using a patient-like dummy arm allows for faster assistive or rehabilitative exoskeleton development. However, the translation of the exoskeleton performance with the dummy arm to the intended target population should be further investigated.

Lastly, it is challenging to objectively compare the performance of exoskeletons with respect to each other, especially as the performance metric (e.g., perceived level of provided support) can become very subjective and differ across the reachable workspace. Using standardized dummy arm and objective evaluation methods allows for a more objective

comparison of exoskeleton performance, which is relevant for the patients as well for the developers, as it can point to possible areas of improvement.

## **6.5 Conclusions**

The current dummy arm successfully mimicked the characteristics of the human arm and was proven to be a helpful development and verification tool for the developed investigational DAROR exoskeleton. Since the design is relatively simple, reproducible, and cost-effective, it promises to serve more arm exoskeleton applications, and is therefore shared. The design allows for easy adjustment of the mechanical properties (e.g., mass, CoM), outer dimensions, and eJimp torque-angle profiles to fit the specific characteristics of a (vulnerable) intended target population. Using such dummy limbs, like the dummy arm, enhances the fast iteration and objective evaluation of new control strategies, and can save time, labor, and the burden of voluntary participants, who may be exposed to safety risks in an early stage of exoskeleton development.

## References

- [1] W. S. Barrutia, J. Bratt, and D. P. Ferris. A Human Lower Limb Mechanical Phantom for the Testing of Knee Exoskeletons. *IEEE Transactions on Neural Systems and Rehabilitation Engineering*, 31:2497–2506, 2023. doi: 10.1109/TNSRE.2023.3276424.
- [2] J. Bessler-Etten, L. Schaake, G. B. Prange-Lasonder, and J. H. Buurke. Assessing effects of exoskeleton misalignment on knee joint load during swing using an instrumented leg simulator. *Journal of NeuroEngineering and Rehabilitation*, 19(1):1–18, 2022. doi: 10.1186/s12984-022-00990-z.
- [3] R. F. Chandler, C. E. Clauser, J. T. McConville, H. M. Reynolds, and J. W. Young. Investigation of Inertial Properties of the Human Body. Technical Report March, U.S. Department of Transportation, Washington, D.C., 1975.
- [4] C. E. Clauser, J. T. McConville, and J. W. Young. Weight, volume, and center of mass of segments of the human body. Technical report, Wright-Paterson Air Force Base, Ohio, 1969. URL <http://oai.dtic.mil/oai/oai?verb=getRecord&metadataPrefix=html&identifier=AD0710622>.
- [5] R. Contini. Body Segment Parameters, Part II 1. Technical report.
- [6] J. Dávila-Vilchis, Laz-Avilés, J. C. Ávila Vilchis, and A. H. Vilchis-González. Design methodology for soft wearable devices-the MOSAR case. *Applied Sciences (Switzerland)*, 9(22), 2019. doi: 10.3390/app9224727.
- [7] M. P. de Looze, T. Bosch, F. Krause, K. S. Stadler, and L. W. O’Sullivan. Exoskeletons for industrial application and their potential effects on physical work load. *Ergonomics*, 59(5):671–681, May 2016. doi: 10.1080/00140139.2015.1081988.
- [8] W. T. Dempster and G. R. Gaughran. Properties of body segments based on size and weight. *American Journal of Anatomy*, 120(1):33–54, jan 1967. doi: 10.1002/aja.1001200104.
- [9] M. Dežman, S. Massardi, D. Pinto-Fernandez, V. Grosu, C. Rodriguez-Guerrero, J. Babič, and D. Torricelli. A mechatronic leg replica to benchmark human–exoskeleton physical interactions. *Bioinspiration and Biomimetics*, 18(3), 2023. doi: 10.1088/1748-3190/acda8.
- [10] A. M. Dollar and H. Herr. Lower extremity exoskeletons and active orthoses: Challenges and state-of-the-art. *IEEE Transactions on Robotics*, 24(1):144–158, feb 2008. doi: 10.1109/TRO.2008.915453.
- [11] C. A. M. Doorenbosch, J. Harlaar, and D. H. E. J. Veeger. The globe system: An unambiguous description of shoulder positions in daily life movements. *Journal of Rehabilitation Research and Development*, 40(2):147–155, 2003. doi: 10.1682/jrrd.2003.03.0149.
- [12] R. Drillis, R. Contini, and M. Bluestein. Body Segment Parameters 1 A Survey of Measurement Techniques. Technical report.

- [13] S. J. Filius, M. M. H. P. Janssen, H. van der Kooij, and J. Harlaar. Comparison of Lower Arm Weight and Passive Elbow Joint Impedance Compensation Strategies in Non-Disabled Participants. In *2023 International Conference on Rehabilitation Robotics (ICORR)*, pages 1–6, 2023. doi: 10.1109/ICORR58425.2023.10304707.
- [14] S. J. Filius, J. Harlaar, L. Alberts, S. Houwen-van Opstal, H. van der Kooij, and M. M. Janssen. Design requirements of upper extremity supports for daily use in Duchenne muscular dystrophy with severe muscle weakness. *Journal of Rehabilitation and Assistive Technologies Engineering*, 11(March):1–18, 2024. doi: 10.1177/20556683241228478.
- [15] M. Gandolla, A. Antonietti, V. Longatelli, and A. Pedrocchi. The Effectiveness of Wearable Upper Limb Assistive Devices in Degenerative Neuromuscular Diseases: A Systematic Review and Meta-Analysis. *Frontiers in Bioengineering and Biotechnology*, 7(January):1–16, 2020. doi: 10.3389/fbioe.2019.00450.
- [16] M. A. Gull, S. Bai, and T. Bak. A review on design of upper limb exoskeletons. *Robotics*, 9(1):1–35, mar 2020. doi: 10.3390/robotics9010016.
- [17] A. S. Koopman, I. Kingma, G. S. Faber, M. P. de Looze, and J. H. van Dieën. Effects of a passive exoskeleton on the mechanical loading of the low back in static holding tasks. *Journal of Biomechanics*, 83:97–103, 2019. doi: 10.1016/j.jbiomech.2018.11.033.
- [18] T. Madani, B. Daachi, and K. Djouani. Non-singular terminal sliding mode controller: Application to an actuated exoskeleton. *Mechatronics*, 33:136–145, 2016. doi: 10.1016/j.mechatronics.2015.10.012.
- [19] S. Maggioni, A. Melendez-Calderon, E. Van Asseldonk, V. Klamroth-Marganska, L. Lünenburger, R. Riener, and H. Van Der Kooij. Robot-aided assessment of lower extremity functions: A review. *Journal of NeuroEngineering and Rehabilitation*, 13(1):1–25, 2016. doi: 10.1186/s12984-016-0180-3.
- [20] T. Noda, T. Teramae, B. Ugurlu, and J. Morimoto. Development of an upper limb exoskeleton powered via pneumatic electric hybrid actuators with bowden cable. *unpublished*, (Iros):3573–3578, 2014. doi: 10.1109/IROS.2014.6943062.
- [21] Paul H. Tidwell. Wrapping Cam Mechanisms. Technical report, 1995. URL <https://www.proquest.com/dissertations-theses/wrapping-cam-mechanisms/docview/304228797/se-2>.
- [22] A. Plaza, M. Hernandez, G. Puyuelo, E. Garces, and E. Garcia. Lower-Limb Medical and Rehabilitation Exoskeletons: A Review of the Current Designs. *IEEE Reviews in Biomedical Engineering*, 16:278–291, 2023. doi: 10.1109/RBME.2021.3078001.
- [23] A. Schiele and F. C. T. van der Helm. Kinematic design to improve ergonomics in human machine interaction. *IEEE Transactions on Neural Systems and Rehabilitation Engineering*, 14(4):456–469, 2006. doi: 10.1109/TNSRE.2006.881565.
- [24] J. S. Schroeder, J. C. Perry, and S. W. Beyerlein. Application of Wrapping Cams in an Unpowered, Upper-Limb Assistive Device. Technical report, 2016. URL <https://www.proquest.com/dissertations-theses/application-wrapping-cams-unpowered-upper-limb/docview/1868839422/se-2>.



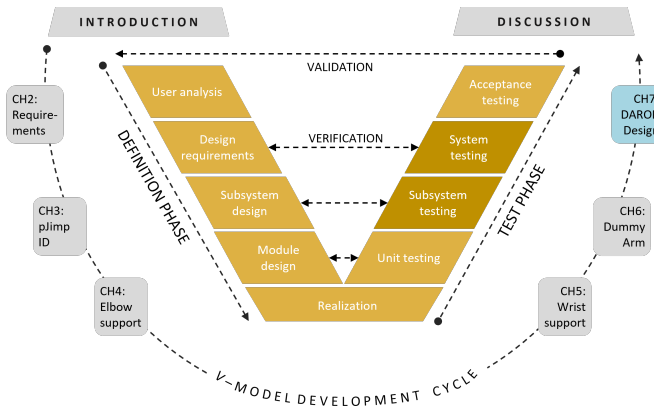
- [25] A. H. A. Stienen and A. Q. L. Keemink. Visualization of shoulder range of motion for clinical diagnostics and device development. *IEEE International Conference on Rehabilitation Robotics*, 2015-Sept:816–821, 2015. doi: 10.1109/ICORR.2015.7281303.
- [26] A. Story. Right Hand Reference, 2020. URL <https://grabcad.com/library/right-hand-reference-1>.
- [27] A. Toth, T. Pilissy, M. O. Bauer, G. Al-Absi, S. David, and G. Fazekas. Testing the Limit Range of Motion Safety Function of Upper Limb Rehabilitation Robots with an Anthropometrically Adjustable and Sensorized Dummy Limb. *IEEE International Conference on Rehabilitation Robotics*, 2022-July:25–29, 2022. doi: 10.1109/ICORR55369.2022.9896575.
- [28] W. Van Diik, T. Van De Wijdeven, M. M. Hölscher, R. Barents, R. Könemann, F. Krause, and C. L. Koerhuis. Exobudy - A Non-Anthropomorphic Quasi-Passive Exoskeleton for Load Carrying Assistance. In *IEEE International Conference on Biomedical Robotics and Biomechatronics (Biorob)*, volume Augustus 2, pages 336–341, Enschede, 2018. doi: 10.1109/BIOROB.2018.8487794.
- [29] G. Wu, F. C. T. Van Der Helm, H. E. J. Veeger, M. Makhsous, P. Van Roy, C. Anglin, J. Nagels, A. R. Karduna, K. McQuade, X. Wang, F. W. Werner, and B. Buchholz. ISB recommendation on definitions of joint coordinate systems of various joints for the reporting of human joint motion - Part II: Shoulder, elbow, wrist and hand. *Journal of Biomechanics*, 38(5):981–992, 2005. doi: 10.1016/j.jbiomech.2004.05.042.



# 7

## A 4DOF Motorized Upper Limb Assistive Exoskeleton with Weight and Elbow Stiffness Compensation

Chapter 6 discussed the design of the Dummy Arm. This tool was used in the development and verification of the compensation strategies for the motorized arm exoskeleton.



This chapter will present the design the realized Duchenne ARM ORthosis and verifies whether the design requirements of Chapter 2 were met.

This chapter was submitted for publication to *IEEE Transactions on Neural Systems and Rehabilitation Engineering* on September 11, 2024 as:

Filius, S.J., Keemink, A.Q.L, Meijneke, C., Gregoor, W., Kuenen, K., Lunshof, S., Janssen, M., Harlaar, J., and van der Kooij, H. (*under revision*). A 4DOF Motorized Upper Limb Assistive Exoskeleton with Weight and Elbow Stiffness Compensation. Upon acceptance, a supporting video will be available as supplementary material.

## A 4DOF Motorized Upper Limb Assistive Exoskeleton with Weight and Elbow Stiffness Compensation

**Abstract** *Duchenne Muscular Dystrophy (DMD) causes severe progressive muscle weakness, and currently no, suitable assistive arm support for personal use exists for the advanced stage (Brooke Scale 4). Motorized exoskeletons that compensate for weight and joint stiffness seem promising but face technological challenges. This work 1) presents the design of the Duchenne ARm Orthosis (DAROR), 2) compares two methods to estimate weight and elbow stiffness parameters for compensation using impedance control, and 3) verifies compliance with design requirements. Weight and elbow stiffness are estimated through: 1) ID, which personalizes parameters from joint angles and moments, and 2) AP, which uses general arm anthropometric data. DAROR's design is unique in its compactness (close to the body), strength (16 Nm), and intuitive human-exoskeleton interaction (without joysticks or buttons) compared to other wheelchair-attachable assistive exoskeletons. Verification tests involved a co-creator with DMD, a reference user without muscle weakness, and a dummy arm. The DAROR meets the predefined design requirements for the range of motion, support torque, and compensation performance, making it suitable for individuals with DMD Brooke Scale 4. The AP balances 39% more shoulder and 25% elbow configurations with known dummy arm parameters, whereas ID appears more feasible for individuals with atypical anthropometrics like our co-creator. On average, the DAROR reduces the required shoulder lift torque to 1 Nm (12%–55% of Brooke 4 scale muscle strength) and elbow lift to 0.5 Nm (10%–63%). Future clinical evaluation should validate our preliminary results in the target population.*

### 7.1 Introduction

Duchenne Muscular Dystrophy (DMD) is a progressive neuromuscular disease caused by a mutation on the dystrophin gene that is located on the X-chromosome. This mutation results in a lack of the dystrophin protein, causing severe muscle weakness that leads to functional limitations and loss of independence. People with DMD often start using a wheelchair around the age of 12, while they deal with functional loss in the upper extremities [7, 17].

Despite much research being done [36], no cure exists, but due to various medical technologies, life expectancy has increased [21]. This implies that their lifespan in a wheelchair becomes longer and the dependency on their upper extremity function increases, while the muscle strength in their arms progressively weakens [16, 23, 24]. Moreover,

during disease progression, muscle shortening and connective tissue development cause the formation of joint contractures and lead to an increased passive joint impedance [22, 30, 38]. This results in elevated mechanical resistance in the joint to an applied motion [25]. The joint impedance is found to be non-linear, time-varying and has different torque-angle curves across people with disabilities [11, 22, 30]. The stiffness is assumed to be the most dominant component [3, 10, 22], so from hereon called ‘joint impedance’. This combination of increased joint impedance and reduced muscle strength makes movement even more difficult, thereby expanding the need for arm function assistance.

By compensating for the weight of the arm, assistive arm supports can lower the shoulder and elbow moments [8] and improve the functional ability of the arm in daily activities [37]. Since the currently commercially available assistive arm supports are non- or semi-motorized [12], they provide insufficient support for people in the advanced disease stages (Brooke Scale  $\geq 4$  [2]) [5, 10, 13, 19, 20, 24, 28].

In our previous work (Chapter 2), we investigated the design requirements for people with DMD Brooke Scale 4. This population cannot benefit from existing available arm supports but have just enough strength to reach their own mouth independently. Although, some design requirements require more investigation, a motorized arm support with an intuitive force-based weight with joint impedance compensation is expected best to match their needs [10]. Concerning intuitiveness, impedance controllers are assumed to be more intuitive than admittance or position controllers since this is how people usually interact with objects in the environment. With an impedance controller the (supporting) joint torques are determined based on the configuration (change) of the exoskeleton.

Recent advancements in research projects have led to, e.g., the hybrid semi-motorized Power-Assist (Talem Technologies, US) system described in [4, 26]. Unlike other semi-motorized systems, their system automatically adjusts the level of support to the desired workplane height using admittance control. This seems promising, however, similar to the commercially available semi-motorized systems, it does not consider joint impedance compensation. Moreover, this device is interfaced with a forearm brace and does not follow the human arm’s anatomy. Such devices are also referred to as *end-effector* systems, while supports that follow the anatomy of the limb are referred to as *exoskeletons* [12]. Using the same degrees of freedom (DOF) and following the human arm’s anatomy is expected to allow for better alignment, natural behavior [6, 9], and sleek design compared to end-effector designs.

There exist two types of motorized upper limb exoskeletons, therapeutic robots for (neuro)rehabilitation training purposes in a clinical setting and assistive exoskeletons to support daily activities for personal home use. Although, on a conceptual level, there may be similarities between therapeutic and assistive exoskeletons, the design requirements of therapeutic devices are not tailored to the needs of people with DMD. Only a few motorized exoskeletons intended for daily use that are suitable to fixate to a wheelchair for people with severe muscle weakness have been explored. Table 7.1 summarizes their characteristics. Of these, two systems appear not to have reached the stage of being tested on individuals with muscle weakness [20, 28]. Additionally, none of these four systems utilize impedance control.

To test our formulated design requirements of Chapter 2 we built the investigational DAROR (Duchenne ARm ORthosis) exoskeleton. The hardware is built to allow for the

**Table 7.1:** Wheelchair fixable motorized assistive exoskeleton projects

Device	PDOF	Control	Sensor	ID	Ref.
Active A-Gear	4	Admittance	F/T, EMG	y	[20]
Powered WREX	2	Amplification	F/T	y <sup>1</sup>	[30],[29] <sup>1</sup>
Bridge	4	Position	Joystick, Voice	n	[5, 13]
Exo for SCI	4	Position	GUI	n	[14]

Abbreviations: ID, studies that include identification of passive joint torques (i.e., weight and joint stiffness identification); Ref, Reference; Exo, exoskeleton, PDOF, Powered degrees of freedom; SCI, cervical spinal cord injury; F/T, force torque; EMG: electromyography.

comparison of various control strategies in the future (e.g., EMG- or force-based admittance). In this work, we compare two estimation strategies to find parameters to compensate for the weight of the arm and elbow stiffness. One estimation method, *A Priori* (AP), estimates the human arm weight and elbow stiffness parameters based on anthropometric models and data from the literature. The other, named *Identified* (ID), estimates the parameters by an identification (i.e., calibration) process. The advantage of the ID method is that it does not require body measurements to estimate arm anthropometrics. Estimating the mass and CoM of the human arm segments is inherently less accurate, particularly for populations with atypical anthropometrics [15, 32, 39]. However, this method has the drawback that the identification procedure can be a time-consuming process that needs to be performed accurately and may need to be repeated periodically. Considering the possible configurations across the entire 4DOF workspace, selecting the correct configurations to identify the parameters is challenging. Selecting the sub-optimal configurations can lead to a low compensation performance across the workspace.

The advantage of the AP parameters is that no identification procedure is needed, and only a few body measurements are required to provide semi-personalized weight compensation. However, it is a quick-and-dirty approach that can lead to inaccuracies in compensation torque due to deviations from the anthropometrics models. These inaccuracies can be reduced by manually tuning the human arm model parameters, though this can be a time-consuming process counteracting its advantage over ID. We hypothesize that the ID method is more accurate than the conventional AP method in the case of atypical anthropometrics but that the AP method is easier and faster.

This study aims to 1) present the DAROR design, 2) compare the ID and AP methods, and 3) verify whether the in Chapter 2 predefined design requirements are met to assist people with DMD Brooke Scale 4.

The contribution of this work is to present (Section 7.2) the design of the newly developed DAROR, including a mobile power station and custom-built series elastic actuators (SEA) for compliant human-exoskeleton interaction. It presents (Section 7.3) the modeling and control, including an optimized identification procedure. To the authors' knowledge, this is the first impedance-controlled arm exoskeleton designed for intuitive assistance in daily activities. Additionally, it (Section 7.4) verifies the design requirements and introduces a new method to quantify high-level compensation and transparency performance objectively. Here, the high-level transparency refers to the device's ability to move with

ease, with low mechanical impedance (e.g., resistance), so that the user can move without the feeling of wearing the exoskeleton.

## 7.2 Design

### 7.2.1 Mechanical skeleton design

The kinematic design is built upon the kinematic design of the passive Exone (Yumen Bionics, The Netherlands), a continuation of the FlexTension A-Gear Project [19, 20]. This design follows the anatomical DOFs of the human glenohumeral (GH) shoulder joint and the elbow joint. Three actuators are placed at the shoulder and one at the elbow. The axes of rotation of the three shoulder actuators intersect the spherical joint of the human shoulder in the shoulder's Center of Rotation (CoR). The elbow actuator axis is aligned with the human elbow joint axis.

The upper arm structure can be adapted in length between 235 and 335 mm to match the upper arm length of the user. The forearm structure contains a textile sleeve (designed by Yumen Bionics, The Netherlands). The interaction point between the sleeve and the rigid forearm structure is equipped with a 6 DOF force/torque (F/T) sensor.

The future design perspective is to mount Actuator 1 to an (electrical) wheelchair. For research purposes, the device is mounted on an in-width and in-height adjustable mobile frame. By doing so, the set-up can easily be adapted to different users and their personalized wheelchairs.

### 7.2.2 Actuator design

Four SEAs were designed for this application to provide high torque demands while being compact enough to fit within the design space. The spring element (SE) enhances a safe and compliant human-robot interaction [28, 34, 42].

All SEAs are equipped with a motor (T-Motor MN4006 KV380), gearbox (Leader drive LCsG-14-100), and SE element. Each SEA is equipped with 3 absolute encoders (ICHaus, Germany) attached to a custom sensor slave running at 1 kHz that monitors the state of the gearbox (14 bits), rotor, and SE (19 bits, each). The SE element has a stiffness of approx. 289 Nm/rad and can handle a peak torque of 16 Nm. Each actuator weighs about 0.59 kg.

### 7.2.3 Software and system architecture

Each actuator is connected to an Ingenia Everest Servo Drive and is controlled in torque mode. The control models were created in Simulink (version 2018b, Matlab, Mathworks). The SEAs are connected to the industrial PC (Beckhoff C 6025 0020 IPC, Windows 7) in the mobile power station that runs the control software in real-time (1000 Hz) using TwinCAT. The mobile power station is connected to an operator's PC, which can activate or deactivate the control in TwinCAT. Using a Matlab graphical user interface (GUI), the live state and settings can be observed and modified.

### 7.2.4 Mobile power station design

The mobile power station provides 4 h/day continuous operating power and allows easy hot-swapping of the Lithium Ion battery packs. This station enables the set-up, when



**Figure 7.1:** Left) Snapshots of video where co-creator with DMD in his electrical wheelchair is supported by the assistive 4DOF motorized upper extremity support, the DAROR arm is mounted on a displaceable width- and height-adjustable support frame to align Actuators 1-3 with the shoulder of the user. Right) Structural overview of components.

assembled to a wheelchair, to be mobile, which is a step towards a product phase.

## 7.2.5 Sensor performance

A detailed description of the sensor performance analyses can be found in the Appendix D.1.

### 7.2.5.1 Joint angle resolution

Together, the encoders of the gearbox and SE element give an accurate measurement of the joint angle, with an effective resolution of  $0.07^\circ$ , thrice the standard deviation (SD) of the noise.

### 7.2.5.2 SEA torque sensor performance

The deflection of the SE element is used to calculate the joint torque and has an effective resolution of 0.025 Nm. A torque accuracy of 0.5 Nm was found for Actuators 3 and 4 within the DAROR set-up. This was determined with the root-mean-squared-error (rmse) between a theoretical applied and measured torque. This accuracy assessment was not feasible for Actuators 1 and 2 due to their positioning in the configuration. The precision of all SEAs was found to be 0.4 Nm (rmse between repeated measurements with same load). However, the performance of the actuators varies, with Actuator 2 performing the worst (max absolute error: 2.2 Nm) and Actuator 3 the best (max absolute error: 0.2 Nm). The SEA torque readings show some non-linearity and hysteresis (e.g., energy loss caused by frictions and sliding of components) [1] affecting the sensor performance. For good sensor accuracy and precision, it is important that the SE element behaves linearly and has low hysteresis without death-band [1].

### 7.2.5.3 F/T force sensor performance

The analogue signal of the 6 DOF F/T sensor (SI-40-mini F/T, Schunk, ATI Industrial Automation, USA) was digitized to 12 bits at 1 kHz. The effective resolution of the force



magnitude is 0.30 N. The force accuracy has a rmse of 0.23 N. When transformed to shoulder or elbow joint torque the F/T sensor has a torque accuracy  $\leq 0.09$  Nm.

## 7.2.6 Safety measures

To prevent discomfort from overstretching, both soft- and hardware end-stops, together with torque guards, are implemented. For each user, personalized software end-stops can be set to match the allowable range of motion (ROM), depending on their joint contractures. A state machine organizes the system's functionality, ensuring the software limits are set before transitioning to the operational state. These limits create a four-dimensional (4D) configuration space, defining the operational workspace of the Human Exoskeleton Combination (HEC). Both the user and operator can press a stop button at any time to immediately stop the device if they experience any discomfort or unexpected behavior. Furthermore, the mobile power station has a main power switch to improve electrical safety.

When the stop button is pressed, an electrical brake is activated for 10 seconds to ensure a slow downward movement of the HEC. To improve user safety, 3D-printed guards are placed around the shoulder to prevent skin or finger pinching from the 'scissor mechanisms' at the rotating parts. Additionally, operators are instructed to handle the device using the safety handle and read the safety instructions in the manual.

## 7.3 Modeling and Control

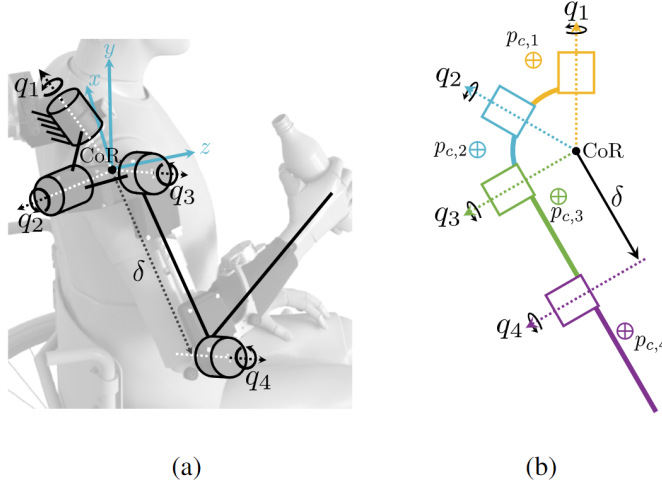
### 7.3.1 Kinematics

Fig. 7.2 shows the kinematic overview and Center of Mass (CoM) location model of the DAROR. It is assumed that the HEC moves as if rigidly connected at the forearm. As a consequence, they are modelled together as a four-segment rigid body system in which the joint-angles of the set-up joints are denoted by  $q = [q_1 \ q_2 \ q_3 \ q_4]^T$ .

We describe the kinematics of the right-arm set-up with a static CoR inside the shoulder. Seen from the user, the coordinate frame in which we express motions is given by:

- global x-axis points from the shoulder CoR into the user;
- global y-axis points from the shoulder CoR upward;
- global z-axis points from the shoulder CoR forward.

The rotation-axis of Actuator 1 is rotated with respect to y, as is visible in both Fig. 7.1 and 7.2a. This axis is the intersection of two planes, one tilted  $-30^\circ$  around x (positive being counter-clockwise) and one plane tilted  $-10^\circ$  around z. The actuator is subsequently also rotated  $-45^\circ$  around its own axis which defines its zero angle. From that configuration onwards, the zero-angle ( $q = 0_{4 \times 1}$  rad) configuration is as shown in Fig. 7.2b (i.e., the whole planar structure undergoes the three previous rotations). The two connecting arcs between the three shoulder joint actuators are both evenly spaced and span  $60^\circ$  around local y. The rotation axis of  $q_4$  is parallel to the one of  $q_3$ . The detailed kinematic model and how to solve for the inverse kinematics is further explained in Appendix D.2.



**Figure 7.2:** Schematic kinematic overview of the HEC. a) kinematic view of actuator DOFs. Note that the shoulder joints have a common Center of Rotation (CoR), while the elbow-actuator axis is offset from the CoR by  $\delta$ . b) The HEC placed in a flat plane, showing the zero-angle configuration of all joints. The segment Centers of Mass (CoMs) are indicated as  $\oplus$ , their color indicating with respect to which actuator rotation they are stationary.

## 7

### 7.3.2 Weight compensation model

Considering the relatively slow arm movements, the velocity- and inertia-induced torques are considerably lower than the gravitational torques [13]. Therefore, we are not interested in compensating dynamic effects and only model the weight of the HEC, so that it can be actively compensated.

By determining the potential energy contribution of each of the four HEC segments  $V_i, i = 1, 2, 3, 4$ , the torques induced by gravity  $\hat{\tau}_g(q)$  are modelled to be

$$\hat{\tau}_g(q) = \frac{\partial \sum V_i}{\partial q} = K_g(q)\theta_g, \quad (7.1)$$

with  $K_g(q) \in \mathbb{R}^{4 \times 12}$  a nonlinear function of the joint angles and  $\theta_g \in \mathbb{R}^{12}$  the model parameters containing information about gravity, masses and moment arms. How to actually obtain the potential energy and  $K_g(q)$  is explained in detail in Appendix D.3.

### 7.3.3 Elbow stiffness compensation

Besides weight compensation, optionally, compensation for the user's elbow joint impedance can be provided. If the stiffness is also compensated, a + is added to the model/parameters name (i.e., following Section 7.1, we would have ID+ and AP+). In Chapter 4, the joint impedance of 12 healthy male participants was measured and modelled as a pure linear stiffness. Data on shoulder stiffness is lacking to model the stiffness for the AP+ method accurately. Therefore, we decided to investigate the feasibility of the stiffness compensa-

tion for the elbow joint first to make a fair comparison between ID+ and AP+. Moreover, elbow joint stiffness is perceived as more problematic in daily activities than shoulder stiffness [33].

We approached the general joint impedance model as, at most, a fifth-order polynomial over the elbow angle  $q_4$ . A lower-order model can still be enforced by setting some polynomial coefficients to zero. The option for first- to fifth-order polynomial was chosen to accommodate the more complex angle-torque relationships, as [29, 30] found varying relationships in children with disabilities and recommended a subject-specific approach. According to [29], a third-order polynomial seems most suitable for non-weakened individuals. The 4D torque induced by the stiffness is given as

$$\hat{\tau}_j(q) = \begin{bmatrix} 1 & 0_{3 \times 6} & q_4 & \dots & q_4^5 \end{bmatrix} \begin{bmatrix} c_1 \\ \vdots \\ c_6 \end{bmatrix} = K_j(q)\theta_j, \quad (7.2)$$

with polynomial coefficients  $c_1, \dots, c_6$ .

The total weight plus elbow joint impedance compensation model ( $\tau_c(q)$ ) is then the combination of Eq. (7.1) and (7.2):

$$\begin{aligned} \tau_c(q) &= \hat{\tau}_g(q) + \hat{\tau}_j(q) = K_g(q)\theta_g + K_j(q)\theta_j \\ &= K(q)\theta, \end{aligned} \quad (7.3)$$

where  $\theta$  now contains both the weight and joint impedance related parameters.

### 7.3.4 Parameters of the compensation model

Two sets of model parameters, one found via identification and one chosen a priori (i.e., ID(+) and AP(+) respectively, as discussed in Section 7.1, are used to determine the required torques ( $\tau_c(q) \in \mathbb{R}^4$ ) for weight (and stiffness) compensation of the HEC.

#### 7.3.4.1 ID(+)

The ID(+) parameters are those that best predict the weight (and elbow stiffness) compensation torques of the HEC by fitting, in a least squares sense, the measured SE joint torques from an identification procedure. During this procedure, the user must sit still and remain as relaxed as possible while the HEC is moved between several configurations in the reachable workspace.

The HEC is moved to a set ( $P$ ) of  $N$  static 4D configurations in the workspace of the user, in which the required torque to stay there is measured ( $\tau_m(q)$ ). This gives a set of torque measurements:  $T = \{\tau_m(q), \forall q \in P\}$ . Given the dataset  $\{T, P\}$  we assume that the model in Eq. (7.3) holds for each of the  $i = 1, \dots, N$  measurements

$$K(iq)\theta = {}^i\tau_m(iq) + \epsilon_i, \quad (7.4)$$

with error term  $\epsilon_i$ . The error for all  $N$  measurements can be stacked as  $\epsilon = [\epsilon_1^T, \dots, \epsilon_N^T]^T \in \mathbb{R}^{4N}$ . The parameters  $\theta$  that minimize  $\epsilon^T \epsilon$  and, therefore, give the best model fit, in terms of rmse:

$$\text{rmse} = \sqrt{\epsilon^T \epsilon / (4N)}, \quad (7.5)$$

can be obtained through linear regression. In the experiments and results discussed where the elbow stiffness is not compensated,  $\theta_j = 0_{6 \times 1}$  was a constraint during regression for ID.

The identification procedure and choice of best configurations ( $P$ ) optimized for how much information they add to the parameters is described in detail in Appendix D.5. The amount of best configurations selected was limited by the maximal identification duration of (approx. 5 min) to ensure the user can remain comfortable while fully relaxing the arm.

#### 7.3.4.2 AP(+)

The AP parameters use human arm parameters based upon body measurements (body mass, arm segment lengths, and arm width) and anthropometric models from [27, 41]. The human arm model parameters (CoM and mass of forearm and upper arm) are tunable up to 80–120% of the initial body mass and segment length values given in the GUI.

The parameters of the DAROR itself (mass and CoM) are, however, identified for a set upper arm length. This underscores a disadvantage of the AP, which is that, unlike with ID, the upper arm CoM parameter of the DAROR, which changes with different upper arm lengths, does not automatically update. This needs to be either manually adapted for each length or set to an average upper arm length.

For the AP+ coefficients, a first-order model of the joint impedance is used. In the model in Eq. (7.2),  $c_1 = -1.29$  Nm,  $c_2 = 1.14$  Nm/rad,  $c_3, c_4, c_5 = 0$ , based on the group average found in Chapter 4, see also Chapter 6. This first-order approach simplifies the tuning of the stiffness (slope) and offset, which are also real-time tunable up to 80–120% of their initial values.

In the experiments and results discussed where the elbow stiffness is not compensated,  $\theta_j = 0_{6 \times 1}$  was set for AP.

7

### 7.3.5 Control for compensation and transparency

For each motor, a disturbance-observer-based torque controller is used to ensure high bandwidth torque tracking with little output impedance [31]. The weight and stiffness compensation are used as the desired torque for the torque controller to track. This actively controls the SEA, making it easier for the user to move the HEC with the desired weight and (when used) elbow joint stiffness compensation.

## 7.4 Verification tests

This section includes both methods and results of the verification tests. The verification tests involved a co-creator with DMD (estimated arm mass of 2.7 kg, by anthropometric models [27, 41]), a reference user without muscle weakness (estimated arm mass of 3.1 kg), and a dummy arm (arm mass of 2.8 kg). The dummy arm represents the human arm with adjustable mass and CoM. It ensures the absence of muscle activation and allows for accurate mass and CoM determination (which is not possible in the human arm). Moreover, it has the option to simulate elevated elbow joint impedance by the use of mechanical springs. For this study, we chose a somewhat extreme elbow joint impedance (3.7 Nm/rad, with an equilibrium at 63°), to illustrate the working principle of the elbow joint impedance compensation. The design of this dummy arm is elaborated in Chapter 6. The verification

**Table 7.2:** Verification design requirements

	Requirement	Achieved	Target
SEA	Breakaway $\tau$ (Nm)	0.3±0.1	< 0.4
	$\tau$ precision [rmse] (Nm)	0.4	< 1
	$\tau$ accuracy [rmse] (Nm)	0.5	< 1
Control	Sensor interface	F/T-based	intuitive
	Support gain	tunable	tunable
	Compensation for	$\tau_g, \tau_{je}$	$\tau_g, \tau_j$
	Minimal required user $\tau$ (Nm)	$e: 0.5\pm0.1$ $s: 1.0\pm0.1$	$\leq 0.8$ $\leq 1.8$
System	Weight (kg)	3.6	2.5 [20]
	Max distance from body (cm)	12	15 [20]
	Continuous operating time (hour)	$\geq 4$	4
	Misalignment $e$ joint (cm)	approx. 2	< 10
	Time to doff (min)	approx. 4	< 15
	Time to don (min)	approx. 5	< 15
ROM	GH elevation (deg)	[11 137]	[30 75]
	GH horizontal (deg)	[-46 138]	[5 110]
	GH axial (deg)	[-113 65]	[-80 -5]
	El flexion/extension (deg)	[2 150]	[70 145]
Safety	Quick release sleeve (s)	approx. 30	< 30
	Sound level (dBA)	65 (peak 80)	< 80
	Actuator temperature (°C)	< 40	< 48

Abbreviations: rmse: root mean square error;  $\tau$ : torque;  $g$ : weight components;  $j$ : joint stiffness components;  $e$ : elbow joint;  $s$ : shoulder joint; F/T: force/torque. The color in the Achieved column is used to indicate whether the target defined in Chapter 2 were met (green), almost met (orange), or the value was compared to literature if there was no pre-defined target (grey).

tests that involved human participants were executed under ethical approval from Delft University of Technology on April 10th, 2024 (ID4098).

Table 7.2 summarizes the device specifications and verifies the SEA, control, system design, the ROM (also in Fig.7.3), and safety requirements to the intended *must-haves* target requirements as defined in Chapter 2.

### 7.4.1 Range of motion

Table 7.2 shows the ROM of the set-up's GH shoulder and elbow joints without a user. Due to the configuration of the three shoulder actuators, not all combinations of the GH rotations as presented here are possible. For example, a GH elevation rotation with 90° GH horizontal rotation (clinical ante-flexion) of approx. 137° is achieved, while with no GH horizontal rotation (clinical abduction), a GH elevation rotation of maximally 88° is possible.

Therefore, the combined ROM of the shoulder joint of the HEC with a reference user without muscle weakness is visualized in Fig. 7.3 and compared to the target ROM defined in Chapter 2. The GH elevation is shown on the vertical axis, the GH horizontal rotation

on the horizontal axis, and the GH axial rotation is represented by the arches. Additionally, the ROM with the reference user is smaller than the ROM of the device alone due to limited joint ROM and collisions of the user's hand with the body and of the device with the user. For example, when the GH elevation rotation rises above approx.  $80^\circ$  in combination with a horizontal rotation of approx.  $60^\circ$ , the second shoulder actuator rotates towards the human scapula, which limits the shoulder ROM in this area, this varies across users.

Fig. 7.3 shows that the targeted ROM for the GH horizontal and elevation rotation is achieved. Only the target GH axial rotation is not achieved over the full workspace. However, the defined target ROM in Chapter 2 reports the minimal required ROM per axis without consideration of the combinations of the GH rotations. This limited GH axial rotation is not expected to hinder the in Chapter 2 defined target activities of daily living (ADL).

For the elbow, the targeted flexion angle of  $150^\circ$  is achieved within the DAROR. However, due to the length of the interface sleeve that collides with the upper arm of the user, the elbow flexion angle of the HEC is limited to approx.  $120^\circ$ . Moreover, the pro- and supination of the forearm is in the current design, limited to the soft tissue rotation in the sleeve.

As a reference, the ROM of our co-creator with DMD reached during the identification procedure to identify the ID parameters is also presented in Fig. 7.3. Our co-creator (Brooke Scale 5, i.e., cannot raise hands to the mouth but can use hands to hold a pen or pick up pennies from the table [2]), who was closely involved during the development process, has a limited passive ROM as a result of joint contractures. However, the ROM presented here is further limited by the aforementioned HEC shoulder configuration limits, the software limits (set with an additional safety buffer zone of  $3^\circ$  and  $8^\circ$  for elbow and shoulder, respectively), and is affected by the selected configurations of the identification procedure.

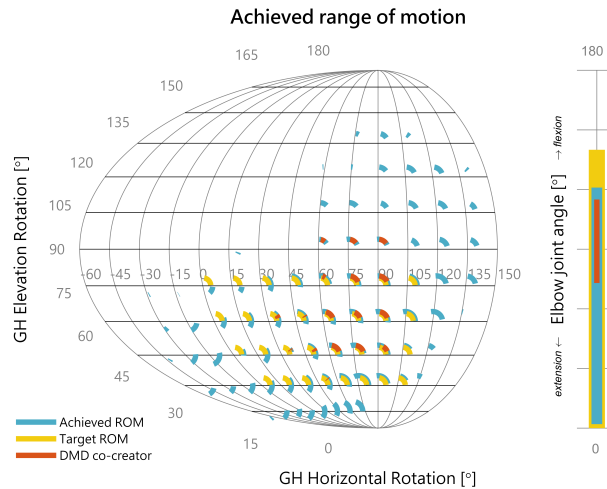








**Figure 7.3:** Achieved range of motion of the glenohumeral (GH) and elbow joints of the DAROR with reference and co-creator user (*note:* limited by safety limits and collision avoidance), compared to the target defined in Chapter 2. Visualization method for the shoulder adapted from [35].

### 7.4.2 DAROR support torque

The required support torque depends on the weight and joint impedance of the user's arm and the weight of the device itself. To verify that the actuators of the DAROR are strong enough we evaluated a set of static ADL configurations from the functional requirements in the must, should, and could category as stated in Chapter 2.

Table 7.3 presents the measured SEA torques for both the HEC (reference user) and Dummy arm Exoskeleton Combination (DEC) in the ADL configurations. The ADL configurations slightly differed between the HEC and DEC analyses, which could lead to different load distributions across the actuators. The device has proven to be powerful enough to move through the ADL activities with the reference user as well as with the dummy arm.

**Table 7.3:** Measured SEA torques (Nm) in HEC and DEC in six ADL poses

Must		Should						Could				
												
	HEC	DEC	HEC	DEC	HEC	DEC	HEC	DEC	HEC	DEC	HEC	DEC
$q_1$	3.5	2.6	3.3	-2.4	3.3	-2.6	1.8	-2.6	2.2	1.3	2.7	1.3
$q_2$	-7.5	-6.2	-9.1	-5.5	-6.2	-2.4	-3.7	-5.2	-8.7	-7.5	-9.3	-8.1
$q_3$	4.9	2.4	7.9	5.5	8.9	4.6	9.3	5.9	14.1	9.5	15	10.8
$q_4$	5.0	2.7	0.3	3.9	-3.1	-0.1	-1.5	4.4	4.4	1.0	4.7	1.7

Activities of daily living (ADL) from left to right: tabletop activities, feeding activities, reach top head, bring object to head (200 g), and reach at shoulder height without and with object (200 g). Performed with human reference user (HEC) who was instructed to fully relax the arm and dummy arm (DEC). *Note:* the poses can slightly differ between HEC and DEC. Human model representing activities retrieved from DAZ Productions [40].

### 7.4.3 High-level compensation and transparency performance

**Motivation** Verifying the compensation performance in a motorized exoskeleton is challenging due to the interdependence of actuator configurations. Assessing performance with a human user adds complexity, as compensation is affected by deviations from the anthropometric tables, the user's joint impedance and the user's relaxation state during the identification procedure. Additionally, humans may be biased or do not perceive small differences in compensation torques of the evaluated settings, leading to subjective evaluations. This newly developed method can be used to compare different compensation settings, models, or conditions across multiple configurations in the workspace.

**Method** First, the ID parameters were found for the DEC using the identification procedure. The parameters of the AP were set to the prior known dummy arm segment mass and com. For the AP+, the first-order model parameters ( $c_1 + c_2 q_4$ , with  $c_1 = -2.6$  Nm,  $c_2 = 3.0$  Nm/rad) were used to compensate for the mimicked elbow joint impedance by the springs in the dummy arm.

Then, using position control, the DEC is brought to a set configuration, after which the shoulder joint is released to torque control with either the ID(+) or AP(+) compensation. If the DEC maintains its configuration, the compensation torque is considered to be adequate. However, the DEC could also remain in its position due to friction in the system, which is part of the system's mechanical impedance, which is a relevant performance metric. This mechanical impedance negatively affects the high-level transparency. This is a relevant performance metric because the user needs to overcome this friction to bring the arm to a new configuration. Therefore, the required external applied 'push' force to move the DEC was measured. Conversely, if the DEC does not maintain its position and drifts from the desired configuration, the external required 'hold' force to maintain the configuration is recorded.

The *hold* or *push* forces were applied to the end-point (wrist location) of the dummy arm and recorded with the 6DOF F/T sensor<sup>1</sup>. For each measurement, three consecutive pushes or holds were performed and averaged. For the shoulder evaluation, the elbow joint was fixated at (65°), and since the moment arm of the applied force is affected by the chosen elbow joint angle, the measured forces were transformed into shoulder torques in the global frame. To reduce the effects of noise, the magnitude of the shoulder torques measured in the three global axes (i.e.,  $x$ ,  $y$ ,  $z$ ) was filtered by a phase-lag-free 1<sup>st</sup>-order low-pass Butterworth filter, with a cut-off frequency of 25 Hz. At the start of each push or hold recording, the filtered magnitude of the applied torque was zeroed to ensure that only the applied torque was observed. Then, the peak torque that was required to move the magnitude of the three shoulder actuators combined, at least 1°, was taken as the applied push torque.

The elbow joint was evaluated on 10, 40, 70, and 100° while the shoulder was fixed to a neutral configuration (GH elevation 10°, horizontal and axial 0°). The elbow joint was released in torque control at each configuration with either the AP(+) or ID(+) compensation method. Again, three consecutive pushes up (i.e., flexion) or downward (i.e., extension) were given at the dummy arm wrist in case the DEC remained in its position. This time, the F/T measurements were transformed to elbow joint torque.

**Results** Fig. 7.4 presents the results of the ID and AP model, where the size of the circles and lines of the crosses scale with the measured input torque. For instance, for the GH joint, the ID model shows in the configuration 0° horizontal with 60° elevation rotation, the applied torque to push the DEC upward was 0.17 Nm, which is substantially lower than the downward push torque of 1.42 Nm, indicating an over-compensation after the breakaway torque ( $0.3 \pm 0.1$  Nm) is overcome by the applied push. For the hold experiments, for instance, the configuration with 90° horizontal and 120° elevation rotation, the hold torque was 0.40 Nm for the ID model and 0.76 Nm for the AP. This indicates that the AP has a bigger tendency to drift away at this configuration. For the elbow, for example, at 100°, the ID hold input torque was 2.0 Nm, while with joint impedance compensation the ID+ was 0.6 Nm.

As a reference, also the minimal required user torque *target* and the maximum elbow and shoulder torques applied by the co-creator with DMD while pushing up, down, in-, and outward in a single configuration are added as reference values.

<sup>1</sup>The F/T sensor offset was calibrated at the start of each recording day, explained in detail in Appendix D.6



### High-level compensation and transparency performance

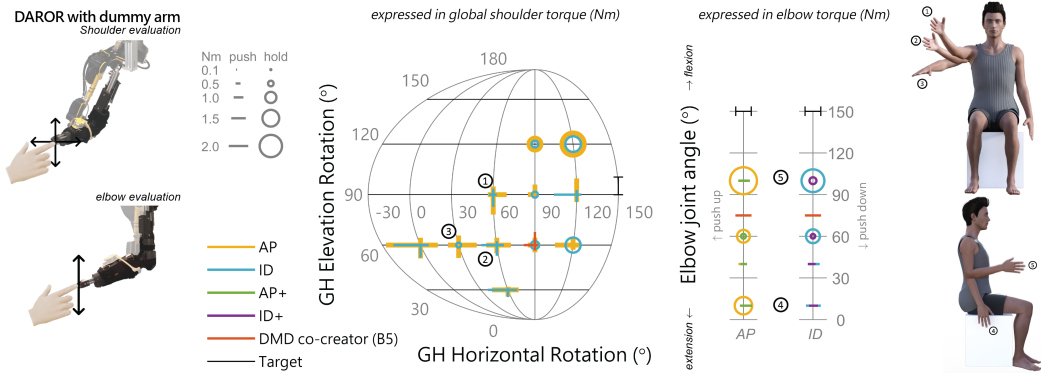


**Figure 7.4:** The high-level compensation and transparency performance expressed in global shoulder torque (Nm) and elbow joint torque (Nm). On the left, a representation of how the external *push* forces are applied to the dummy arm. In the middle, the results for the GH shoulder joint. The GH configurations are plotted on the nearest cross-section of the globe for visual clarity. The circles represent the external applied *hold* input. The crosses represent the external applied *push* input. For GH, the vertical line corresponds with an upward and downward push (GH elevation rotation), and the horizontal line with an inward and outward push (GH horizontal rotation). On the right, the elbow torques are presented on two vertical axes. The vertical axis on the left shows the AP(+) model, and on the right, the ID(+). As a reference, the minimal user input target torque based on muscle strength of people with DMD Brooke Scale 4 reported in Chapter 2 are shown in black (i.e., 1.8 N shoulder abduction, 0.8 N elbow flexion/extension). Moreover, the maximal push input of the co-creator with DMD with Brooke Scale 5 (B5) is plotted for the shoulder and elbow torque measured in a single configuration. The human model on the right represents five of the evaluated arm configurations for illustration, the model was retrieved from DAZ Productions [40].

The variation between the three consecutive pushes was generally low ( $SD = 0.15$  Nm), except for the outward push in the shoulder configuration GH  $0^\circ$ , GH horizontal  $60^\circ$ , where the shoulder actuators nearly collided ( $SD = 1.0$  Nm). Here, the outward push torque was considerably higher because of the software limits that prevent the shoulder actuators from colliding, propelling a force in the opposite direction when pushing outwards, explained in Appendix D.4.

Table 7.4 summarizes the mean (M) and SD of the push and hold applied joint torques. Moreover, it shows the error between the predicted and measured joint torques by the rmse values, as in Eq. (7.5). The measured joint torques are retrieved from an identification procedure with the dummy arm and co-creator with DMD. For each method, 20% of the randomized samples were used to calculate the rmse, whereas 80% of the randomized samples were used to train the ID(+) parameters. Further interpretation of these results is discussed in Section 7.5.1.

**Table 7.4:** High-level compensation and transparency performance

DEC HEC RMSE (Nm)			push/hold nr	push M $\pm$ SD (Nm)	hold M $\pm$ SD (Nm)
AP ID					
		GH	11/2 6/7	1.1 $\pm$ 0.3 1.0 $\pm$ 0.2	1.5 $\pm$ 0.7 0.8 $\pm$ 0.4
AP	1.745	1.890	1/3	0.3	1.7 $\pm$ 0.6
AP+	1.385	1.839	3/1	0.6 $\pm$ 0.3	0.4
ID	1.263	0.874	2/2	0.8 $\pm$ 0.1	1.6 $\pm$ 0.6
ID+	0.443	0.691	2/2	0.4 $\pm$ 0.2	0.5 $\pm$ 0.2

The mean (M) and standard deviation (SD) push or hold torque for the magnitude of glenohumeral (GH) and elbow joint for DEC. The root mean square error (RMSE, Eq. (7.5)) for the dummy arm (DEC) and co-creator with DMD (HEC).

## 7.5 Discussion

### 7.5.1 Verification of the design requirements

As can be seen in Table 7.2, most of the intended target requirements were met. The supplementary video gives an impression of the DAROR performance. The following sections will discuss the important verification results in more detail.

**Donning** Donning the DAROR arm with our co-creator with DMD takes approx. 5 min after the wheelchair and set-up frame are positioned at the right location and preset settings are set. To find the settings (i.e., back- and headrest wheelchair adjusted, armrest removed, upper arm length corrected, hardware end-stops installed) took approx. 20 min. A reference user can don and doff independently, the arm in approx. 30 s by connecting 2 velcro straps.

**Joint alignment** After donning, the misalignment was approximately  $\leq 2$  cm for the elbow and shoulder joint (estimated by a ruler). During free shoulder movement with the co-creator with DMD, the employed trunk compensation movements increased the shoulder joint misalignment up to approx. 10 cm (visually estimated). With reference user, the shoulder misalignment remained  $\leq 4$  cm during movement and for the elbow  $\leq 2$  cm. Fixating the trunk with a trunk vest could improve shoulder alignment.

**Obtrusiveness** With the relatively slender exoskeleton design, we managed to stay close to the body, with a maximum distance away from the body of 12 cm. This was considered to be an important design requirement [6, 19]. The DAROR is 3 cm closer to the body than the Active A-gear, which was claimed to be the most light-weight and slender active upper-extremity exoskeleton developed in 2016 [20]. Moreover, the DAROR delivers double the support torque compared to the A-Gear.

**ROM** The ROM analysis shows that the *must* target is achieved with the DAROR. However, in the HEC the elbow joint is slightly limited. Nevertheless, the reference user was able to perform all formulated ADL activities of Table 7.3. To further improve the ROM

of the shoulder, the actuators might be slightly moved outwards (further from the body). Moreover, shortening the interface sleeve will make it easier to reach the mouth.

**Support torque** The actuators (16 Nm each) proved to be strong enough to support the passive human arm in ADL activities, for both the DEC and HEC (both reference user as co-creator with DMD). This delivered support torque is double the actuator torque of the Active A-gear [20]. However, when a broader, heterogeneous target population is desired (arm mass of  $\geq 4$  kg) it is recommended to increase the maximum motor torque for shoulder elevation to approx. 20 Nm for the current HEC. Alternatively, additional use of passive springs parallel could be explored to reduce the load on the actuators [20]. The DAROR design already incorporates attachment points for parallel springs similar to those in the passive EXone (Yumen Bionics, The Netherlands) to facilitate this in a follow-up.

**SEA performance** Although the disturbance observer aims to minimize the SEA output impedance, unmodeled dynamics remain (e.g., static friction, the HEC's inertia and friction caused by off-axis bearing loads). This results in an increased breakaway torque that varies across the actuators and their workspace. The off-axis bearing load demands seem to be the least favorable in Actuator 2. A re-design of the output bearing mechanism (double-sided) might reduce the output impedance.

Moreover, the SE torque accuracy of 0.5 Nm, in combination with the precision of 0.4 Nm, presumably resulting from SE hysteresis, has a negative effect on the compensation performance. On average, the sensor precision met the in Chapter 2 stated 'must' requirement of  $<1.0$  Nm. However, the max absolute error of 2.2 Nm measured in Actuator 2 is undesirable. For the ID(+) method, this effect is twofold: it affects the identified model parameters and causes torque tracking errors. This latter holds also for the AP(+) methods. Different SE design (e.g., geometry, stiffness, and attachment) might improve the hysteresis, as was investigated in [1].

**High-level compensation and transparency performance** The minimal required input torque to bring the DEC to the new configuration was, on average  $1.0 \pm 0.1$  Nm for the shoulder and  $0.5 \pm 0.1$  Nm for the elbow (for all applied push torques of both AP and ID methods combined).

In the configurations where the DEC drifted from the desired position, the user needs to apply hold torques to remain in the position. For the shoulder, the average hold torque was  $0.9 \pm 0.6$  Nm and for the elbow with stiffness compensation, the average hold torque was  $0.5 \pm 0.1$  Nm.

We compare these results with the muscle strength of individuals with DMD Brooke Scale 4 reported in Chapter 2, estimated to be 1.8 to 9.1 Nm for the shoulder abduction, 0.8 to 4.8 Nm for the elbow flexion, and 0.8 to 6.6 Nm for the elbow extension. Based on these numbers, the required user input to bring the arm to a new configuration for both ID and AP methods is, on average, 12% to 55% of the shoulder muscle strength of individuals with DMD Brooke Scale 4 and 10% to 62.5% of the elbow flexion strength. So, theoretically, people with a Brooke Scale of 4 would be strong enough to move the HEC and, therefore, profit from the support of the DAROR.

The relatively high hold torques in the elbow joint for the AP and ID methods result from the high spring stiffness (3.7 Nm/rad) in the dummy arm, which simulates an elevated elbow joint impedance. This elbow joint impedance increases towards the joint limits. With the elbow stiffness compensation, the required push or hold torque is more consistent throughout the full ROM, illustrating the effectiveness of the joint impedance compensation. Follow-up studies could further investigate like how to estimate and compensate for shoulder stiffness in people with DMD similar to [29].

### 7.5.1.1 Comparison AP(+) and ID(+)

The AP model could balance the DEC in 85% for the shoulder, and AP+ 75% of the elbow configurations. Whereas the ID model balanced 46% and ID+ model 50% of the configurations for the elbow, respectively. In the statically balanced configurations, the users can use their muscle strength to overcome the system's mechanical impedance and maneuver their arm to a new configuration rather than lifting the arm's weight.

Since we know the dummy arm's exact mass and CoM parameters, it was to be expected that the AP would outperform the ID in the DEC. However, when looking at the RMSE values for the HEC (co-creator with DMD), the ID+ (RMSE 0.691 Nm) shows a substantially lower error between the predicted and measured torques than the AP+ model (RMSE 1.84 Nm), as shown in Table 7.4. This RMSE is expected to improve with longer identification procedures (> 5 min).

However, a drawback of the ID(+) method is that the identified parameters may be influenced by measurement inaccuracies, including sensor errors, involuntary muscle activity, misalignment of the HEC joint axis, and unmodeled system dynamics (such as stiction or friction due to off-axis bearing loads).

### 7.5.1.2 Intuitiveness of the control interface

As discussed in Section 7.1, an impedance controller was expected to be more intuitive than an admittance controller. With an admittance controller as in [20, 26], a force-sensor is used to measure the movement intention and translate this to a movement of the arm. This can have the disadvantage that the device is effectively blind to any other forces acting on the robot, pushing through constraints such as a table or collisions with the user's body. Also, poorly tuned admittance control can become unstable during interactions with users or objects [18], making the method inherently more unsafe. These problems cannot arise with our impedance controller. However, the intuitiveness of the controller is affected by how easily the HEC can be moved, i.e., the high-level compensation and transparency performance.

The admittance-controlled Power-Assist reports a minimum system activation force required to operate the system of 0.22 N [26], thus substantially less than the minimal required user torque achieved with our controller. The intuitiveness of an impedance controller versus an admittance controller can be explored in a follow-up study. The integrated F/T sensor allows for such comparison within the same hardware set-up.

## 7.5.2 Study Limitations

Although designed for people with Brooke Scale 4, at the current development phase we have not evaluated the performance of the DAROR with this population yet. At the

start of the co-creation, our pilot could reach his mouth independently (Brooke Scale 4). Natural disease progression (i.e., Brooke Scale 5) led to increased muscle weakness during development. In the following validation phase of the project, after the proposed improvements, the DAROR will be tested within the intended Brooke Scale 4 population to confirm our results. With this work we first verify whether the design of the DAROR design is safe and sound before we can validate the overall performance and users' acceptance in a larger population. This step-down approach prevents unnecessary burden of a vulnerable population that easily gets fatigued.

### 7.5.3 Conclusions

This study aimed to present the DAROR design, compare two estimation methods for weight and elbow joint stiffness parameters, and verify the compliance of the design requirements specified in Chapter 2. Compared to the existing wheelchair-attachable assistive exoskeletons, DAROR's design is unique in its slenderness (max distance of 12 cm from the body), support torque (16 Nm), and intuitive human-exoskeleton interaction using impedance control (without joysticks or buttons).

This work introduces an effective method for identifying the weight and elbow stiffness parameters through an optimized identification procedure, reducing the calibration time and improving feasibility. Moreover, it presents a new method to objectively quantify and visualize the high-level compensation and transparency performance across the workspace.

Our verification showed that most target design requirements are met in the current design. The achieved ROM, support torque, and high-level compensation and transparency performance is expected to be sufficient for the intended target population with Brooke Scale 4.

The relatively high minimal required torques to bring the DEC to a new configuration are expected to be the result of the torque sensing inaccuracies and the residual system's impedance. Preferably, the hardware should be improved to enhance the performance at the source. However, elaborate control models that contribute to the torque sensing performance, such as modeling the current SEA friction and SE hysteresis, might improve the current compensation performance. Such improvements could potentially make the set-up also suitable for people with higher Brooke Scales  $\geq 5$ .

The following step, after optimizing the torque sensing and system transparency, is to validate the user's acceptance and whether the design requirements are sufficient for the intended target population in a clinical trial, for which Medical Ethical Committee approval is obtained.

This evaluation should focus on the intuitiveness of the human-exoskeleton interaction and the feasibility of the DAROR in daily activities. Moreover, we will compare various control interfaces within the same hardware set-up, such as F/T or EMG admittance, with our current impedance controller. Later, we plan to evaluate the advancement of our fully active versus available (semi-)active (end-effector) systems.

The results of this study will guide the next design iteration, and by sharing our insights, we aim to accelerate the overall development toward a feasible and effective arm support that enhance the quality of life in individuals with severe arm muscle weakness.

## References

- [1] G. Bodo, F. Tessari, S. Buccelli, L. De Guglielmo, G. Capitta, M. Laffranchi, and L. De Michieli. Customized Series Elastic Actuator for a Safe and Compliant Human-Robot Interaction: Design and Characterization. In *2023 International Conference on Rehabilitation Robotics (ICORR)*, pages 1–6, 2023. doi: 10.1109/ICORR58425.2023.10304680.
- [2] M. H. Brooke, R. C. Griggs, J. R. Mendell, G. M. Fenichel, J. B. Shumate, and R. J. Pellegrino. Clinical trial in Duchenne dystrophy. I. The design of the protocol. *Muscle & nerve*, 4(3):186–197, 1981. doi: 10.1002/mus.880040304.
- [3] C. Cornu, F. Goubel, and M. Fardeau. Muscle and joint elastic properties during elbow flexion in Duchenne muscular dystrophy. *The Journal of Physiology*, 533(2):605–616, 2001. doi: 10.1111/j.1469-7793.2001.0605a.x.
- [4] M. C. Corrigan, B. Mathie, and R. A. Foulds. Translation of an upper extremity exoskeleton to home and community use for individuals with duchenne muscular dystrophy. *2017 International Symposium on Wearable Robotics and Rehabilitation, WeRob 2017*, pages 1–2, 2018. doi: 10.1109/WEROB.2017.8383820.
- [5] S. Dalla Gasperina, M. Gandolla, A. Manti, L. Aquilante, V. Longatelli, M. G. D’Angelo, F. Molteni, E. Biffi, M. Rossini, M. Gfoehler, M. Puchinger, F. Braghin, and A. Pedrocchi. Upper-limb actuated exoskeleton for muscular dystrophy patients: Preliminary results. *Proceedings of the Annual International Conference of the IEEE Engineering in Medicine and Biology Society, EMBS*, pages 4431–4435, 2019. doi: 10.1109/EMBC.2019.8857725.
- [6] A. G. Dunning, M. M. H. P. Janssen, P. N. Kooren, and J. L. Herder. Evaluation of an arm support with trunk motion capability. *Journal of Medical Devices, Transactions of the ASME*, 10(4):1–4, 2016. doi: 10.1115/1.4034298.
- [7] A. E. Emery. The muscular dystrophies. *The Lancet*, 359(9307):687–695, feb 2002. doi: 10.1016/S0140-6736(02)07815-7.
- [8] J. M. Essers, K. Meijer, A. Murgia, A. Bergsma, and P. Verstegen. An inverse dynamic analysis on the influence of upper limb gravity compensation during reaching. *IEEE International Conference on Rehabilitation Robotics*, pages 1–5, 2013. doi: 10.1109/ICORR.2013.6650368.
- [9] J. M. Essers, A. Murgia, A. A. Peters, M. M. H. P. Janssen, and K. Meijer. Recommendations for studies on dynamic arm support devices in people with neuromuscular disorders: a scoping review with expert-based discussion. *Disability and Rehabilitation: Assistive Technology*, 0(0):1–14, 2020. doi: 10.1080/17483107.2020.1806937.
- [10] S. J. Filius, J. Harlaar, L. Alberts, S. Houwen-van Opstal, H. van der Kooij, and M. M. Janssen. Design requirements of upper extremity supports for daily use in Duchenne muscular dystrophy with severe muscle weakness. *Journal of Rehabilitation and Assistive Technologies Engineering*, 11(March):1–18, 2024. doi: 10.1177/20556683241228478.

- [11] D. Formica, S. K. Charles, L. Zollo, E. Guglielmelli, N. Hogan, and H. I. Krebs. The passive stiffness of the wrist and forearm. *Journal of Neurophysiology*, 108(4):1158–1166, 2012. doi: 10.1152/jn.01014.2011.
- [12] M. Gandolla, A. Antonietti, V. Longatelli, and A. Pedrocchi. The Effectiveness of Wearable Upper Limb Assistive Devices in Degenerative Neuromuscular Diseases: A Systematic Review and Meta-Analysis. *Frontiers in Bioengineering and Biotechnology*, 7(January):1–16, 2020. doi: 10.3389/fbioe.2019.00450.
- [13] M. Gandolla, S. Dalla Gasperina, V. Longatelli, A. Manti, L. Aquilante, M. G. D’Angelo, E. Biffi, E. Diella, F. Molteni, M. Rossini, M. Gföhler, M. Puchinger, M. Bocciolone, F. Braghin, and A. Pedrocchi. An assistive upper-limb exoskeleton controlled by multi-modal interfaces for severely impaired patients: development and experimental assessment. *Robotics and Autonomous Systems*, 143, 2021. doi: 10.1016/j.robot.2021.103822.
- [14] M. A. Gull, M. Thøgersen, S. H. Bengtson, M. Mohammadi, L. N. Andreassen Struijk, T. B. Moeslund, T. Bak, and S. Bai. A 4-dof upper limb exoskeleton for physical assistance: design, modeling, control and performance evaluation. *Applied Sciences (Switzerland)*, 11(13), 2021. doi: 10.3390/app11135865.
- [15] S. L. Houwen-van Opstal, L. Rodwell, D. Bot, A. Daalmeyer, M. A. Willemsen, E. H. Niks, and I. J. de Groot. BMI-z scores of boys with Duchenne muscular dystrophy already begin to increase before losing ambulation: a longitudinal exploration of BMI, corticosteroids and caloric intake. *Neuromuscular Disorders*, 32(3):236–244, 2022. doi: 10.1016/j.nmd.2022.01.011.
- [16] M. M. H. P. Janssen, J. Horstik, P. Klap, and I. J. de Groot. Feasibility and effectiveness of a novel dynamic arm support in persons with spinal muscular atrophy and duchenne muscular dystrophy. *Journal of NeuroEngineering and Rehabilitation*, 18(1):1–13, 2021. doi: 10.1186/s12984-021-00868-6.
- [17] I. Y. Jung, J. H. Chae, S. K. Park, J. H. Kim, J. Y. Kim, S. J. Kim, and M. S. Bang. The correlation analysis of functional factors and age with Duchenne muscular dystrophy. *Annals of Rehabilitation Medicine*, 36(1):22–32, 2012. doi: 10.5535/arm.2012.36.1.22.
- [18] A. Q. Keemink, H. van der Kooij, and A. H. Stienen. Admittance control for physical human–robot interaction. *International Journal of Robotics Research*, 37(11):1421–1444, 2018. doi: 10.1177/0278364918768950.
- [19] P. N. Kooren, A. G. Dunning, M. M. H. P. Janssen, J. Lobo-Prat, B. F. Koopman, M. I. Paalman, I. J. De Groot, and J. L. Herder. Design and pilot validation of A-gear: A novel wearable dynamic arm support. *Journal of NeuroEngineering and Rehabilitation*, 12(1):1–12, 2015. doi: 10.1186/s12984-015-0072-y.
- [20] P. N. Kooren, J. Lobo-Prat, A. Q. Keemink, M. M. H. P. Janssen, A. H. Stienen, I. J. de Groot, M. I. Paalman, R. Verdaasdonk, and B. F. Koopman. Design and Control of the Active A-Gear: a Wearable 5 DOF Arm Exoskeleton for Adults with Duchenne Muscular Dystrophy. *6th IEEE RAS/EMBS International Conference on Biomedical*



- Robotics and Biomechanics (BioRob)* June 26-29, 2016. UTown, Singapore, 2016-June (26-29):637–642, 2016. doi: 10.1109/BIOROB.2016.7523801.
- [21] E. Landfeldt, R. Thompson, T. Sejersen, H. J. McMillan, J. Kirschner, and H. Lochmüller. Life expectancy at birth in Duchenne muscular dystrophy: a systematic review and meta-analysis. *European Journal of Epidemiology*, 35(7):643–653, 2020. doi: 10.1007/s10654-020-00613-8.
  - [22] J. Lobo-Prat, A. Q. L. Keemink, B. F. J. M. Koopman, A. H. A. Stienen, and P. H. Veltink. Adaptive gravity and joint stiffness compensation methods for force-controlled arm supports. In *IEEE International Conference on Rehabilitation Robotics*, volume 2015-Septe, pages 478–483. IEEE, 2015. doi: 10.1109/ICORR.2015.7281245.
  - [23] J. Lobo-Prat, P. N. Kooren, M. M. H. P. Janssen, A. Q. Keemink, P. H. Veltink, A. H. Stienen, and B. F. Koopman. Implementation of EMG-and force-based control interfaces in active elbow supports for men with duchenne muscular dystrophy: a feasibility study. *IEEE Transactions on Neural Systems and Rehabilitation Engineering*, 24(11):1179–1190, 2016. doi: 10.1109/TNSRE.2016.2530762.
  - [24] V. Longatelli, A. Antonietti, E. Biffi, E. Diella, M. G. D’Angelo, M. Rossini, F. Molteni, M. Bocciolone, A. Pedrocchi, and M. Gandolla. User-centred assistive SystEm for arm Functions in neUromuscuLar subjects (USEFUL): a randomized controlled study. *Journal of NeuroEngineering and Rehabilitation*, 18(1):1–17, 2021. doi: 10.1186/s12984-020-00794-z.
  - [25] S. Maggioni, A. Melendez-Calderon, E. Van Asseldonk, V. Klamroth-Marganska, L. Lünenburger, R. Riener, and H. Van Der Kooij. Robot-aided assessment of lower extremity functions: A review. *Journal of NeuroEngineering and Rehabilitation*, 13(1):1–25, 2016. doi: 10.1186/s12984-016-0180-3.
  - [26] B. Mathie, M. Grimm, J. Cavanaugh, R. Foulds, Z. Smith, and R. Smith. Restoration of Arm Mobility with Power-Assist Exoskeletons for Young Men with Duchenne Muscular Dystrophy. 2020.
  - [27] S. Plagenhoef, F. Gaynor Evans, and T. Abdelnour. Anatomical Data for Analyzing Human Motion. *Research Quarterly for Exercise and Sport*, 54(2):169–178, 1983. doi: 10.1080/02701367.1983.10605290.
  - [28] D. Ragonesi, S. Agrawal, W. Sample, and T. Rahman. Series elastic actuator control of a powered exoskeleton. *Proceedings of the Annual International Conference of the IEEE Engineering in Medicine and Biology Society, EMBS*, pages 3515–3518, 2011. doi: 10.1109/IEMBS.2011.6090583.
  - [29] D. Ragonesi, S. K. Agrawal, W. Sample, and T. Rahman. Quantifying anti-gravity torques in the design of a powered exoskeleton. In *Proceedings of the Annual International Conference of the IEEE Engineering in Medicine and Biology Society, EMBS*, volume 21, pages 7458–7461. IEEE, 2011. doi: 10.1109/IEMBS.2011.6091749.



- [30] D. Ragonesi, S. K. Agrawal, W. Sample, and T. Rahman. Quantifying anti-gravity torques for the design of a powered exoskeleton. *IEEE Transactions on Neural Systems and Rehabilitation Engineering*, 21(2):283–288, 2013. doi: 10.1109/TNSRE.2012.2222047.
- [31] W. F. Rampeltshammer, A. Q. Keemink, and H. Van Der Kooij. An Improved Force Controller with Low and Passive Apparent Impedance for Series Elastic Actuators. *IEEE/ASME Transactions on Mechatronics*, 25(3):1220–1230, 2020. doi: 10.1109/TMECH.2020.2970532.
- [32] V. Ricotti, M. R. Evans, C. D. Sinclair, J. W. Butler, D. A. Ridout, J. Y. Hogrel, A. Emira, J. M. Morrow, M. M. Reilly, M. G. Hanna, R. L. Janiczek, P. M. Matthews, T. A. Yousry, F. Muntoni, and J. S. Thornton. Upper limb evaluation in duchenne muscular dystrophy: Fat-water quantification by MRI, muscle force and function define endpoints for clinical trials. *PLoS ONE*, 11(9):1–15, 2016. doi: 10.1371/journal.pone.0162542.
- [33] A. J. Skalsky and C. M. McDonald. Prevention and management of limb contractures in neuromuscular diseases. *Physical Medicine and Rehabilitation Clinics of North America*, 23(3):675–687, 2012. doi: 10.1016/j.pmr.2012.06.009.
- [34] A. H. Stienen, E. E. Hekman, H. T. Braak, A. M. Aalsma, F. C. Van Der Helm, and H. Van Der Kooij. Design of a rotational hydroelastic actuator for a powered exoskeleton for upper limb rehabilitation. *IEEE Transactions on Biomedical Engineering*, 57(3):728–735, 2010. doi: 10.1109/TBME.2009.2018628.
- [35] A. H. A. Stienen and A. Q. L. Keemink. Visualization of shoulder range of motion for clinical diagnostics and device development. *IEEE International Conference on Rehabilitation Robotics*, 2015-Sept:816–821, 2015. doi: 10.1109/ICORR.2015.7281303.
- [36] S. Takeda, P. R. Clemens, and E. P. Hoffman. Exon-Skipping in Duchenne Muscular Dystrophy. *Journal of neuromuscular diseases*, 8(s2):S343–S358, 2021. doi: 10.3233/JND-210682.
- [37] L. A. van der Heide, G. J. Gelderblom, and L. P. De Witte. Effects and effectiveness of dynamic arm supports: A technical review. *American Journal of Physical Medicine and Rehabilitation*, 94(1):44–62, 2015. doi: 10.1097/PHM.0000000000000107.
- [38] J. F. Wang, J. Forst, S. Schröder, and J. M. Schröder. Correlation of muscle fiber type measurements with clinical and molecular genetic data in Duchenne muscular dystrophy. *Neuromuscular Disorders*, 9(3):150–158, 1999. doi: 10.1016/S0960-8966(98)00114-X.
- [39] L. M. Ward, S. Hadjiyannakis, H. J. McMillan, G. Noritz, and D. R. Weber. Bone health and osteoporosis management of the patient with Duchenne muscular dystrophy. *Pediatrics*, 142(Suppl 2):S34–S42, 2018. doi: 10.1542/peds.2018-0333E.
- [40] R. Whisenant, C. Jones, A. Diether, and B. Lamming. DAZ 3D Studio, 2023. URL <https://www.daz3d.com/>. Version 4.10.0.123 Pro Edition (64-bit) For Windows.
- [41] D. A. Winter. *Biomechanics and Motor Control of Human Movement: Fourth Edition*. 2009. doi: 10.1002/9780470549148.

- [42] K. Wu, Y. Su, Y. Yu, K. Lin, and C. Lan. Series Elastic Actuation of an Elbow Rehabilitation Exoskeleton with Axis Misalignment Adaptation. pages 1–6, 2017.

# IV

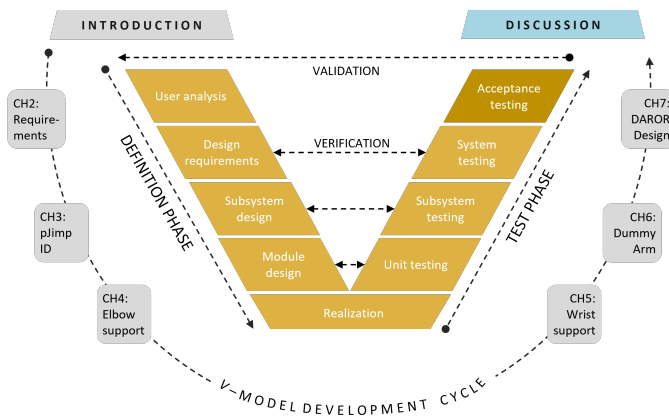
## General Discussion



# 8

## Discussion

In Part I, II and III, we have touched upon the left and right sides of the V-model. Now it is time for the top part, ‘*acceptance testing*’, and reflecting on the formulated design requirements.



The discussion provides an overview of the main findings from the chapters, followed by the preliminary validation results with our co-creator. It then reflects on the lessons learned during the development process and the design choices made. Finally, it concludes with recommendations for future directions.

## 8.1 Overview of main results

The overall aims of this project were fourfold. The first aim was to identify and define the design requirements for motorized arm supports to assist individuals with Duchenne Muscular Dystrophy (DMD) Brooke Scale 4 in daily activities. This population suffers from severe muscle weakness and cannot benefit from the currently available arm supports. This was addressed in Chapter 2. The second aim of this project was to develop a method to estimate and compensate for the arm weight and the stiffness component of the passive joint impedance (pJimp) using an impedance controller. This was addressed, first only for the forearm in Chapter 4, and later expanded to the full arm in Chapter 7. Thirdly, it aimed to design an investigational platform, the Duchenne ARm ORthosis (DAROR), to evaluate those control methods and, finally, verify the formulated design requirements within this set-up. The third and fourth objectives were both addressed in Chapter 7. For the development of the DAROR, we followed the V-model concept, which also guided the division of the thesis into three main parts. The following sections will provide an overview of the key findings from each part.

### 8.1.1 Part I – User Analysis and Design Requirements

In Chapter 2, the clinical characteristics of the target population were matched to functional and technical design requirements. People with DMD Brooke Scale 4 have approximately <22% of arm strength compared to individuals without muscle weakness. This leads to no effective shoulder function and severely limited elbow movement. Based on the identified clinical characteristics and functional user needs, a form of motorized actuator technology with intuitive movement intention detection is recommended. Moreover, it revealed that the pJimp seems a relevant clinical characteristic to consider in the compensation strategy. However, Chapter 2 also revealed that essential knowledge about how the pJimp evolves over disease progression and how the pJimp can be modelled for compensation is lacking. So, in Chapter 3, methods used in literature to examine pJimp were explored by a literature review. For the application of pJimp compensation in motorized arm supports, it is recommended to apply a very slow movement ramp-type perturbation with constant velocity over the full pROM of the arm and measure the resulting joint moment. This gives the torque-angle profile of the pJimp, which can be used to model the behavior for compensation. Chapter 3 also overviews the parameters that have an effect on pJimp, such as the joint's position, history, and velocity, but also the cross-coupling effects of multi-articular muscles. These parameters should be considered when designing the measurement method or identification procedure of the pJimp.

### 8.1.2 Part II – Subsystem Design, Module Design, and Unit Testing

Chapter 4 explored strategies to measure and compensate for the pJimp in twelve non-weakened participants in a subsystem of the DAROR setup, an active elbow support. This setup was built with the alpha-version, or 'test actuator', of the custom-made actuators intended for the DAROR. It showed that even in non-weakened individuals, the pJimp contributes substantially to the passive forces in the human arm. On average, the range of the isolated pJimp took up  $60 \pm 14\%$  of the total torque-angle curve (i.e., weight and pJimp), with measurements taken over a ROM of 80% of the elbow's pROM. This underlines the

relevance of compensating for pJimp in arm-supportive devices. Variations in constant movement velocity (i.e., 0.05, 0.1, 0.2 rad/s) and the bi-articular nature of the m. biceps brachii and m. triceps brachii muscles (i.e.,  $\pm 45^\circ$  horizontal rotation) were taken into consideration. However, the results from the student project [15] showed no significant effects under the investigated variations. The joint angle-dependent stiffness component appears to be the most dominant component of the pJimp, particularly given the relatively slow arm movements for our application. These findings support the decision to determine the elbow pJimp at low velocity in a single shoulder configuration. The torque-angle curve did show a direction dependency (e.g., hysteresis), with a mean absolute difference between the flexion and extension cycles of approximately  $< 0.5$  Nm on average. We decided to level this out by averaging the flexion and extension phases for control stability. The shape of this curve resembles a flattened S-shape, where the pJimp appears mostly linear over the measured 80% of the pROM but steeply increases near the joint limits.

Moreover, it compared four different compensation strategies for weight compensation and a combination of weight and elbow stiffness. One of them being the *scaled-model*, solely compensating for the weight of the arm using a simplified gravitational model. This model is semi-personalized, as it is scaled to the ‘a priori known’ arm biometrics, i.e., mass, and segment center of mass (CoM) locations of the user. A slightly more advanced model, called *hybrid*, also includes the measured elbow joint stiffness in addition to the scaled model. The other two, *measured* and *fitted-model*, compensate for both weight and stiffness and are more personalized. Where the measured compensates for the combined passive forces directly measured in the arm; and the fitted-model combines a simplified linear (i.e., first-order) model for the elbow stiffness to the scaled-model, but then fitted to the measured data.

When comparing these models, the scaled-model and hybrid seem to overestimate the gravitational component. Therefore, the measured and fitted-model strategies were considered to be more accurate but have the drawback that they require an identification process to identify the passive forces in the arm. In this identification procedure, it is crucial to fully relax the arm while the setup moves it through its ROM and accurately measures the joint moments. When extrapolating this to the entire arm, the gravitational model becomes more complex, as the direction of gravity changes for each joint depending on the orientation of the other joints.

This latter holds also for the wrist joint, as discussed in Chapter 5. The required support torque for the weight of the hand depends on the orientations of the shoulder, elbow, and wrist joints. This interdependence makes it more challenging to compensate for the weight of the hand with a lightweight passive add-on module. Additionally, the design space becomes smaller and more constrained further distally on the arm. Therefore, Chapter 5 evaluates simplified torque profiles to compensate for the weight of the hand. It was found that the simplified ‘constant’ torque profile, which is only dependent on the forearm orientation (instead of both forearm and wrist), was not statistically different from the ‘theoretical ideal’ sinusoidal profile. This makes (semi-)passive solutions as add-on modules to the DAROR more feasible. A conceptual design of such a wrist module was explored in a student project [18] and Wearable Robotics consortium [14]. Moreover, for the wrist joint, we found that the theoretically ideal profile does not provide perfect support, as factors beyond weight (such as pJimp) are likely to influence the required compensation torque.

### 8.1.3 Part III – System Design and System Testing

Part III presents in Chapter 6 the design of a verification tool, the Dummy Arm, that mimics the characteristics of a human arm (e.g., mass, and CoM location) that are tuneable to a desired target population. Moreover, it demonstrates that it can replicate various elbow stiffness torque-angle profiles. This simple, cost-effective verification tool enhanced the development process of the DAROR. It offered quick iteration, objective comparison, reduced safety risks, and minimized the burden on voluntary pilots.

In Chapter 7, the design of the investigational DAROR, that supports both the elbow and shoulder is presented. Moreover, two methods to estimate and compensate for the weight and elbow stiffness using an impedance-based controller are compared. This investigational platform allowed us to verify the formulated design requirements and recommend future directions for arm supports. The two compensation approaches are inspired by the compensation strategies explored in Chapter 4 but extrapolated to the four degrees of freedom (DOF). The first method is semi-personalized and inspired by the hybrid and scaled model, and the second is personalized similar to the measured or fitted model of the elbow support study. The first approach, referred as AP(+), based on the ‘a priori’ knowledge of the arm characteristics plus, optionally, a general first-order model of the elbow joint stiffness. The second approach is called ID(+), based on an optimized ‘identification’ procedure that estimates the parameters for a gravitation model only or, optionally, combined with a higher-order model of elbow stiffness. Moreover, it introduced a novel method to objectively quantify both high-level compensation and transparency performance. The high-level compensation performance measures how well the human-exoskeleton combination (HEC) is statically balanced across the workspace and whether the user input torque required to hold a pose is acceptable. While, high-level compensation performance quantifies the residual system impedance, assessing how much user input torque is needed to move the system.

The verification results showed that the DAROR meets the predefined design requirements for the range of motion (ROM), support torque, and high-level compensation and transparency performance while remaining close to the body (i.e., not stigmatizing), making it suitable for individuals with DMD Brooke Scale 4. The ID and AP perform similarly in the Dummy arm exoskeleton combination (DEC) with known arm anthropometric parameters. However, there is confidence that the ID is more suitable for individuals with atypical anthropometrics.

This chapter successfully addressed the final research objective and concluded the V-model system testing by *verifying* if the design requirements are met (i.e., are we building the product in the right way?). The next step is to *validate* the device’s system acceptance with the target population (i.e., are we building the right product?). To this end, we obtained medical ethical approval to conduct a clinical evaluation of the DAROR in its current form, in accordance with medical device regulations.

## 8.2 General Discussion

This section will further discuss the results of the system testing and reflect upon what design requirements need some refinement to improve the performance. Additionally, it presents the preliminary validation results from acceptance testing with our co-creator



with DMD, covering the iterative feedback loop at the top region of the V-Model.

## 8.2.1 System verification and refinement of design requirements

The results of Chapter 7 demonstrated that the ‘must’ design requirements defined in Chapter 2 were met, demonstrating that the investigational DAROR is suitable to test with individuals with DMD. However, to further improve the robustness and performance of the DAROR, a few design requirements benefit from some refinement.

### 8.2.1.1 High-level compensation and transparency performance

As discussed in the introduction (Chapter 1) of this thesis, an impedance-based controller is expected to be more intuitive than a position- or admittance-based controller; since this is how humans naturally interact with objects in the environment. However, the intuitiveness of such an impedance-based controller is also affected by how easily the HEC can be moved. This requires a high system transparency (i.e., low system mechanical impedance) and reliable torque-sensing (i.e., accuracy and precision) to effectively balance the HEC and facilitate easy movement to new poses (i.e., good high-level compensation and transparency performance).

Despite meeting the ‘must’ torque sensing and residual actuator impedance (e.g., transparency) requirements formulated in Chapter 2, the current torque sensing and overall system impedance performance seem to negatively impact controller performance. The results in Chapter 7 show that the torque readings of the SEAs deal with hysteresis that can result in torque reading and tracking errors. Moreover, presumably unfavorable off-axis load demands on the bearings increase the SEA friction, which reduces the system’s impedance. Refinement of the formulated design requirements might be considered for a better and more robust high-level compensation and transparency performance. Nevertheless, based on the reported muscle strength in Chapter 2, the target population appears strong enough to move the HEC arm, but future validation with individuals with DMD at Brooke Scale 4 is needed to confirm these conclusions.

For the torque sensing accuracy, the ‘must’ requirement was defined at  $<1.0$  Nm (0.1 Nm for the should/could category). With the current experiences, a must requirement of 0.1 Nm might be more appropriate for our impedance-based controller ( $\leq 0.1$  Nm for the should/could category).

Considering the transparency, the must requirement for the residual actuator impedance was based on 50% of the average elbow flexion strength of the population and defined at  $\leq 0.4$  Nm (with  $\leq 0.3$  Nm for should/could). The isolated actuator breakaway torque (e.g., to overcome the static friction) was found to be  $0.3 \pm 0.1$  Nm (determined in the alpha-version) and seems sufficient. However, the requirement for the overall system impedance was not defined in Chapter 2. Within the DAROR set-up, the actuator impedance varies under different loading conditions, and unfavorable loading of the bearings seems to affect the overall system impedance negatively. Additionally, the overall system impedance is affected by the controller’s performance, as inaccuracies in estimation can cause (a tendency) to drift the system in a particular direction. Therefore, we recommend adding this ‘missing’ design requirement to the list of requirements. It should at least be lower than the muscle strength of the target population (i.e., must requirement), but preferably even lower (e.g.,  $\leq 50\%$ , should/could). Although the results of Chapter 7 identified an overall user input

torque to move the system of  $0.5 \pm 0.1$  Nm for the elbow and  $1.0 \pm 0.1$  Nm for the shoulder, which is lower than the in Chapter 2 estimated muscle strength of 0.8 Nm and 1.8 Nm for the elbow and shoulder, respectively (Brooke Scale 4); we believe the intuitiveness of the DAROR controller could be enhanced by further reducing the required input torque.

### 8.2.1.2 Semi-personalized or personalized parameter estimation?

As we have seen in the dummy arm exoskeleton combination (DEC) results of Chapter 7, the semi-personalized (AP) method statically balances more poses across the workspace than the personalized (ID) method. However, in the case of the DEC the exact anthropometrics are measured and used as input for the AP method, making the AP, in fact, a personalized method. With a human exoskeleton combination (HEC), especially in people with atypical anthropometrics, estimating the required parameters is inherently less accurate. This is often the case in DMD because of muscle atrophy, reduced bone mineral density, and contractures. Based on the results with the co-creator of the residual error between the predicted and measured model joint torques in Chapter 7, there is confidence that the ID model is more suitable for individuals with deviating anthropometrics.

However, with the personalized method (ID), it is important to identify the passive forces with high accuracy. It requires an accurate joint alignment, full relaxation of the arm and accurate torque sensing. Making the personalized method (ID) more prone to measurement errors than the semi-personalized method (AP). The personalized method is affected by the torque sensing performance two-fold: by parameter identification and by torque tracking, both of which are directly affected by the quality of the torque sensing. Meanwhile, the semi-personalized model (AP) is more robust in measuring inaccuracies since it is only affected by tracking performance. Nevertheless, the co-creator had a preference for the ID over the AP model (further discussed in Section 8.2.4), and we expect that when the transparency and torque sensing performance is improved, this will outperform the semi-personalized strategy.

## 8

### 8.2.2 The importance of joint stiffness compensation

In Chapter 4, we confirmed that the stiffness component of the pJimp contributes substantially to the passive forces in the arm and that it is important to consider this in the compensation strategies. This holds for both force-based impedance- and admittance-based controllers.

The results from Chapter 7 demonstrated that with the compensation of elbow joint stiffness (i.e., ID+ and AP+) in the DEC with simulated elevated joint stiffness (3.7 Nm), the interaction forces remained more consistent across the full elbow ROM, highlighting the effectiveness of the joint stiffness compensation. Currently, this joint stiffness of the elbow is considered as a polynomial tunable between first to fifth order for the compensation in ID+ and simplified to a first-order in AP+. However, we are still unsure of what order is most appropriate for the population, and the shoulder was left outside the scope of this project for feasibility reasons.

In the work of Ragonesi et al. [16, 17], they measured the passive forces of both the shoulder and elbow joint in adults, children without muscle weakness, and children with various pathologies (i.e., muscular dystrophy but type not specified, spinal muscular atrophy and arthrogryposis). They found that the adults and children without disability

had a similar torque-angle profile of the passive forces that could be described by a third-order polynomial, while the children with disabilities had a deviating curve and could not be averaged across disabilities [16]. They recommended using a subject-specific model. Therefore, we implemented the option to adjust the elbow stiffness polynomial from first to fifth order to accommodate complex behaviors.

However, using higher-order polynomials, such as fifth order, is prone to over-fitting and might also capture complex behavior resulting from measurement inaccuracies (e.g., joint misalignment, voluntary contraction, torque sensing errors) during the identification process. A more accurate identification process (e.g., ensure correct alignment, relaxation state and torque sensing) could improve the performance. However, a good following step is to collect more data from both the elbow and shoulder pJimp in a larger group of DMD to get more insight into the behavior and what order can be used best.

### 8.2.3 Kinematic design alterations

The results in Chapter 7, show that the current shoulder actuator configuration slightly limits the HEC in its ROM. In movements with low glenohumeral (GH) horizontal rotation in combination with GH elevation, the shoulder actuators can collide with each other, the human shoulder, or the users' wheelchairs. Although the requirements, the 'must' activities of daily living (ADL) as stated in Chapter 2 are met. A modification in the segments of the shoulder joint configuration could improve the shoulder ROM and potentially also allow for the 'should' ADL. This might, however, have the disadvantage of a DAROR design becoming further away from the body. Moreover, the current forearm sleeve interface is relatively long and positioned proximally to the elbow joint, causing it to interfere with the upper arm during elbow flexion. Modifying the size and placement of the interface sleeve on the forearm could enhance elbow flexion, making it easier to reach the mouth.

A different shoulder configuration could also enable the shoulder to be positioned fully horizontally. Although this was not a design requirement initially, such a configuration would facilitate horizontal arm measurements similar to those in the elbow study in Chapter 4. This would allow us to identify the behavior of the pJimp more accurately since the gravitational forces on the arm remain constant in these positions. Therefore, it is recommended to adopt the requirement for the kinematic design to allow the elbow and shoulder joint to move horizontally through its ROM.

### 8.2.4 Preliminary validation results from co-creation

During this project, we established a co-creation with a volunteer pioneer with DMD who was willing to be the first user with DMD of the DAROR. Our co-creator was involved in various steps in the development cycle, including the risk analysis for medical device regulations. He visited us multiple times to fit the DAROR, evaluate the compensation models, and give his feedback. We would like to mention that at the start of the co-creation project, our pilot was within our intended target population (Brooke Scale 4). During the project, natural disease progression led to increased muscle weakness, which did not allow our pilot to raise his hand to his mouth anymore (i.e., Brooke Scale 5).

During the first evaluations, applying sufficient shoulder torque to reposition the upper arm was challenging, which necessitated him to use trunk compensation strategies. At this point, it is yet unclear whether these compensation strategies are necessary because

the residual impedance in the system was too high for him (i.e., low system transparency) or whether he also lost the selectivity of his voluntary movement directions along with the functional loss (see quotation 4 in box below). Moreover, misalignments, or voluntary contractions (since EMG was not measured during identification to assess relaxation levels), and torque sensing inaccuracies might have negatively influenced the ID controller performance.

On the contrary, the support in the elbow joint successfully supported his forearm and hand with both AP and ID methods. He could move the HEC easily over the elbow ROM, he could bring a weight of 200g to his mouth and shake someone's hand, things he could not do without the support.

He preferred the ID over the ID+ and AP(+). Although there is not enough data from these preliminary results to make solid conclusions; the ID+ seemed to push his forearm more towards the joint limits, which made it harder for him to move the elbow smoothly. It is possible that joint torques measured during the identification process were incorrectly attributed to the fifth-order polynomial of the pJimp. For instance, caused by joint misalignment, torque sensing inaccuracies, or voluntary contractions (since EMG was not measured during identification to assess relaxation levels). These moments might have been incorrectly assigned to the polynomial. As discussed in Section 8.2.2 further research is needed to determine which type of polynomial best fits the population.

#### Some preliminary quotes from the co-creator:

Please note that I have taken the liberty to summarize and translate the statement for clarity and brevity:

1. How would you rank the support on a scale from 1-5? *"A ten!"* (after the first time he moved his arm again independently)
2. *"I did not expect it to be so intuitive to move my arm"*
3. *"I had to get used to the system, but I didn't feel unsafe"*
4. *"I probably can bring my arm in that direction, but I forgot how to do so"*
5. *"With some movements, I wish it [the DAROR] better knew [through intuitive sensing] where I want to go" [Sjoerd Lunshof]*

#### About the design of the DAROR our co-creator said the following:

Note: I took the liberty to summarize and translate his response for clarity and brevity. *"The size of the DAROR is on the large side, but considering the current development state I assume the actuators cannot be much smaller. ... The color is fine, but when it becomes a product, I think black would suit better for a more discreet look. For the future it would be nice if the arm support is more integrated in the wheelchair as a whole."* [Sjoerd Lunshof]

## 8.3 Lessons learned

This section will reflect on the lessons learned during the overall project process. It highlights the importance of thoroughly testing and highlights the value of a network and collaboration within the project.

### 8.3.1 Applying the V-model: Test, Test, and... Test!

The first important lesson learned is the importance of testing across each level of the development cycle in the V-model. Both hardware and software implementations need extensive testing as soon as possible and in the most representative use case.

For instance, after the first alpha-version of the actuator was ready to be tested (V-model: *unit testing*), we made the elbow support (V-model: *subsystem design*) for Chapter 4 to get familiar with both the hardware and software. Various early-stage issues arose during this first-time usage (e.g., encoder's sensitivity to magnetic fields produced by the rotor, non-linearity, hysteresis, and off-axis load demands). Some of these issues could be addressed in the next-generation actuators for the DAROR setup (V-model: *system integration*).

However, it is a challenge to define all hardware design requirements upfront and thus also to verify whether the component meets the requirements. Especially since some requirements depend on the total configuration and selected control approach, as different control approaches require different actuator characteristics. For instance, the choice for impedance- versus admittance-based control affects the desired actuator compliance [9, 19]. Moreover, considering the configuration, in retrospect, a double-sided bearing would have been more suitable for actuators with high off-axis load demands in the DAROR configuration. Extensive testing of the alpha-version actuator under all loading conditions in a simple proof-of-principle setup might have revealed this issue earlier in the process. Learning by doing is part of the engineering process, and projects like this are constrained by budget and time. Nevertheless, extensive testing under representative load cases would have been a valuable step we overlooked. This provides a lesson for future projects and suits the V-model approach's unit testing and subsystem testing phase.

The Dummy Arm of Chapter 5 is a successful example of a relatively simple, cost-effective verification tool that promotes extensive testing with a representative load case. The Dummy Arm proved to have great benefits in the development and verification of compensation strategies and minimized unnecessary burdens and safety risks for voluntary participants. The idea to develop this tool emerged from the IEEE ICORR RehabWeek 2023 conference in Singapore, where I was inspired by the work of others in the field [1, 3], highlighting the value of attending and networking at conferences. Testing with such a dummy limb for exoskeleton development is a great way to test with a representative load case, and starting with this in an earlier development phase would have been even more beneficial.

Testing with the target population remains, however, the most representative approach. Therefore, involving our co-creator with DMD was a crucial and valuable step forward. However, such construction falls outside the standard practice of the regional medical ethical or the university's human ethical research committee approval, making it difficult to arrange. Which, in our case, further delayed our collaboration with the target population.

Therefore, it is advisable to begin the application process for such construction early and, during volunteer recruitment, consider including individuals with lower Brooke Scales, given the rapid progression of the disease.

During this collaboration, we also learned that the time available to collect data or test control settings in a single session is limited due to the fatiguing nature of the sessions for the co-creator. This includes traveling to the setup, performing all safety checks, readjusting the wheelchair seating (and disabling this function during tests), relying on the people or exoskeleton to move the arm, and addressing questions and providing feedback.

### 8.3.2 Collaboration is key

This lesson learned is related to the Epigraph at the beginning of this thesis:

*The ideal engineer is a composite ... [S]He is not a scientist, [s]he is not a mathematician, [s]he is not a sociologist or a writer; but [s]he may use the knowledge and techniques of any or all of these disciplines in solving engineering problems.*

Nathan W. Dougherty

This project required a high level of expertise in various disciplines. Unfortunately, unlike other application projects in the Wearable Robotics program (see page xxi), only a single PhD candidate was assigned to this project, making it hard to composite all required skills on an expert level. Therefore, it was of great importance to establish effective collaborations across multiple disciplines. We established fruitful collaborations with the target population, as well as medical clinicians, physio- and occupational therapists, bio-medical scientists, and various mechanical, electrical, and control engineers.

The established collaborations were key to this project's success. Starting with our user committee. We established a good relationship with Yumen Bionics (The Netherlands). They successfully continued the *passive* A-Gear research project [10] and, after making significant improvements, brought it to market with CE marking. Yumen Bionics now has more than 10 years of experience with the target population. They provided the researcher with a workspace at their office during the University's restricted access due to the pandemic. This close collaboration enabled us to build on their lessons learned, participate in patient home visits, and accelerate our hardware development by building further on their design.

Moreover, we collaborated with DEMO (TU Delft), who took the time to listen closely, explain patiently, and create the required hardware and low-level software needed for this application. Without this collaboration, there was only a limited understanding of the low-level building blocks needed to build the DAROR. In fact, the DAROR itself would not have existed. Once again, a workplace was offered to the researcher, which allowed the researcher to quickly learn the technical details of the hardware and low-level software during a crucial phase of the project.

For medical-related questions during the development of the arm support, we frequently consulted the clinicians on our user committee, who work daily with individuals with

DMD at Radboud University Medical Center (UMC). When the pandemic finally allowed us to join the patient visits of physio- and occupational therapists at the Radboud UMC.

We set up an expert team composed of two patients with different disease stages, including their personal medical practitioner, assistants, and a parent, together with a physiotherapist, human movement scientists, clinical technology professor, and a mechanical-, constructor-, control-, and electrical engineer. This group of experts had the expertise and skills to make an accurate assessment of the potential risks and required mitigations to prevent those risks. We performed multiple cycles of risk analyses which were required to obtain the approval in accordance with medical device regulations. This led to a safe user manual, user protocol and design.

When the hardware of the DAROR was realized, the software, including the exploded compensation strategies in the elbow support study (Chapter 4), could be extrapolated to the four DOF. After recognizing that this was beyond our former team's expertise (as Nathan W. Dougherty knew, I am not a mathematician), we met just the right person at the Wearable Robotics Symposium (which was finally held in person again after the pandemic). After this symposium, we established a close collaboration with the University of Twente and extended our research team with a new member. This collaboration brought the project to the next level and accelerated the control development as presented in Chapter 7.

Finally, our collaborator and user committee partner, Duchenne Parent Project, which is a patient organization, facilitated the essential collaboration with our co-creator with DMD. We are grateful for his contribution and his collaboration is of great value.

## 8.4 Study limitations and recommendations

Unfortunately, the start of this project coincided with the onset of the COVID-19 pandemic in the Netherlands. Besides hindering rapid progress in the researcher's work and establishing collaborations with expert colleagues, the Wearable Robotics consortium, and our own user committee, it delayed the initiation of contact with the DMD population. Hospitals did not allow external visitors, and ethical approval applications for research proposals were postponed to protect the vulnerable health of the DMD population.

Preferably, we would have performed the elbow study of Chapter 4 also in individuals with DMD. Due to the pandemic and time constraints, this was not feasible. Moreover, since the DAROR configuration does not allow the horizontal orientation of the arm, it was also not possible to evaluate the isolated elbow (and potentially shoulder) pJump in the DAROR setup with the co-creator. Such evaluation would have given us more insights into the behavior of the (elevated) pJump in the target population and how to model the pJump in Chapter 7 for the AP+ and ID+ approach (i.e., currently implemented as a polynomial tunable between first to fifth-order). So, this remains a valuable direction for future follow-up.

Moreover, we believe that a co-creator approach is more valuable in the verification phase than a clinical evaluation with a single contact moment, even with a larger participant group. Therefore, we recommend conducting more Brooke Scale 4 co-creator trajectories when soft- or hardware improvements are implemented in a follow-up. Either simultaneously or sequentially, which would benefit the development process and alignment to the user needs. Such an approach can help to understand better each co-creator's



specific characteristics, preferences, and physical limitations. This approach allows for data collection on one day and testing of compensation strategies on another, facilitating quick interactions in control development. The subsequent use of the Dummy Arm with characteristics similar to those of the co-creators in between sessions can help to evaluate new control settings to minimize unnecessary burdens and safety risks.

## 8.5 Future outlook

This section will discuss alternatives and additions to look into when following up on this project.

### 8.5.1 Alternative control approaches

Our impedance-based controller was intended for intuitive control, given a low system impedance and accurate torque sensing performance. As discussed in Chapter 7, admittance controllers have the advantage of requiring less user activation force to initiate a movement but are assumed to be less intuitive.

With admittance control, similar to impedance-based, accurate identification of the joint stiffness is required to distinguish between the voluntary movement intention and elevated pJimp. Alternatively, to a force-based interface, electromyography (EMG) interfaces might be considered. With an EMG interface, a distinction between weight and joint stiffness is not required, but such interfaces have other practical drawbacks. Such as being more time-consuming to install, prone to incorrect sensor placement, having low long-term stability, and the skin-sensor interface can become uncomfortable for long-wearing duration. However, for the higher Brooke scores, who have almost no muscle strength left, EMG-based approaches are perceived as less fatiguing than force-based and might, therefore, be more suitable [12].

The same holds for devices that are position-controlled [2, 6, 7], that make use of a joystick or predefined movement trajectories (e.g., activated by voice or GUI commands). They can assist people who have no voluntary force left, to the disadvantage of being less intuitive and do not promote making use of the residual muscle strength. Nevertheless, these other approaches might be a workable solution for the more advanced disease stages (i.e., Brooke Scale 5 and 6).

Since our design incorporated the force/torque (F/T) sensor that can accurately measure the user's movement intention, the DAROR can compare admittance-based versus impedance-based control in the same hardware set-up. The feasibility and intuitiveness of an impedance-based controller versus an admittance-based controller should be further evaluated in a follow-up clinical evaluation. Functional performance outcomes (e.g., task completion time, surface EMG, or success rate) of a set of tasks combined with subjective performance metrics (e.g., the System Usability Scale or NASA-Task Load Index) can be used to quantify and compare the perceived intuitiveness, usability, and task load demands of different approaches.

When clinical evaluation in DMD has proven the concept of the DAROR and shown the added value of motorized arm support, expansion to other pathologies can be explored. Starting with pathologies that have similar functional profiles and needs as DMD patients.



### 8.5.2 Generalization of the results

The design requirements identified for individuals with DMD Brooke Scale 4 may also apply to conditions with similar levels of upper limb weakness, such as Spinal Muscular Atrophy, Myopathies, or other Muscular Dystrophies like advanced stages of Becker and Limb-Girdle. However, conditions involving neurological dysfunction, such as Cerebral Palsy, Multiple Sclerosis, Amyotrophic Lateral Sclerosis, or partial Spinal Cord Injury, introduce challenges due to involuntary muscle contractions like spasticity. These may interfere with the current impedance-based control approach, posing safety risks for users and bystanders. When broadening the inclusion criteria, one should carefully consider the residual muscle strength of the population and the absence of significant involuntary movements to ensure safe and effective device use. For users with lower muscle strength (higher Brooke Scales) or for other pathologies with similar functional profiles, exploring alternative control interfaces may be necessary.

### 8.5.3 Alternative hardware configurations

The additional weight of the actuators on the arm increases the HEC's weight and inertia. Relocation of the actuators to the back of the wheelchair while transmitting the actuation power through, for instance, Bowden cables was suggested in Kooren et al. [11] for the next generation of the Active A-gear. This would reduce the HEC's arm weight and improve the ease of bringing the HEC to a new pose. However, this would drastically affect the control approach and raise additional mechanical challenges, including cable transmission friction compensation [20].

Another alternative configuration that can be considered is the position-controlled 4DOF upper limb wheelchair-mounted exoskeleton described by Gull et al. [7], developed for individuals with cervical spinal cord injury (SCI). In this design, the shoulder is supported by only two actuators (i.e., extension/flexion and internal/external rotation), along with actuators for the elbow and wrist for radial/ulnar deviation. This simplified approximation of the shoulder joint still seems to achieve a considerable area of the human workspace for daily activities [7].

As discussed in the introduction (Chapter 1) of this thesis, an important consideration is a choice for *exoskeleton* (i.e., close to the body) versus an *end-effector* design (i.e., further away from the body). Essers et al. [5] recommend using the same number of DOF as a human arm for better alignment and natural behavior, based on the findings of [4]. Being close to the body is assumed to have better aesthetics and is less stigmatizing [10]. It is also less obtrusive and does not 'hit' objects in the surroundings while moving the arms, as can happen with protruding arm supports. However, considering the functional ROM, and collision with the body or wheelchair, it might be preferred to have a design that is slightly less close to the body than the current DAROR design. A follow-up study could compare user's preference for exoskeleton versus end-effector designs.

### 8.5.4 Compensate for additional lifted objects

Although beyond the scope of this thesis, a great advantage of motorized arm supports over passive supports is that it theoretically can automatically adjust for additional lifted objects in the hand. We conducted an exploratory student project [8] to investigate the

effectiveness of a data classification algorithm to distinguish between different handheld weights (i.e., 0 to 1 kg) during assisted elbow flexion and extension movements using the elbow support of Chapter 4. Two classification algorithms (i.e., K Nearest Neighbor and Support Vector Machine) were used to distinguish the weights using four sensor signals, i.e., F/T, Inertial Measurement Unit (IMU), and EMG. The preliminary results indicated some potential for discriminating higher weights (e.g., 1 kg) but showed a tendency to misclassify lower weights (e.g., 200 g), which are more relevant for ADL activities. Additionally, the effects of picking up and placing the weights were not included in the analysis. Further research exploring alternative approaches is needed to automatically detect and compensate for handheld objects.

In the admittance-controlled Power-Assist described in [13], they make use of additional wrist support that supports the handheld loads. Depending on the chosen control approach, different solutions for compensation of handheld loads might be possible. When the feasibility of the DAROR controller(s) is proven, automatic adjustment and compensation for lifted objects is an interesting follow-up step.

### 8.5.5 Towards a product phase

In the design of the DAROR, we prioritized its role as an investigation platform over being an end product. After the working principle of the system has proven to be effective and accepted by the users, some of these choices need to be reconsidered when transitioning towards a product phase.

For instance, donning and doffing with ease is a very important practical requirement and should be addressed in future product phases. Currently, the DAROR is supported by an adjustable frame that can change width and height, but it does not adjust to the tilt of the wheelchair backrest, complicating the donning process. Preferably, the user can don or doff independently. However, given the limited arm function in the target population, it is more feasible to aim for quick and safe donning and doffing with minimal assistance from a caretaker.

When mounted on a wheelchair, the design needs an IMU sensor to measure the changing direction of gravity. Moreover, the device needs to be dust- and water-resistant to be able to be used outdoors. The integrated mobile base station, however, already powers the set-up for the intended duration of 4h/day and provides an easy hot-swapping ability of the battery pack. It is possible to be assembled to the back of the wheelchair, which is already a good step towards a product phase.

Future designs could explore additional re-designs to assist or allow, for example, for the forearm pro- and supination (as they are an integral part of the feeding movement [5]) and trunk motion (to allow compensatory strategies that are typical for DMD) [5]. Essers et al. [5] highlights the importance of the trunk movements. In the current design, trunk movements are possible but cause misalignments between the HEC shoulder joints. A trunk vest could be used to prevent misalignment of the shoulder, but it may restrict the user's ability to use compensatory strategies typical for DMD. Allowing trunk movements by design could be a solution to this, as suggested in [5, 10].

Moreover, the current design allows for simultaneous usage of parallel springs similar to the passive EXone (Yumen Bionics, The Netherlands) for more efficient power usage or exploration of a hybrid system but is left outside the scope of the current project but could

be explored in a follow-up.

Finally, when a more end-product design is established, a clinical evaluation should investigate the benefits of motorized arm support compared to no support and other existing devices, such as passive and semi-active systems, including a follow-up on long-term compliance and potential long-term effects.

## References

- [1] J. Bessler-Etten, L. Schaake, G. B. Prange-Lasonder, and J. H. Buurke. Assessing effects of exoskeleton misalignment on knee joint load during swing using an instrumented leg simulator. *Journal of NeuroEngineering and Rehabilitation*, 19(1):1–18, 2022. doi: 10.1186/s12984-022-00990-z.
- [2] S. Dalla Gasperina, M. Gandolla, A. Manti, L. Aquilante, V. Longatelli, M. G. D’Angelo, F. Molteni, E. Biffi, M. Rossini, M. Gfoehler, M. Puchinger, F. Braghin, and A. Pedrocchi. Upper-limb actuated exoskeleton for muscular dystrophy patients: Preliminary results. *Proceedings of the Annual International Conference of the IEEE Engineering in Medicine and Biology Society, EMBS*, pages 4431–4435, 2019. doi: 10.1109/EMBC.2019.8857725.
- [3] M. Dežman, S. Massardi, D. Pinto-Fernandez, V. Grosu, C. Rodriguez-Guerrero, J. Babič, and D. Torricelli. A mechatronic leg replica to benchmark human–exoskeleton physical interactions. *Bioinspiration and Biomimetics*, 18(3), 2023. doi: 10.1088/1748-3190/acda8.
- [4] A. G. Dunning, M. M. H. P. Janssen, P. N. Kooren, and J. L. Herder. Evaluation of an arm support with trunk motion capability. *Journal of Medical Devices, Transactions of the ASME*, 10(4):1–4, 2016. doi: 10.1115/1.4034298.
- [5] J. M. Essers, A. Murgia, A. A. Peters, M. M. H. P. Janssen, and K. Meijer. Recommendations for studies on dynamic arm support devices in people with neuromuscular disorders: a scoping review with expert-based discussion. *Disability and Rehabilitation: Assistive Technology*, 0(0):1–14, 2020. doi: 10.1080/17483107.2020.1806937.
- [6] M. Gandolla, S. Dalla Gasperina, V. Longatelli, A. Manti, L. Aquilante, M. G. D’Angelo, E. Biffi, E. Diella, F. Molteni, M. Rossini, M. Gföhler, M. Puchinger, M. Bocciolone, F. Braghin, and A. Pedrocchi. An assistive upper-limb exoskeleton controlled by multi-modal interfaces for severely impaired patients: development and experimental assessment. *Robotics and Autonomous Systems*, 143, 2021. doi: 10.1016/j.robot.2021.103822.
- [7] M. A. Gull, M. Thøgersen, S. H. Bengtson, M. Mohammadi, L. N. Andreasen Struijk, T. B. Moeslund, T. Bak, and S. Bai. A 4-dof upper limb exoskeleton for physical assistance: design, modeling, control and performance evaluation. *Applied Sciences (Switzerland)*, 11(13), 2021. doi: 10.3390/app11135865.
- [8] K. A. F. L. Heyns. Weight classification during actively assisted elbow flexion and extension extension, 2023. URL <http://resolver.tudelft.nl/uuid:3903b806-a9c5-4d5b-9bd6-4505c83fdb3a>.
- [9] A. Q. Keemink, H. van der Kooij, and A. H. Stienen. Admittance control for physical human–robot interaction. *International Journal of Robotics Research*, 37(11):1421–1444, 2018. doi: 10.1177/0278364918768950.
- [10] P. N. Kooren, A. G. Dunning, M. M. H. P. Janssen, J. Lobo-Prat, B. F. Koopman, M. I. Paalman, I. J. De Groot, and J. L. Herder. Design and pilot validation of A-gear: A

- novel wearable dynamic arm support. *Journal of NeuroEngineering and Rehabilitation*, 12(1):1–12, 2015. doi: 10.1186/s12984-015-0072-y.
- [11] P. N. Kooren, J. Lobo-Prat, A. Q. Keemink, M. M. H. P. Janssen, A. H. Stienen, I. J. de Groot, M. I. Paalman, R. Verdaasdonk, and B. F. Koopman. Design and Control of the Active A-Gear: a Wearable 5 DOF Arm Exoskeleton for Adults with Duchenne Muscular Dystrophy. *6th IEEE RAS/EMBS International Conference on Biomedical Robotics and Biomechanics (BioRob) June 26-29, 2016. UTown, Singapore, 2016-June (26-29):637–642, 2016. doi: 10.1109/BIOROB.2016.7523801.*
- [12] J. Lobo-Prat, K. Nizamis, M. M. H. P. Janssen, A. Q. Keemink, P. H. Veltink, B. F. Koopman, and A. H. Stienen. Comparison between sEMG and force as control interfaces to support planar arm movements in adults with Duchenne: A feasibility study. *Journal of NeuroEngineering and Rehabilitation*, 14(1):1–17, 2017. doi: 10.1186/s12984-017-0282-6.
- [13] B. Mathie, M. Grimm, J. Cavanaugh, R. Foulds, Z. Smith, and R. Smith. Restoration of Arm Mobility with Power-Assist Exoskeletons for Young Men with Duchenne Muscular Dystrophy. 2020.
- [14] A. A. Nobaveh and B. Caasenbrood. Design Feasibility of an Energy-efficient Wrist Flexion-Extension Exoskeleton using Compliant Beams and Soft Actuators. *2022 International Conference on Rehabilitation Robotics (ICORR)*, pages 1–6, jul 2022. doi: 10.1109/ICORR55369.2022.9896528.
- [15] K. Papa. Passive Elbow Joint Impedance Identification with the use of an Elbow Device, 2023. URL <https://resolver.tudelft.nl/uuid:1f6e5d56-66e1-4cea-b626-266c9aded162>.
- [16] D. Ragonesi, S. K. Agrawal, W. Sample, and T. Rahman. Quantifying anti-gravity torques in the design of a powered exoskeleton. In *Proceedings of the Annual International Conference of the IEEE Engineering in Medicine and Biology Society, EMBS*, volume 21, pages 7458–7461. IEEE, 2011. doi: 10.1109/IEMBS.2011.6091749.
- [17] D. Ragonesi, S. K. Agrawal, W. Sample, and T. Rahman. Quantifying anti-gravity torques for the design of a powered exoskeleton. *IEEE Transactions on Neural Systems and Rehabilitation Engineering*, 21(2):283–288, 2013. doi: 10.1109/TNSRE.2012.2222047.
- [18] B. J. van der Burgh. Constant torque gravity compensation - Designing a wrist support for Duchenne Muscular Dystrophy patients., 2022. URL <https://resolver.tudelft.nl/uuid:cd089772-150a-49ab-833c-681e9c368dd3>.
- [19] H. van der Kooij, J. Veneman, and R. Ekkelenkamp. Compliant Actuation of Exoskeletons. *Mobile Robots: towards New Applications*, 281(December), 2006. doi: 10.5772/4688.
- [20] J. F. Veneman, R. Ekkelenkamp, R. Kruidhof, F. C. Van Der Helm, and H. Van Der Kooij. A series elastic- and bowden-cable-based actuation system for use as torque actuator in exoskeleton-type robots. *International Journal of Robotics Research*, 25(3): 261–281, 2006. doi: 10.1177/0278364906063829.



# 9

## Conclusion

This thesis explored the needs of individuals with Duchenne Muscular Dystrophy (DMD) Brooke Scale 4, who cope with severe muscle weakness and cannot benefit from existing arm supports. It demonstrated that compensating for both arm weight and the elevated passive joint impedance (pJimp) using a motorized arm support best matches the needs of this population. Our findings highlighted the important role of pJimp in the passive forces of the elbow joint, which behaves mostly linearly with a steep increase near the joint limits. We showed that its behavior, together with the weight of the arm, can be approximated by a mathematical model. We compared two strategies to find the parameters of this model. The personalized approach aligned better with atypical body measurements but was more error-prone and time-consuming than the semi-personalized method, which relied on standardized anthropometric data. The developed Duchenne ARm ORthosis (DAROR) met the key design requirements for Brooke Scale 4 users, including sufficient support, range of motion, and intuitive control performance. Its compact and strong design remains close to the body and includes a mobile power station that can be mounted on an (electric) wheelchair. Preliminary validation with our co-creator with DMD Brooke Scale 5 also revealed some limitations in the torque sensing and mechanical impedance, which increases the required residual muscle strength to operate the device. Refinements of the formulated design requirements are proposed to enhance performance. Future efforts should focus on these refinements while staying in close contact with additional co-creators to ensure alignment with the user-specific preferences. Followed by clinical validation of the DAROR to further investigate the users' acceptance in individuals with Brooke Scale 4, for which ethical approval has been obtained. The current design has the potential to compare various control methods to extend the DAROR's suitability to individuals with lower muscle strength or conditions with similar functional profiles and intact neuromuscular control. Through this work, we aim to bridge the gap in commercially available arm supports and contribute to the development of assistive technologies that enhance movement independence and quality of life of those with limited mobility.





# Appendices





# Appendix A

This appendix provides the supplementary materials of Chapter 3.

## A.1 Search terms used in literature review of Chapter 3

### PuBMed Search Terms

(((((stiffness[Title/Abstract]) OR (stiff[Title/Abstract]) OR (stiffnesses[Title/Abstract])) OR ((elasticity[Title/Abstract]) OR (elastance[Title/Abstract]) OR (elastances [Title/Abstract]) OR (elastic[Title/Abstract]) OR (elastical [Title/Abstract]) OR (elastically[Title/Abstract]) OR (elasticities [Title/Abstract]) OR (elastics[Title/Abstract])OR (elasticity[MeSH Terms])) OR ((coactivation[Title/Abstract]) OR (co-activation[Title/Abstract])) OR (contractures [Title/Abstract]) OR (((range[Title/Abstract]) AND (motion [Title/Abstract])) OR (articular range of motion[Title/Abstract]) OR (range of motion[Title/Abstract]) OR (range of motion, articular[MeSH Terms])) OR ((excursion[Title/Abstract]) OR (excursions[Title/Abstract])) OR ((fibrosis[Title/Abstract]) OR (fibrosis[MeSH Terms]) OR (fibro-adipose[Title/Abstract]) OR (fibrotic[Title/Abstract]) OR (fibrosi[Title/Abstract]) OR (fibroses[Title/Abstract]) OR (fibrose[Title/Abstract]))) AND ((muscle[MeSH Terms]) OR (joint[MeSH Terms]) OR (muscle[Title/Abstract]) OR (muscles[Title/Abstract]) OR (muscle's[Title/Abstract]) OR (joint[Title/Abstract]) OR (joints[Title/Abstract]) OR (joint's[Title/Abstract])) AND ((becker [Title/Abstract]) OR (neuromuscular disease [Title/Abstract]) OR (neuromuscular diseases [Title/Abstract]) OR (muscular dystrophy[Title/Abstract]) OR ( muscular dystrophies[Title /Abstract]) OR (muscular dystrophies [MeSH Terms]) OR (duchenne [Title/Abstract]) OR (duchenne's [Title/Abstract]) OR (duchenne's[Title/Abstract]) OR (muscular dystrophy, duchenne[MeSH Terms])) AND (((upper[Title/Abstract]) AND ((limb[Title/Abstract]) OR (limbs[Title/Abstract]) OR (extremity[Title/Abstract]) OR (extremities[Title/Abstract]))) OR (upper extremity[MeSH Terms]) OR (arm[Title/Abstract]) OR (arms[Title/Abstract]) OR (elbow[Title/Abstract]) OR (elbows[Title/Abstract]) OR (elbow joint[MeSH Terms]) OR (wrist[Title/Abstract]) OR (wrists[Title/Abstract]) OR (wrist joint[MeSH Terms]) OR (shoulder[Title/Abstract]) OR (shoulders[Title/Abstract]) OR (shoulder joint[MeSH Terms])) AND ((adolescent[Filter]) OR (adult[Filter]) OR (youngadult[Filter]))

## A

**SCOPUS Search Terms**

(TITLE-ABS-KEY (human) OR INDEXTERMS (human) OR KEY("normal human") OR TITLE-ABS-KEY ( Duchenne ) OR INDEXTERMS ( Duchenne ) OR TITLE-ABS-KEY ( duchenne ) OR KEY(DMD) OR KEY("Duchenne muscular dystrophy") OR KEY("muscular dystrophy, duchenne") OR TITLE-ABS-KEY ( becker ) OR KEY("becker muscular dystrophy") OR TITLE-ABS ( "muscular dystrophy" ) OR TITLE-ABS-KEY ( "muscular dystrophies" ) OR INDEXTERMS ( "muscular dystrophy" ) OR TITLE-ABS-KEY ( "neuromuscular disease" ) OR TITLE-ABS-KEY ( "neuromuscular diseases" ) OR KEY(male) OR KEY(biomechanics)) AND (TITLE-ABS-KEY ( stiffness ) OR TITLE-ABS ( stiffnesses) OR TITLE-ABS ( stiff ) OR TITLE-ABS ( elasticity ) OR TITLE-ABS ( elasticities ) OR TITLE-ABS ( elastance ) OR TITLE-ABS ( elastances ) OR TITLE-ABS ( elastic ) OR TITLE-ABS ( elastics ) OR TITLE-ABS ( elastical ) OR TITLE-ABS ( elastically) OR INDEXTERMS ( elasticity ) OR TITLE-ABS ( coactivation ) OR TITLE-ABS ( co-activation ) OR TITLE-ABS ( contractures ) OR TITLE-ABS ( excursion ) OR TITLE-ABS ( excursions ) OR TITLE-ABS ( "range of motion" ) OR TITLE-ABS ( range motion ) OR INDEXTERMS ( "range of motion" ) OR INDEXTERMS ( "articular range of motion" ) OR KEY("range of motion, articular") OR TITLE-ABS-KEY ( fibrosis) OR TITLE-ABS ( fibrosi ) OR TITLE-ABS ( fibrotic ) OR TITLE-ABS-KEY ( fibro-adipose ) OR TITLE-ABS ( fibroses ) OR TITLE-ABS ( fibrose )) AND (TITLE-ABS-KEY ( muscle ) OR TITLE-ABS ( muscles ) OR TITLE-ABS-KEY ( joint ) OR TITLE-ABS ( joints )) AND (TITLE-ABS-KEY ( "upper extremity" ) OR TITLE-ABS-KEY ( "upper extremities" ) OR TITLE-ABS-KEY ( arm ) OR TITLE-ABS-KEY ( arms ) OR TITLE-ABS-KEY ( wrist ) OR TITLE-ABS-KEY ( shoulder ) OR TITLE-ABS-KEY ( shoulders ) OR TITLE-ABS-KEY ( elbow ) OR KEY ( "elbow joint" ) OR KEY ( "shoulder joint" ) OR INDEXTERMS ( elbow ) OR KEY ( "wrist joint" ) OR KEY ( wrist ) OR TITLE-ABS-KEY ( "upper limb" ) OR TITLE-ABS-KEY ( "upper limbs" )) AND ( SUBJAREA ( neur ) OR SUBJAREA ( engi )) AND (EXCLUDE ( DOCTYPE,"no" )) AND (LIMIT-TO ( LANGUAGE,"English" )) AND (LIMIT-TO ( EXACTKEYWORD,"Adult" ) OR LIMIT-TO ( EXACTKEYWORD,"Young Adult" ) OR LIMIT-TO ( EXACTKEYWORD, "Adolescent" ) OR EXCLUDE ( EXACTKEYWORD,"Diagnostic Imaging" ) OR EXCLUDE ( EXACTKEYWORD,"Aged, 80 And Over" ) OR EXCLUDE ( EXACTKEYWORD,"Leg" ) OR EXCLUDE ( EXACTKEYWORD,"Knee" ) OR EXCLUDE ( EXACTKEYWORD,"Trunk" ) OR EXCLUDE ( EXACTKEYWORD,"Stroke Rehabilitation" ))

**IEEEExplore Search Terms**

((((stiffness) OR (stiff) OR (stiffnesses)) OR ((elasticity) OR (elastance) OR (elastances) OR (elastic) OR (elastical) OR (elastically) OR (elasticities) OR (elastics)) OR ((coactivation) OR ("co-activation")) OR (contractures) OR (((range) AND (motion)) OR ("articular range of motion") OR ("range of motion")) OR ((excursion) OR (excursions)) OR ((fibrosis) OR ("fibro-adipose") OR (fibrotic) OR (fibrosi) OR (fibroses) OR (fibrose))) AND ( (muscle) OR (muscles) OR (joint) OR (joints) ) AND ((becker) OR (neuromuscular disease) OR (neuromuscular diseases) OR (muscular dystrophy) OR (muscular dystrophies) OR (duchenne) OR (duchenne's) OR (duchenne) ) AND (((upper) AND ((limb) OR (limbs) OR (extremity) OR (extremities))) OR ("upper extremity") OR (arm) OR (arms) OR (elbow) OR (elbows) OR ("elbow joint") OR (wrist) OR (wrists) OR ("wrist joint") OR ("shoulder joint"))

## WebOfScience Search Terms

(ALL=((stiffness) OR (stiff) OR (stiffnesses)) OR ((elasticity) OR (elastance) OR (elastances) OR (elastic) OR (elastical) OR (elastically) OR (elasticities) OR (elastics)) OR ((coactivation) OR (co-activation)) OR (contractures) OR (((range) AND (motion)) OR (articular range of motion) OR (range of motion)) OR ((excursion) OR (excursions)) OR ((fibrosis) OR (fibro-adipose) OR (fibrotic) OR (fibrosi) OR (fibroses) OR (fibrose)))) AND (ALL=((muscle) OR (joint) OR (muscles) OR (muscle's) OR (joints) OR (joint's))) AND (ALL=((becker) OR (neuromuscular disease) OR (neuromuscular diseases) OR (muscular dystrophy) OR (muscular dystrophies) OR (duchenne) OR (duchennes) OR (duchenne's))) AND (ALL=((upper) AND ((limb) OR (limbs) OR (extremity) OR (extremities)) OR (arm) OR (arms) OR (elbow) OR (elbows) OR (elbow joint) OR (wrist) OR (wrists) OR (wrist joint) OR (shoulder joint))))



# B

## Appendix B

This appendix provides the supplementary materials of Chapter 4.

### B.1 Direction dependency of passive joint moments

Figure B.1 illustrates the direction dependency of the passive moments measured in the elbow joint. The gray lines present the flexion, extension and average curve of the passive forces measured in the horizontal plane where the effect of gravity is minimal. Therefore, this curve represents the passive joint impedance of the elbow joint. The black lines present the passive forces measured in the near vertical plane, affected by the gravity and passive joint impedance.

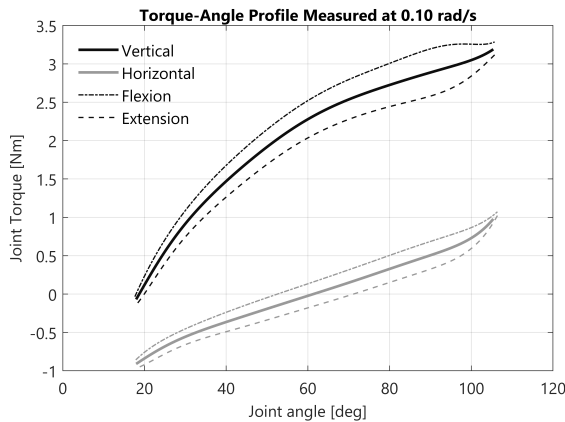


**Figure B.1:** A representative measurement of torque-angle profiles flexion and extension cycles measured at 0.10 rad/s in session 2.





# C

## Appendix C

This appendix provides the supplementary materials for Chapter 5, authored by B. J. van der Burgh, who shares first authorship of the chapter.

### C.1 Torque models

When looking at current wrist supports [2, 5], which aim to support the hand against gravity, such as the Ambroise Dynamic Wrist Orthosis [1], they primarily focus on supporting palmar-dorsal flexion of the wrist. As such gravity compensation of the hand for palmar-dorsal flexion is considered here. Consequently, as only one degree of freedom of the wrist is considered it can be simplified as a revolute joint. Thus, the required torque to compensate for the weight of the hand can be expressed as

$$T = mgL \cos(\theta - \phi) \cos \psi \quad (\text{C.1})$$

Where  $m$  is the mass of the hand,  $L$  the distance from the wrist joint to the hand's center of mass,  $g$  the gravitational acceleration,  $\phi$  the angle of the wrist with respect to the forearm,  $\theta$  the inclination of the forearm and  $\psi$  the pronation-supination angle at zero inclination (Figure C.1). The weight of the hand can be perfectly compensated by attaching a balance weight opposite to the center of mass (Figure C.2), resulting in a sinusoidal torque profile. To simplify the required torque profile, it can be approximated using Taylor expansions. Here the 0<sup>th</sup> and 1<sup>st</sup> order expansion will be considered. The 0<sup>th</sup> order expansion around the neutral wrist position  $\phi_0 = 0$  can be expressed as

$$T = mgL \cos \theta \cos \psi \quad (\text{C.2})$$

From this it can be noticed that the required torque only depends on the orientation of the forearm and no longer on the position of the wrist. Thus, the torques are constant for each position of the wrist. The 1<sup>st</sup> order expansion is given by

$$T = mgL (\cos \theta + \phi \sin \theta) \cos \psi \quad (\text{C.3})$$

Consequently, the torque depends linearly on the wrist position. This linear term can be considered as a torque generated by a linear spring with torsional stiffness  $k_\phi = mgL \sin \theta$  or  $k = mg \frac{L}{r^2} \sin \theta$  for an ordinary coil spring attached to a pulley of radius  $r$ .

The orientations considered during the experiment correspond to  $\psi=0^\circ$ ,  $\theta=0, 25, 50^\circ$  and  $\phi=-25, 0, 25, 50^\circ$ . The angle  $\psi$  is achieved physically through a combination of predominantly pronation of the forearm and a slight abduction of the shoulder. The different angles of  $\theta$  are achieved through a combination of elbow and shoulder flexion. The different angles of  $\phi$  are achieved through dorsal and palmar flexion of the wrist.

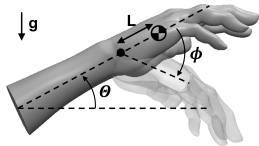


**Figure C.1:** Model of the hand. Note that  $\phi$  is chosen positive for palmar flexion. Hand model adapted from [7]

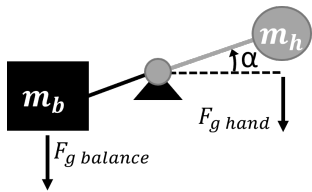


**Figure C.2:** Example of a gravity balancer using a balance weight, which generates a sinusoidal torque profile as a function of  $\alpha$  around the joint

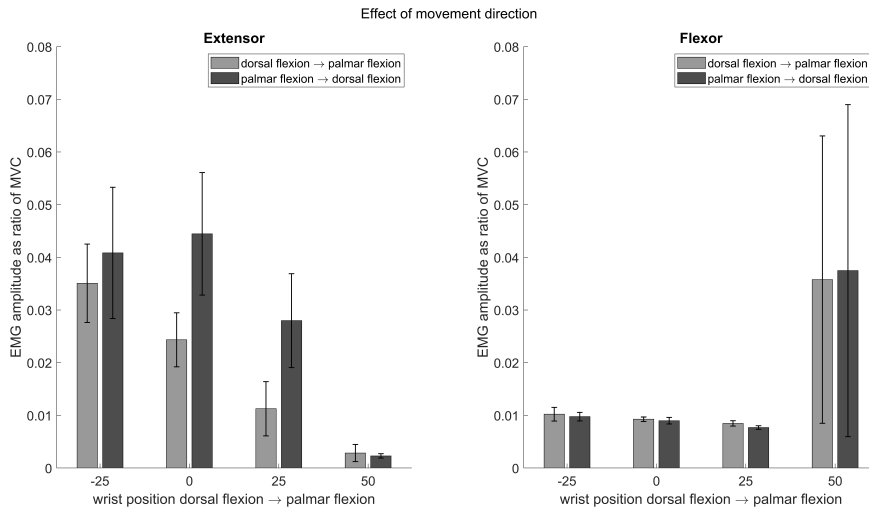
## C.2 Effect of movement direction

To assess the effect of the movement order of the wrist on the muscle activity of the m. extensor carpi radialis and the m. flexor carpi radialis, a separate experiment was performed. This experiment was performed with one subject and each measurement was performed 10 times. The participant was asked to move his hand from  $25^\circ$  dorsiflexion to  $0^\circ$  and then to  $25^\circ$  and  $50^\circ$  palmar flexion, after following the same order backwards. The orientation of the forearm was held constant throughout the experiment and no support was provided.

The biometric data of the participant are depicted in Table C.1. The results of the experiment are depicted in Figure C.3 showing in general higher activity when moving from palmar to dorsal (against gravity) than from dorsal to palmar (with gravity). The first case (dorsal to palmar flexion) involves a concentric contraction (muscle shortens during contraction) while the second (palmar to dorsal flexion) involves an eccentric contraction (muscle lengthens during contraction). These results are also expected as in general the measured activity during a concentric contraction is larger than during eccentric contraction [4].

**Table C.1:** Biometric data of the participant (n=1)

Gender	Age (years)	Weight (kg)	Height (m)	Hand weight (g)	center of mass (mm)
Male	24	61	1.88	353	43.6



C

**Figure C.3:** Mean normalized EMG-amplitude of the m. extensor carpi radialis (left) and m. flexor carpi radialis (right) for two movement directions. Error bars are one standard deviation

### C.3 Effect of different levels of compensation

To assess the effect of different levels of compensation an additional experiment was performed for the constant torque by using different weights. This experiment was performed with one subject and each measurement was performed five times. In sets of three and two. The order of the level of compensation was randomized as well as the order of the wrist positions. The orientation of the forearm was held constant throughout the experiment.

The biometric data of the participant are depicted in Table C.1. The results of the experiment are shown in Figure C.4. From this, it can be concluded that using more compensation results in a larger reduction in the activity of the anti-gravity muscle (extensor). However, a larger level of compensation results in an increase in the flexor muscle activity for palmar flexion. This can also be expected as for larger levels of compensation overcompensation occurs, requiring additional effort of the flexor muscles. When comparing these findings with literature, Coscia et al. [3] observed a decrease in muscle activity of the anti-gravity muscles when increasing the level of support from no to full support. Here, they used perfect balancing, which is comparable to the sinusoidal profile as discussed in this article. Note that in this experiment, non-perfect balancing is used (a constant torque), and the levels are increased beyond the full compensation. A similar effect was observed by Runnalls et al. [6]. Comparing the results of this additional experiment with the main experiment, it can be observed that for the extensor, the outcomes are similar when looking at 0% and 98% support. However, the flexor amplitude is considerably higher when support is used, compared to the mean results from the main experiment. However, this is likely caused by interindividual differences as also, in the main experiment, some participants showed similar results.

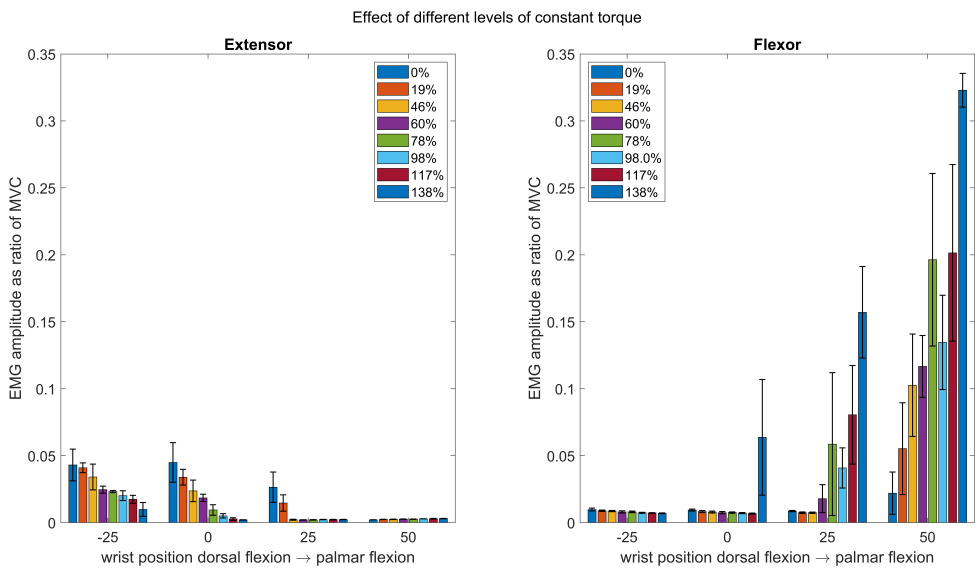


**Figure C.4:** Mean normalized EMG amplitude for different levels of constant torque compensation of the extensor carpi radialis (left) and flexor carpi radialis (right). Error bars are one standard deviation

## References

- [1] Ambroise Dynamische Polsorthese. URL <https://www.ambroise.nl/armorthesen/polsorthesen/ambroise-dynamische-polsorthese/>.
- [2] R. A. Bos, C. J. W. Haarman, T. Stortelder, K. Nizam, J. L. Herder, A. H. A. Stienen, and D. H. Plettenburg. A structured overview of trends and technologies used in dynamic hand orthoses. *Journal of NeuroEngineering and Rehabilitation*, 13(1):62, 2016. doi: 10.1186/s12984-016-0168-z.
- [3] M. Coscia, V. C. K. Cheung, P. Tropea, A. Koenig, V. Monaco, C. Bennis, S. Micera, and P. Bonato. The effect of arm weight support on upper limb muscle synergies during reaching movements. *Journal of NeuroEngineering and Rehabilitation*, 11(1):22, 2014. doi: 10.1186/1743-0003-11-22.
- [4] E. Criswell. *Cram's introduction to surface electromyography*. Jones and Bartlett, Sudbury, MA, second edi edition, 2011.
- [5] P. Heo, G. M. Gu, S. Lee, K. Rhee, and J. Kim. Current hand exoskeleton technologies for rehabilitation and assistive engineering. *International Journal of Precision Engineering and Manufacturing*, 13(5):807–824, 2012. doi: 10.1007/s12541-012-0107-2.
- [6] K. D. Runnalls, G. Anson, S. L. Wolf, and W. D. Byblow. Partial weight support differentially affects corticomotor excitability across muscles of the upper limb. *Physiological Reports*, 2(12):e12183, 2014. doi: 10.14814/phy2.12183.
- [7] A. Story. Right Hand Reference, 2020. URL <https://grabcad.com/library/right-hand-reference-1>.



# D

## Appendix D

This appendix provides the supplementary materials for Chapter 7, which was jointly written by S.J. Filius and A. Keemink.

### D.1 Sensor Analysis

The series elastic actuator (SEA) specifications are summarized in Table D.1. The specifications of the SI-40-mini (Schunk, ATI Industrial Automation, USA) force/torque (F/T) sensor can be found on <https://schunk.com>.

**Table D.1:** SEA specifications

Actuator weight	0.59 <sup>a</sup>	kg
Gear ratio	1:101	-
$\tau$ resolution	<0.01	Nm
$\tau$ constant	0.0251	Nm/A
Spring stiffness	289	Nm/rad
Maximum speed	$\geq 8$	rad/s
Maximum actuator $\tau$	16	Nm

Abbreviations:  $\tau$ : torque. <sup>a</sup>Differs per actuator.

#### D.1.1 Theoretical sensor resolution

For effective sensor resolution we calculate thrice the standard deviation of the noise, see Figure D.1.

#### D.1.2 SEA

Each SEA is equipped with three absolute encoders that monitor the state of the gearbox (14 bits), rotor, and series elastic (SE) element (19 bits, each). Together, the gearbox and SE

### Sensor noise

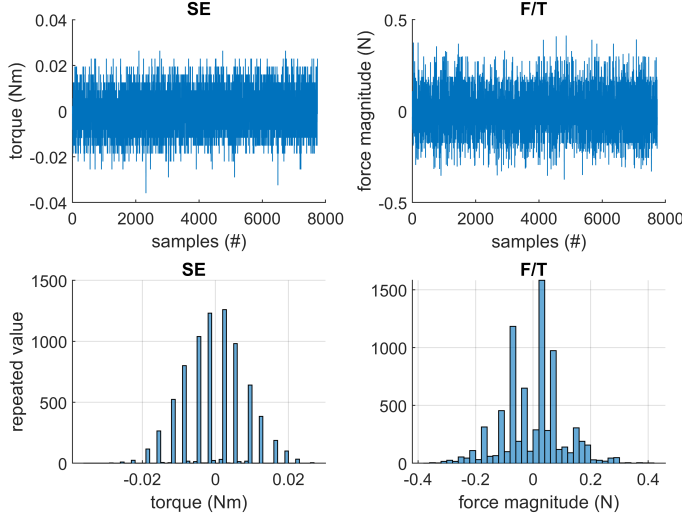


**Figure D.1:** SE and F/T sensor noise

element encoders accurately measure the joint angle. The effective resolution of the joint angle is around 0.0012 rad (thrice the standard deviation of the noise).

The SE element also acts as a torque sensor. With the encoder resolution of 19 bits and a spring stiffness of 289 Nm/rad, the theoretical torque resolution is:

$$\tau_{min} = \frac{2 \cdot \pi \cdot K_{SE}}{\# \text{ counts per revolution}} = \frac{2 \cdot \pi \cdot 289}{2^{19}} = 0.0035 \text{ Nm} \quad (\text{D.1})$$

However, the effective resolution is more in the range of 0.025 Nm (thrice the standard deviation of the noise, which is 0.0083 Nm).

### D.1.3 F/T sensor

For the force/torque (F/T) sensor, thrice the standard deviation of the noise is 0.201 N for the x-axis, 0.171 N for the y-axis, and 0.360 N for the z-axis, Figure D.1 shows the F/T force magnitude of the axes.

### D.1.4 Sensor performance

We performed an accuracy, sensitivity, and precision analysis to evaluate the sensor performance of the SEA and FT sensor. Figures D.2 and D.3 show the results.

#### D.1.4.1 Accuracy and sensitivity analysis

The torque accuracy and sensitivity of the SEAs are determined based on two different experiments. These experiments are only performed for Actuator 4 (R4) and Actuator 3



(R3) since similar experiments are not convenient for Actuators 1 and 2 within the DAROR set-up.

For R4, the elbow, with a known mass of 2.24 kg in the sleeve, was moved through the elbow range of motion (ROM) with static pauses. A simplified pendulum model determined each static interval's theoretical applied torque ( $T_{\text{applied}}$ ). The measured torque ( $T_{\text{measured}}$ ) was then compared with the applied torque.

For Actuator 3 (R3), the DAROR arm was fixated such that the upper arm was parallel to the ground, while known masses (0, 200, 500, 700, 1000 g) were placed on the F/T sensor location (moment arm of 41.5 cm). Again, the theoretical applied torques were calculated and compared to the measured torques. The results are shown in Figure D.2a to h.

For the F/T sensor, a similar experiment was conducted. A box was placed below the sleeve to add calibration masses ranging between 0.15 to 6.2 kg. The results of the force magnitude are shown in Figure D.2c, f, and i and elbow and shoulder joint torque in Figure D.3.

For the sensor accuracy, we calculated the mean absolute error (MAE), the root mean square error (RMSE), the standard deviation (SD) and the maximal error (max), between the measured and applied torque.

For the sensor sensitivity, we calculated the ratio of the change in measured torque ( $T_{\text{measured}}$ ) to the change in applied torque ( $T_{\text{applied}}$ ):

$$S = \frac{\Delta T_{\text{measured}}}{\Delta T_{\text{applied}}} \quad (\text{D.2})$$

The accuracy and sensitivity results of the SEA and F/T sensor are presented in Table D.2.

**Table D.2:** Results from the accuracy and sensitivity analysis for the SEA R3, R4, and for the magnitude of the F/T sensor, including the F/T sensor expressed in shoulder torque (sT) and elbow torque (eT).

Metric	R3 (Nm)	R4 (Nm)	R3+4 (Nm)	F/T (N)	sT (Nm)	eT (Nm)
MAE	0.27	0.52	0.43	0.13	0.06	0.05
SD	0.26	0.30	0.30	0.21	0.08	0.06
Max absolute error	0.55	1.10	1.10	0.72	0.27	0.21
RMSE	0.33	0.60	0.52	0.23	0.09	0.08
Sensitivity fit (-)	0.83	0.85	1.00	1.00	0.97	0.94

Ideally, the sensitivity of a sensor is 1. Since R4 overestimates the theoretical applied torques and R3 underestimates the applied torques, the sensitivity analysis of the combined errors gives a ratio of 1. However, in Chapter 7, we reported the average sensitivity ratio of 0.84 for the R3 and R4 instead.

### D.1.5 Precision analysis

The torque precision is calculated by taking the absolute mean error between the errors of the duplicated loads. First, the static plateaus in the joint angles are identified (rounded by 0.03 rad, 2°). Then, duplicates in the configurations for all four degrees of freedom (DOF)

over the full trajectory are identified, shown in Figure D.4. Since the load of the duplicated samples is approximately the same, it offers a strategy to measure the error in the torque readings. The calculated mean absolute error, standard deviation of the absolute error, the maximal absolute error and root mean square of the absolute errors per actuator are displayed in Table D.3.

**Table D.3:** Results from the torque precision analysis for all actuators. The mean absolute error (MEA), standard deviation (SD), maximal absolute error and root mean square error (RMSE) of the torque measurements of 35 duplicated static joint configurations.

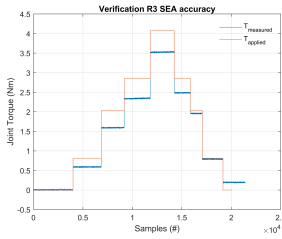
	MAE $\pm$ SD (Nm)	Max absolute error (Nm)	RMSE (Nm)
R1	0.18 $\pm$ 0.15	0.47	0.23
R2	0.50 $\pm$ 0.47	2.21	0.68
R3	0.08 $\pm$ 0.04	0.18	0.09
R4	0.10 $\pm$ 0.10	0.31	0.14
All	0.21 $\pm$ 0.37	2.21	0.37

### D.1.6 SEA linearity and hysteresis

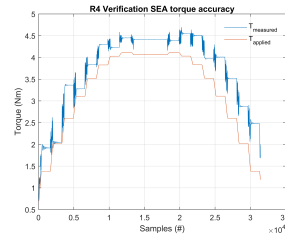
Ideally, the measured SE sensor torque as a function of the deflection of the SE shows a linear relation without death-band for a high sensor precision. As shown in Figure D.5a, the SE is slightly non-linear, affecting the SEA torque reading. To compensate for this non-linearity, we use a polynomial fit to express the joint torque  $\tau_{SE}$  as a function of the SE deflection  $\theta$  in rad by:

$$\tau_{SE} = -2.5 \cdot 10^6 \theta^5 + 2 \cdot 10^5 \theta^4 + 2.1 \cdot 10^4 \theta^3 - 1 \cdot 10^3 \theta^2 + 2.7 \cdot 10^2 \theta \quad (D.3)$$

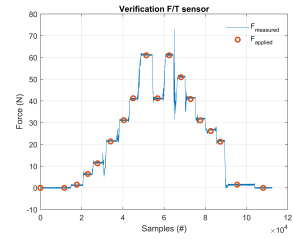
Moreover, Figure D.5b shows the death band indicating energy loss caused by friction and sliding between components, in other words, a hysteresis effect.



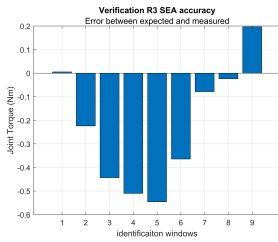
(a) R3 applied (red) and measured torque(blue)



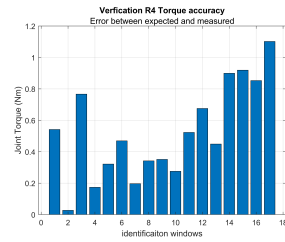
(b) R4 applied (red) and measured torque(blue)



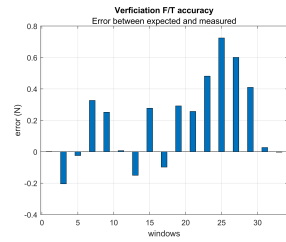
(c) F/T applied and measured torque



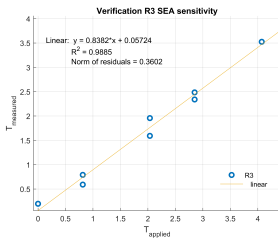
(d) R3 Error between applied and measured torque



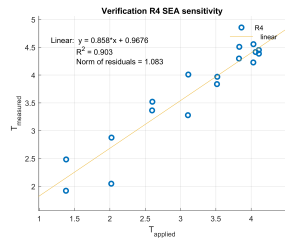
(e) R4 Error between applied and measured torque



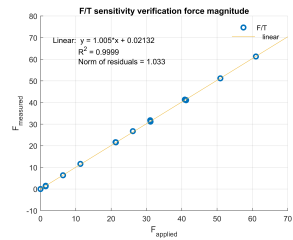
(f) F/T error between applied and measured force



(g) R3 Scatter plot of applied torque to measured torque with linear fit



(h) R4 Scatter plot of applied torque to measured torque with linear fit



(i) F/T Scatter plot of applied force to measured force with linear fit

**Figure D.2:** Accuracy and sensitivity measurements of SEA (R3 and R4) and F/T sensor.

D

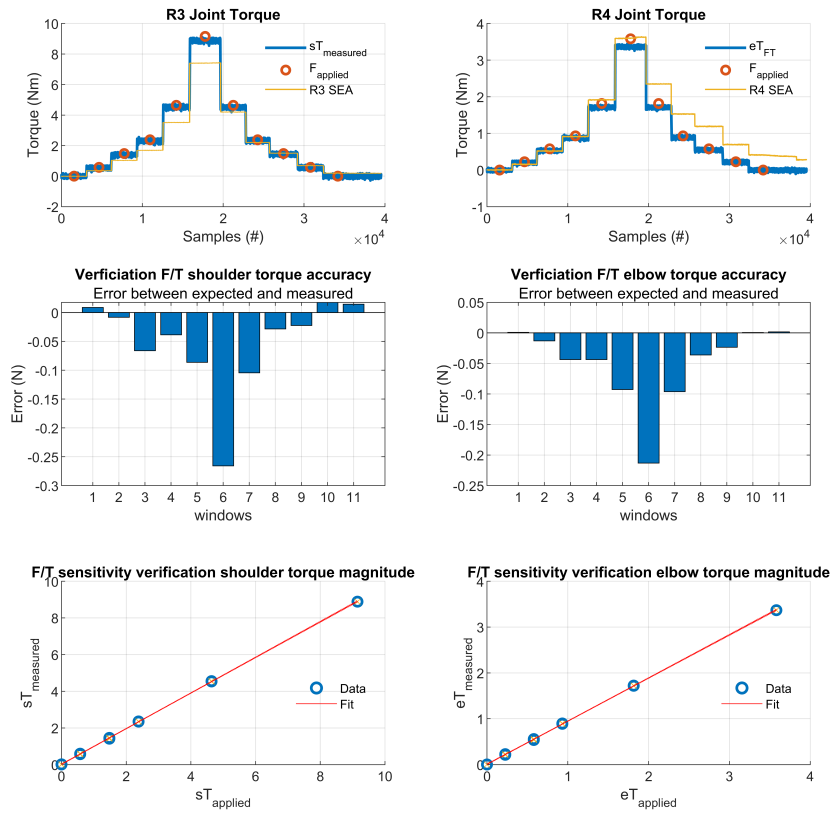
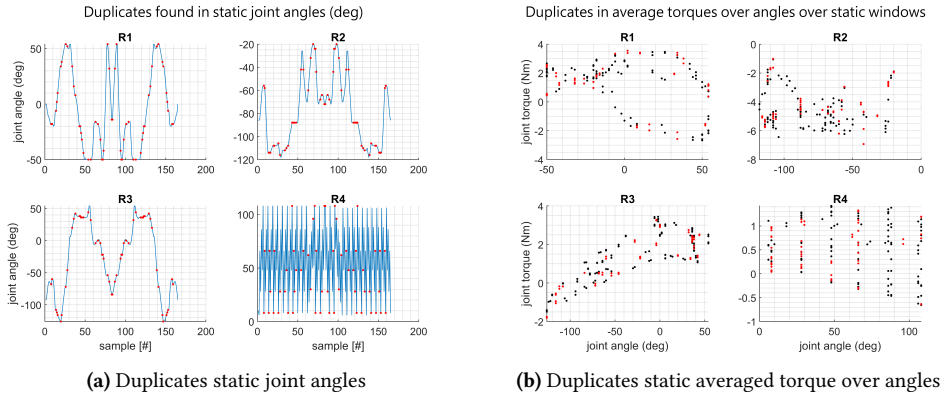


**Figure D.3:** F/T transformed to elbow and shoulder torque. The sensitivity fit are presented in Tab. D.2.



D

**Figure D.4:** In Figure (a), the joint angles are presented over an identification trajectory. In Figure (b), the average measured torques are presented over the averaged joint angles. The red dots present the duplicated joint angles (rounded by  $2^\circ$ ). In 35 samples, the same configurations were found two or three times. The torque errors between these duplicates are used to compare the consistency in the torque measurements to serve as a precision outcome metric.

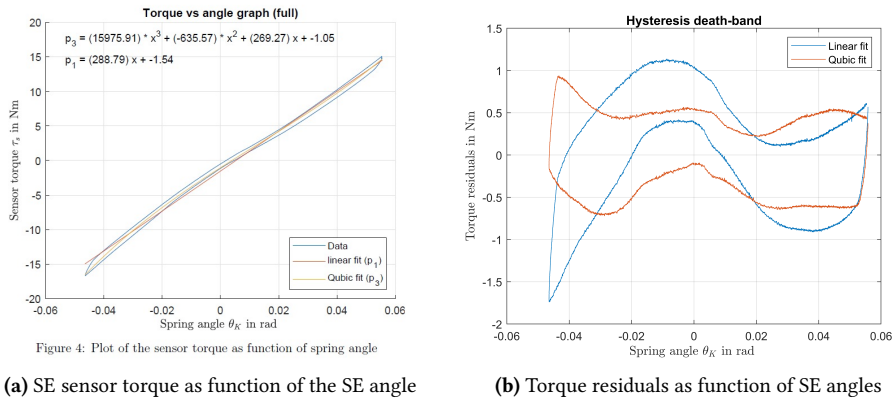


**Figure D.5:** a) Shows the measured SE sensor torque as a function of deflection of the SE (blue), with either a (red) linear or (yellow) cubic fit. b) SEA hysteresis deadband for the linear (blue) and cubic (red) fit.

## D.2 Kinematic model of the HEC

This section describes the kinematic modeling of the human exoskeleton combination (HEC) arm and how to solve the inverse kinematics problem.

### D.2.1 Kinematic Model

We refer to Chapter 7 for a schematic view of the kinematics of the HEC.

#### D.2.1.1 Exoskeleton forward kinematics

With respect to the center of rotation (CoR) in the shoulder, each actuator's rotor-frame  $i$  ( $i = 1, 2, 3, 4$ ) is determined by a chain multiplication of homogeneous transformations, where a homogeneous transform  ${}^{\#}H_i(q) \in SE(3)$  ( $\#$  could be any frame) comprises a rotation and translation in 3D:

$${}^{i-1}H_i(q) = \begin{bmatrix} RR_z(q_i) & {}^{i-1}p_i \\ 0_{1 \times 3} & 1 \end{bmatrix}, \quad (D.4)$$

with  $R, R_z(q_i) \in SO(3)$ , the former being a rotation-matrix because not all joint axes are aligned, and the latter being a canonical rotation-matrix around local  $z$  for the joint's degrees of freedom (DoF)  $q_i$ , and  ${}^{i-1}p_i \in \mathbb{R}^3$  the constant translation between the previous coordinate frame and the current one. The coordinate transformation for the frame of each actuator, or exoskeleton segment,  $i$  is hence found as

$${}^0H_i(q) = {}^0H_1(q) {}^1H_2(q) \dots {}^{i-1}H_i(q) \quad (D.5)$$

This chain multiplication leads to the shoulder frame expressed in the 0-frame (see Chapter 7) being:

$${}^0H_s(q) = {}^0H_{1,s} {}^1H_1(q) {}^1H_2(q) {}^2H_3(q), \quad (D.6)$$

where  ${}^0H_{1,s}$  is the constant rotation from the 0-frame to the stator of the first motor, as described in Chapter 7.

#### D.2.1.2 Human arm, shoulder frame and kinematics

The human glenohumeral joint is defined as a spherical joint with three descriptive DOFs according to the definitions of the ISB [7]. This frame is slightly than our 0-frame mentioned in Chapter 7, namely:

- ISB  $x$ -axis points from the shoulder CoR forward
- ISB  $y$ -axis points from the shoulder CoR upward
- ISB  $z$ -axis points from the shoulder CoR outward ("away from the user")

This coordinate system will be denoted as  $\Psi_I$ .

Transforming between the definition from the 0 and the ISB frame is trivial and is achieved by a canonical rotation around  $y$ :

$${}^I R_s(q) = {}^I R_0 {}^0 R_s(q) = R_y(+90^\circ) {}^0 R_s(q), \quad (D.7)$$

which is invertible:

$${}^0 R_s(q) = {}^0 R_I {}^I R_s(q) = R_y(-90^\circ) {}^I R_s(q). \quad (D.8)$$

We can decompose any ISB rotation matrix into three angles [6] that describe the ‘elevation’  $\gamma_e$  (how much the arm is raised with respect to the downward vertical), the ‘horizontal rotation’  $\gamma_h$  (how much it is rotated in the elevated plane) and the ‘axial rotation’  $\gamma_a$  (how much it is rotated around our upper arm). Together, these angles can be captured in a triplet  $\Gamma_s = [\gamma_h, \gamma_e, \gamma_a]^T$ , or for all four joints, also including the elbow, as  $\Gamma = [\gamma_h, \gamma_e, \gamma_a, q_4]^T$ .

**Inverse Kinematics** To determine the ISB shoulder angles from a rotation matrix of the shoulder, we can define the upper-arm unit vector and rotate it by the rotation matrix to decompose the (ISB) angles. For the elevation angle, we find the angle between the downward vertical and the unit vector of the upper arm ( $u_x$  in  ${}^I R_s(q)$ ):

$$\gamma_e = \arccos({}^I R_s(q)u_x \cdot -u_y) \quad (D.9)$$

The horizontal rotation  $\gamma_h$  is found by projecting onto the  $xz$ -plane and measuring the angle between the projection and the  $z$ -axis (taking the sign from the projection on the  $x$ ):

$$u_p = u_y \times ({}^I R_s(q)u_x \times u_y), \quad \hat{u}_p = u_p / |u_p|, \quad \gamma_h = \arccos(\hat{u}_p \cdot u_z) \text{sign}(\hat{u}_p \cdot u_x) \quad (D.10)$$

The axial rotation  $\gamma_a$  is found by comparing the rotation matrix to one generated by  $\gamma_e, \gamma_h$ :

$$\gamma_a = \arccos([0 \ 0 \ 1] \rho \cdot [0 \ 0 \ 1] {}^I R_s(q)) \text{sign}([1 \ 0 \ 0] \rho \cdot [0 \ 0 \ 1] {}^I R_s(q)) \quad (D.11)$$

with

$$\rho = R_y(\gamma_h)R_x(-\gamma_e). \quad (D.12)$$

**Forward Kinematics** Inverting this relation (i.e., forward kinematics) is much easier, as is shown in [6]:

$${}^I R_s(q) = {}^I R_s(\Gamma_s) = R_y(\gamma_h)R_x(-\gamma_e)R_y(-\gamma_a) \quad (D.13)$$

## D.2.2 Solving the inverse kinematics problem for trajectory generation

In position control mode, the target HEC configuration  $\Gamma$  determines the desired joint angles  $q$  as described in the following.

When the exoskeleton should move from a configuration  $\Gamma_i$  to the next configuration  $\Gamma_{i+1}$ , we can trivially, calculate the rotation matrices for the shoulder, namely *desired* rotation  $R_d(t)$ . Through forward kinematics, any  $\Gamma$  can be transformed to a rotation matrix of the shoulder and an elbow angle, as is shown in the previous section or in [6]. The reference joint angles  $q$  to reach the desired configuration are found via constrained differential inverse kinematics with corrective feedback. This allows the imposition of joint constraints in both coordinate systems, as explained in Section D.2.2.2, so that the exoskeleton use is always safe when in position control mode.

### D.2.2.1 Kinematic Error Correction

We add a feedback velocity term  $\omega_{\text{corr}} \in \mathbb{R}^3$ , to correct for any deviations due to either poor joint conditioning, joint angle or velocity or ISB angle limits. Such a deviation is found as the “difference” between two rotation matrices [4] (omitted dependence on time for readability):

$$\alpha_e [u_e]_{\times} = R_d^0 R_s^T(q) - R_d^{T0} R_s(q). \quad (\text{D.14})$$

Here,  $\alpha_e$  gives the positive scalar rotation error, and  $u_e \in \mathbb{R}^3$  the unit-length rotation axis of the error and notation  $[a]_{\times} b$  denotes the matrix form of the cross product  $a \times b$ . Together with positive kinematic feedback gain  $\kappa_p$  we obtain exponential convergence to the desired trajectory and configuration, if it were to deviate, by choosing

$$\omega_{\text{corr}} = \alpha_e u_e \kappa_p. \quad (\text{D.15})$$

### D.2.2.2 Constrained Differential Inverse Kinematics

The desired shoulder velocity  $\omega_d$  is an addition of 1) the rotation vector that brings the HEC from configuration  $\Gamma_i$  to  $\Gamma_{i+1}$  and 2) the correction term (Section D.2.2.1), in case any limits were hit. This sum is given as

$$\omega_d = \omega v + \omega_{\text{corr}} \in \mathbb{R}^3, \quad (\text{D.16})$$

which relates to the total exoskeleton joint angle velocity  $\dot{q} \in \mathbb{R}^4$  via

$$\dot{r} = \begin{bmatrix} \omega_d \\ \dot{q}_4 \end{bmatrix} = \begin{bmatrix} J(q) & 0 \\ 0 & 1 \end{bmatrix} \dot{q} = \bar{J}_{\omega}(q) \dot{q}. \quad (\text{D.17})$$

The relation between exoskeleton joint velocities and ISB velocities  $\dot{\Gamma}_s \in \mathbb{R}^3$  is

$$\dot{\Gamma}_s = \begin{bmatrix} J_I(q) & 0 \end{bmatrix} \dot{q} = \bar{J}_I(q) \dot{q}. \quad (\text{D.18})$$

Here shoulder joint Jacobian  $J(q)$  or augmented  $\bar{J}_{\omega}(q)$  can readily be constructed as described in many reference works (e.g., [2], or specifically for shoulder rotation joints in [3]). The Jacobian  $J_I(q)$  or augmented  $\bar{J}_I(q)$  that relate joint angle rate to ISB angle rate can be found similarly, or approximated numerically by a finite difference approximation.

The inverse kinematics problem can be solved, while conforming to joint range limits in the following way. If in joint space ( $q$ ) a joint goes beyond a limit angle, its upper or lower limit in *velocity* is set to 0 (no more motion in that direction). Similarly, if in ISB angle space ( $\Gamma$ ) the angle goes beyond a limit (e.g., too high elevation angle), then the ISB angular velocity will be limited to 0 in that ISB direction.

This allows us to formulate the differential inverse kinematics (DIK) problem as a minimization problem, more specifically a quadratic program (QP), that gives the “best” (in least squares sense) choice for joint velocities ( $\dot{q}^*$ ), while ensuring that we never obtain velocities that would bring us into a region of the coordinate space ( $q$  or  $\Gamma$ ) that we should



not be in:

$$\begin{aligned} \dot{q}^* &= \underset{\dot{q}}{\operatorname{argmin}} \|\dot{r} - \bar{J}_\omega(q)\dot{q}\|^2 \\ \text{s.t.} \\ \dot{q}_L &\leq \dot{q} \leq \dot{q}_U \\ \dot{\Gamma}_L &\leq \bar{J}_I(q)\dot{q} \leq \dot{\Gamma}_U, \end{aligned}$$

where  $\square_L$  and  $\square_U$  denote the lower and upper limits of some velocity ( $\dot{q}$  or  $\dot{\Gamma}$ ) that is changed to 0 on the fly as soon as a limit is reached.

This problem is convex (because the product  $\bar{J}_\omega^T \bar{J}_\omega$  is positive definite when  $\bar{J}_\omega$  is invertible and can therefore be solved uniquely in a few microseconds with a dedicated QP solver (we used a custom solver made on cvxgen.com [5]).

If the DIK method is constrained, then the exoskeleton will not be moving directly towards the next desired configuration but move in a way that is “close” (in an LS sense) to a desired motion. The feedback term (Section D.2.2.1) will make sure that when motion is unconstrained (again), the exoskeleton converges back to the direct path towards the desired configuration.

D

### D.3 Derivation of the HEC gravity model

The Center of Mass (CoM) of each segment in the HEC kinematic chain, expressed in frame 0, is given as

$${}^0P_{c,i} = {}^0H_i(q) {}^iP_{c,i}, \text{ with } {}^iP_{c,i} = \begin{bmatrix} {}^ip_{c,i} \\ 1 \end{bmatrix}, \quad (\text{D.19})$$

where  ${}^ip_{c,i} \in \mathbb{R}^3$  are constant vectors of the CoM of HEC segment  $i$ , expressed in frame  $i$ .

The total gravitational potential energy  $V(q)$  of the HEC is given as

$$V(q) = \begin{bmatrix} 0 & 1 & 0 & 0 \end{bmatrix} g \sum_{i=1}^4 {}^0P_{c,i} m_i, \quad (\text{D.20})$$

with  $g$  the gravitational acceleration of  $9.81 \text{ m/s}^2$ , and  $m_i$  the linear mass of HEC segment  $i$ . Writing out the gravitational torque estimate in parameter linear form gives

$$\hat{\tau}_g(q) = \frac{\partial V(q)}{\partial q} = K_g(q) \theta_g, \quad (\text{D.21})$$

with  $\theta_g \in \mathbb{R}^{12}$  the parameters of the gravity model

$$\theta_g = \begin{bmatrix} gm_1^1 p_{c,1} \\ gm_2^2 p_{c,2} \\ gm_3^3 p_{c,3} + gm_4^3 \delta \\ gm_4^4 p_{c,4} \end{bmatrix}, \quad (\text{D.22})$$

and  $K_g(q) \in \mathbb{R}^{4 \times 12}$  a matrix dependent on the joint angles that we obtain in the following. We note that only the elbow joint is offset from the CoR, in terms of position, by a vector  ${}^3\delta$ .

Replacing the homogeneous transformations by rotations and an offset vector from shoulder to elbow ( $\delta$ ), the notation is simplified. The gravitational potential energy becomes

$$V(q) = [0 \quad 1 \quad 0] \begin{bmatrix} {}^0R_1(q) & {}^0R_2(q) & {}^0R_3(q) & {}^0R_4(q) \end{bmatrix} \theta_g. \quad (D.23)$$

These rotation matrices can be readily extracted as the upper-left  $3 \times 3$  sub-matrix of the similarly named homogeneous transformation matrix.

Because all joints rotate around a local  $z$ -axis, the relevant partial derivatives are

$$R'_z(q_i) = \frac{\partial R_z(q_i)}{\partial q_i} = \begin{bmatrix} -\sin q_i & -\cos q_i & 0 \\ \cos q_i & -\sin q_i & 0 \\ 0 & 0 & 0 \end{bmatrix}. \quad (D.24)$$

This makes each row  $K_{g,i}(q)$  ( $i = 1, 2, 3, 4$ ) of  $K_g(q)$  as follows:

$$K_{g,i}(q) = [0 \quad 1 \quad 0] \hat{K}_{g,i}(q) \in \mathbb{R}^{1 \times 4} \quad (D.25)$$

with  $\hat{K}_{g,i}(q) \in \mathbb{R}^{3 \times 4}$  ( $i = 1, 2, 3, 4$ ) given as

$$\begin{aligned} \hat{K}_{g,1}(q) &= [{}^0R_{1,s}R'_z(q_1) \quad {}^0R_{1,s}R'_z(q_1)R_\phi R_z(q_2) \quad \dots \\ &\quad {}^0R_{1,s}R'_z(q_1)R_\phi R_z(q_2)R_\phi R_z(q_3) \quad {}^0R_{1,s}R'_z(q_1)R_\phi R_z(q_2)R_\phi R_z(q_3)R_z(q_4)] \\ \hat{K}_{g,2}(q) &= [0 \quad {}^0R_{1,s}R_z(q_1)R_\phi R'_z(q_2) \quad {}^0R_{1,s}R_z(q_1)R_\phi R'_z(q_2)R_\phi R_z(q_3) \quad \dots \\ &\quad {}^0R_{1,s}R_z(q_1)R_\phi R'_z(q_2)R_\phi R_z(q_3)R_z(q_4)] \\ \hat{K}_{g,3}(q) &= [0 \quad 0 \quad {}^0R_{1,s}R_z(q_1)R_\phi R_z(q_2)R_\phi R'_z(q_3) \quad \dots \\ &\quad {}^0R_{1,s}R_z(q_1)R_\phi R_z(q_2)R_\phi R'_z(q_3)R_z(q_4)] \\ \hat{K}_{g,4}(q) &= [0 \quad 0 \quad 0 \quad {}^0R_{1,s}R_z(q_1)R_\phi R_z(q_2)R_\phi R_z(q_3)R'_z(q_4)], \end{aligned}$$

where  $R_\phi = R_y(60^\circ)$  and  ${}^0R_{1,s}$  is the fixed initial rotation of the first motor's stator (as explained in Chapter 7).

## D.4 Enforcing workspace limits during minimal impedance mode

The user can move the device freely when the controller compensates for weight and possibly joint impedance. Consequently, by making ballistic motions, the device could bring the user to an uncomfortable configuration where the inertia of the exoskeleton will lead to the HEC going beyond the intended ROM.

To alleviate this problem, the workspace is limited by a uni-directional spring-damper force that pushes the HEC back into its allowed workspace. This strategy is quite common in robotics, and hence, a standard Jacobian transpose method is used to transform a force from an operational-space-limiter to generalized forces at the exoskeleton joint level.

We state a static, valid workspace set expressed in limits on joint angles  $Q$  (in practice, eight numbers to describe limits for four exoskeleton joints) and also a static, valid workspace set expressed in limits on arm ISB angles  $G$  (in practice, six numbers to describe limits on three ISB angles  $\Gamma_s$ ).

We check, element-wise, if any of the joints/ISB coordinates  $\xi$  ( $q$  or  $\Gamma_s$ ) outside a closed set of valid configurations  $X$  ( $Q$  or  $G$ , respectively). This set can be box-like, or more complicated and conditional on past trajectories, as long as limit checks can be implemented as conditional statements.

The workspace-limiter torque contribution for any coordinate  $\xi$  is given as

$$\tau_{l,\xi}(\xi) = \begin{cases} J_\xi^T(q)K_p(\xi_l - \xi), & \text{if } \xi \notin X \\ 0_{4 \times 1}, & \text{otherwise,} \end{cases} \quad \in \mathbb{R}^4 \quad (\text{D.26})$$

where  $\xi_l$  is the coordinate of the closest/relevant limit. The bring-back-torque contributions for all coordinates are subsequently summed.

For the ISB angles  $J_\xi = J_i$ , the Jacobian maps differential ISB motion to the rotation of the shoulder. For the joint angles  $q$ , the transposed Jacobian  $J_q^T$  is trivially a column with a single one and three zeros.

If the joint is pushed too far beyond this stated limit, given by some fixed margin  $\mu$ , then the exoskeleton goes into failure mode.

## D.5 Parameter identification procedure

Either the gravity-only ( $g$ ) or gravity plus elbow passive joint impedance ( $g + j$ ) parameters can be identified. The  $g + j$  model combined is as follows:

$$\begin{aligned} \hat{\tau}(q) &= \hat{\tau}_g(q) + \tau_j(q) = K_g(q)\theta_g + K_j(q)\theta_j \\ &= \begin{bmatrix} K_g(q) & K_j(q) \end{bmatrix} \begin{bmatrix} \theta_g \\ \theta_j \end{bmatrix} = K(q)\theta, \end{aligned}$$

with  $K(q) \in \mathbb{R}^{4 \times 18}$  and  $\theta \in \mathbb{R}^{18}$ .

### D.5.1 Configurations and Motions for Identification

#### D.5.1.1 Configurations

During identification, the HEC moves, position controlled, to a number of unique arm configurations within the allowable workspace of the user. These configurations are a selection ( $P_s$ ) from a uniformly sampled set of candidate configurations ( $P$ ) determined by the actuator's ROM and those of the user (as limits on ISB coordinates). The configurations in  $P_s$  are chosen to be  $D$ -optimal (Section 7.5 in [1]). The configurations are weighted in how much information they add to the parameters. The configurations that (sorted in weight) ensure that the movement duration is  $\leq 5$  minutes, determine  $P_s$ .

To obtain a short movement duration, the  $P_s$  configurations are sorted using the nearest neighbor heuristic to find a solution to the traveling salesman problem. This process is guided by a pairwise Euclidean distance matrix among the elements of  $P_s$  (this comparison is doable because there are at most a few dozen configurations). The result is an optimized trajectory that greedily minimizes the travel distance, which is sufficient for our application.

### D.5.1.2 Trajectory generation

Disregarding the trivial elbow angle  $q_4$ , the shoulder components  $\Gamma_s$  for a configuration  $i$  are transformed to a rotation matrix  $R(\Gamma_{s,i})$  for the shoulder. The rotation difference between two configurations ( $i$  and  $i + 1$ ) is then given as a rotation error [4]:

$$\alpha[\omega]_x = R(\Gamma_{s,i+1})R^T(\Gamma_{s,i}) - R^T(\Gamma_{s,i+1})R(\Gamma_{s,i}), \quad (\text{D.27})$$

giving a unit-length rotation axis  $\omega \in \mathbb{R}^3$  between the two rotations, expressed in frame 0, and a positive angle  $\alpha \in \mathbb{R}^+$  between those two rotations. The  $[\omega]_x$  is the skew-symmetric form (for the cross product) of  $\omega$ , which can trivially be reversed. A shoulder rotational velocity that would bring the shoulder joint from configuration  $\Gamma_{s,i}$  to  $\Gamma_{s,i+1}$ , with some scalar speed  $v$ , can then trivially be constructed as the product  $v\omega$ . Hence,  $v$  follows a smooth acceleration and constant velocity profile to, in total, traverse rotation angle  $\alpha$ .

In each configuration  $\Gamma_i \in P_s$ , the device remains stationary for a brief amount of time. The joint torques and angles at these stationary configurations are recorded and used for identification, as explained later in this document.

### D.5.2 Parameter identification as a fitting problem

The  $g$  or  $g + j$  model is found via Linear Least Squares (LLS) regression. We minimize the sum of squares residual of the predicted torque  $\hat{\tau}$  and the experimental torque  $\tau_e$ , for a training dataset of  $N$  measurements. The optimization problem is as follows:

$$\begin{aligned} \min_{\theta} L(\tau_e, [\cdot], q[\cdot], \theta) &= \min_{\theta} \left\| \begin{bmatrix} \tau_{e,[1]} \\ \tau_{e,[2]} \\ \vdots \\ \tau_{e,[N]} \end{bmatrix} - \begin{bmatrix} K(q_{[1]}) \\ K(q_{[2]}) \\ \vdots \\ K(q_{[N]}) \end{bmatrix} \theta \right\|_2^2 \\ &= \min_{\theta} \left\| \tau_{e,[\cdot]} - K(q[\cdot])\theta \right\|_2^2, \end{aligned}$$

where subscript  $[z]$ ,  $z \in [1, N]$  stands for the torque or joint angle data point, while the use of all data points is denoted in MATLAB-like fashion as  $[\cdot]$ . Matrix  $K(q[\cdot])$  is the problem's regressor.

#### D.5.2.1 Uniqueness of solution

At least three unique data points are needed for the  $g$  model ( $3 \cdot 4 \geq 12$ ) and five for the  $g + j$  model ( $5 \cdot 4 \geq 18$ ) to over-determine the regression. Conditioning analysis shows that after using at least those numbers of data points, the rank of the (sub)regressor  $K_g(q)$  is never higher than eight. This is to be expected, as for a gravitational model the induced torque is invariant to link-CoM displacements along the axis of rotation. As a consequence, no unique or physically explanatory parameters might be found via the proposed method. However, we are mostly interested in torque reproduction and not necessarily reconstructing an exact mass and CoM-location combination. Any change in parameter  $\theta_g$  that is in the nullspace of  $K_g(q)$  has no effect on torque prediction. During  $g + j$  model identification, however, the six passive joint impedance coefficients *will* be unique.

The minimization problem is solved via MATLAB's `pinv()` (version 2018b), to deal with the regressor's rank deficiency, giving a  $\theta$  with the smallest  $L_2$  norm.

Given the known nullspace of the gravitational model regressor, an equality-constrained (pseudo-)inverse can also be performed in which some higher-order parameters of the impedance model are also forced to become zero.

## D.6 Zeroing of F/T sensor offset and post-sensor brace contribution

A forearm sleeve containing a metal brace interfaces the user to the exoskeleton (see Fig. 1 in Chapter 7). An ATI SI-40-mini 6DOF F/T sensor attaches to this brace. This sensor allows for measurements of the user's interaction forces on the exoskeleton. However, there are two challenges: 1) bias voltage on the sensor when not under load, and 2) the sleeve has non-zero weight, generating a force and moment on the force sensor that is configuration-dependent.

During a "zeroing procedure" (without user), both the bias voltage and brace contribution can be identified and can consequently be negated for any configuration of the HEC. This helps distinguish user input from irrelevant biases. Note that we are not identifying inertial parameters here, and hence those will not be negated.

### D.6.1 F/T Sensor Workings

The F/T sensor measures six voltages  $u \in \mathbb{R}^6$  that can be transformed to a 6D vector of forces and torques  ${}^F F \in \mathbb{R}^6$ , where

$${}^F F = \begin{bmatrix} {}^F f \\ {}^F \tau \end{bmatrix} \quad (\text{D.28})$$

with  ${}^F f \in \mathbb{R}^3$  the linear force acting on the sensor and  ${}^F \tau \in \mathbb{R}^3$  the net moment around the center of the force sensor, all expressed in the force sensor frame  $F$ .

The measured voltage is related to the measured forces ( ${}^F F_m$ ), via a dense static calibration matrix  $C \in \mathbb{R}^{6 \times 6}$ :

$${}^F F_m = Cu = C(u_F + u_0) = {}^F F + {}^F F_u \quad (\text{D.29})$$

where we split  $u$  into a component that is dependent on real forces/torques ( $u_F$ ) and, unfortunately, a bias voltage ( $u_0$ ) that might differ between sessions, days and temperature.

### D.6.2 Determining bias forces and torques

It is more convenient to think of  $u_0$  of providing a (quasi-)static offset F/T vector,  ${}^F F_u \in \mathbb{R}^6$ . When there is no user in the system, we "should" be measuring zero external F/T ( ${}^F F_{\text{external}}$ ), however we measure a contaminated signal

$${}^F F_m = \underbrace{0_{6 \times 1}}_{{}^F F_{\text{external}}} + {}^F F_{\text{slv}}(q) + {}^F F_u. \quad (\text{D.30})$$

The contribution of the offset  ${}^F F_u$  and a gravitational contribution  ${}^F F_{\text{slv}}$ , of an always-present sleeve with mass  $m$ , located at  ${}^F r$ , can be combined to a total configuration-dependent bias F/T that has to be negated:

$${}^F \hat{F}_b(q) = \begin{bmatrix} {}^F g(q)m \\ {}^F r \times {}^F g(q)m \end{bmatrix} + {}^F F_u. \quad (\text{D.31})$$

The gravitational acceleration ( ${}^F g(q)$ ) in the sensor frame (rotated by  ${}^0 R_F(q)$ ) is given via forward kinematics of the robot arm as:

$${}^F g(q)m = {}^F R_0(q) {}^0 g m, \quad (D.32)$$

where  ${}^0 g = [0 \quad -9.81 \quad 0]^T$ . The torque contribution due to the brace can be rewritten as:

$$\begin{aligned} {}^F r \times {}^F g(q)m &= -{}^F g(q)m \times {}^F r \\ &= -{}^F R_0(q) {}^0 g \times {}^F r m \\ &= -[{}^F R_0(q) {}^0 g]_{\times} {}^F r m, \end{aligned}$$

where  $[a]_{\times} b$  describes the matrix form of the cross product  $a \times b$ .

Then the total bias F/T can be written in parameter linear form:

$${}^F \hat{F}_b(q) = \begin{bmatrix} {}^F R_0(q) {}^0 g & 0_{3 \times 3} & I_{3 \times 3} & 0_{3 \times 3} \\ 0_{3 \times 1} & -[{}^F R_0(q) {}^0 g]_{\times} & 0_{3 \times 3} & I_{3 \times 3} \end{bmatrix} \begin{bmatrix} m \\ mr_x \\ mr_y \\ mr_z \\ F_{u,1} \\ F_{u,2} \\ F_{u,3} \\ F_{u,4} \\ F_{u,5} \\ F_{u,6} \end{bmatrix}, \quad (D.33)$$

which we can write in short as:

$${}^F \hat{F}_b(q) = \rho(q) \theta_F, \quad (D.34)$$

with  $\rho(q) \in \mathbb{R}^{6 \times 10}$  the nonlinear matrix function of  $q$  and  $\theta_F \in \mathbb{R}^{10}$  the parameters.

By taking at least two F/T sensor measurements in two different configurations ( $2 \times 6 \geq 10$ ), the ten parameters can be identified by repeated stacking of  $\rho(q)$  for multiple  $q$  to over-determine the system of equations. However, to reduce sensitivity to noise, many more measurements than two should be used, in similar fashion to the ID described in Section D.5.2.

### D.6.3 Compensating bias forces and torques

After parameters  $\theta_F$  are identified, they can “zero” the F/T sensor by subtracting the bias model from the “raw” measured F/T:

$${}^F \hat{F} = {}^F F_m - {}^F \hat{F}_b(q). \quad (D.35)$$

This gives us the voluntary F/T estimate  ${}^F \hat{F}$  from the user, or approximately zero for each configuration  $q$  in the workspace of the exoskeleton when used without a user.

Note that this compensation is kinematic-model based since it requires the calculation of the frame of the force sensor  ${}^F R_0(q)$  as a function of  $q$ .

## References

- [1] S. Boyd and L. Vandenberghe. *Convex optimization*. Cambridge university press, 2004.
- [2] S. Brunp, L. Sciavicco, L. Villani, and G. Oriolo. *Robotics: Modelling, Planning and Control*. Springer, 2009.
- [3] A. Q. Keemink, H. van der Kooij, and A. H. Stienen. Admittance control for physical human–robot interaction. *International Journal of Robotics Research*, 37(11):1421–1444, 2018. doi: 10.1177/0278364918768950.
- [4] T. Lee, M. Leok, and N. H. McClamroch. Geometric tracking control of a quadrotor UAV on SE(3). *Proceedings of the IEEE Conference on Decision and Control*, pages 5420–5425, 2010. doi: 10.1109/CDC.2010.5717652.
- [5] J. Mattingley and S. Boyd. CVXGEN: A code generator for embedded convex optimization. *Optimization and Engineering*, 13:1–27, 2012.
- [6] A. H. A. Stienen and A. Q. L. Keemink. Visualization of shoulder range of motion for clinical diagnostics and device development. *IEEE International Conference on Rehabilitation Robotics*, 2015-Sept:816–821, 2015. doi: 10.1109/ICORR.2015.7281303.
- [7] G. Wu, F. C. T. Van Der Helm, H. E. J. Veeger, M. Makhsous, P. Van Roy, C. Anglin, J. Nagels, A. R. Karduna, K. McQuade, X. Wang, F. W. Werner, and B. Buchholz. ISB recommendation on definitions of joint coordinate systems of various joints for the reporting of human joint motion - Part II: Shoulder, elbow, wrist and hand. *Journal of Biomechanics*, 38(5):981–992, 2005. doi: 10.1016/j.jbiomech.2004.05.042.





# End Matter



# Acknowledgments

With my bare feet in the grass and a nice September-after-summer sun on my face, it is finally time to express my gratitude to all the people who helped me complete this journey. It was an enjoyable yet challenging expedition. It required me to step outside my comfort zone and do things I had never done or experienced before. For many things, I initially had no idea how to approach, handle, or solve the challenges we encountered along the way. Luckily, I did not have to do it (and could not have done it) alone. Therefore, I would like to express my gratitude to all who contributed, supported and encouraged me along the way.

Starting with my promoter and supervisor **Jaap**. Our paths first crossed in 2017 at VU Amsterdam, where you remotely supervised my master's internship in Lucerne, Switzerland. Although our contact was limited to a few email exchanges, they were always supportive and helpful. Coincidentally, our paths crossed again when I pursued a second master's in BioMedical Engineering, just as you became a professor in Clinical Technology at the TU Delft. After an extensive search for my next thesis assignment, the topics you proposed appealed to me the most, so you became my supervisor again. When I left academia to start my career in industry, I didn't expect to return to TU Delft nor to work under your supervision again, but I'm glad I did! I am very grateful for your trust in me by selecting me for this role. I hope I have met your expectations. Over the years, I have greatly appreciated your support, guidance, and fatherly advice. There was always room for a joke, casual chitchat, or a safe space to share my feelings and concerns. I admire your insights, communication and strategic skills in the academic world. With you, I could openly share my thoughts and have trustful conversations. When it was needed, you truly listened and came to action, which makes you a great supervisor and coach. The Frisian saying, your grandmother taught you: *"As it net kin sa't it moat, dan moat it mar sa't it kin"* (If it can't be done the way it should, then it should be done the way it can), will always stay with me. You often repeated it during our projects, which helped me set aside my perfectionism from time to time and finish the work within the targeted deadlines. A great lesson I will take along with me, thank you for everything!

Next, I would like to thank my copromotor **Mariska**. We got to know each other on a computer screen. After one year of extensive online meetings and collaboration due to the pandemic, we finally met in real life. Even though most of our contact was remote due to the distance (Amsterdam - Nijmegen), and sometimes took longer than planned or went off-topic due to our chitchat, I always felt heard and understood during our meetings. You listened to me, thought along with me, and gave me good advice, suggestions, and tips. We closely collaborated on the first chapter of this thesis, which we even got to present in Mexico at the ISPO World Congress. We explored the city of Guadalajara together, including the cocktail and taco bars. It was a pleasure to be supervised by you, and I found it very valuable to have another woman and friend on the project team!

My second promotor **Herman**. After approximately the first year of my PhD you stepped-in as supervisor in our project. Your additional input and expertise in the field were of great value, and your vision of the Wearable Robotics Project consortium led the project in the right direction. Thank you for reviewing our papers and giving strong feedback that helped improve the structure, clarity, and coherence. You also strengthened this project by enlisting the support of Arvid from the University of Twente. Thank you for making this possible and bringing this additional experienced resource to the team!

**Arvid**, we first met at the Wearable Robotics Symposium, which was finally held in person after two virtual editions. We were on the same footgolf team and you showed interest in our prototype. It was immediately clear to me that you had some experience with arm supports, actuators and control, so I was thrilled when you agreed to join the team to strengthen our control approaches. I enjoyed our collaboration, especially the three intensive months we worked together in the lab in UTwente with master student **Thom**. It felt like we were part of a small R&D team, making rapid improvements to the controller, an experience I truly appreciated! Tom and Arvid, thanks for your valuable contribution to 'The DAROR project' and our enjoyable time in the lab! Tom, your high motivation and passion for the project even led to constructing a student job for you besides your graduation project. Thank you both very much, for all the good ideas, time, and inputs you put into this project, you were of great value!

I had a similar lab experience with "the guys of DEMO", **Wouter**, and **Cor**. In particular, during the project's first three years, both of you were highly involved. You warmly welcomed me into the DEMO assembly room, where I could settle and feel at ease. I always enjoyed working with you guys. There was always room for a joke, good conversation or a small and always very interesting lecture from Cor. I always left the room wiser than when I arrived. Cor, you have a talent for explaining complex stuff in a nice and understandable manner. Even though your time was limited due to your new function at DEMO and a PhD of your own, you helped us set up the low-level controllers and provide the software building blocks we needed. Wouter, your design skills, engineering experience, and vision for the appearance of our prototype have resulted in the safe, robust, and (if I may say) good-looking, slender DAROR. The DAROR was brought to life by DEMO, including **Giel**, **Hans**, and **Perry**, and this thesis wouldn't have been possible without you.

**Lonneke**, thank you for your commitment to the project. Your assistance in the METC approval and reviewing our work was very welcome! Thank you for the hours you spent testing the DAROR performance with me and improving our protocols. I always enjoyed our casual talks during the lunch and WR outings!

During my PhD project, I also have had the opportunity to supervise master students **Zhangyue**, **Kyriacos**, **Bas**, **Kirsten**, and **Kevin**; I thank you for your interest, hard work and willingness to spend a lot of hours in the lab and assisted the project where it was needed! Also, thank you for the trust you put in me by choosing me as your supervisor. I especially want to thank Kyriacos and Bas for your extra motivation and additional work after your graduation projects to establish our joined publications. I enjoyed sharing first authorship with you two. It made the publication process a lot more fun to work on; you can be proud of yourselves! Bas, your interest in the project went beyond your master thesis project. You were always willing to help and demonstrated a deep commitment to the work. We established a side job for you to develop the Dummy Arm. Your dedication

to help led to a great product and our second shared publication. Well done! Thank you for your hard work!

Next, I would like to thank the organizations and companies within our user committee. **Yumen Bionics**, your dedication and high motivation to help people with Duchenne is inspiring. During the pandemic, you were offering me to work at your nice location near the IJ in Amsterdam. Thank you for this kind offer and hospitality. **Paulien, David, and Sjaak**, I always enjoyed our conversations and hearing about your visions and experiences in the field.

**Imelda and Saskia from RadboudUMC**, thank you for your medical insights and advice; your input and clinical view at the user committee meetings were always very helpful.

**Duchenne Parents Project**, thank you for your contribution, facilitating the co-creation, and providing access to the Dutch Dystrophinopathy Database.

**Jan from Festo**, thank you for your participation in the user committee, your hospitality in inviting us to FESTO and your contribution in assembling the actuators.

**Anjen from NWO, Arthur from Baat Medical, the FSHD Stichting, and Spieren voor Spieren**, thank you all for your input, participation and financial support of our project.

Special gratitude goes to **Sjoerd**, including your parents **Jolanda**, and **Halbe**. Thank you for voluntarily participating as a co-creator and giving honest opinions and feedback. Sjoerd, I know the sessions were quite an operation and tiring for you. So, thank you very much for all the energy and time you put into this project besides your school activities. You trusted us and our technology to support and move your arm, which can be difficult. I was happy we had such good contact with each other. Good luck with pursuing your studies and I really hope a suitable arm support solution becomes available soon.

Next, I would like to thank my Wearable Robotics Project consortium colleagues. Thank you **Edwin and Christina** for organizing the enjoyable summer school. **Ali**, my only WR TU Delft and ex-Laevo colleague, thank you for our talks and hilarious dance lesson in Spain (I still start to laugh when I think about our performance). Thank you **Eline Z.**, for exploring Madrid with me, I had a great time with you. **Ander**, and **Maura**, thanks for taking me out for dinner and doing some sightseeing in Enschede. You made me feel welcome at UTwente. **Alejandro, Brandon, Niels, Michelle, Ali, Martijn, and Nauzef**, it was nice to get to know you and have you as PhD peers in the consortium.

**Laura, Alex, Raphael, and Stéfano**, I very much enjoyed our time at the RehabWeek in Singapore and exploring the city with you.

My dear colleagues of the BioMedical Engineering department of the TU Delft: **Anton, Teddy, Martijn, Marit, Bart**, and our adopted colleague **Thijs**. Thanks for being fun 'Office 1' mates! I very much enjoyed having nice Padel and boulder sessions with you and, not to forget, making the dancefloor at the BME conference in Egmond unsafe. Later on, **Christoph, Gabriele, and Hassan**, I enjoyed your companion at the office.

I very much enjoyed working in the BioRobotLab in the basement due to the company of **Lucy, Katy, Patricia, Andries, Nianlei, Jonathan, and Bob** (still look forward to surf together in Scheveningen once). Thank you for the nice (outdoor) lunch walks and talks!

**Katerina and Jette**, it was great to organize the bonding *Pirates of the CaribBME* sailing

trip together. Dear colleagues, **Niko** (loved our spontaneous after-work swim at the Schie), **Kirsten** (thanks for your great advice on how to finish up a PhD), **Pier, Vera, Anneke, Robin, Indra, Ludovica, Federica, Dirk, Judith, Italo, Jelle, Ebi, Merle, Lennart, Rick**, and many more I might forget, I enjoyed bumping into you for a hallway talk and hanging out with you during work (outings)!

Then, to my dear and kind friends, **Leandra** and **Lisa**. We know each other from high school and I'm so glad we continued being friends. Although we live different and busy lives, we update each other regularly and celebrate important life events. Your friendship is very valuable to me and I our spontaneous Padel and boulder sessions, diners, music bingo, and not to forget dancing at the most beautiful wedding in Italy, were nice distractions from my work! I appreciate how we can continue our conversations every time we meet. Thanks for being you!!

**Jaap K., Niels, Sam, Jeroen** and **Ashira**, you are amazing people, and I very much enjoy our philosophical and psychological discussions during our weekends away in 'la France' and 'Zeeland'.

To my surf, skate, and bouldering mates, **IJsbrand, Pieter, Ryu, Greta**, and **Anne**, the days spent with you on the beach, in the water, and at Vondelpark are the ones I cherish most! Those moments I can enjoy nature, recharge my body and clear my mind.

**Fabiene & Joey, Nikki & Rowen, Joy & Joris, Lauren & Sjors, Niene & Sjef, Jolanda & David, Louise & Robin, Fabeya & Yorick, Quinty & Tim Kuijl, Noud, Sander, Tom**, thank you for all the great moments we have had together and are going to make! Who knows how many double-date weddings and babies await us. Some of you I've known for quite a while now, and you guys feel like brothers to *Tim*. I truly appreciate each of you and thanks for understanding that I was sometimes occupied with work or a bit stressed. You encouraged me not to give up and provided me, but more important *Tim* pleasant distractions when needed! Thanks for that!

To my dear dear and best friends **Yoni, Anne, Rozemarijn, Jaimie**, and **Wieke**, I'm so grateful to have met you during our Human Movement Studies in Amsterdam. I know I can always trust and rely on you. You girls feel like family, and you've supported and encouraged me throughout my PhD journey. You've taken the time to listen, to be there for me, and to help me navigate my doubts and big life decisions over the past decade. Thank you for accepting me as I am, even when I go off radar to focus on work or am feeling stressed. You've always checked in and put effort to nicely distracting me with our creative and sportive hobbies, memorable holidays and weekends away! Each of you is an incredible woman, and I hope to enjoy our friendship for the rest of our lives.

To my family, my brothers and sisters, **Joscha, Eline & Peter, Leon & Marlen**, and adorable baby **Nathan**; To my parents **Rens & Diny**, and parents-in-law **Ger & Anja**, thank you for the interest you showed in my project, for the support you provided when I needed it, and for the hours you spent listening to my thoughts and reflections. I love you all and feel deeply loved by you. I know I can always knock on your door, and please, feel free to knock on mine, whether you need help, a chat, a laugh, a cry, or simply a cup of coffee.

Dad, wise man, you were a great example to me throughout my education and academic career. Whenever I truly needed help with homework, literature reviews, or my master's

theses, you made time in your busy schedule to listen and offer valuable advice. You even took the time to review my entire thesis before it was sent to the printer, which I interpret as a great gesture of love. Thank you for being so intelligent and supportive.

Mom, thank you for your endless patience and always lending a listening ear. You have a gift for asking the questions that help me clarify my thoughts. I know my talk about work sometimes bored you ;), but you let me go on when I needed to. You are a great support to me. Thank you!

Finally, to my partner, **Tim**. I don't think words can truly capture what you mean to me or how grateful I am for your support throughout my PhD journey. I hope I've shown you how much it means to me, but I'll still try to put some of it into words. Thank you for all the delicious meals you prepared when I came home late (please keep that up ;)). Thank you for the countless hours of listening to my work/life challenges and doubts, offering consulting advice, supporting me in stressful times, and encouraging my sporty addictions. You accept me as I am, and I feel supported by you no matter what. I can be truly open and honest with you. You are my number-one colleague, roommate, best friend, travel companion, first love, and now fiancé. I can't wait for all the adventures and memories we'll create together.





# List of Publications

## Publications related to PhD project:

6. **Filius S.J.**, Keemink, A.Q., Meijneke, C., Gregoor, W.F., Kuenen, T. Lunshof, S., Janssen, M.M.H.P., Harlaar, J., & van der Kooij, H. (2024). *A 4DOF Motorized Upper Limb Assistive Exoskeleton with Weight and Elbow Stiffness Compensation (under revision)*
5. **Filius, S.J.**, Papa, K., Harlaar, J. (2024). *Review of Upper Extremity Passive Joint Impedance Identification for People with Duchenne Muscular Dystrophy (under revision)*
4. **Filius S.J.**, van der Burgh B.J., and J. Harlaar, J. (2024). *The Design of the Dummy Arm: A Verification Tool for Arm Exoskeleton Development*. Biomimetics 9, no. 10: 579. pp. 1–11. doi:10.3390/biomimetics9100579
3. **Filius, S.J.**, Harlaar, J., Alberts, L., Houwen-van Opstal, S., van der Kooij, H., & Janssen, M.M.H.P. (2024). *Design Requirements of Upper Extremity Supports for Daily Use in Duchenne Muscular Dystrophy with Severe Muscle Weakness*. Journal of Rehabilitation and Assistive Technologies Engineering 11(March). pp. 1–18. doi: 10.1177/20556683241228478
2. van der Burgh, B.J., **Filius, S.J.**, Radaelli, G., & Harlaar, J. (2024). *The Efficacy of Different Torque Profiles for Weight Compensation of the Hand*. Wearable Technologies 5. doi: 10.1017/wtc.2023.23. (Shared first authorship with B. van der Burgh)
1. **Filius, S.**, Janssen, M., van der Kooij, H. & Harlaar J. (2023). *Comparison of Lower Arm Weight and Passive Elbow Joint Impedance Compensation Strategies in Non-Disabled Participants*. pp. 1–6 in 2023 International Conference on Rehabilitation Robotics (ICORR) 101469. doi: 10.1109/ICORR58425.2023.10304707

## Other publication:

1. Vanbellingen, T., **Filius, S. J.**, Nyffeler, T., & van Wegen, E.E.H. (2017). *Usability of Videogame-Based Dexterity Training in the Early Rehabilitation Phase of Stroke Patients: A Pilot Study*. Frontiers in Neurology 8(DEC). doi: 10.3389/fneur.2017.00654.

## MSc thesis projects supervised:

- Zhangyue Wei, *Gravity compensation of wearable upper extremities support system for DMD patients*, (2023, April)
- Kyriacos Papa, *Passive Elbow Joint Impedance Identification with the use of an Elbow Device*, (2023, August)
- Kisten Heyns, *Classifying external loads in human elbow flexion and extension arm movements with arm weight compensation executed by an active-assistive device*, (2023, September)
- Bas van der Burgh, *Constant torque gravity compensation*, (2022, Oktober)

## BSc thesis project supervised:

- Tijmen Hartuijker, Gijs de Jong, Jurriën Smits, & Koen Tack, *Glenohumeral exoskeleton configuration for people with Duchenne Muscular Dystrophy*, (2020, December)

## Internship supervised:

- Kevin Laban, *Developer research assistant internship*, (2024, February)

# Curriculum Vitæ

## Suzanne J. Filius

1994/12/08    Born in Uithoorn, The Netherlands

### Experience

- 2019-2020    *Human-factors engineer*  
Laevo Exoskeletons, Rijswijk, The Netherlands
- 2018-2019    *Work Internship*  
InteSpring, Delft, The Netherlands
- 2017          *Research Internship*  
Luzerner Kantonsspital, Lucerne, Switzerland

### Education

- 2020-2024    *PhD in Advancing motorized arm support technology for severe muscle weakness*  
Department of BioMechanical Engineering  
Delft University of Technology, Delft, The Netherlands  
Thesis title: *The Duchenne ARm ORthosis project*  
Promotor: *Prof. dr. ir. Jaap Harlaar*  
Promotor: *Prof. dr. ir. Herman van der Kooij*  
Copromotor: *Dr. Mariska M.H.P. Janssen*
- 2017-2019    *MSc Biomedical Engineering*  
Delft University of Technology, Delft, The Netherlands  
Thesis: *Instantaneous Cost Mapping the Energy Cost of Walking: Validation in Ankle-Foot-Orthosis Evaluation*  
Supervisor: *Prof. dr. ir. Jaap Harlaar*

- 2016-2018    *MSc Human Movement Sciences: Sport, Exercise and Health - Rehabilitation*  
VU University Amsterdam, The Netherlands  
Thesis: *Usability of Videogame-Based Dexterity Training in the early rehabilitation phase of stroke patients: a pilot study*  
Supervisor: *Dr. Tim Vanbellinghen*
- 2013-2016    *BSc in Human Movement Science*  
VU University Amsterdam, The Netherlands  
Thesis: *Do people minimize metabolic energy by choosing a pathway in walking?*  
Supervisor: *Dr. Knoek van Soest*
- 2007-2013    *VWO (Pre-university Secondary Education)*  
Alkwin College, Uithoorn, The Netherlands  
Thesis: *Can music improve runners' performances?*

PEOPLE WITH DUCHENNE MUSCULAR DYSTROPHY, ESPECIALLY THOSE WITH SEVERE MUSCLE WEAKNESS ( BROOKE SCALE 4), STILL LACK ACCESS TO SUITABLE ARM SUPPORTS. DUE TO VARIATIONS AMONG THE POPULATION, IT IS DIFFICULT TO FIND A ONE-SIZE-FITS-ALL SOLUTION. ADDITIONALLY, IT IS TECHNOLOGICALLY CHALLENGING TO ACHIEVE AN INTUITIVE HUMAN-EXOSKELETON INTERACTION WITH STRONG BUT COMPACT ACTUATION THAT FITS THE LIMITED DESIGN SPACE. THIS THESIS WILL GUIDE YOU THROUGH THE STEPS WE TOOK TO DEVELOP OUR PROTOTYPE, THE **DUCHENNE ARM ORTHOSIS (DAROR)**. STARTING WITH FORMULATING THE DESIGN REQUIREMENTS, EXPLORING DIFFERENT CONTROL STRATEGIES AND VERIFYING THESE STRATEGIES WITHIN THE REALIZED HARDWARE, INCLUDING CUSTOM-MADE ACTUATORS. THROUGH THIS WORK, WE HOPE TO BRIDGE THE GAP IN CURRENT SOLUTIONS AND ADVANCE THE DEVELOPMENT OF EFFECTIVE ARM SUPPORTS THAT CAN GREATLY IMPROVE THE QUALITY OF LIFE AND HELP THOSE STILL WAITING FOR THE RIGHT TECHNOLOGY.

